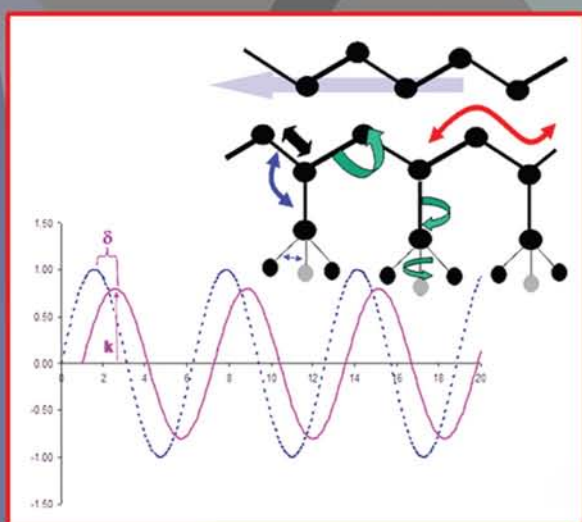


Second Edition

DYNAMIC MECHANICAL ANALYSIS

A Practical Introduction



Kevin P. Menard



CRC Press
Taylor & Francis Group

S e c o n d E d i t i o n

**DYNAMIC
MECHANICAL
ANALYSIS**

A Practical Introduction

S e c o n d E d i t i o n

DYNAMIC MECHANICAL ANALYSIS

A Practical Introduction

Kevin P. Menard



CRC Press

Taylor & Francis Group

Boca Raton London New York

CRC Press is an imprint of the
Taylor & Francis Group, an **informa** business

CRC Press
Taylor & Francis Group
6000 Broken Sound Parkway NW, Suite 300
Boca Raton, FL 33487-2742

© 2008 by Taylor & Francis Group, LLC
CRC Press is an imprint of Taylor & Francis Group, an Informa business

No claim to original U.S. Government works
Printed in the United States of America on acid-free paper
10 9 8 7 6 5 4 3 2 1

International Standard Book Number-13: 978-1-4200-5312-8 (Hardcover)

This book contains information obtained from authentic and highly regarded sources. Reasonable efforts have been made to publish reliable data and information, but the author and publisher cannot assume responsibility for the validity of all materials or the consequences of their use. The authors and publishers have attempted to trace the copyright holders of all material reproduced in this publication and apologize to copyright holders if permission to publish in this form has not been obtained. If any copyright material has not been acknowledged please write and let us know so we may rectify in any future reprint.

Except as permitted under U.S. Copyright Law, no part of this book may be reprinted, reproduced, transmitted, or utilized in any form by any electronic, mechanical, or other means, now known or hereafter invented, including photocopying, microfilming, and recording, or in any information storage or retrieval system, without written permission from the publishers.

For permission to photocopy or use material electronically from this work, please access www.copyright.com (<http://www.copyright.com/>) or contact the Copyright Clearance Center, Inc. (CCC), 222 Rosewood Drive, Danvers, MA 01923, 978-750-8400. CCC is a not-for-profit organization that provides licenses and registration for a variety of users. For organizations that have been granted a photocopy license by the CCC, a separate system of payment has been arranged.

Trademark Notice: Product or corporate names may be trademarks or registered trademarks, and are used only for identification and explanation without intent to infringe.

Library of Congress Cataloging-in-Publication Data

Menard, Kevin P.

Dynamic mechanical analysis : a practical introduction / Kevin P. Menard.
p. cm.

Includes bibliographical references and index.

ISBN 978-1-4200-5312-8 (alk. paper)

1. Materials--Testing. 2. Rheology. I. Title.

TA418.32.M46 2008

620.1'12--dc22

2007048967

Visit the Taylor & Francis Web site at
<http://www.taylorandfrancis.com>

and the CRC Press Web site at
<http://www.crcpress.com>

Dedication

To my wife, Connie,

*Tecum vivere amen,
tecum obeam libens.*

—*Homer, Epodes, ix*

Contents

Author's Preface	xi
Foreword to the First Edition	xiii
Foreword to the Second Edition	xv
Acknowledgments	xvii
Author	xix
Chapter 1 An Introduction to Dynamic Mechanical Analysis	1
1.1 A Brief History of DMA	1
1.2 Basic Principles	2
1.3 Sample Applications	4
1.4 Creep–Recovery Testing	9
1.5 Aggressive Environments	10
Notes	12
Chapter 2 Basic Rheological Concepts <i>Stress, Strain, and Flow</i>	15
2.1 Force, Stress, and Deformation	15
2.2 Applying the Stress	17
2.3 Hooke's Law: Defining the Elastic Response	20
2.4 Geometry, Sample Shape, and Aspect Ratio	24
2.5 Liquid-Like Flow or the Viscous Limit	25
2.6 Another Look at Stress–Strain Curves	28
2.7 Appendix: Conversion Factors	32
Notes	35
Chapter 3 Rheology Basics <i>Creep–Recovery and Stress Relaxation</i>	37
3.1 Creep–Recovery Testing	37
3.2 Models to Describe Creep–Recovery Behavior	40
3.3 Analyzing a Creep–Recovery Curve to Fit the Four-Element Model	41
3.4 Analyzing a Creep Experiment for Practical Use	44
3.5 Creep Ringing	45
3.6 Other Variations on Creep Tests	45
3.7 Superposition: The Boltzmann Principle	48
3.8 Retardation and Relaxation Times	49
3.9 Structure–Property Relationships in Creep–Recovery Tests	50

3.10	Stress Relaxation Experiments.....	51
3.11	Constant Gauge Length Tests.....	53
	Notes	54
Chapter 4 Thermomechanical Analysis.....		57
4.1	Theory of Thermomechanical Analysis.....	57
4.2	Experimental Considerations with TMA Samples.....	59
4.3	Expansion and CTE.....	61
4.4	Flexure and Penetration.....	64
4.5	Dilatometry and Bulk Measurements	65
4.6	Mechanical Tests	65
4.7	PVT Relationship Studies.....	67
	Notes	68
Chapter 5 Dynamic Testing and Instrumentation.....		71
5.1	Applying a Dynamic Stress to a Sample	71
5.2	Calculating Various Dynamic Properties.....	74
5.2.1	Calculation from Deformation and Phase Lag.....	75
5.2.2	Calculating Properties from a Measured Stiffness	76
5.3	Instrumentation for DMA Tests	76
5.3.1	Forced Resonance Analyzers	76
5.3.2	Stress and Strain Control.....	77
5.3.3	Axial and Torsional Deformation.....	79
5.3.4	Free Resonance Analyzers	79
5.4	Fixtures or Testing Geometries	81
5.4.1	Axial	83
5.4.1.1	Three-Point and Four-Point Bending	84
5.4.1.2	Dual and Single Cantilever	85
5.4.1.3	Parallel Plate and Variants	86
5.4.1.4	Bulk.....	87
5.4.1.5	Extension/Tensile.....	87
5.4.1.6	Shear Plates and Sandwiches	87
5.4.2	Torsional	88
5.4.2.1	Parallel Plates.....	88
5.4.2.2	Cone-and-Plate.....	89
5.4.2.3	Couette	89
5.4.2.4	Torsional Beam and Braid.....	90
5.5	Sample Handling Issues	90
5.6	Calibration Issues	91
5.7	Dynamic Experiments.....	92
	Notes	93

Chapter 6	Time and Temperature Scans Part I	
	<i>Transitions in Polymers</i>	95
6.1	Time and Temperature Scanning in the DMA.....	95
6.2	Transitions in Polymers: Overview	98
6.3	Sub- T_g Transitions.....	101
6.4	The Glass Transition (T_g or T_α).....	103
6.5	The Rubbery Plateau, T_α^* and T_{11}	106
6.6	The Terminal Region.....	110
6.7	Frequency Dependencies in Transition Studies.....	112
6.8	Applications.....	114
6.9	Time-Based Studies.....	117
6.10	Conclusions.....	118
	Notes	119
Chapter 7	Time and Temperature Scans Part II	
	<i>Thermosets</i>	123
7.1	Thermosetting Materials: A Review	123
7.2	Studying Curing Behavior in the DMA: Cure Profiles	127
7.3	Photocuring	132
7.4	Modeling Cure Cycles.....	133
7.5	Isothermal Curing Studies.....	133
7.6	Kinetics by DMA: The Roller Model and Other Approaches.....	134
7.7	Mapping Thermoset Behavior: The Gillham–Enns Diagram.....	137
7.8	Quality Control Approaches to Thermoset Characterization	138
7.9	Postcure Studies.....	140
7.10	Conclusions.....	141
	Notes	142
Chapter 8	Frequency Scans	145
8.1	Methods of Performing a Frequency Scan.....	145
8.2	Frequency Effects on Materials.....	147
8.3	The Deborah Number.....	155
8.4	Frequency Effects on Solid Polymers	155
8.5	Frequency Effects During Curing Studies	158
8.6	Frequency Studies on Polymer Melts	158
8.7	Normal Forces and Elasticity	159
8.8	Master Curves and Time–Temperature Superposition.....	161
8.9	Transformations of Data.....	167
8.10	Molecular Weight and Molecular Weight Distributions	169
8.11	Conclusions.....	171
	Notes	171

Chapter 9	Unusual Conditions and Specialized Tests	175
9.1	UV Studies	175
9.1.1	UV Photocures	177
9.1.2	UV Photodegradations	178
9.2	Humidity Studies	179
9.2.1	Equilibration Times	181
9.2.2	Effects of Humidity in the DMA	182
9.3	Immersion	182
9.3.1	Effects of Solvent on Instrumentation and Measurement	183
9.3.2	DMA in Solution	184
9.4	Hyphenated Techniques	186
9.5	Modeling Other Mechanical Tests	187
	Notes	188
Chapter 10	DMA Applications to Real Problems	
	<i>Guidelines</i>	191
10.1	The Problem: Material Characterization or Performance	191
10.2	Performance Tests: To Model or to Copy	191
10.3	Choosing a Type of Test	192
10.4	Characterization	194
10.5	Choosing the Fixture	194
10.6	Checking the Response to Loads	197
10.7	Checking the Response to Frequency	197
10.8	Checking the Response to Time	197
10.9	Checking the Temperature Response	198
10.11	Putting It Together	199
10.12	Verify the Results	199
10.13	Supporting Data from Other Methods	200
10.14	Appendix: Sample Experiments for the DMA	201
10.14.1	TMA Experiments	201
10.14.2	Stress–Strain Scans	201
10.14.3	Creep–Recovery Experiments	201
10.14.4	Stress Relaxation	202
10.14.5	Dynamic Strain Sweeps	202
10.14.6	Dynamic Temperature Scans	202
10.14.7	Curing Studies	202
10.14.8	Frequency Scans	202
	Notes	202
Index		205

Author's Preface

In the last eight years since the first edition was published, dynamic mechanical analysis (DMA) or spectroscopy has become a common tool in the analytical laboratory. However, information on the use of DMA is still scattered among a range of books and articles, many of which are rather formidable looking. It is still common to hear “I heard about DMA. What is it and what will it tell me?” This is often expressed as “I want a DMA in my lab, but can't justify its cost.” Novices in the field have to dig through thermal analysis, rheology, and materials science texts for the basics. Then they have to find articles on the specific application. Having once been in that situation, and now helping others in similar straits, I believed eight years ago there was a need for an introductory book on dynamic mechanical analysis. The assumption proved to be true. There have been enough changes in the last eight years that a new edition seems to be justified.

This book attempts to give the chemist, engineer, or materials scientist a starting point to understand where and how dynamic mechanical analysis can be applied, how it works (without burying the reader in calculations), and the advantages and limits of the technique. There are some excellent books for someone with familiarity with the concepts of stress, strain, rheology, and mechanics, and I freely reference them throughout the text. In many ways, DMA is the most accessible and usable rheological test available to the laboratory. Often its results give clear insights into material behavior. However, DMA data is most useful when supported by other thermal data and the use of DMA data to complement thermal analysis is often neglected. I have tried to emphasize this complementary approach to get the most information for the cost in this book as budget constraints seem to tighten each year. DMA can be a very cost-effective tool when done properly as it tells you quite a bit about material behavior quickly.

The approach taken in this book is the same I use in the DMA training course taught for PerkinElmer and as part of the University of North Texas' course in thermal analysis. After a review of the topic, we start off with a discussion of the basic rheological concepts and the techniques used experimentally that depend on them. Because I work mainly with solids, we start with stress–strain. I could as easily start with flow and viscosity. Along the way, we will look at what experimental considerations are important, and how data quality is assured. Data handling will be discussed, along with the risks and advantages of some of the more common methods. Applications to various systems will be reviewed and both experimental concerns and references are supplied.

The mathematics has been minimized and a junior or senior undergraduate or new graduate student should have no trouble with it. I probably should apologize now to some of my mentors and the members of the Society of Rheology for what may

be oversimplifications. However, my experience suggests most users of DMA don't want, may not need, and are discouraged by an unnecessarily rigorous approach. For those who do, references to more advanced texts are provided. I do assume some exposure to thermal analysis and a little more to polymer science. Although the important areas are reviewed, the reader is referred to a basic polymer text for details.

Kevin P. Menard
Denton, Texas

Foreword to the First Edition

As an educator, and also because of my involvement in short courses preceding the International Conferences on Materials Characterization (POLYCHAR), I have repeatedly found that some practitioners of polymer science and engineering tend to stay away from dynamic mechanical analysis (DMA). Possibly because of its use of complex and imaginary numbers, such people call the basic DMA definitions impractical and sometimes do not even look at the data. This is a pity, because DMA results are quite useful for the manufacturing of polymeric materials and components as well as for the development of new materials.

Year after year, listening to Kevin Menard's lectures at the POLYCHAR Short Courses on Material Characterization, I have found that he has a talent for presentation of ostensibly complex matters in a simple way. He is not afraid of going to a toy store to buy Slinkies™ or Silly Putty™, and he uses these playthings to explain what DMA is about. Those lectures and the DMA course he teaches for PerkinElmer, which is also part of the graduate level thermal analysis course he teaches at UNT, form the basis of this text.

The following book has the same approach: explaining the information that DMA provides in a practical way. I am sure it will be useful for both beginning and advanced practitioners. I also hope it will induce some DMA users to read more difficult publications in this field, many of which are given in the references.

Witold Brostow
University of North Texas
Denton, in July 1998

Foreword to the Second Edition

This is a second edition of the book by Kevin P. Menard on dynamic mechanical analysis (DMA). This while Menard is not Agatha Christie, nor Erle Stanley Gardner, nor J.K. Rowling either. This also while billions of people read novels, but only a very small fraction of that set reads technical literature. Clearly, the first edition of this book has filled a need that existed before.

The applications of the DMA technique are growing, and the author of this book is now reporting progress achieved since the first edition in 1999. I believe I know why that first edition was so popular. In the preface to the first edition I wrote: “Some practitioners of polymer science and engineering tend to stay away from DMA. Possibly because of its use of complex and imaginary numbers, such people call the basic DMA definitions impractical and sometimes do not even look at the data. This is a pity, because DMA results are quite useful for the manufacturing of polymeric materials and components as well as for the development of new materials.” I also said then that Prof. Menard explains “the information that DMA provides in a practical way. I am sure (the book) will be useful for both beginners and advanced practitioners.” Today, instead of polymeric materials I would have simply said materials, given the increase in the use of polymer-based composites and also of applications of DMA to other materials that *do not contain polymers at all*, such as thermoelectric coolers.¹

What must have happened was that many of those skeptics did listen! They must have read and used the Menard book, which is why now a second edition is needed.

Success like this does not occur by itself. Menard had a natural ability to explain complex things in a simple way to begin with. But he also has an unusually good opportunity to sharpen those skills—an opportunity he created himself. In 1990, he, Michael Hess (now at the University of Duisburg-Essen, then a visiting professor at North Texas), and the author of this preface started what is now called the POLYCHAR World Forum on Advanced Materials.² For several years POLYCHAR was held at North Texas, then it started moving around: Portugal, Singapore, and Japan. POLYCHAR 15 was held in April 2007 in Buzios in the state of Rio de Janeiro in Brazil, organized by Elizabete F. Lucas. POLYCHAR 16 is planned for February 2008 at the University of Lucknow in India, organized by Ram P. Singh. POLYCHAR (Polymer Characterization) starts each year with a course on that subject, and each year DMA is covered. The course helps the participants to follow research presentation during the forum. You will not be surprised that a survey of the participants resulted in Menard being elected the best course instructor.

Let me also express my personal gratitude to Menard. I knew something about DMA, but I learned much more about it from the first edition of his book. In the spring of 2006 we were talking about brittleness of materials. The word had been used—again and again—in hand-waving discussions, but there was no definition.

Together with Haley Hagg Lobland of North Texas in Denton and Moshe Narkis of Technion in Haifa, we have defined brittleness.³ Our definition involves the storage modulus E' , which is obtained in every DMA experiment (and there is no other way to measure it). We have solved this problem because of the influence of the author of this book.

NOTES

1. W. Brostow, K.P. Menard, and J.B. White, *e-Polymers* 2004, no. 045.
2. <http://www.unt.edu/POLYCHAR/>.
3. W. Brostow, H.E. Hagg Lobland, and M. Narkis, *J. Mater. Res.*, 2006, 21, 2422.

Witold Brostow
University of North Texas
September 2007

Acknowledgments

I need to thank and acknowledge the help and support of a lot of people, more than could be listed here. This book would never have been started without Dr. Jose Sosa. After roasting me extensively during my job interview at Fina, Jose introduced me to physical polymer science and rheology, putting me through the equivalent of a second Ph.D. program while I worked for him. One of the best teachers and finest scientists I have met, I am honored to also consider him a friend. Dr. Letton and Dr. Darby at Texas A&M got me started in their short courses. Jim Carroll and Randy O'Neal were kind enough to allow me to pursue my interests in DMA at General Dynamics, paying for classes and looking the other way when I spent more time running samples than managing that lab. Charles Rohn gave me just tons of literature when I was starting my library. Chris Macosko's short course and its follow-up opened the mathematical part of rheology to me.

Witold Brostow of the University of North Texas, who was kind enough to preface and review this manuscript, has been extremely tolerant of my cries for help and advice over the years. While he runs my tail off with his International Conference on Polymer Characterization each winter, his friendship and encouragement (translation: nagging) were instrumental in getting this done. Dr. Charles Earnest of Berry College has also been more than generous with his help and advice. His example of and advice on how to teach science was instrumental in deciding to use an informal style. Dr. George Martin of Syracuse University read the first edition cover to cover for me. Dr. John Duncan of Triton Technologies gave me tons of data and was also kind enough to read over the second edition. Dr. Bryan Bilyeu, now of Xavier University, and Ms. Wunpen Chonkaew were invaluable in helping me get samples run and data collected.

My colleagues at PerkinElmer Life and Analytical Science have been wonderfully supportive. Without my management's support, I could have never done this. Mike Divvito and Steffen Ball were very supportive of my writing. Dr. Jesse Hall, my friend and mentor while at PerkinElmer, supplied lots of good advice for the first edition. My colleagues in the Material Characterization group, Svenja Goth, Krista Swanson, and Peng Ye, were always helpful. Dave Norman, BC Tan, Tiffany Kang, Larry Fletcher, and Farrell Summers helped with examples, juicy problems, and feedback. Bob Schwartz, Kenny Uliano, and Greg Curran also gave me more help than they realize. Likewise, our customers, who are too numerous to list here, were extremely generous with their samples and data. Dr. John Enns gets my thanks for his efforts in keeping me honest over the years and pushing the limits of the current commercially available instrumentation. John Rose of Rose Consulting has been always a source of interesting problems and an adviser of wide experience. Many people cannot be mentioned as I promised not to tell where the samples came from. Many of the figures were reproduced due to the kindness of others. I'm sure I

missed more than a few people who helped over the years; it is unintentional and I apologize.

More personally, a large group of friends helped keep me sane and Tom Morrissey and Paul Albert were always ready to listen to me whine. Jonathon Plant, my editor, put up endlessly with my lack of a concept of deadline. Finally, thanks are offered to my wife, Connie, and my sons, Noah and Benjamin, for letting me write on nights when I should have been an attentive husband and father.

Author

Kevin P. Menard is a chemist with research interests in materials science and polymer properties. He has published or presented more than 130 papers and holds 13 patents. Currently the global product manager for mechanical analysis for the PerkinElmer Life and Analytical Science's Material Characterization Division, he is also an adjunct professor in materials science at the University of North Texas.

After earning his doctorate from Wesleyan University and spending two years at Rensselaer Polytechnic Institute, he joined the Fina Oil and Chemical Company where he worked for several years on toughened polymers and metallocene catalysts. He then moved to the General Dynamics Corporation where he managed the Advanced Process Engineering Group and Process Control Laboratories. He joined PerkinElmer in 1992 as a senior product specialist in thermal and elemental analysis.

Dr. Menard has been elected as a fellow of the Royal Society of Chemistry, a fellow of the American Institute of Chemists, and a certified professional chemist. He is active in the American Chemical Society and Society of Plastic Engineers, where he is on the board of directors for the Polymer Analysis Division as well as a member of the Technical Program Committee for ANTEC. He has been treasurer for the North American Thermal Analysis Society and served on its long-range planning committee. He also has participated in the ASTM E37 and D20 committees, briefly acted as chair of the DMA subcommittee, and is a member of the Materials Research Society, the Society of Rheology, the American Institute of Chemists, and the American Association of Pharmaceutical Scientists.

Married to an incredibly tolerant woman for twenty-five years, he has two sons and a very spoiled dog. His hobbies include outdoor sports, mandolin, martial arts, woodworking, and running a small research group in the Materials Science Department of the University of North Texas.



1 An Introduction to Dynamic Mechanical Analysis

Dynamic mechanical analysis (DMA) is becoming more and more commonly seen in the analytical laboratory as a tool rather than a research curiosity. This technique is still treated with reluctance and unease, probably due to its importation from the field of rheology. Rheology, the study of the deformation and flow of materials, has a reputation of requiring a fair degree of mathematical sophistication. Although many rheologists may disagree with this assessment,¹ most chemists have neither the time nor the inclination to delve through enough literature to become fluent. Neither do they have an interest in developing the constituent equations that are a large part of the literature. DMA is a technique that does not require a lot of specialized training to use for material characterization. It supplies information about major transitions as well as secondary and tertiary transitions not readily identifiable by other methods. It also allows characterization of bulk properties directly affecting material performance.

Depending on whom you talk to, the same technique may be called dynamic mechanical analysis (DMA), forced oscillatory measurements, dynamic mechanical thermal analysis (DMTA), dynamic thermomechanical analysis, and even dynamic rheology. This is a function of the development of early instruments by different specialties (engineering, chemistry, polymer physics) and for different markets. In addition, the names of early manufacturers are often used to refer to the technique, the same way that Kleenex™ has come to mean tissues. In this book, DMA will be used to describe the technique of applying an oscillatory or pulsing force to a sample.

1.1 A BRIEF HISTORY OF DMA

The first attempts that I found reported in the literature to do oscillatory experiments to measure the elasticity of a material were by Poynting² in 1909. Other early works gave methods to apply oscillatory deformations by various means to study metals³ and many early experimental techniques were reviewed by te Nijenhuis in 1978.⁴ Miller's book on polymer properties referred to dynamic measurements in this early discussion of molecular structure and stiffness.⁵ Early commercial instruments included the Weissenberg rheogoniometer (approximately 1950) and the Rheovibron (approximately 1958). The Weissenberg rheogoniometer, which dominated cone-and-plate measurements for over 20 years following 1955, was the commercial version of the first instrument to measure normal forces.⁶ By the time Ferry wrote *Viscoelastic Properties of Polymers* in 1961,⁷ dynamic measurements were an integral part of polymer science and he gives the best development of the theory available. In 1967,

McCrum et al. collected the current information on DMA and DEA (dielectric analysis) into their landmark textbook.⁸ The technique remained fairly specialized until the late sixties when commercial instruments became more user-friendly. About 1966, Gillham developed the torsional braid analyzer and started the modern period of DMA.⁹ In 1971, Macosko and Starita built a DMA that measured normal forces and from this came the Rheometrics Corporation.¹⁰ In 1976, Bohlin also developed a commercial DMA and started Bohlin Rheologia. Both instruments used torsional geometry. The early instruments were, regardless of manufacturer, difficult to use, slow, and limited in their ability to process data. In the late seventies, Murayani¹¹ and Read¹² wrote books on the uses of DMA for material characterization. Several thermal and rheological companies introduced DMA's in the same time period and currently most thermal and rheological vendors offer some type of DMA. Polymer Labs offered a dynamic mechanical thermal analyzer (DMTA) using an axial geometry in the early 1980s. This was soon followed by an instrument from Du Pont. PerkinElmer developed a controlled stress analyzer based on its thermomechanical analyzer (TMA) technology, which was designed for increased low-end sensitivity. The competition between vendors has led to easier to use, faster, and less expensive instruments. The revolution in computer technology, which has so affected the laboratory, changed instrumentation in many ways and DMAs of all types became more user-friendly as computers and software evolved. We will look at instrumentation briefly in Chapter 5. Since the first edition of this book was published, several articles have appeared that review the state of the art.¹³

1.2 BASIC PRINCIPLES

DMA can be simply described as applying an oscillating force to a sample and analyzing the material's response to that force (Figure 1.1). This is a simplification and we will discuss it in Chapter 5 in greater detail. From this, one calculates properties like the tendency to flow (called viscosity) from the phase lag and the stiffness (modulus) from the sample recovery. These properties are often described as the ability to lose energy as heat (damping) and the ability to recover from deformation (elasticity). One way to describe what we are studying is the relaxation of the polymer chains.¹⁴ Another description would be to discuss the changes in the free volume of the polymer that occur.¹⁵ Both descriptions allow one to visualize and describe the changes in the sample. We will discuss stress, strain, and viscosity in Chapter 2.

The applied force is called stress and is denoted by the Greek letter σ . When subjected to a stress, a material will exhibit a deformation or strain, γ . Most of us working with materials are used to seeing stress–strain curves as shown in Figure 1.2. These data have traditionally been obtained from mechanical tensile testing at a fixed temperature. The slope of the line gives the relationship of stress to strain and is a measure of the material's stiffness, the modulus. The modulus is dependent on the temperature and the applied stress. The modulus indicates how well a material will work in a specific application in the real world. For example, if a polymer is heated so that it passes through its glass transition and changes from glassy to rubbery, the modulus will often drop several decades. (A decade is an order of magnitude.) This drop in stiffness can lead to serious problems if it occurs at a temperature different

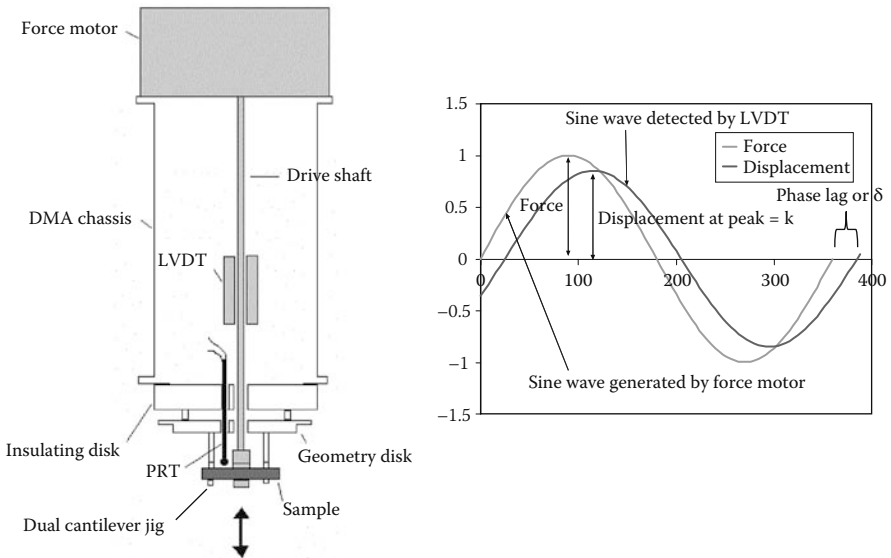


FIGURE 1.1 How a DMA works. The DMA supplies an oscillatory force, causing a sinusoidal stress to be applied to the sample, which generates a sinusoidal strain. By measuring both the amplitude of the deformation at the peak of the sine wave and the lag between the stress and strain sine waves, quantities like the modulus, the viscosity, and the damping can be calculated. The schematic above shows the PerkinElmer DMA 8000; other instruments use force–balance transducers and optical encoders to track force or position. Used with the permission of the PerkinElmer LAS, Shelton, Connecticut.

from expected. One advantage of DMA is that we can obtain a modulus each time a sine wave is applied, allowing us to sweep across a temperature or frequency range. So if we were to run an experiment at 1 hertz (Hz) or 1 cycle/second, we would be able to record a modulus value every second. This can be done while varying temperature at some rate like 5°C–10°C/min so that the temperature change per cycle is not significant. We can then with a DMA record the modulus as a function of temperature

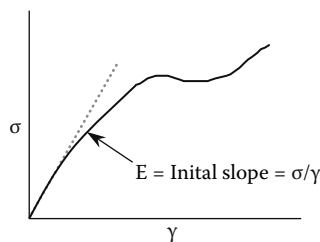


FIGURE 1.2 The ratio of stress to strain is the modulus, which is a measurement of the material’s stiffness. Young’s modulus, the slope of the initial linear portion of the stress–strain curve (shown here as a dotted line), is commonly used as an indicator of material performance in many industries. Since stress–strain experiments are one of the simplest tests for stiffness, Young’s modulus provides a useful evaluation of material performance.

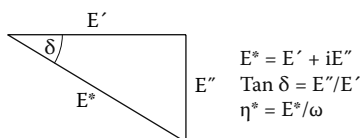


FIGURE 1.3 DMA uses the measured phase angle and amplitude of the signal to calculate damping, $\tan \delta$, and a spring constant, k . From these values, the storage and loss moduli are calculated. As the material becomes elastic, the phase angle, δ , becomes smaller and E^* approaches E' .

over a 200°C range in 20–40 minutes. Similarly we can scan a wide frequency or shear rate range of 0.01 to 300 Hz in less than 2 hours assuming a rate of 2°C/min. In the traditional approach, we would have to run the experiment at each temperature or strain rate to get the same data. For mapping modulus or viscosity as a function of temperature, this would require heating the sample to a temperature, equilibrating, performing the experiment, loading a new sample, and repeating at a new temperature. To collect the same 200°C range this way would require several days of work.

The modulus measured in DMA is, however, not exactly the same as the Young's modulus of the classic stress–strain curve (Figure 1.3). Young's modulus is the slope of a stress–strain curve in the initial linear region. In DMA, a complex modulus (E^*), an elastic modulus (E') and an imaginary (loss) modulus (E'')¹⁶ are calculated from the material response to the sine wave. These different moduli allow better characterization of the material because we can now examine the ability of the material to return energy (E'), to lose energy (E''), and the ratio of these effects ($\tan \delta$), which is called damping. Chapter 5 discusses dynamic moduli along with how DMA works.

Materials also exhibit some sort of flow behavior, even materials we think of as solid and rigid. For example, the silicon elastomer sold as Silly Putty™ will slowly flow on sitting even though it feels solid to the touch. Even materials considered rigid have finite, although very large, viscosities and “if you wait long enough everything flows.”¹⁷ Now to be honest, sometimes the times are so long as to be meaningless to people but the tendency to flow can be calculated. This tendency to flow is measured as viscosity. Viscosity is scaled so it increases with resistance to flow. Because of how the complex viscosity (η^*) is calculated in the DMA, we can get this value for a range of temperatures or frequencies in one scan. The Cox–Mertz rules¹⁸ relate the complex viscosity, η^* , to traditional steady shear viscosity, η_s , for very low shear rates, so that a comparison of the viscosity as measured by dynamic methods (DMA) and constant shear methods (for example, a spinning disk viscometer) is possible.

1.3 SAMPLE APPLICATIONS

Let's quickly look at a couple of examples on using the DMA to investigate material properties. First, if we scan a sample at a constant ramp rate, we can generate a graph of elastic modulus versus temperature. In Figure 1.4a, this is shown for nylon. The glass transition can be seen at ~50°C. Note that there are also changes in the modulus at lower temperatures. These transitions are labeled by counting back from the melting temperature, so the glass transition (T_g) here is also the alpha transition (T_α). As the T_g

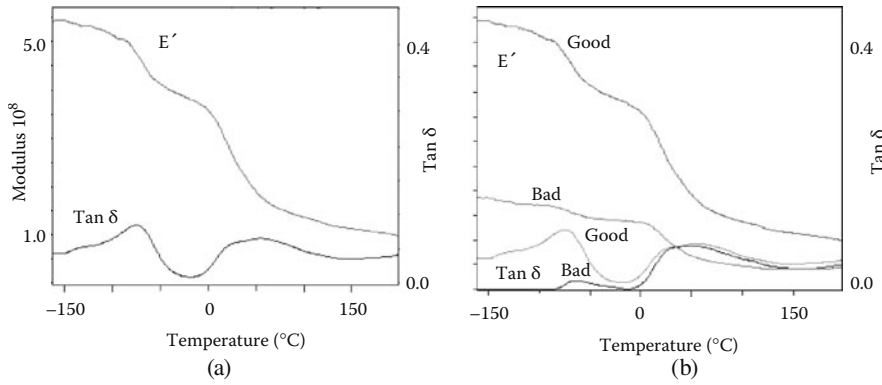


FIGURE 1.4 (a) The importance of higher transitions in material behavior is well known. The first figure shows a sample of material with good impact toughness. We can see in the storage modulus, E' , both a T_g at -50°C and a strong T_β at -80° . These are also seen as peaks in the $\tan \delta$. (b) The curves for the material that fails impact testing are overlaid. Note the lower modulus values and the relatively weaker T_β in the bad sample. Comparisons of the relative peak areas for T_β suggest that the second material is less able to damp vibrations below the T_g .

or T_α can be assigned to gradual chain movement, so can the beta transition (T_β) be assigned to other changes in molecular motions. The beta transition is often associated with side chain or pendant group movements and can often be related to the toughness of a polymer.¹⁹ Figure 1.4b also shows the above nylon overlaid with a sample that fails in use. Note the differences in both the absolute size (the area of the T_β peak in the $\tan \delta$) and the size relative to the T_g of T_β . The differences suggest the second material would be much less able to dampen impact via localized chain movements. An idealized scan of various DMA transitions is shown in Figure 1.5, along with the molecular motions associated with the transitions. The use of molecular motions and free volume to describe polymer behavior will be discussed in Chapter 6. Another use of this kind of information is determining the operating range of a polymer, for example PET. In the range between T_α and T_β , the material possesses the stiffness

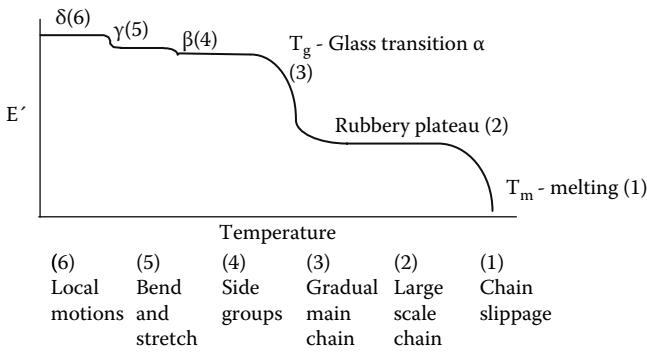


FIGURE 1.5 An idealized scan showing the effect of various molecular relaxations on the storage modulus, E' , curve.

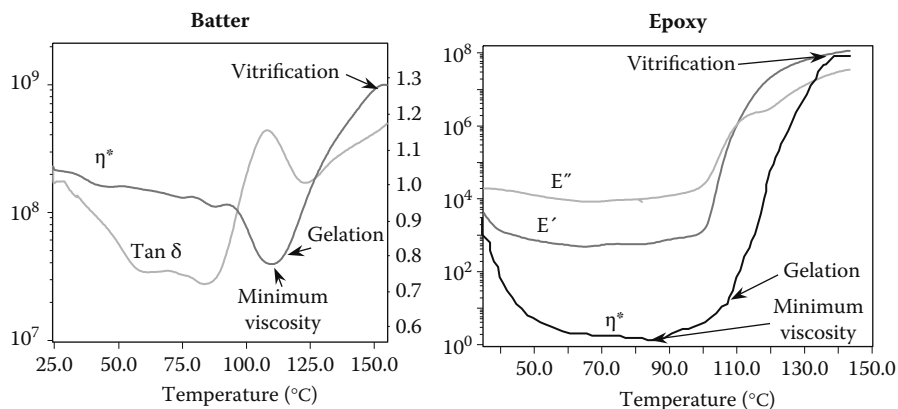


FIGURE 1.6 The curing of very different materials has similar requirements and problems. Note the similarities between a cake batter and an epoxy adhesive. Both show the same type of curing behavior, an initial decrease in viscosity to a minimum followed by a sharp rise to a plateau. Note that gelation is often taken as the E' – E'' crossover or where $\text{tan } \delta$ equals one. Other points of interest are labeled.

to resist deformation and the flexibility to not shatter under strain. It is important to note that beta and gamma transitions are too faint to be detected in the differential scanning calorimeter (DSC) or thermomechanical analyzer (TMA).²⁰ The DMA is much more sensitive than these techniques and can easily measure transitions not apparent in other thermal methods. This sensitivity allows the DMA to detect the T_g of highly crosslinked thermosets or of thin coatings. Recently, the use of a material pocket allows one to extend this sensitivity even to powders.²¹

If we look at a thermoset instead of a thermoplastic, we can follow the material through its cure by tracking either viscosity or modulus changes. This is done for everything from hot melt adhesives to epoxies to angel food cake batter (Figure 1.6). The curves show the same initial decrease in modulus and viscosity to a minimum, corresponding to the initial melting of the uncured material, followed by an increase in viscosity as the material is cured to a solid state. Figure 1.6a shows a cure cycle for an epoxy resin. From one scan, we can estimate the point of gelation (where the material is gelled), the minimum viscosity (how fluid it gets), and when it is stiff enough to bear its own weight.²² At the last point, we can free up the mold and finish curing in an oven. As we allow the sample to cool back to room temperature, notice that the modulus increases. We can even make a crude relative estimation of the activation energy (E_{act}) from the slope of the viscosity increase during curing.²³ If we want a more exact value for E_{act} , we can use isothermal runs (Figure 1.7) to get values closer to the accuracy of DSC.²⁴ Chapter 7 looks at these applications in detail.

Often the response of a material to the rate of strain is as important as the temperature response. Chapter 8 addresses the use of frequency scans in the DMA. This is one of the major applications of DMA for polymer melts, suspensions, and solutions and is normally studied with a torsional DMA. Similar to how DMA can be used to rapidly map the modulus of a material as a function of temperature, we can also use DMA to quickly look at the effect of shear rate or frequency on viscosity.

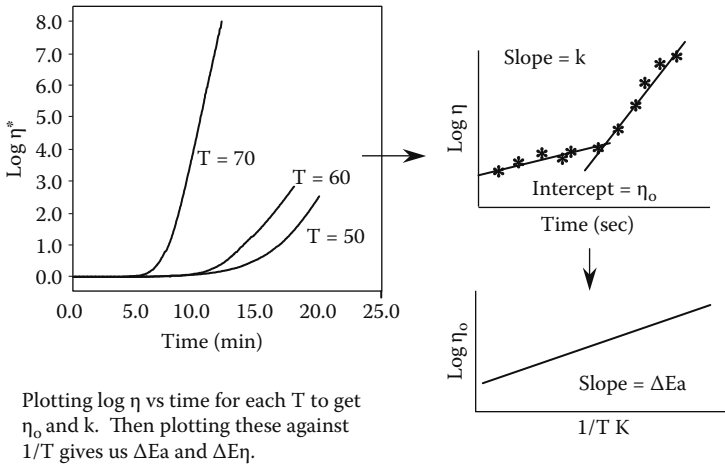


FIGURE 1.7 Isothermal runs allow the development of models for curing. Plotting the log of the measured viscosity, η^* , against time for each temperature gives the true initial viscosity, η_0 , and the rate constant, k . Then we obtain the two activation energies, ΔE_a and ΔE_η , by plotting the initial viscosities and rate constants against the inverse temperature ($1/T$). This approach is discussed in Chapter 7.

For example, a polymer melt can be scanned in a DMA for the effect of frequency on viscosity in less than 2 hours over a range of 0.01 Hz to 300 Hz. A capillary rheometer study for similar rates would take days. For a hot melt adhesive, we may need to see the low frequency modulus (for stickiness or tack) as well as the high frequency response (for peel resistance).²⁵ We need to keep the material fluid enough to fill the pores of the substrate without the elasticity getting so low the material pulls out of the pores too easily. By scanning across a range of frequencies (Figure 1.8) we can collect information about the elasticity and flow of the adhesive as E' and η^* at the temperature of interest.

The frequency behavior of materials can also give information on molecular structure. The crossover point between either E' and η^* or between E' and E'' can be related to the molecular weight²⁶ and the molecular weight distribution²⁷ by the Doi–Edwards theory. As a qualitative assessment of two or more samples, this crossover point allows a fast comparison of samples that may be difficult or impossible to dissolve in common solvents. In addition, the frequency scan at low frequency will level off to the zero-shear plateau (Figure 1.9). In this region, changes in frequency do not result in a change in viscosity because the rate of deformation is too low for the chains to respond. A similar effect, the infinite shear plateau, is found at very high frequencies. The zero-shear plateau viscosity can be directly related to molecular weight, above a critical molecular weight by

$$\eta = k(M^{3.4}) \quad (1.1)$$

where k is a material specific constant.²⁸ This method has been found to be as accurate as gel permeation chromatography (GPC) over a very wide range of molecular weights for the polyolefins.²⁹

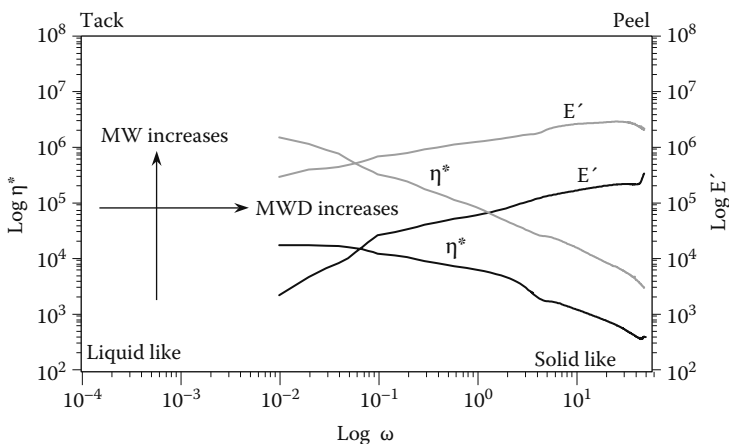
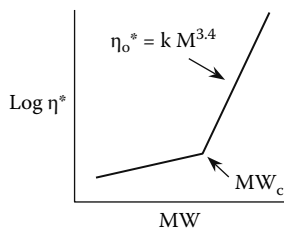
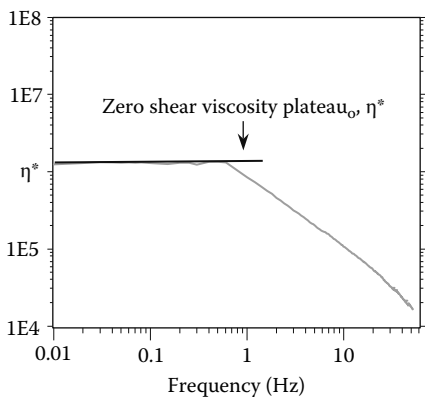


FIGURE 1.8 Frequency responses depend on molecular structure and can be used to probe the molecular weight and distribution of the material. Properties like relative tack (stickiness) and peel (resistance to removal) responses can also be studied. Modern DMAs, which can scan both temperature and frequency in the same experiment, make these studies more accessible to the nonspecialist.

Frequency data are often manipulated in various ways to extend the range of the analysis by exploiting the Boltzman superposition principle.³⁰ Master curves from superpositioning strain, frequency, time, degree of cure, humidity, and so forth allow one to estimate behavior outside the range of the instrument or of the experimenter's patience.³¹ Most familiar is the Williams–Landel–Ferry (WLF) model, which was



The zero shear plateau can be used to calculate the MW of a polymer if the material constant k is known and the MW is above a critical value. This MW_c is normally about 10,000 amu.

FIGURE 1.9 One of the main uses of frequency data is estimation of molecular weight. The zero-shear plateau can be used to calculate the molecular weight of a polymer by the above equation if the material constant k is known and the MW is above a critical value. This critical molecular weight, M_w , is typically about 10,000 amu.

developed for rubbers. Like all accelerated aging and predictive techniques, one needs to remember that this is a bit like forecasting the weather and care is required.

Recently, the testing of materials in nonstandard environments has become more common. For years, solvent contact, humidity levels, and UV exposures were all known to have effects on materials but testing could be tricky.³² Recent developments addressed in Chapter 9 have made it more accessible and a wealth of data on how materials act under real-world conditions is becoming available.

1.4 CREEP–RECOVERY TESTING

Finally, most DMAs on the market also allow creep-recovery testing. Creep is one of the most fundamental tests of material behavior and is directly applicable to a product's performance.³³ We discuss this in Chapter 3 as part of the review of basic principles as it is the basic way to study polymer relaxation. Creep–recovery testing is also a very powerful analytical tool. These experiments allow you to examine a material's response to constant load and its behavior on removal of that load. For example, how a cushion on a chair responds to the body weight of the occupant, how long it takes to recover, and how many times it can be sat on before it becomes permanently compressed can all be studied by creep–recovery testing. The creep experiment can also be used to collect data at very low frequencies³⁴ and the recovery experiment to get data at high frequencies by free oscillations,³⁵ extending the range of the instrument. This is discussed in Chapter 3, Section 3.3 and Chapter 4, Section 4.3, respectively. More important, creep–recovery testing allows you to gain insight into how a material will respond when kept at a constant load, like a plastic wheel on a caster.

Note that creep is not a dynamic test as a constant load is applied during the creep step and removed for the recovery step (Figure 1.10). Several approaches to quantifying the data can be used as shown in Figure 1.10³⁶ and will be discussed in Chapter 3. Comparing materials after multiple cycles can be used to magnify the differences between materials as well as to predict long-term performance

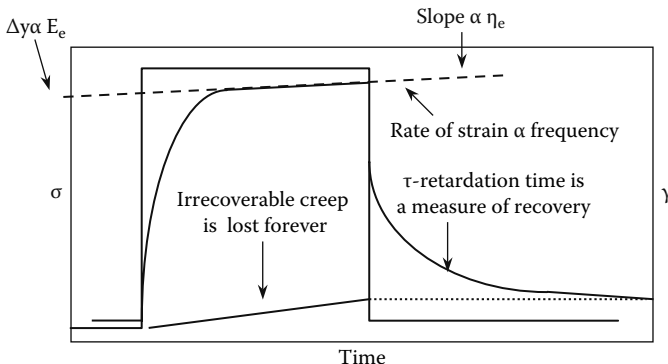


FIGURE 1.10 Creep–recovery experiments allow the determination of properties at equilibrium like modulus, E_e , and viscosity, η_e . These values allow the prediction of material behavior under conditions that mimic real-life applications.

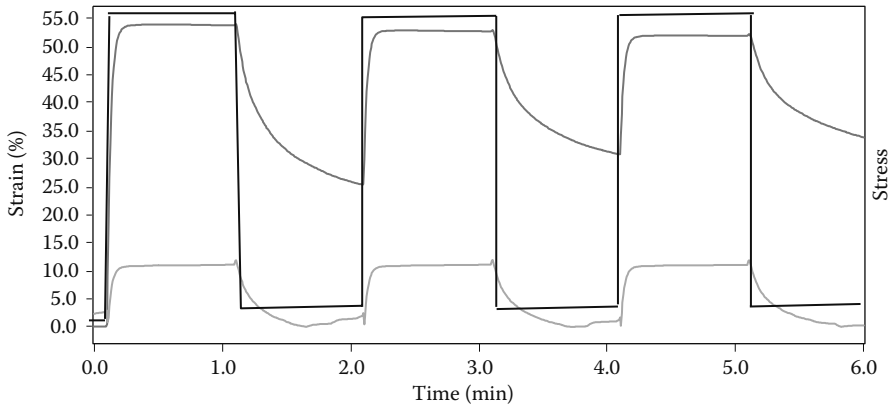


FIGURE 1.11 Various programs can be used to simulate the in-service stressing of a sample, including multiple cycles, temperature changes, and other environmental factors. Here the specimen is loaded three times and the changes in sample response over three cycles are significant. The relaxation time increases and percent recovery decreases. This could lead to poor performance if this product is used under repetitive applications of load.

(Figure 1.11). Repeated cycles of creep–recovery show how the product will wear in the real world and the changes over even three cycles can be dramatic. Other materials, like a human hair coated with commercial hair spray, may require testing for over a hundred cycles. Temperature programs can be applied to make the test more closely match what the material is actually exposed to in end use. This can also be done to accelerate aging in creep studies by using oxidative or reductive gases, UV exposure, or solvent leaching.³⁷

1.5 AGGRESSIVE ENVIRONMENTS

Any of these tests mentioned in the previous section can be done in more aggressive environmental conditions to match the operating environment of the samples. Examples include hydrogels tested in saline,³⁸ fibers in solutions,³⁹ and collagen in water.⁴⁰ UV light can be used to cure samples⁴¹ to mimic processing or operating conditions. A specialized example of environmental testing is shown in Figure 1.12, where the position control feature of a DMA is exploited to perform a specialized stress relaxation experiment called constant gauge length (CGL) testing. The response of the fibers is greatly affected by the solution in which it is tested. Similar tests in both dynamic and static modes are used in the medical, automotive, and cosmetic industries. The adaptability of DMA to match real-world conditions is yet another advantage of the technique. Controlled humidity can also be used to induce changes in a material's behavior⁴² similar to the way that frequency and light are. For example, in Figure 1.13 we see a sample of a piece of nylon under a controlled humidity ramp. On changing the humidity to higher levels at constant temperature, the material gives a response similar to what one sees with a temperature scan across glass transition. These types of

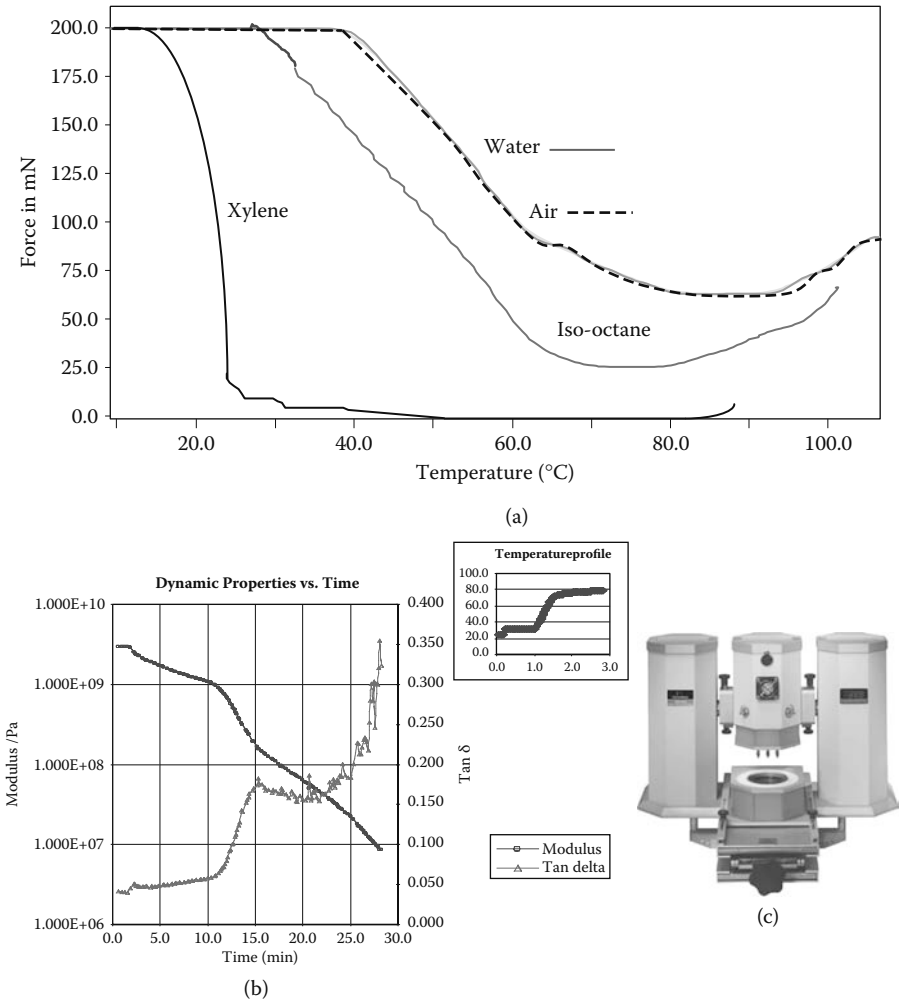


FIGURE 1.12 Testing in the presence of solvents allows one to evaluate a material under operating conditions. (a) Polypropylene fibers show very different responses when run in different solvents in a constant gauge length experiment. (b) The response of pasta in water shows the modulus change on cooking. (c) The PerkinElmer DMA 8000 with fluid bath for immersion studies.

experiments are discussed in Chapter 9. The DMA's ability to give insight into the molecular structure and to predict in-service performance makes it a necessary part of the modern thermal laboratory.

Finally we will very briefly look at putting all this together by deciding which test to run, how to validate the data we collect, and exploiting other techniques that complement the DMA. Several thermal, spectroscopic, and mechanical tests can be used to help interpret the data. A quick overview of these is given in Chapter 8, along with some guidelines on using DMA tests.

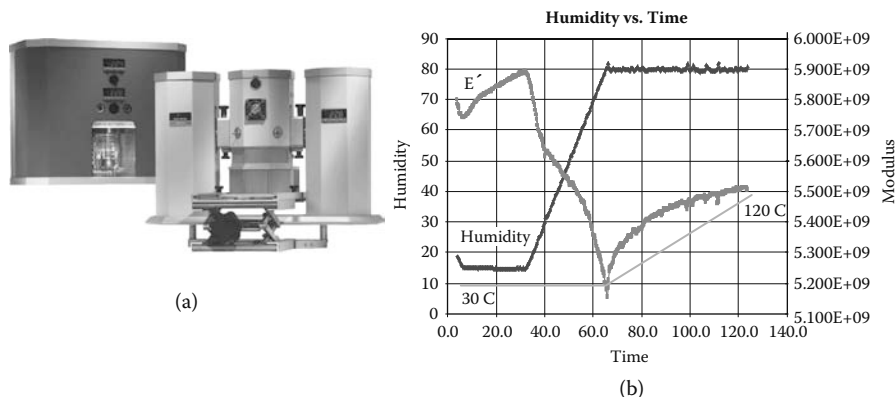


FIGURE 1.13 The effect of humidity on a material's properties is a serious concern in many materials from sugars and other food products to nylon and polymers to paper goods and coated materials. Interest in using DMA to measure these properties is growing. (a) A PerkinElmer DMA 8000 with its integrated humidity generator, used with permission of PerkinElmer LAS, Shelton, Connecticut. (b) The effect on a sample of nylon of changing the humidity level while holding the temperature constant. Used with the permission of Triton Technologies, Keyworth, UK.

NOTES

1. C. Macosko, *Rheology Principles, Measurements, and Applications*, VCH, New York, 1994.
2. J. H. Poyntang, Proc. Royal Society, Series A, 82, 546, 1909.
3. A. Kimball and D. Lovell, *Trans. Amer. Soc. Mech. Eng.*, 48, 479, 1926.
4. K. te Nijenhuis, *Rheology, Volume 1: Principles*, G. Astarita et al., Eds., Plenum Press, New York, 263, 1980.
5. M. L. Miller, *The Structure of Polymers*, Reinhold, New York, 1966.
6. J. Dealy, *Rheometers for Molten Plastics*, Van Nostrand Reinhold, New York, pp. 136–137, 234–236, 1992.
7. J. Ferry, *Viscoelastic Properties of Polymers*, 3rd ed., John Wiley and Sons, New York, 1980.
8. N. McCrum, G. Williams, and B. Read, *Anelastic and Dielectric Effects in Polymeric Solids*, Dover, New York, 1991. This is a reprint of the 1967 edition.
9. J. Gillham and J. Enns, *Trends Polym. Sci.*, 2, 406, 1994.
10. C. Macosko and J. Starita, *SPE Journal*, 27, 38, 1971.
11. T. Murayama, *Dynamic Mechanical Analysis of Polymeric Materials*, Elsevier, New York, 1977. This book is the ultimate reference on the Rheovibron.
12. B. E. Read and G. D. Dean, *The Determination of the Dynamic Properties of Polymers and Composites*, John Wiley and Sons, New York, 1978.
13. J. Duncan, Dynamic mechanical analysis, in *Principles and Applications of Thermal Analysis*, P. Gabbott, Ed., Blackwell Publishing, Oxford, 2008. K. Menard, Dynamic Mechanical Analysis, in *The Encyclopedia of Polymer Technology*, 3rd ed., Jacqueline Kroschwitz, Ed., John Wiley and Sons, New York, 2005. K. Menard, Dynamic mechanical thermal analysis, in *The Encyclopedia of Chemical Processing*, S. Lee, Ed., Marcel Dekker, 2005, p. 799. K. Menard, Thermomechanical and dynamic mechanical analysis, in *Handbook of Polymer Analysis*, H. Lobo and J. Bonilla, Eds., Marcel Dekker, New York, 2003.

14. S. Matsuoka, *Relaxation Phenomena in Polymers*, Hanser, New York, 1992.
15. W. Brostow and R. Corneliussen, Eds., *Failure of Plastics*, Hanser, New York, 1986.
16. N. McCrum, B. Williams, and G. Read, *Anelastic and Dielectric Effects in Polymeric Solids*, Dover, New York, 1991.
17. H. Barnes, J. Hutton, and K. Walters, *An Introduction to Rheology*, Elsevier, New York, 1989.
18. J. Dealy and K. Wissbrum, *Melt Rheology and Its Role in Plastics Processing*, Van Nostrand, New York, 1990.
19. This is admittedly a generalization of a very complex subject. B. Twombly, K. Fielder, R. Cassel, and W. Brennan, *NATAS Proc.*, 20, 28, 1991. D. Van Krevelen, *Properties of Polymers*, Elsevier, New York, 1972. R. Boyd, *Polymer*, 26, 323, 1123, 1985. N. McCrum, G. Williams, and B. Read, *Anelastic and Dielectric Effects in Polymeric Solids*, Dover, New York, 1991.
20. R. Cassel and B. Twombly, in *Material Characterization by Thermomechanical Analysis*, M. Neag, Ed., ASTM, Philadelphia, STP 1136, 108, 1991.
21. P. G. Royall, C.-Y. Huang, S.-W. Jai Tang, J. Duncan, G. Van-de-Velde, M. B. Brown, *Int. J. Pharmaceutics*, 301, 181–191, 2005.
22. S. Crane and B. Twombly, *NATAS Proc.*, 20, 386, 1991.
23. K. Hollands and I. Kalnin, *Adv. Chem. Ser.*, 92, 80, 1970.
24. M. Roller, *Polym. Eng. Sci.*, 15(6), 406, 1975.
25. C. Rohm, Proc. 1988 Hot Melt Symp., 77, 1988.
26. R. Rahalkar and H. Tang, *Rubber Chem. Tech.*, 61(5), 812, 1988. W. Tuminello, *Polym. Eng. Sci.*, 26(19), 1339, 1986.
27. R. Rahalkar, *Rheologica Acta*, 28, 166, 1989. W. Tuminello, *Polym. Eng. Sci.*, 26(19), 1339, 1986.
28. L. Sperling, *Introduction to Physical Polymer Science*, 2nd ed., Academic Press, New York, 1993.
29. J. Sosa and J. Bonilla, private communication. B. Shah and R. Darby, *Polym. Eng. Sci.*, 22(1), 53, 1982.
30. J. Ferry, *Viscoelastic Properties of Polymers*, John Wiley, New York, 1980.
31. A. Goldman, *Prediction of the Properties of Polymeric and Composite Materials*, ACS, Washington, 1994. W. Brostow and R. Corneliussen, Eds., *Failure of Plastics*, Hanser, New York, 1986.
32. G. Ehrenstein, G. Riedel, and P. Trawiel, *Thermal Analysis of Plastics*, Hanser, Cincinnati, OH, 2004.
33. L. Nielsen, *Mechanical Properties of Polymers*, Reinhold, New York, 1965, ch. 4.
34. L. Nielsen, *Mechanical Properties of Polymers and Composites*, Vol. 1, Marcel Dekker, New York, 1974.
35. U. Zolzer and H. Eicke, *Rheologica Acta*, 32, 104, 1993.
36. L. Nielsen, *Mechanical Properties of Polymers*, Vol. 2, Reinhold, New York, 1965. L. Nielsen, *Polymer Rheology*, Marcel Dekker, New York, 1977.
37. Y. Goldman, *Predication of Polymer Properties and Performance*, American Chemical Society, Washington D.C., 1994.
38. Q. Bao, *NATAS Proc.*, 21, 606, 1992. J. Enns, *NATAS Proc.*, 23, 606, 1994.
39. C. Daley and K. Menard, *SPE Tech. Pap.*, 39, 1412, 1994. C. Daley and K. Menard, *NATAS Notes*, 26(2), 56, 1994.
40. B. Twombly, R. Cassel, and A. Miller, *NATAS Proc.*, 23, 288, 1994.
41. J. Enns, unpublished results.
42. I. Yakimets, N. Wellner, A. C. Smith, R. H. Wilson, I. Farhat, J. Mitchell, Effect of water content on the fracture behaviour of hydroxypropyl cellulose films studied by the essential work of fracture method, *Mech. Mater.*, in press.

2 Basic Rheological Concepts

Stress, Strain, and Flow

The term *rheology* seems to generate a slight sense of terror in the average worker in materials. Rheology is defined as the study of the deformation and flow of materials. The term was coined by Bingham to describe the work being done in modeling how materials behave under heat and force. Bingham thought that chemists would be frightened away by the term *continuum mechanics*,¹ which was the name of the branch of physics concerned with these properties. This renaming was one of science's less successful marketing ploys, as most chemists think rheology is something only done by engineers with degrees in non-Newtonian fluid mechanics and most likely in dark rooms.

More seriously, rheology does have an undeserved reputation of requiring a large degree of mathematical sophistication. Parts of it do require a familiarity with mathematics. However, many of the principles and techniques are understandable to anyone who survived physical chemistry. Enough understanding of its principles to use a dynamic mechanical analyzer and successfully interpret the results doesn't need even that much. For those who find they would like to see more of the field, Shaw and MacKnight have rewritten a classic introduction to rheology² and Macosko has published the text of his short course offered annually at the University of Minnesota.³ Both are very readable introductions. We are now going to take a nonmathematical look at the basic principles of rheology so we have a common terminology to discuss dynamic mechanical analysis (DMA). This discussion is an elaboration of a lecture given as a short course by the author at various meetings of the International Conference on Polymer Characterization (POLYCHAR) called "Rheology for the Mathematically Insecure."

2.1 FORCE, STRESS, AND DEFORMATION

If you apply a force to a sample, you get a deformation of the sample. The force, however, is an inexact way of measuring the cause of the distortion. Now we know the force exerted by a probe equals the mass of the probe (m) times its acceleration (a). This is given as

$$F = m \times a \quad (2.1)$$

However force doesn't give the true picture, or rather it gives an incomplete picture. For example, which would you rather catch? A 25 pound medicine ball or a

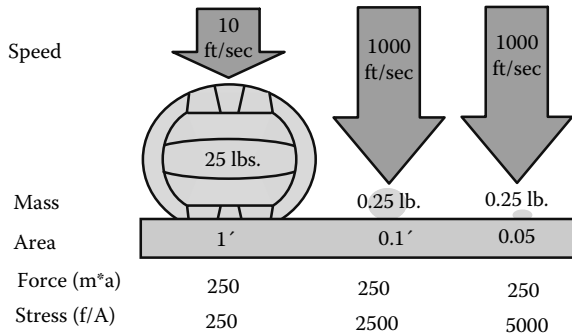


FIGURE 2.1 Stress is force divided by area. While the force is a constant at 250 ft-lb, the stress changes greatly as the area changes.

hardball with 250 ft-lbs of force? The above equation tells the force exerted by a 25 pound medicine ball moving at 10 feet per second is equal to the force exerted by a hardball (0.25 pounds) at 1000 feet per second! We expect that the impact from the hardball is going to do more damage. This damage is called a deformation.

So what we really need to include is a measure of the area of impact. The product of a force (F) across an area (A) is a stress, σ . The stress is normally given in either psi or pascals and can be calculated for the physical under study. If we assume the medicine ball has an area of impact equivalent to a 1 foot diameter, while the superball's is 1 inch, we can calculate the stress by

$$\sigma = F \times A \quad (2.2)$$

Figure 2.1 gives a visual interpretation of the results. Despite the forces being equal at 250 ft-lbs, the stress seen by the sample varies from 250 psi to 2000 psi. We are making an assumption about the contact area here to simplify the math. In real life, we would measure the diameter of the impact, assuming it was round, and calculate the area of that circle. Here I am just trying to show how stress affects strain and we are going to skip that step. If we program a test in forces and our samples are not exactly the same size, the results will differ because the stresses are different. This even occurs in the linear viscoelastic region⁴ though in the nonlinear region the effects are magnified. While stress gives a more realistic view of the material environment, in real life most people choose to operate their instruments in forces or in deformation. This allows you to track your instruments' limits more easily than having to remember the maximum stress or strain in each geometry would be. Stress is what is affecting the material, not force, and that means with proper sample preparation, the force limits of the instrument can be worked around.

The applied stress causes a deformation of the material and this deformation is called a strain, γ . A mnemonic for the difference is to remember that if your boss is under a lot of stress, his personality changes are a strain. Strain is calculated as

$$\gamma = \Delta Y/Y \quad (2.3)$$

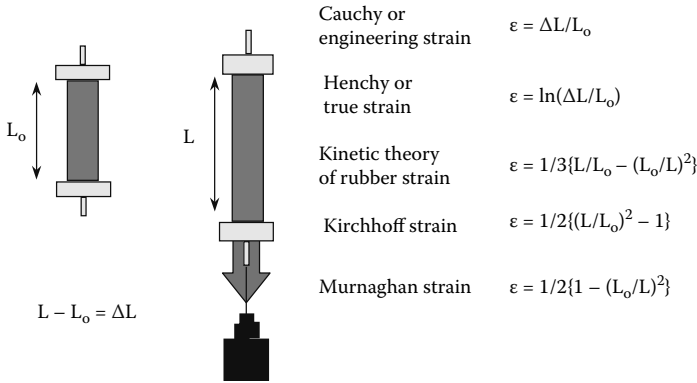


FIGURE 2.2 The result of applying a stress is a strain. There are a lot of types of strain developed for specific problems.

where Y is the original sample dimension and ΔY is the change in that dimension under stress. This is often multiplied by 100 and expressed as percent strain. The application of a stress to a sample and recording the resultant strain is a commonly used technique. Going back to the balls in the earlier example, the different stresses can cause very different strains in the material, be it a sheet of plastic or your catching hand. Figure 2.2 shows how some strains are calculated.

2.2 APPLYING THE STRESS

How the stress is applied can also affect the deformation of the material. Without considering yet how changes in the material’s molecular structure or processing enter the picture, we can see different behavior depending on how a static stress⁵ is applied and what mode of deformation is used. Figure 2.3 summarizes the main ways of applying a static stress. If we consider the basic stress–strain experiment from materials testing, we increase the applied stress over time at a constant stress rate ($\dot{\sigma}$).⁶ As shown in

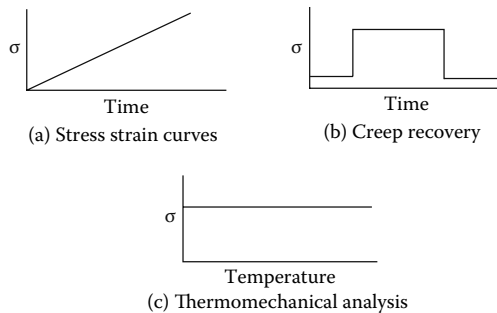


FIGURE 2.3 Applications of a static stress to a sample. The three most common cases are shown plotted against time or temperature. (a) Shows a stress-strain curve where stress is plotted against strain; (b) shows a creep recovery curve with the stepwise application of a stress; and (c) shows a TMA run where a constant stress is applied while temperature is varied.

Figure 2.3a, we can track the change in strain as a function of stress. This is done at constant temperature and generates the stress–strain curve. Classically, this experiment was done by a strain-controlled instrument, where one deforms the sample at a constant strain rate, $\dot{\gamma}$, and measures the stress with a load cell resulting a stress (y-axis)–strain (x-axis) curve. Alternatively, we could apply a constant stress as fast as possible and watch the material deform under that load. This is the classical engineering creep experiment. If we also watch what happens when that stress is removed, we have the creep–recovery experiment (Figure 2.3b). These experiments complement DMA and are discussed in Chapter 3. Conversely, in the stress relaxation experiment a set strain is applied and the stress decrease over time is measured. Finally, we could apply a constant force or stress and vary the temperature while watching the material change (Figure 2.3c). This is a TMA (thermomechanical analysis) experiment. Thermomechanical analysis is often used to determine the glass transition (T_g) in flexure by heating a sample under a constant load. The heat distortion test used in the polymer industry is a form of this. Figure 2.4 shows the strain response for these types of applied stresses.

While we are discussing applying a stress to generate a strain, you can also look at it as if an applied strain has an associated stress. This approach was often used by older controlled deformation instruments, for example, most mechanical testers used for traditional stress–strain curves and failure testing. The analyzers worked by using a mechanical method, like a screw driver, to apply a set rate of deformation to a sample and measured the resulting stress with a load cell. The differences between stress control and strain control are still being discussed and it has been suggested that stress control, because it gives the critical stress, is more useful.⁷ We will assume for most of this discussion that the differences are minimal.

The stress can also be applied in different orientations as shown in Figure 2.5. These different geometries give different appearing stress–strain curves and, even in an isotropic homogeneous material, give different results. Flexural, compressive, extensile, shear, and bulk moduli are not the same although some of these can be interconverted as discussed in Section 2.3. For example, in compression, a limiting case is reached where the material becomes practically incompressible. This limiting

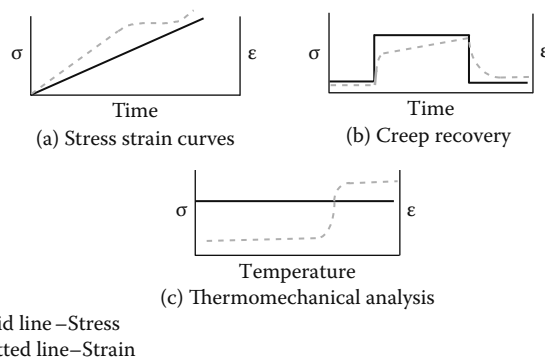
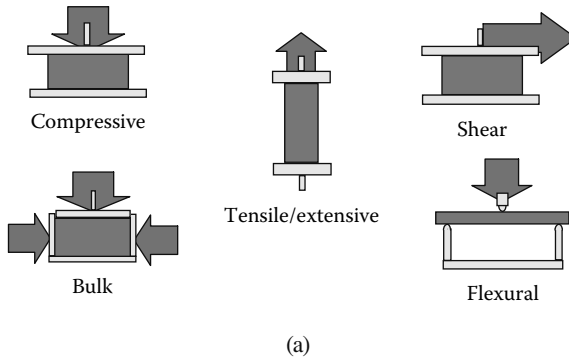
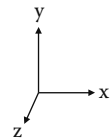


FIGURE 2.4 Strains resulting from static stress testing. For (a) the stress is applied at a constant rate while in (b) a stepwise application of stress gives the classical shark fin strain curve. In (c) the probe position rather than strain is normally reported.



For rectangular specimens, force is applied on the y axis.
 For dual cantilever and 3 point bending, x is the length from the center point to one end.

Geometry	B (shape factor)
Single cantilever	$z(y/x)^3$
Dual cantilever	$2z(y/x)^3$
Compression or tension	xz/y
3 point bending	$z/2(y/x)^3$
Shear	$2(z/y/x)$



(b)

FIGURE 2.5 (a) Geometric arrangements or methods of applying stress are shown. All of the bottom fixtures are stationary. Bulk is 3-D compression, where sides are restrained from moving. (b) Geometry factors used with various shapes.

modulus is not seen in extension, where the material may neck and deform at high strains. In shear, the development of forces or deformation normal or orthogonal to the applied force may occur.

The relation of a material load to its deformation can be considered stiffness. Notice I said load to deformation, not stress to strain. This is what a DMA or TMA actually measures and the calculations above allow us to normalize the response. You can look at stiffness as the response of the sample to a load. Stiffness is a way of relating stress to strain with including the geometry factor. So if we apply 100 pounds to a maple board 4 feet by 1 foot by 1 inch, we'll see a stiffness of some value. That stiffness may be the same as measured with the same load on a piece of steel plate 4 feet by 1 foot by 1/8 inch. A pine board, a weaker wood, might have the same stiffness when it is 2 inches thick. So while the stiffness would be the same, something is different. If we apply a geometry factor to the stiffness, we can obtain a modulus, which can be viewed as the stiffness adjusted for sample size or mathematically

$$E = bS \tag{2.4}$$

where b is the geometry factor to normalize for sample size. These were given in Figure 2.5b and are the same used in the earlier discussion of stress and strain. Having a modulus to characterize the material allows us to define one limit of material response. This also turns out to be a very practical approach as it allows us to decide how thick a bookshelf would need to be to hold all the rheology books one collects. Some instruments actually calculate their values from a measured stiffness, for example, the PerkinElmer DMA 8000.

2.3 HOOKE'S LAW: DEFINING THE ELASTIC RESPONSE

Material properties can be conceived of as being between two limiting extremes. The limits of elastic or Hookean behavior⁸ and viscous or Newtonian behavior can be looked at as brackets on the region of DMA testing. In traditional stress–strain curves, we are concerned mainly with the elastic response of a material. This behavior can be described as what one sees when you stress a piece of tempered steel to a small degree of strain. The model we use to describe this behavior is the spring and Hooke's law relates the stress to the strain of a spring by a constant, k . This is graphically shown in Figure 2.6.

Hooke's law states that the deformation or strain of a spring is linearly related to the force or stress applied by a constant specific to the spring. Mathematically this becomes

$$\sigma = k \times \gamma \quad (2.5)$$

where k is the spring constant. As the spring constant increases, the material becomes stiffer and the slope of the stress–strain curve increases. As the initial slope is also Young's modulus, the modulus would also increase. Modulus, then, is a measure of

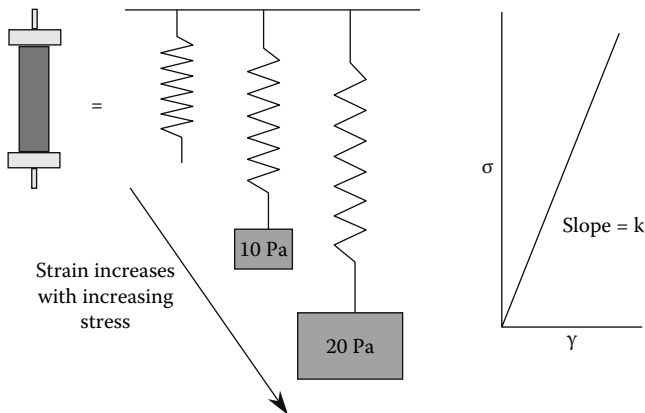


FIGURE 2.6 Hooke's law and stress–strain curves. Elastic materials show a linear and reversible deformation on applying stress (within the linear region). The slope, k , is the modulus, a measure of stiffness, for the material. For a spring, k would be the spring constant.

a material's stiffness and is defined as the ratio of stress to strain. For an extension system, we can then write the modulus, E , as

$$E = d\sigma/d\varepsilon \quad (2.6)$$

If the test is done in shear, the modulus is denoted by G and in bulk as B . If we then know the Poisson's ratio, ν , which is a measure of how the material volume changes with deformation when pulled in extension, we can also convert one modulus into another (assuming the material is isotropic) by

$$E = 2G(1 - \nu) = 3B(1 - 2\nu) \quad (2.7)$$

For a purely elastic material, the inverse of modulus is the compliance, J . The compliance is a measure of a material's willingness to yield. The relationship of

$$E = 1/J \quad (2.8)$$

is only true for purely elastic materials as it does not address viscous or viscoelastic contributions.

Ideally elastic materials give a linear response when the modulus is independent of load and of loading rate. Unfortunately, as we know, most materials are not ideal. If we look at a polymeric material in extension, we see that the stress–strain curve has some curvature to it. This becomes more pronounced as the stress increases and the material deforms. In extension, the curve assumes a specific shape where the linear region is followed by a nonlinear region (Figure 2.7). This is caused by necking of the specimen and its subsequent drawing out. In some cases, the curvature makes it difficult to determine the Young's modulus.⁹ In DMA tests, where the strains will be kept small, the response in the glassy region is normally strain-independent.

Figure 2.8a also shows the analysis of a stress–strain curve. Usually, we are concerned with the stiffness of the material, which is obtained as the Young's modulus from the initial slope. Most of the time, this value is what is of interest in stress–strain studies. Figure 2.8b shows some real data, for single- and two-layer films. In addition, we would like to know how much stress is needed to deform the material.¹⁰ This is the yield point. At some load, the material will fail (break) and this is known as the ultimate strength. It should be noted that this failure at the ultimate strength

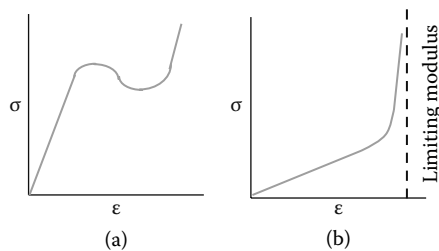


FIGURE 2.7 The stress–strain curves vary depending on the geometry used for the test. Stress–strain curves for (a) tensile and (b) compressive.

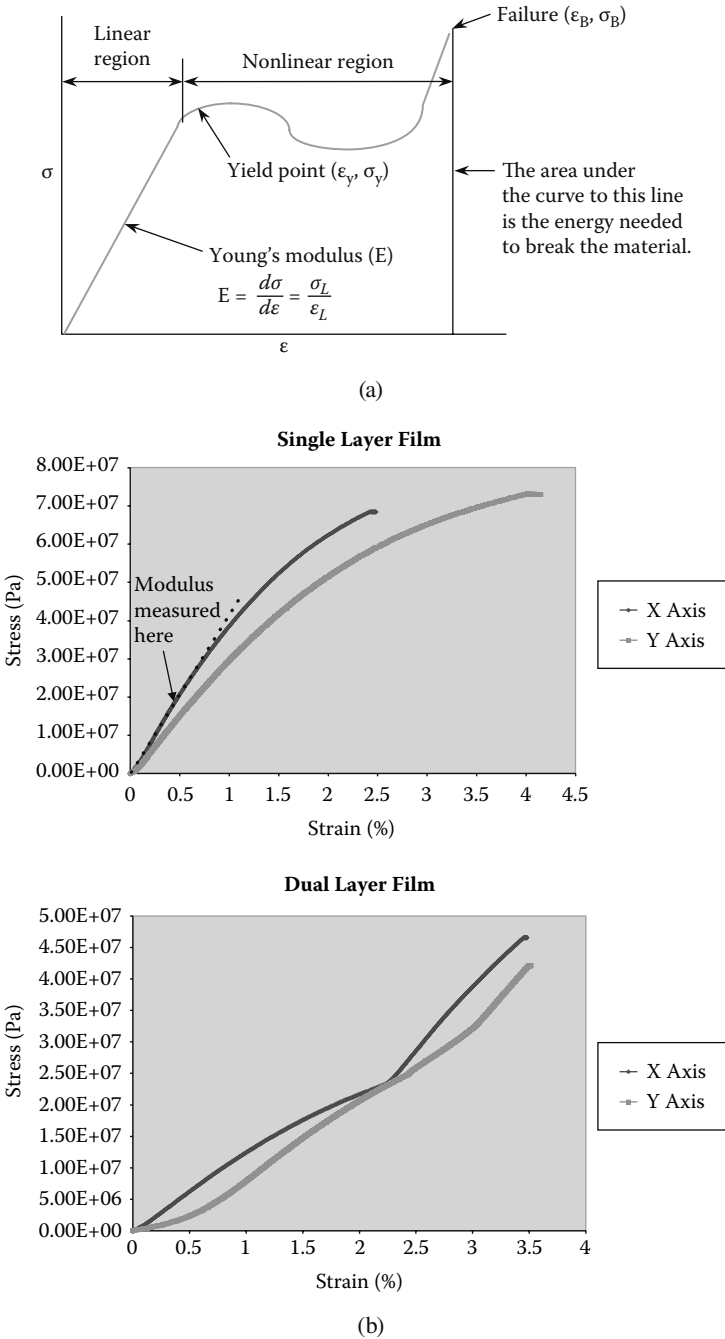


FIGURE 2.8 (a) Analysis of a typical stress–strain curve in extension. This is one of the most basic and most common tests done on solid materials. (b) A real-world example of single and dual layer films collected by BC Tan and used with the permission of PerkinElmer LAS.

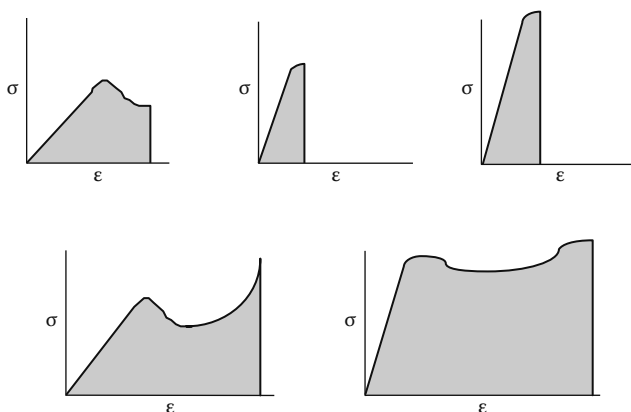


FIGURE 2.9 Stress–strain curves in extension for various types of materials with different mixtures of strength and toughness. The area under the curve is often integrated to obtain the energy needed to break the sample and used as an indicator of toughness of the material.

follows massive deformation of the sample. The area under the curve is proportional to the energy needed to break the sample. The shape of this curve and its area tells us about whether the polymer is tough or brittle or weak or strong. These combinations are shown in Figure 2.9. Interestingly, as the testing temperature is increased, a polymer's response moves through some or all of these curves (Figure 2.10a). This change in response with temperature leads to the need to map modulus as a function of temperature (Figure 2.10b) and represents another advantage of DMA over isothermal stress–strain curves. Obviously, we need to explain the curvature seen in what Hooke's law says should be a straight line. We will look at that in Section 2.5. However before we discuss that, let's consider some experimental concerns with the sample itself.

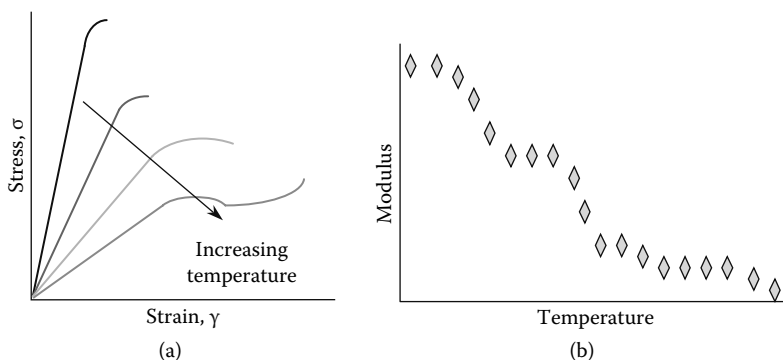


FIGURE 2.10 (a) Stress–strain curves change as the testing temperature increases. As a polymer is heated, it becomes less brittle and more ductile. (b) These data can be graphically displayed as a plot of the modulus versus temperature.

2.4 GEOMETRY, SAMPLE SHAPE, AND ASPECT RATIO

We have been considering stress, strain and modulus, all properties where the sample size was taken into consideration. This tends to, in practice, often get forgotten. For any sample we discuss, modulus values are dependent on the accuracy of the measurement of not only the deformation of the sample, but also by the measurement of the sample itself. A small error in a sample measurement can result in a significant change in the modulus value. Figure 2.11 shows the change that results from small mismeasurements of the sample. This drawing is based on a real problem we saw when a die was cut to the English system equivalent of a metric die by a machine shop. Use of the new die caused a shift in modulus values. Since everyone assumed both were the same diameter, several days of production were lost until someone actually measured the sample size. Corrected for the new diameter, the moduli now matched. Similarly, small changes in a three-point bending bar shift the modulus, too. This geometry is less sensitive to changes in certain directions and therefore is a bit more “error-tolerant.” If we want to measure a modulus, we need precise dimensions for the sample.

We actually need more than that. In all geometries, the ratio of sample length to width to thickness needs to be controlled. As we apply a load or deformation to a sample, we also generate stress by the clamping mechanism, the way the sample is loaded, how the sample changes under the load, and so forth. For example, think of a dual cantilever specimen, where a beam is clamped at three points. Not only do we have tension on one side of the beam and compression on the other, but we can see shear and compression stresses at the clamping points. All of these generate errors in the modulus. One way to handle these is to keep the aspect ratio of the materials the same. Aspect ratio¹¹ is defined as the height divided by the diameter for cylinders, or the length divided by the thickness for cubic beams, and for rectangular beams, the length divided by the crosssection area. In the latter case, a proportion is often given. For example, for a three-point bending or flexural test, Duncan gives an aspect ratio of 5:2:1 (10 mm long to 4 mm wide to 2 mm thick).¹² ASTM methods will often call out aspect ratios as well as standard sample sizes for mechanical tests. This can be a span–depth ratio like the 16:1 for flexure tests in ASTM D-790, where a 10% overhang on each end of the fixture is also recommended. A European aerospace

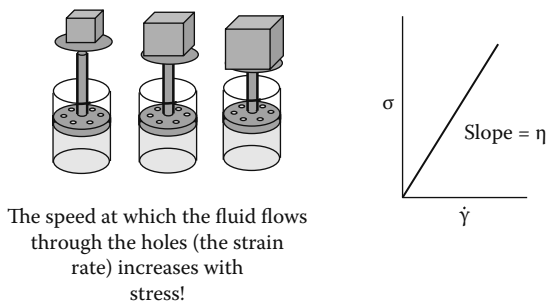


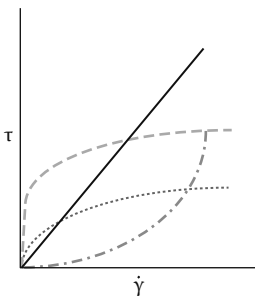
FIGURE 2.11 Newton’s law and dashpot. Flow is dependent of the rate of shear and there is no recovery seen. A dashpot, examples of which include a car’s shock absorber or a French press coffee pot, acts as an example of flow or viscous response.

specification asked for samples to have a span depth ratio of 20, so samples must be 20 times as long as the thickness of an 8-ply laminate (~2 mm). So a 40 mm free length is required and the total sample should be 48 mm long. While this all may seem a bit persnickety, a lot of the literature is devoted to how aspect ratio affects modulus and neglecting it leads to erroneous results.¹³ Not surprisingly, it's probably the most common questions that I get called about.

2.5 LIQUID-LIKE FLOW OR THE VISCOUS LIMIT

So assuming we have a decent specimen and are running our experiment under reasonable conditions, why do we still see curvature in the stress–strain curves? To explain the curvature in the stress–strain curves of polymers, we need to look at the other end of the material behavior continuum. The other limiting extreme is liquid-like flow, which is also called the Newtonian model. We will diverge a bit here, to talk about the behavior of materials as they flow under applied force and temperature. We will begin to discuss the effect of the rate of strain on a material. This takes us into the area of viscosity testing, where the flow properties of fuel oils, lotions, paints, suspensions, lubricants, cooking oils, emulsions, and so forth are studied.¹⁴ Viscosity was originally defined by Isaac Newton back in 1687.¹⁵ A simple way to imagine the behavior of a Newtonian fluid is by using the dashpot as a model. An example of a dashpot would be a car's shock absorber or a French press coffee pot. These have a plunger header, which is pierced with small holes through which the fluid is forced. Figure 2.12 shows the response of the dashpot model. Note that as the stress is applied, the material responds by slowly deforming. As the rate of the shear is increased, the rate of flow of the material also increases. For a Newtonian fluid, the stress–strain rate curve is a straight line, which can be described by the following equation

$$\sigma = \eta \dot{\gamma} = \eta \frac{\partial \gamma}{\partial t} \quad (2.9)$$



- Newtonian behavior is linear and the viscosity is independent of rate.
- Pseudoplastic (.....) fluids get thinner as shear increases.
- Dilatant fluids (- · - · -) increase their viscosity as shear rates increase.
- Plastic fluids (-----) have a yield point with pseudoplastic behavior.
- Thixotropic and rheopectic fluids (not shown) exhibit viscosity-time nonlinear behavior. For example, the former shear thin and then reform its gel structure.

FIGURE 2.12 Non-Newtonian behavior in solutions. The major departures from Newtonian behavior are shown.

where stress is related to shear rate by the viscosity. This linear relationship is analogous to the stress–strain relation. While many oils and liquids are Newtonian fluids, materials like polymers, food products, suspensions, and slurries are not.

The study of material flow is one of the largest areas of interest to rheologists, materials scientists, chemists, and food scientists. Commonly, fluid properties for many Newtonian or near-Newtonian fluids are studied by techniques like viscosity tubes, continuous shear rheometer, and so forth. In many industries, the glass viscometer or viscosity tube, shown in Figure 2.13a, is the standard method as it is easy and adaptable to automation. It works on the principle of capillary rheometry, measuring the flow rate of a material through a precisely sized small tube with a large aspect ratio (length to diameter). The speed of which the material moves through the tube is measured as volume per time and then the viscosity calculated. Values for viscosity from fractions of a centistokes (cSt) to a few hundred Stokes can be measured, and stress values are about 1 to 1000 Pa. In automated instruments, like shown in Figure 2.13b, Malkin claims errors can be as small as .01%.¹⁶

Since many materials are non-Newtonian, a lot of work has been done in this area. Non-Newtonian materials can be classified in several ways, depending on how they deviate from ideal behavior. These deviations are shown in Figure 2.14. The most common deviation is shear thinning. Almost all polymer melts are of this type. Shear thickening behavior is rare in polymer systems but often seen in suspensions.

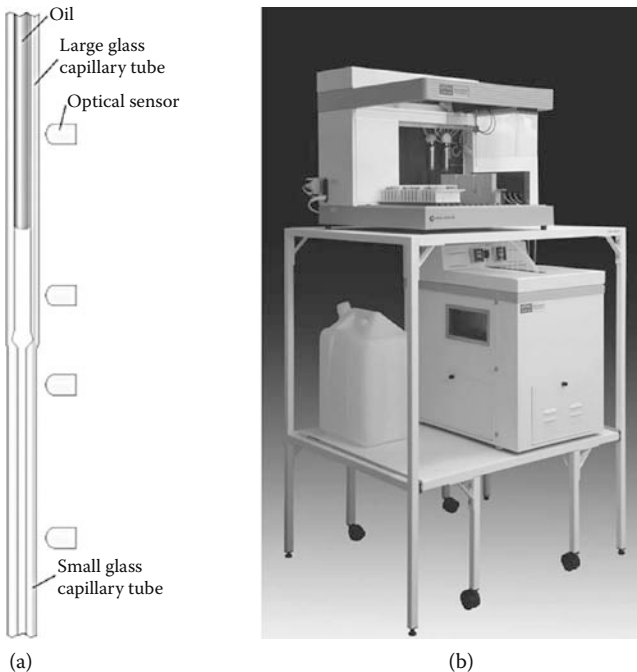


FIGURE 2.13 Viscometry. (a) A glass viscometry tube used for measuring Newtonian fluids. This version uses optical sensors and is a patented system designed for automate measurement. (b) The qVISC 4320, an automated system using glass viscometry tubes, sold by PerkinElmer LAS (used with permission).

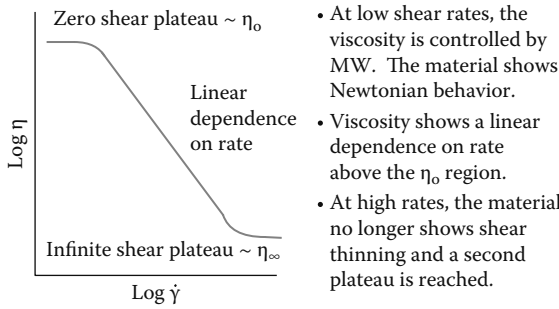


FIGURE 2.14 A polymer melt under various shear rates. Note Newtonian behavior is seen at very high and very low shear rates or frequencies. This is shown as a log–log–log plot as is normally done by commercial thermal analysis software. Better ways of handling the data are now available. For example, the Carreau model described in Armstrong et al.¹⁴ can be fitted using a regression software package like PolyMath™ or Mathematica™.

Yield stress behavior is also observed in suspensions and slurries. Let’s just consider a polymer melt as shown in Figure 2.15 under a shearing force. Initially, a plateau region is seen at very low shear rates or frequency. This region is also called the zero-shear plateau. As the frequency (rate of shear) increases, the material becomes nonlinear and flows more. This continues until the frequency reaches a region where increases in shear rate no longer cause increased flow. This infinite shear plateau occurs at very high frequencies.

Wide ranges of material properties can be measured by both capillary rheometers and continuous shear rheometers. Capillary rheometers are commonly used on polymers for quality control and can be as simple as a melt indexer.¹⁷ On the low end, we can immerse a spinning disk into a solution and measure the resistance to the spin. This is commonly done for paints, coatings, food products, and cosmetics. We can also use a parallel plate or cone-and-plate geometry in a laboratory instrument. Most DMAs designed for shear testing can also run these kinds of tests. Figure 2.16a

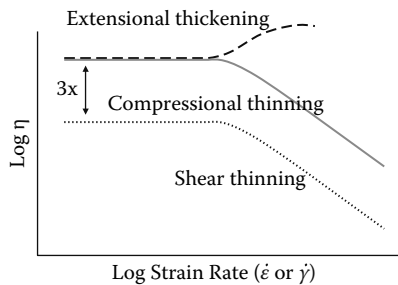


FIGURE 2.15 Shear, compressive, and extensional flows. While both compressive and shear cause an apparent thinning of the material, extensional flow causes a thickening. Note also that the modulus difference between shear and compression can be related as $1/3 E = G$ for cases when Poisson’s ratio, ν , is equal to 0.5.

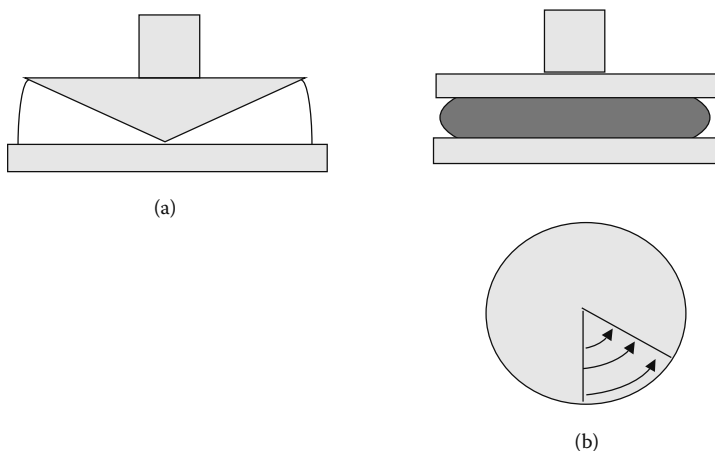


FIGURE 2.16 Cone and plate rheometers. (a) Cone and plate arrangement from a shear rheometer showing the gap and cone. The cone angle and gap are selected to generate a more even stress field across the sample. (b) A parallel plate arrangement means material at the center barely moves while edges move more, generating a greater stress in the material. The angle of a cone and plate corrects this to some extent.

shows a cone and plate arrangement. Cone and plate is used instead of parallel plate to help maintain a more constant rate of shear across the sample (Figure 2.16b). Rohn,¹⁸ Malkin,¹⁹ and Dealy²⁰ discuss these kind of tests in greater details.

Like with solids, the behavior you see in a fluid is dependent on how you strain the material. In shear and compression, we see a thinning or reduction in viscosity (Figure 2.15). If the melt is tested in extension, a thickening or increase in the viscosity of the polymer is observed. These trends are also seen in solid polymers. Suspension also exhibits similar effects. Both a polymer melt and a polymeric solid under frequency scans show a low frequency Newtonian region before the shear thinning region. When polymers are tested by varying the shear rate, we run into four problems that have been the drivers for much of the research in rheology and are what complicate the life of polymer chemists.

These four problems are defined by Macosko²¹ as: (1) shear thinning of polymers, (2) normal forces under shear, (3) time dependence of materials, and (4) extensional thickening of melts. The first two can be solved by considering Hooke's law and Newton's law in their three-dimensional forms.²² Time dependence can be addressed by the linear viscoelastic theory. Extensional thickening is more difficult and the reader is referred to one of several references on rheology if more information is required.²³

2.6 ANOTHER LOOK AT STRESS–STRAIN CURVES

Before our discussion of flow, we were looking at a stress–strain curve. The curves of real polymeric materials are not perfectly linear and a rate dependence is seen. Testing a Hookean material under different rates of loading shouldn't change the modulus. Yet, both curvature in the stress–strain curves and rate dependence are common enough in polymers for commercial computer programs to be sold that

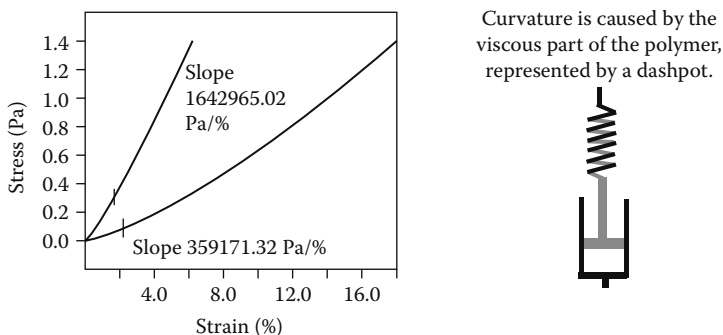


FIGURE 2.17 The Maxwell model, an early attempt to explain material behavior, is a dashpot and a spring in parallel. The dashpot introduces curvature into the graph, representing the ability of the material to flow.

address these issues. Adding the Newtonian element to the Hookean spring gives a method of introducing flow into how a polymer responds to an increasing load (Figure 2.17). The curvature can be viewed as a function of the dashpot, where the material slips irreversibly. As the amount of curvature increases, the increased curvature indicates the amount of liquid-like character in the material has increased. This is not to suggest that the Maxwell model, the parallel arrangement of a spring and a dashpot seen in Figure 2.17, is currently used to model a stress–strain curve. Better approaches exist. However, the introduction of curvature to the stress–strain curve comes from the viscoelastic nature of real polymers.

Several trends in polymer behavior are summarized in Figure 2.18.²⁴ Molecular weight and molecular weight distribution have, as expected, significant effects on the stress–strain curve. Above a critical molecular weight (M_c), which is where the material begins exhibiting polymer-like properties, mechanical properties increase with molecular weight. The dependence appears to correlate best with the weight average molecular in the GPC. There is also a T_g value above which the corresponding

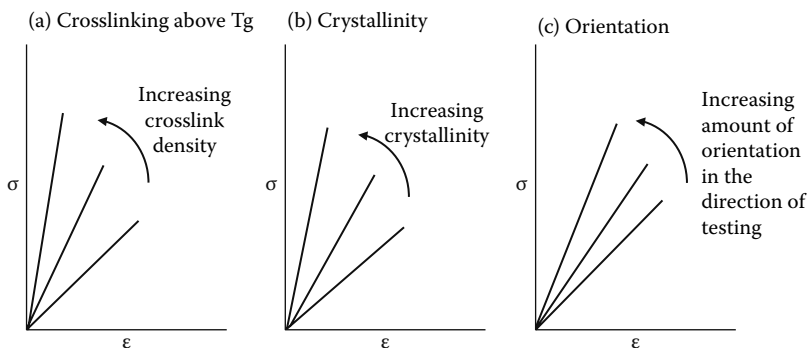


FIGURE 2.18 Effects of structural changes on stress–strain curves are shown for (a) crosslinking, (b) crystallinity, and (c) orientation. As the structure of the polymer changes, certain changes are expected in the stress–strain curves.

increases in modulus are so small as to not be worth the cost of production. Distribution is important as the width of the distributions often has significant effects on the mechanical properties.

In crystalline polymers, the degree of crystallinity may be more important than the molecular weight above the M_c . As crystallinity increases, both modulus and yield point increase and elongation at failure decreases. Increasing the degree of crystallinity generally increases the modulus, however, the higher crystallinity can also make a material more brittle. In unoriented polymers, increased crystallinity can actually decrease the strength whereas in oriented polymers, increased crystallinity and orientation of both crystalline and amorphous phases can greatly increase modulus and strength in the direction of the orientation. Side chain length causes increased toughness and elongation, but lowers modulus and strength as the length of the side chains increases. As density and crystallinity are linked to side chain length, these effects are often hard to separate.

As temperature increases we expect modulus will decrease, especially when the polymer moves through the glass transition (T_g) region. In contrast, elongation-to-break will often increase and many times goes through a maximum near the midpoint of tensile strength. Tensile strength also decreases but not to as great an extent as the elongation-to-break. Modifying the polymer by drawing or inducing a heat set is also done to improve the performance of the polymer. A heat set is an orientation caused in the polymer by deforming it above its T_g and then cooling. This is what makes polymeric fibers feel more like natural fabrics instead of feeling like fishing line. The heat set polymer will relax to an unstrained state when the heat set temperature is exceeded. In fabrics, this relaxation causes a loss of the feel or “hand” of the material, so knowing the heat set temperature is very important in the fiber industry. Cured thermosets, which can have decomposition temperature below the T_g , do not show this behavior to any great extent. The elongation-to-break of thermosets is limited to a small percentage of its length by the crosslinks present.

The addition of plasticizers to a polymer causes changes that look similar to that of increased temperature as shown in Figure 2.19. Plasticizers also cause an increase to width of the T_g region. Fillers can act several ways, all with a dependence on loading. Rigid fillers raise the modulus, whereas soft microscopic particles can lower the modulus while increasing toughness. The form of the filler is important as powders will decrease elongation and ultimate strength as the amount of filler

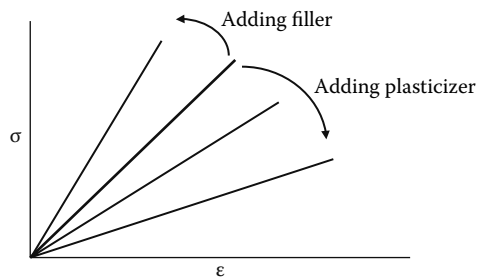


FIGURE 2.19 Plasticizers and fillers effects. Some filler, specifically elastomers added to increase toughness and called tougheners, can also act to lower the modulus.

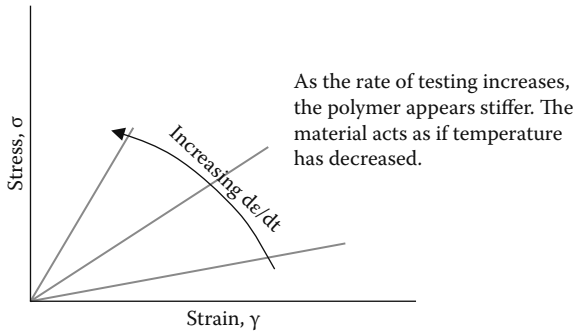


FIGURE 2.20 Rate of testing affects polymers because they are viscoelastic, not Hookean solids. Increasing the rate of applying stress acts as if we raised the temperature. All materials are at least slightly rate dependent, but the effect is small in elastic materials.

increases. Long fibers, on the other hand, cause an increase in both the modulus and the ultimate strength. In both cases, there is an upper limit to the amount of filler that can be used and still maintain the desired properties of the polymer. For example, if a too high weight percent of fibers is used in a fiber reinforced composite, there will not be enough polymer matrix to hold the composite together.

The speed of the application of the stress can show an effect on the modulus and this is often a shock to people from a ceramics or metallurgical background. Because of the viscoelastic nature of polymers, one does not see the expected Hookean behavior where the modulus is independent of rate of testing. Increasing the rate causes the same effects one sees with decreased temperature: higher modulus, lower extension to break, less toughness (Figure 2.20). Rubbers and elastomers often are exceptions as they can elongate more at high rates. In addition, removing the stress at the same rate it was applied will often give a different stress–strain curve than obtained on the application of increasing stress (Figure 2.21). This hysteresis is also caused by the viscoelastic nature of polymers.

As mentioned earlier, polymer melts and fluids also show non-Newtonian behavior in their stress–strain curves. This is also seen in suspensions and colloids. One common behavior is the existence of a yield stress. This is a stress level below which one does not see flow in a predominately fluid material. This value is very important

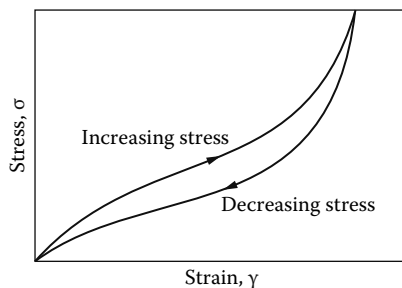


FIGURE 2.21 Hysteresis in polymers is an indicator of nonlinear behavior.

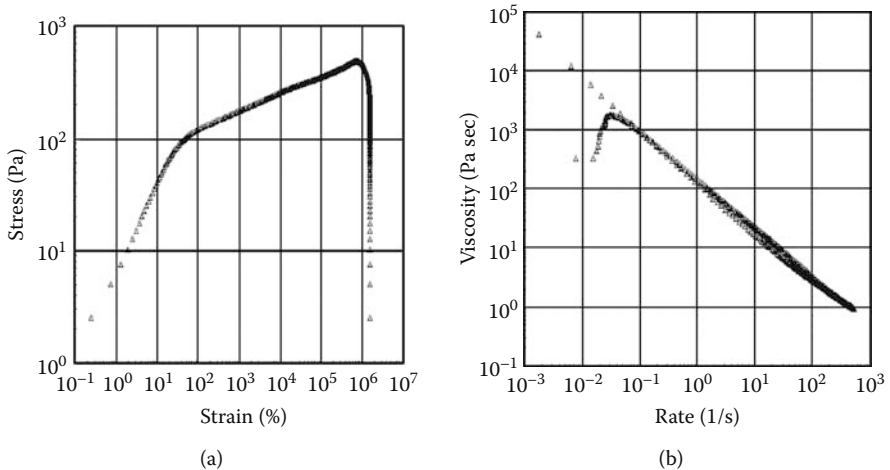


FIGURE 2.22 The yield stress in mayonnaise shows the affect of an important non-Newtonian behavior in food products. (a) A stress–strain curve with a visible knee at the yield stress. (b) Detecting the yield stress from a viscosity–rate plot. Data collected by the author.

in industries like food, paints, coating, and personal products (cosmetics, shampoo, etc.) where the material is designed to exhibit two different types of behavior. For example, mayonnaise is designed to spread easily when applied (one stress applied) but to cling to the food without dripping (another lower stress). The stress–strain curve for mayonnaise is shown in Figure 2.22a, where the knee or bend in the curve represents the value of the yield stress. The yield stress can also be determined from the viscosity–shear rate curve as shown in Figure 2.22b. Note the values don't agree. One needs to make sure the method used to determine the yield stress is a good representation of the actual use of the material. None of these data are really useful for looking at how a polymer's properties depend on time. In order to start considering polymer relaxations, we need to consider creep–recovery and stress relaxation testing.

2.7 APPENDIX: CONVERSION FACTORS

Length

$$1 \text{ mil} = 0.0000245 \text{ m}$$

$$1 \text{ thou} = 0.0254 \text{ mm}$$

$$1 \text{ in} = 2.54 \text{ mm}$$

$$1 \text{ ft} = 304.8 \text{ mm}$$

$$1 \text{ yd} = 914.4 \text{ mm}$$

$$1 \text{ mi} = 1.61 \text{ km}$$

Area

$$1 \text{ in}^2 = 645.2 \text{ mm}^2$$

$$1 \text{ ft}^2 = 0.092 \text{ m}^2$$

$$1 \text{ yd}^2 = 0.8361 \text{ m}^2$$

$$1 \text{ acre} = 4047 \text{ m}^2$$

Volume

$$1 \text{ oz} = 29.6 \text{ cm}^3$$

$$1 \text{ in}^3 = 16.4 \text{ cm}^3$$

$$1 \text{ qt(l)} = 0.946 \text{ dm}^3$$

$$1 \text{ qt(s)} = 1.1 \text{ dm}^3$$

$$1 \text{ ft}^3 = 0.028 \text{ dm}^3$$

$$1 \text{ yd}^3 = 0.0765 \text{ dm}^3$$

$$1 \text{ gal(l)} = 3.79 \text{ dm}^3$$

Time

$$1 \text{ sec} = 9.19\text{E-}09 \text{ period } 55\text{Cs}133\text{s}$$

Velocity

$$250 \text{ m/s} = 55.9 \text{ mph}$$

$$250 \text{ m/s} = 90.6 \text{ kph}$$

$$55 \text{ mph} = 89.1 \text{ kph}$$

$$55 \text{ mph} = 245.9 \text{ m/s}$$

$$90 \text{ kph} = 55.6 \text{ mph}$$

Acceleration

$$1 \text{ ft/s}^2 = 0.3 \text{ m/s}^2$$

$$1 \text{ free fall (g)} = 9.806650 \text{ m/s}^2$$

Frequency

$$1 \text{ cycle/second} = 1 \text{ Hz (hertz)}$$

$$1 \text{ w} = \text{rad/s} = 0.15915494 \text{ Hz}$$

$$1 \text{ Hz} = 6.283185429 \text{ w rad/s}$$

$$1 \text{ Hz} = 60.00 \text{ rpm (revolutions per minute)}$$

$$1 \text{ rpm} = 0.1047198 \text{ r/s (radians/second)}$$

$$1 \text{ rpm} = 0.017 \text{ Hz}$$

Plane angle

$$1 \text{ degree} = 0.017453293 \text{ rad (radian)}$$

$$1 \text{ rad} = 57.29577951 \text{ degree}$$

Mass

$$1 \text{ carat(m)} = 0.2 \text{ g (gram)}$$

$$1 \text{ grain} = 0.00000648 \text{ g}$$

$$1 \text{ oz(ay)} = 28.35 \text{ g}$$

$$1 \text{ oz(troy)} = 31.1 \text{ g}$$

$$1 \text{ lb} = 0.4536 \text{ kg}$$

$$1 \text{ ton (2000 lb)} = 907.2 \text{ Mg}$$

Force

$$1 \text{ dyne} = 1.0000\text{E-}05 \text{ N (newton)}$$

$$1 \text{ oz Force} = 278 \text{ mN}$$

$$1 \text{ g Force} = 9.807 \text{ mN}$$

$$1 \text{ mN} = 0.101967982 \text{ g Force}$$

$$1 \text{ lb Force} = 4.4482\text{E+}00 \text{ N}$$

$$1 \text{ ton Force (US) (2000 lb)} = 8.896 \text{ kN}$$

1 ton Force (UK) = 9.964 kN

1 ton (2000 lbf) = 8.8964E+03 N

Pressure

1 mm H₂O = 9.80E+00 Pa (pascal)

1 lb/ft² = 4.79E+01 Pa

1 dyne/cm² = 1.00E+01 Pa

1 mm Hg @ 0°C = 1.3332E+02 Pa

40 psi = 2.7579E+05 Pa 275790

300000 Pa = 4.3511E+01 psi 44

1 atm = 1.01E+05 Pa

1 Torr = 1.33E+02 Pa

1 Pa = 7.5000E-03 Torr

1 bar = 1.0000E+05 Pa

1 kPa = 1.00E+03 Pa

1 MPa = 1.00E+06 Pa

1 GPa = 1.00E+09 Pa

1 Tpa = 1.00E+12 Pa

Viscosity (dynamic)

1 cP = 1.00E-03 Pa*s (pascal second)

1 Poise = 1.00E-01 Pa*s

1 kp*s/m² = 9.81E+00 Pa*s

1 kp*h/m² = 3.53E+04 Pa*s

Viscosity (kinematic)

1 Stokes = 1.00E-04 m²/s

1 cSt = 1.00e-06 m²/s

1 ft²/s = 0.0929 m²/s

Work (energy)

1 ft*lb = 1.36 J (joule)

1 Btu = 1.05 J

1 Cal = 4.186 kJ

1 kW*h = 3.6 MJ

1 eV = 1.6E-19 J

1 erg = 1.60E-07 J

1 J = 0.73 ft*lbF

1 J = 0.23 cal

1 kJ = 1 Btu

1 MJ = 0.28 kW*h

Power

1 Btu/min = 17.58 W (watt)

1 ft-lb/sec = 1.4 W

1 cal/sec = 4.2 W

1 hp (electric) = 0.746 kW

1 W = 44.2 ft*lb/min

1 W = 2.35 Btu/h

1 kW = 1.34 hp (electric)

1 kW = 0.28 ton (HVAC)

Temperature

$$32^{\circ}\text{F} = 491.7^{\circ}\text{R}$$

$$32^{\circ}\text{F} = 0^{\circ}\text{C}$$

$$32^{\circ}\text{F} = 273.2\text{K}$$

$$0^{\circ}\text{C} = 32^{\circ}\text{F}$$

$$0^{\circ}\text{C} = 273.2\text{K}$$

NOTES

1. R. Steiner, *Physics Today*, 17, 62, 1969.
2. M. Shaw and W. MacKnight, *Introduction to Polymer Viscoelasticity*, 3rd ed., Wiley and Sons, New York, 2005.
3. C. Macosko, *Rheology Principles, Measurements, and Applications*, VCH, New York, 2007.
4. Viscoelasticity is discussed later. For this chapter, we are assuming linear behavior unless we specifically state otherwise.
5. In this book, I will use the term *static stress* or *static force* to refer to the nonoscillatory stress applied to a sample to hold it in place. This is sometimes called the clamping force. The stress used in a creep example will be called a constant stress to indicate a constant load.
6. The addition of the dot over a symbol means we are using the rate of that property. In this case, the term could also be written as $\dot{\delta\sigma}/\delta t$.
7. D. Holland, *J. Rheol.*, 38(6), 1941, 1994. L. Kasehagen, *University of Minnesota Rheometry Short Course*, University of Minnesota, Minneapolis, 1996.
8. For a fuller development of Hookean behavior, see L. Nielsen et al., *Mechanical Properties of Polymers, and Composites*, 3rd ed., Marcel Dekker, New York, 1994. S. Krishnamachari, *Applied Stress Analysis of Plastics*, Van Nostrand Reinhold, New York, 1993. C. Macosko, *Rheology Principles, Measurements, and Applications*, VCH, New York, 1994.
9. G. Gordon and M. Shaw, *Computer Programs for Rheologists*, Hanser, New York, 1994.
10. D. Askeland, *The Science and Engineering of Materials*, PWS, Boulder, 1994.
11. W. Brostow, *Science of Materials*, Robert Krieger, Malabar, FL, 1985.
12. J. Duncan, Dynamic mechanical analysis, in *Principles and Applications of Thermal Analysis*, P. Gabbott, Ed., Blackwell, Oxford, 2007.
13. See for example, F. Garner et al., *J. Nucl. Mater.*, 283, 1014, 2000. M. Braden and R. Clarke, *Biomaterials*, 14, 781, 1993. R. Rockford, M. Braden, and R. Clarke, *Biomaterials*, 15, 75, 1994. I. Mirza and J. Lelievre, *J. Textural Mater.*, 23, 57, 1992. E. Blackstone et al., *J. Biomed. Eng.*, 31, 526, 2003. Z. Rácz and L. Vas, *Composite Interfaces*, 12, 325, 2005. J. Cirne, R. Dormeval, et al., *J. Phys. IV France*, 134, 851, 2006.
14. For a more detailed discussion of flow, viscosity, and melt rheology, the following are suggested: J. Dealy et al., *Melt Rheology and Its Role in Polymer Processing*, Van Nostrand Reinhold, Toronto, 1990. J. Dealy, *Rheometers for Molten Plastics*, Van Nostrand Reinhold, Toronto, 1982. H. Barnes et al., *An Introduction to Rheology*, Elsevier, New York, 1989. N. Cheremisinoff, *An Introduction to Polymer Processing*, CRC Press, Boca Raton, FL, 1993. R. Tanner, *Engineering Rheology*, Oxford University Press, New York, 1988. R. Armstrong et al., *Dynamics of Polymer Fluids*, Vols. 1 and 2, John Wiley, New York, 1987. C. Rohn, *Analytical Polymer Rheology*, Hanser-Gardner, New York, 1995.
15. H. Barnes, J. Hutton, and K. Walters, *An Introduction to Rheology*, Elsevier, Oxford, UK, 1989.

16. A. Malkin and A. Isayev, *Rheology*, ChemTech Publishing, Toronto, 2006.
17. J. Dealy and K. Wissbrum, *Melt Rheology and Its Role in Polymer Processing*, Van Nostrand Reinhold, New York, 1989. J. Dealy, *Rheometers for Molten Plastics*, Van Nostrand Reinhold, New York, 1982.
18. C. Rohn, *Analytical Polymer Rheology*, Hanser-Gardner, New York, 1995.
19. A. Malkin and A. Isayev, *Rheology*, ChemTech Publishing, Toronto, 2006.
20. J. Dealy and P. Saucier, *Rheology in Quality Control*, Hanser-Gardner, Cincinnati, OH, 2000.
21. M. Tirrell and C. Macosko, *Rheological Measurements Short Course Text*, University of Minnesota, Minneapolis, 1996.
22. M. Tirrell and C. Macosko, *Rheological Measurements Short Course Text*, University of Minnesota, Minneapolis, 1996.
23. In addition to the references in notes 8 and 14, see J. D. Ferry, *Viscoelastic Properties of Polymers*, 3rd ed., Wiley, New York, 1980. M. Shaw and W. J. MacKnight, *Introduction to Polymer Viscoelasticity*, 2nd ed., Wiley, New York, 2005. L. C. E. Struik, *Physical Aging in Amorphous Polymers and Other Materials*, Elsevier, New York, 1978. W. Brostow and R. Corneliussen, Eds., *Failure of Plastics*, Hanser, New York, 1986, ch. 3. S. Matsuoka, *Relaxation Phenomena in Polymers*, Hanser, New York, 1992. N. McCrum, G. Williams, and B. Read, *Anelastic and Dielectric Effects in Polymeric Solids*, Dover, New York, 1994. M. Doi and S. Edwards, *The Dynamics of Polymer Chains*, Oxford University Press, New York, 1986. A. Malkin and A. Isayev, *Rheology*, ChemTech Publishing, Toronto, 2006.
24. The following discussion was extracted from several books. The best summaries are found in L. Nielsen et al., *Mechanical Properties of Polymers and Composites*, 3rd ed., Marcel Dekker, New York, 1994. C. Rohn, *Analytical Polymer Rheology*, Hanser-Gardner, New York, 1995. R. Seymour et al., *Structure Property Relationships in Polymers*, Plenum Press, New York, 1984. D. Van Krevelen, *Properties of Polymer*, 2nd ed., Elsevier, New York, 1990.

3 Rheology Basic

Creep–Recovery and Stress Relaxation

The next area we will review before moving on to dynamic testing is creep, recovery, and stress relaxation testing. Creep testing is a basic probe of polymer relaxations and a fundamental form of polymer behavior. It has been said that while creep in metals is a failure mode that implies poor design, in polymers it is a fact of life.¹ The importance of creep can be seen by the number of courses dedicated to it in mechanical engineering curriculums as well as the collections of data available from technical societies.²

Creep testing involves loading a sample with a set weight and watching the strain change over time. Recovery tests look at how the material relaxes once the load is removed. The tests can be done separately but are most useful together. Stress relaxation is the inverse of creep: a sample is pulled to a set length, held there, and the force it generates is measured. These are shown schematically in Figure 3.1. In the following sections we will discuss the creep–recovery and stress relaxation tests as well as their applications. This will give us an introduction to how polymers relax and recover. As most commercial DMAs will perform creep tests, this will also give us another tool to examine material behavior.

Creep and creep–recovery tests are especially useful for studying materials under very low shear rates or frequencies, under long test times, or under real use conditions. Since the creep–recovery cycle can be repeated multiple times and the temperature varied independently of the stress, it is possible to mimic real-life conditions fairly accurately. This is done for everything from rubbers to hair coated with hair spray to the wheels on a desk chair.

3.1 CREEP–RECOVERY TESTING

If a constant static load is applied to a sample, for example, a 5 pound weight is put on top of a gallon milk container, the material will obviously distort. After an initial change, the material will reach a constant rate of change that can be plotted against time (Figure 3.2). This is actually how a lot of creep tests are done and it is still common to find polymer manufacturers with a room full of parts under load that are being watched. This checks not only the polymer but also the design of the part.

More accurately representative samples of polymer can be tested for creep. The sample is loaded with a very low stress level, just enough to hold it in place, and allowed to stabilize. The testing stress is then applied very quickly, with instantaneous application being ideal, and the changes in the material response are recorded

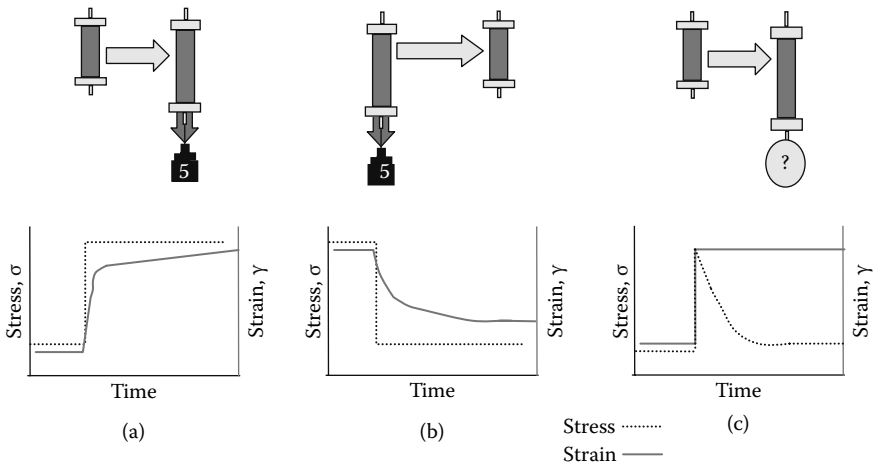


FIGURE 3.1 Creep, recovery, and stress relaxation tests. (a) Creep testing is performed by applying a load or stress to a sample. (b) When the stress is removed and the material is allowed to recover, this is called a recovery test. These two tests are often cycled. (c) Stress relaxation is the reverse of creep. Holding a sample at a set length, the change in stress as a function of time or temperature is recorded.

as percent strain. The material is then held at this stress for a period of time until the material reaches equilibrium. Figure 3.3 shows a creep test and the recovery step.

We can use creep tests in two ways: to gain basic information about the polymer or to examine the polymer response under conditions that approximate real use. In the former case, we want to work within the linear viscoelastic region so we can calculate equilibrium values for viscosity (η), modulus (E), and compliance (J). Compliance is the willingness of the material to deform and is the inverse of modulus for an elastic material. However, for a viscoelastic material this is not true and a Laplace transform is necessary to make that conversion.³ As we mentioned in the previous chapter, polymers have a range over which the viscoelastic properties are linear. We can determine this region for creep–recovery by running a series of tests on different

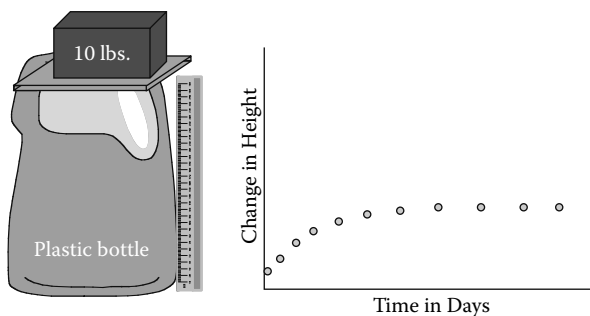


FIGURE 3.2 A representation of a simple creep test where the specimen is loaded with a stress that it would see in real life and its deformation tracked as a function of time.

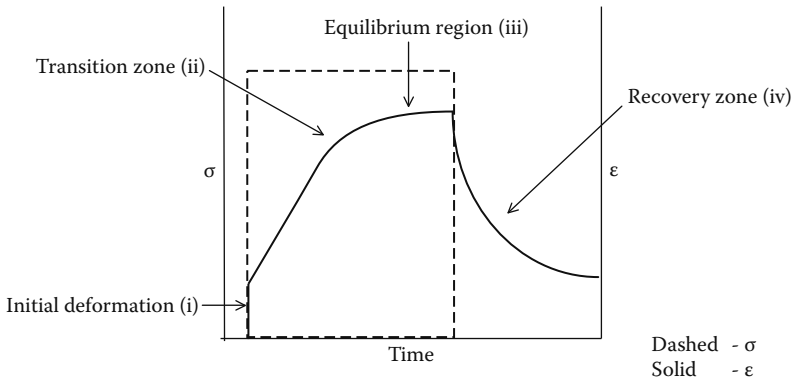


FIGURE 3.3 A creep–recovery curve as seen from a modern DMA operating in the creep–recovery mode showing (a) the applied stress curve and (b) the resulting strain curve. Note the idealized strain curve shows distinct regions of behavior related to (i) the initial deformation, (ii) a transition zone, (iii) the equilibrium region, and (iv) the recovery region.

specimens from the sample and plotting the creep compliance, J , versus time, t .⁴ Where the plots begin to overlay on top of each other, this is the linear viscoelastic region. Another approach to finding the linear region is to run a series of creep tests and observe under what stress no flow occurs in the equilibrium region over time (Figure 3.4). A third way to estimate the linear region is to run the curve at two stresses and add the curves together, using the Boltzmann superposition principle, which states the effect of stresses is additive in the linear region. So if we look at the

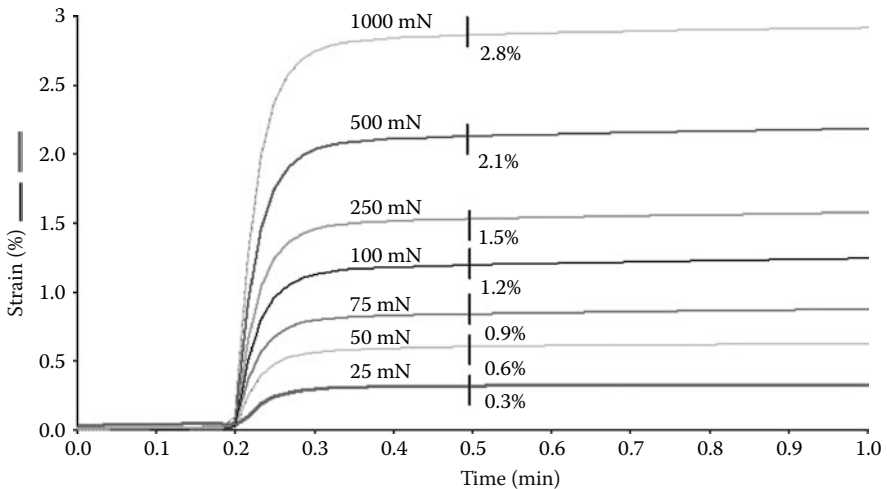


FIGURE 3.4 A plot of percent strain against time showing two methods of determining the linear region for a creep curve. One can look for the region where the equilibrium region shows no flow as a function of time or where the stress–strain relationship ceases being linear.

25 mN curve in Figure 3.4 and take the strain at 0.5 minutes, we notice the strain increases linearly with the stress until about 100 mN where it starts to diverge and at 250 mN the strains are no longer linear. Once we have determined the linear region, we can run our samples within it and analyze the curve. This does not mean you cannot get very useful data outside this limit, but we will discuss that later.

Creep experiments can be preformed in a variety of geometries, depending on the sample, its modulus or viscosity, and the mode of deformation that it would be expected to be seen in use. Shear, flexure, compression, and extension are all used. The extension or tensile geometry will be used for the rest of this discussion unless otherwise noted. When discussing viscosity, it will be useful to assume that the extensional or tensile viscosity is three times that of shear viscosity for the same sample when Poisson's ratio, ν , is equal to 0.5.⁵ For other values of Poisson's ratio, this does not hold.

3.2 MODELS TO DESCRIBE CREEP-RECOVERY BEHAVIOR

In the preceding chapter, we discussed how the dashpot and the spring are combined to model the viscous and elastic portions of a stress-strain curve. The creep-recovery curve can also be looked at as a combination of springs (elastic sections) and dashpots (viscous sections).⁶ However, the models discussed in the last chapter are not adequate for this. The Maxwell model, with the spring and dashpot in series (Figure 3.5a), gives a strain curve with sharp corners where regions change. It also continues to deform as long as it is stressed, for the dashpot continues to respond. So despite the fact the Maxwell model works reasonably well as a representation of stress-strain curves, it is inadequate for creep.

The Voigt-Kelvin model with the spring and the dashpot in parallel is the next simplest arrangement we could consider. This model, shown in Figure 3.5b, gives a curve somewhat like the creep-recovery curve of a solid. This arrangement of the spring and dashpot gives us a way to visualize a time-dependent response as the resistance of the dashpot slows the restoring force of the spring. However, it doesn't show the instantaneous response seen in some samples. It also doesn't show the continued flow under equilibrium stress that is seen in many polymers.

In order to address these problems, we can continue the combination of dashpots and springs to develop the four-element model. This combining of the various dashpots and spring is used with fair success to model linear behavior.⁷ Figure 3.5c shows the model and the curve that results from it. This curve shows the same regions as seen in real material, including a small instantaneous region, a leveling off of the equilibrium region, and a realistic recovery curve. We can use the four-element model to help us understand the strain curve. We can also add additional elements if needed to adjust the behavior and tie it back to structural units. This is a common approach and Shoemaker et al.⁸ reported the use of a six-element model to predict the behavior of ice cream when various parts of that mixture were assigned to specific elements of the model. For example, they assigned the independent spring to ice crystals, the independent dashpot to butterfat, and the Voigt elements to stabilizer gels, air cells, and fat crystals. This doesn't always work this well (and there are some

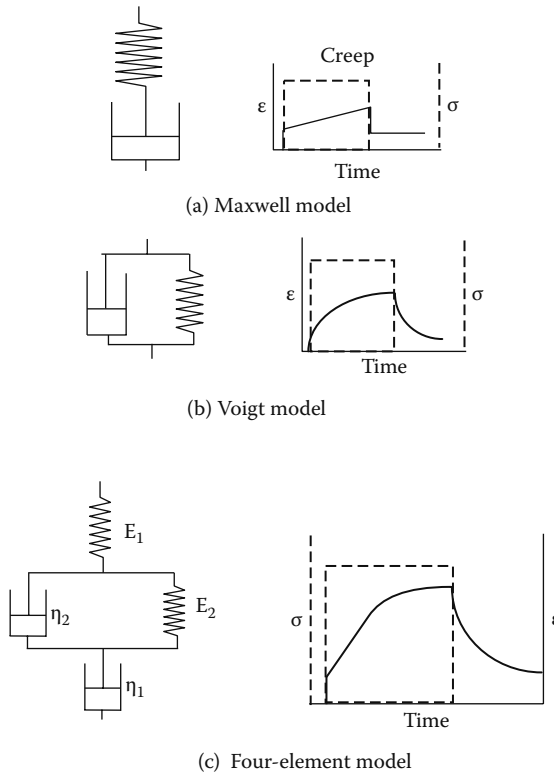


FIGURE 3.5 Models for approximating creep–recovery response. Neither the Maxwell (a) nor the Voigt model (b) work well to explain creep. The four-element model (c) does a better job. More complex models exist.

doubts as to the validity of these assignments in this particular case, too⁹), and better approaches exist. While real polymers do not have springs and dashpots in them, the idea allows us an easy way to explain what is happening in a creep experiment.

3.3 ANALYZING A CREEP–RECOVERY CURVE TO FIT THE FOUR-ELEMENT MODEL

If we now examine a creep–recovery curve, we have three options in interpreting the results. These are shown graphically in Figure 3.6. We can plot strain versus stress and fit the data to a model, in this case to the four-element as shown in Figure 3.6. Alternately we could plot strain versus stress and analyze quantitatively in terms of irrecoverable creep, viscosity, modulus, and relaxation time. A third choice would be to plot creep compliance, J , versus time.¹⁰

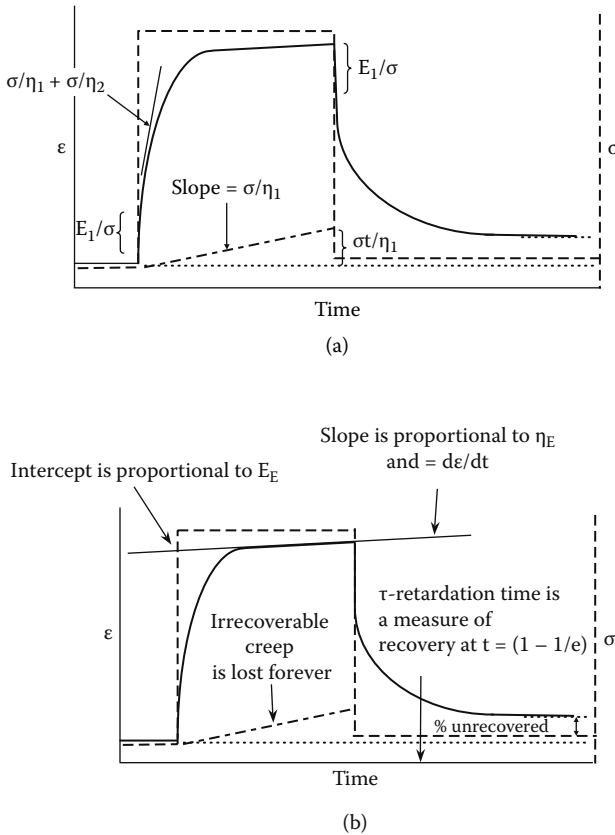


FIGURE 3.6 Analysis of a creep–recovery curve when viewed as either strain or compliance versus time. (a) The terms correspond to the parts of the four-element model discussed in the chapter. (b) The displayed values are the most commonly used ones in the author’s experience.

In Figure 3.6a, we show the relationship of the resultant strain curve to the parts of the four-element model. This analysis is valid for materials in their linear viscoelastic regions and only those that fit the model. However, it is a simple way to separate sample behavior into elastic, viscous, and viscoelastic components. As the stress, σ_0 , is applied, there is an immediate response by the material. The point at which σ_0 is applied is when time is equal to zero for the creep experiment. (Likewise for the recovery portion, time zero is when the force is removed.) The height of this initial jump is equal to the applied stress, σ_0 , divided by the independent spring constant, E_1 . This spring can be envisioned as stretching immediately and then locking into its extended condition. In practice, this region may be very small and hard to see, and the derivative of strain may be used to locate it. After this spring is extended, the independent dashpot and the Voigt element can respond. When the force is removed, there is an immediate recovery of this spring that is again equal to σ_0/E_1 . This is useful as sometimes it is easier to measure this value in recovery than

in creep. From a molecular perspective, we can look at this as the elastic deformation of the polymer chains, angles, and bonds.

The independent dashpot's contribution, η_1 , can be calculated by the slope of the strain curve when it reaches the region of equilibrium flow. This equilibrium slope is equal to the applied stress, σ_0 , divided by η_1 . The same value can be obtained determining the permanent set of the sample, and extrapolating this back to t_f , the time at which σ_0 was removed. A straight line drawn for t_0 to this point will have a slope equal to

$$\text{slope} = \sigma_0(t_f)/\eta_1 \quad (3.1)$$

The problem with this method is that the time required to reach the equilibrium value for the permanent set may be very long. If you can actually reach the true permanent set point, you could also calculate η_1 from the value of the permanent set directly. This dashpot doesn't recover because there is nothing to apply a restoring force to it and molecularly it represents the slip of one polymer chain past another.

The curved region between the initial elastic response and the equilibrium flow response is described by the Voigt element of the Berger model. Separating this into individual components is much trickier as the region of the retarded elastic response is described by the parallel combination of the spring, E_2 , and dashpot, η_2 . In addition, some contribution from the independent dashpot exists. This region responds slowly due the damping affect of the dashpot until the spring is fully extended. The presence of the spring allows for a slow recovery as it pushes the dashpot back to its original position. Molecularly we can consider this dashpot to represent the resistance of the chains to uncoiling, whereas the spring represents the thermal vibration of chain segments that will tend to seek the lowest energy arrangement.

Since the overall deformation of the model is given as

$$\varepsilon(f) = (\sigma_0/E_1) + (\sigma_0/\eta_1) + (\sigma_0/E_2)(1 - e^{-t/(\eta_2/E_2)}) \quad (3.2)$$

we can get the value for the Voigt unit by subtracting the first two terms from the total strain, so

$$\varepsilon(f) - (\sigma_0/E_1) - (\sigma_0/\eta_1) = (\sigma_0/E_2)(1 - e^{-t/(\eta_2/E_2)}) \quad (3.3)$$

The exponential term, η_2/E_2 , is the retardation time, τ , for the polymer. The retardation time is the time required for the Voigt element to deform to 63.21 percent (or $1-1/e$) of its total deformation. If we plot the log of strain against the log of time, the creep curve appears sigmoidal and the steepest part of the curve occurs at the retardation time. Taking the derivative of the above curve puts the retardation time at the peak. Having the retardation time we can now solve the above equation for E_2 and then get η_2 . The major failing of this model is it uses a single retardation time when real polymers, due to their molecular weight distribution, have a range of retardation times.

A single retardation time means this model doesn't fit most polymers well, but it allows for a quick, simple estimate of how changes in formulation or structure can

affect behavior. Much more exact models exist¹¹ including four-element models in 3-D and with multiple relaxation times, but these tend to be mathematically non-trivial. A good introduction to fitting the models to data and to multiple relaxation times can be found in Sperling's book.¹²

3.4 ANALYZING A CREEP EXPERIMENT FOR PRACTICAL USE

The second of the three methods of analysis, shown in Figure 3.6b, is more suited to the real world. Often we intentionally study a polymer outside of the linear region because that is where we plan to use it. More often, we are working with a system that does not obey the Berger model. If we look at Figure 3.6, we can see that the slope of the equilibrium region of the creep curve gives us a strain rate, $\dot{\epsilon}$. We can also calculate the initial strain, ϵ_0 , and the recoverable strain, ϵ_r . Since we know the stress and strain for each point on the curve, we can calculate a modulus (σ/ϵ) and, with the strain rate, a viscosity ($\sigma/\dot{\epsilon}$). If we do the latter, where the strain rate has become constant, we can measure an equilibrium viscosity, η_e . Extrapolating that line back to t_0 we can calculate the equilibrium modulus, E_e . Percent recovery and a relaxation time can also be calculated. These values help quantify the recovery cure; percent recovery is simply how much the polymer comes back after the stress is released while the relaxation time here is simply the amount of time required for the strain to recover to 36.79% (or $1/e$) of its original value.

We can actually measure three types of viscosity from this curve. The simple viscosity is given above and by multiplying the denominator by 3 we approximate the shear viscosity, η_s . Nielsen suggests that a more accurate viscosity, $\eta_{\Delta\epsilon}$, can be obtained by inverting the recovery curve and subtracting it from the creep curve. The resulting value, $\Delta\epsilon$, is then used to calculate a strain rate, multiplied by 3, and divided into the stress, σ_0 . Finally, we can calculate the irrecoverable viscosity, η_{irr} , by extrapolating the strain at permanent setback to t_r and taking the slope of the line from t_0 to t_r . This slope can be used to calculate a irrecoverable strain rate, which is then multiplied by 3 and divided into the initial stress, σ_0 . This value tells us how quickly the material flows irreversibly.

If we instead choose to plot creep compliance against time, we can calculate various compliance values. Extrapolating the slope of the equilibrium region back to t_0 gives us J_e^0 while the slope of this region is equal to t/η_0 . At the very low shear rates seen in creep, this term reduces to $1/\eta_0$. We can also use the recovery curve to independently calculate J_e^0 by allowing the polymer to recover to equilibrium. Since we know

$$\lim_{t \rightarrow \infty} J_r(t) = J_e^0 \text{ for } \dot{\epsilon}(t) = \dot{\epsilon}_\infty \quad (3.4)$$

then we can watch the change in $\dot{\epsilon}$ until it is zero or, more practically, very small. This can be done by watching the second derivative of the strain as it approaches zero. At this point, J_r is equal to J_e^0 . If we are in steady-state creep, the two measurements of J_e^0 should agree. If we actually measure the J_e^0 , we can estimate the longest retardation time (λ_0) for the material by $\eta_0 * J_e^0$.

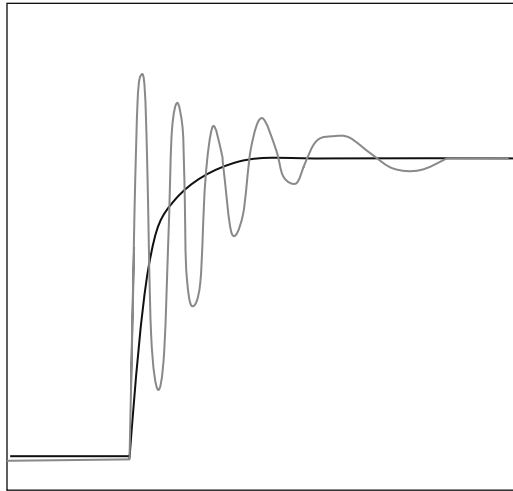


FIGURE 3.7 Creep ringing is sometimes seen in samples. Experimentally one tries to find different conditions to run the sample under to suppress it. Techniques exist for using the data.

3.5 CREEP RINGING

A major problem with many creep tests, especially with very elastic samples, is that one gets ringing when the force is applied to the sample. This is shown in Figure 3.7. Often this can be corrected by changing the load, the geometry, or sample dimensions, but sometimes it cannot. I should note that sometimes you want to induce ringing so you can use the data to study the free resonance decay and we will discuss that in Chapter 5. The most common approach to this is to either discard the data or to average it out so one has a line approximating a normal creep response. While most people using DMA don't worry too much about it, it is a serious concern and Ewoldt and McKinley¹³ discuss some approaches to handling this.

3.6 OTHER VARIATIONS ON CREEP TESTS

Before we discuss the structure–property relationships or concepts of retardation and relaxation times, let's quickly look at variations of the simple creep–recover cycle we discussed earlier. As mentioned before, a big advantage of a creep test is its ability to mimic the conditions seen in use. By varying the number of cycles and the temperature, we can impose stresses that approximate many end-use conditions.

Figure 3.8 shows three types of tests that are done to simulate real applications of polymers. In Figure 3.8a, multiple creep cycles are applied to a sample. This can be done for a set number of cycles to see if the properties degrade over multiple cycles (for example, to test a windshield wiper blade) or until failure (for example, on a resealable o-ring). Creep tests for failure are also occasionally called creep rupture experiments. One normally analyzes the first and last cycle to see the degree of degradation or plots a certain value, say η_c , as a function of cycle number.

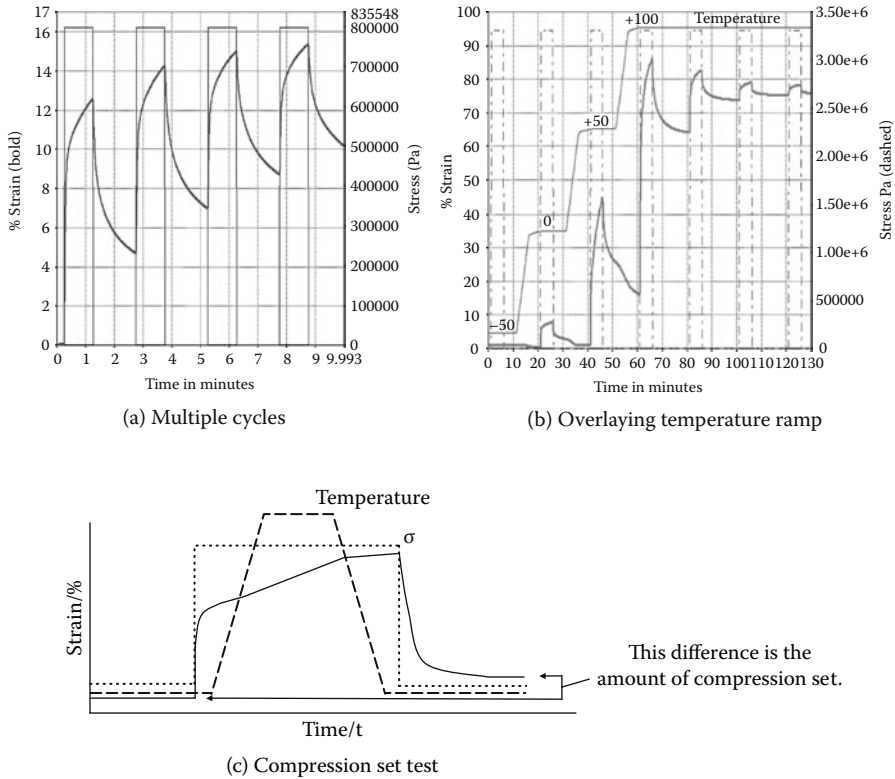


FIGURE 3.8 Examples of types of creep tests: (a) multiple creep recovery cycles, (b) multiple creep cycles with overlaying temperature ramp, and (c) heat set cycle.

You can also vary the temperature with each cycle to see where the properties degrade as temperature increases. This is shown in Figure 3.8b. The temperature can be raised and lowered to simulate the effect of an environmental thermal cycle. It can also be just raised or lowered to duplicate the temperature changes caused by placing the part into a specific environment, like a gasket in a pump in an oil well or a plastic pipe in an Alaskan winter. This environmental testing is not limited to temperature as creep–recovery tests can also be run in solvents or in controlled atmospheres.

You can also vary the temperature within one creep cycle as shown in Figure 3.8c. This is the equivalent of the rubber industry’s heat set test used for materials that will be heated and squeezed at the same time. The creep stress is applied and the material is heated to a set temperature and cooled back to room temperature while still under the load. The stress is removed and the amount of recovery recorded.

A final comment on creep testing is that the ASTM does have standard procedures for creep tests that supply guidelines for both testing and data interpretation.¹⁴ The main method for plastics is D2990-91. It covers tensile, compressive and flexural creep, and creep rupture. A selection of test methods for creep is given in Table 3.1.

TABLE 3.1
ASTM Standards

D2293-96(2002)	Standard Test Method for Creep Properties of Adhesives in Shear by Compression Loading (Metal-to-Metal)
D2294-96(2002)	Standard Test Method for Creep Properties of Adhesives in Shear by Tension Loading (Metal-to-Metal)
D2656-06	Standard Specification for Crosslinked Polyethylene Insulation for Wire and Cable Rated 2001 to 35000 V
D2659-95(2005)	Standard Test Method for Column Crush Properties of Blown Thermoplastic Containers
D2990-01	Standard Test Methods for Tensile, Compressive, and Flexural Creep and Creep-Rupture of Plastics
D3555-07	Standard Specification for Track-Resistant Black Crosslinked Polyethylene Insulation for Wire and Cable
D3916-02	Standard Test Method for Tensile Properties of Pultruded Glass-Fiber-Reinforced Plastic Rod
D3930-93a(2005)	Standard Specification for Adhesives for Wood-Based Materials for Construction of Manufactured Homes
D4027-98(2004)	Standard Test Method for Measuring Shear Properties of Structural Adhesives by the Modified-Rail Test
D4101-07	Standard Specification for Polypropylene Injection and Extrusion Materials
D4680-98(2004)	Standard Test Method for Creep and Time to Failure of Adhesives in Static Shear by Compression Loading
D4762-04	Standard Guide for Testing Polymer Matrix Composite Materials
D4896-01	Standard Guide for Use of Adhesive-Bonded Single Lap-Joint Specimen Test Results
D5262-07	Standard Test Method for Evaluating the Unconfined Tension Creep and Creep Rupture in Geosynthetics
D5456-07	Standard Specification for Evaluation of Structural Composite Lumber Products
D5574-94(2005)	Standard Test Methods for Establishing Allowable Mechanical Properties of Wood-Bonding Adhesives
D5592-94(2002)e1	Standard Guide for Material Properties Needed in Engineering Design Using Plastics
D5857-07	Standard Specification for Polypropylene Injection and Extrusion Materials Using ISO Methodology
D6108-03	Standard Test Method for Compressive Properties of Plastic Lumber and Shapes
D6112-97(2005)	Standard Test Methods for Compressive and Flexural Creep and Creep-Rupture of Plastic Lumber and Shapes
D6147-97(2002)	Test Method of Stress Relaxation in Compression for Vulcanized Rubber & Thermoplastic Elastomer
D6383-99(2005)	Standard Practice for Creep-Rupture of Adhesive Joints Fabricated from EPDM Roof Membrane Material
D6465-99(2005)	Standard Guide for Selecting Aerospace and General Purpose Adhesives and Sealants
D6555-03	Guide for Evaluating System Effects in Repetitive-Member Wood Assemblies
D6648-01	Standard Test Method for Determining the Flexural Creep Stiffness of Asphalt Binder
D6662-07	Standard Specification for Polyolefin-Based Plastic Lumber Decking Boards

(Continued)

TABLE 3.1
ASTM Standards (Continued)

D6815-02a	Standard Specification for Evaluation of Duration of Load and Creep Effects of Wood & Wood-Based Products
D6816-02	Standard Practice for Determining Low-Temperature Performance Grade (PG) of Asphalt Binders
D695-02a	Standard Test Method for Compressive Properties of Rigid Plastics
D6992-03	Standard Test Method for Accelerated Tensile Creep and Creep-Rupture of Geosynthetic Materials Based on Time-Temperature Superposition Using the Stepped Isothermal Method
D7030-04	Standard Test Method for Short Term Creep Performance of Corrugated Fiberboard Containers
D7070-04	Standard Test Method for Creep of Rock Core Under Constant Stress and Temperature
D7107-04	Standard Test Method for Creep Measurement of Self-Lubricating Bushings
D7337/D7337M-07	Standard Test Method for Tensile Creep Rupture of Fiber Reinforced Polymer Matrix Composite Bars
D7406-07	Standard Test Method for Creep Deformation Under Constant Pressure for Geosynthetic Drainage Products
D907-06	Standard Terminology of Adhesives
E139-06	Standard Test Methods for Conducting Creep, Creep-Rupture, and Stress-Rupture Tests of Metallic Materials
E143-02	Standard Test Method for Shear Modulus at Room Temperature
E1457-07	Standard Test Method for Measurement of Creep Crack Growth Times in Metals
E1823-07a	Standard Terminology Relating to Fatigue and Fracture Testing
E21-05	Standard Test Methods for Elevated Temperature Tension Tests of Metallic Materials
E328-02	Standard Test Methods for Stress Relaxation Tests for Materials and Structures
E633-00(2005)	Standard Guide for Use of Thermocouples in Creep and Stress-Rupture Testing to 1800°F (1000°C) in Air

Note: this has been limited to methods from ASTM D and E Committees. If one looks at all ASTM standards, over 200 discussing creep can be found.

3.7 SUPERPOSITION: THE BOLTZMANN PRINCIPLE

The question sometimes arises of how strains act when applied to a material that is already deformed. Boltzmann showed in 1876 that the strains will add linearly and a material's stress at any one time is a function of its strain history. This applies to a linear response whether or not any of the models we discussed are applied. It also works for applied stress and measured strain. There is time dependence in this, as the material will change over time. For example, in stress relaxation the sample will have decreasing stress with time, and therefore, in calculating the sum of the strains, one needs to consider this decay to correctly determine the stress. This decay over time is called a memory function.¹⁵

The superposition of polymer properties is not just limited to the stress and strain effects. Creep and stress relaxation curves collected at different temperatures are also superpositioned to extend the range of data at the reference temperature.

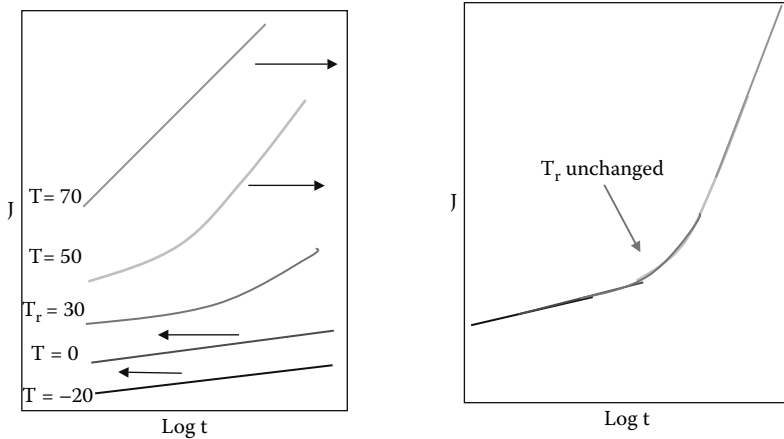


FIGURE 3.9 Shifting creep compliance, J , using $T = 30^\circ\text{C}$ as a reference curve to create a master curve of creep experiments.

Creep data is plotted as creep compliance and then the data is shifted using a shift factor calculated as

$$\text{Log } a_t = \log t/t_r \quad (3.5)$$

where a_t is the shift factor, t is the temperature of the shifted curve, and t_r the reference temperature. Goertzen¹⁶ has an excellent example of this work and its application to a problem using the Williams–Landel–Ferry (WLF) model. Figure 3.9 shows an example of the shifting of creep compliance assuming constant activation energies. A more general model has been proposed by Brostow¹⁷ to allow both stress and temperature superposition in polymer liquid crystals¹⁸ and Polyvinylidene Fluoride (PVDF) monofilaments used as sutures.¹⁹ Similarly we will see these techniques apply to stress relaxation and frequency scans in the DMA.

3.8 RETARDATION AND RELAXATION TIMES

We mentioned in Section 3.4 that one of the failings of the four-element model is that it uses a single retardation where most polymers have a distribution of retardation times. We also mentioned that we could estimate the longest retardation time from the creep compliance, J , versus time plot. The distribution of retardation times, $L(t)$, in a creep experiment or of relaxation times, $H(t)$, in a stress relaxation experiment are what determines the mechanical properties of a polymer. One method estimates $L(t)$ from the slope of the compliance curve against $\log(\text{time})$ plot and $H(t)$ is similarly obtained from the stress relaxation data. Below T_g , these are heavily influenced by the free volume, v_f , of the material. There is considerable interest in determining what the distribution of relaxation or retardation times are for a polymer and many approaches can be found.²⁰ Again, Ferry remains the major lead reference for those interested in this topic.²¹

If you know the retardation time or relaxation time spectra, it is theoretically possible to calculate other types of viscoelastic data. This has not reduced to practice as well as one might hope and the calculations are very complex. Neither $L(t)$ nor $H(t)$ has been used in solving problems. Methods also exist of calculating a discrete spectrum of relaxation and retardation times.²²

3.9 STRUCTURE-PROPERTY RELATIONSHIPS IN CREEP-RECOVERY TESTS

The effects of various structural and environmental parameters on creep-recovery tests are well known.²³ Temperature may be the most important variable as most materials show markedly different behavior above and below the T_g (Figure 3.10a). The glass transition, T_g , of a polymer, where the polymer changes from glassy to rubbery, is where chains gain enough mobility to slide by each other. Below the T_g , the behavior of the polymer is dominated by the free volume, v_f , which limits the ability of the chains to move. In glassy polymers below the T_g where little molecular motion occurs, the amount of creep is small until the deformation is great enough to cause crazing.²⁴ One can decrease the ability of the chains to move by lowering the temperature, increasing the pressure, annealing, increasing the degree of crystallinity, increasing the amount of crosslinking, or decreasing the free volume and that will decrease the amount of creep. Similarly plasticization by increased humidity or reversing the above will increase it.

As the polymer temperature approaches the temperature of its glass transition, the amount of creep becomes very temperature dependent. As we exceed the T_g , the effects of other structural parameters appear. Amorphous polymers without crosslinking have a strong dependence on molecular weight in the amount of flow seen at equilibrium. Branching changes the amount of creep but the effect is difficult to summarize as depending on the branch length and degree of branching.²⁵ For example, the amount of flow can be either increased or decreased depending on whether the branches are long enough to entangle.²⁶ Plasticizers increase the creep. Plasticization acts by lowering the T_g , increasing the molecular weight between entanglements, and diluting the polymer. These effects also decrease the recovery.²⁷

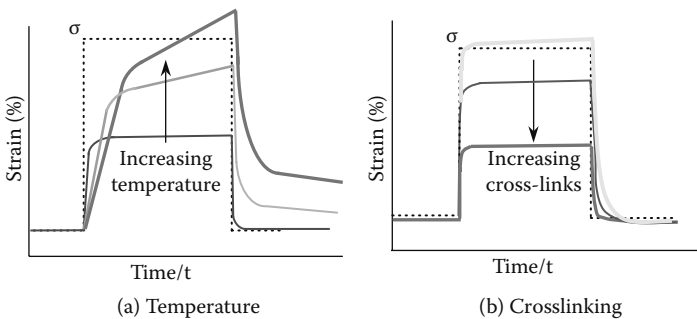


FIGURE 3.10 Various affects from material changes on creep showing the (a) effect of temperature and (b) the effect of crosslinking on the strain curve.

Time can also affect recovery as long creep experiments allow more chains to disentangle and slip, lowering recovery.

Crosslinked polymers show a very specific curve with a flat equilibrium region because the crosslinks do not allow flow. As shown in Figure 3.10b, recovery is normally quite high. While some creep does occur if times are long enough and the crosslink density low enough, in highly crosslinked materials no creep is seen. For highly crystalline polymers below T_g , we see creep responses similar to those seen in a crosslinked polymer because the crystals act as crosslinks and restrain flow. As crystallinity decreases, the material becomes less rigid. However, these materials are very sensitive to the thermal history between the T_g and the melt because of changes to the crystal morphology.

3.10 STRESS RELAXATION EXPERIMENTS

The conceptual inverse of a creep experiment is a stress relaxation experiment (Figure 3.11). A sample is very quickly distorted to a set length, and the decay of the stress exerted by the sample is measured. Experimentally these are often difficult experiments to run because the sample may need to be strained very quickly. While some DMAs can be set up to run these types of tests, many instruments have instrumental response times so long as to limit what can be done experimentally. Where they can be run, they offer another window into material performance. In a stress relaxation experiment, a sample is deformed a known

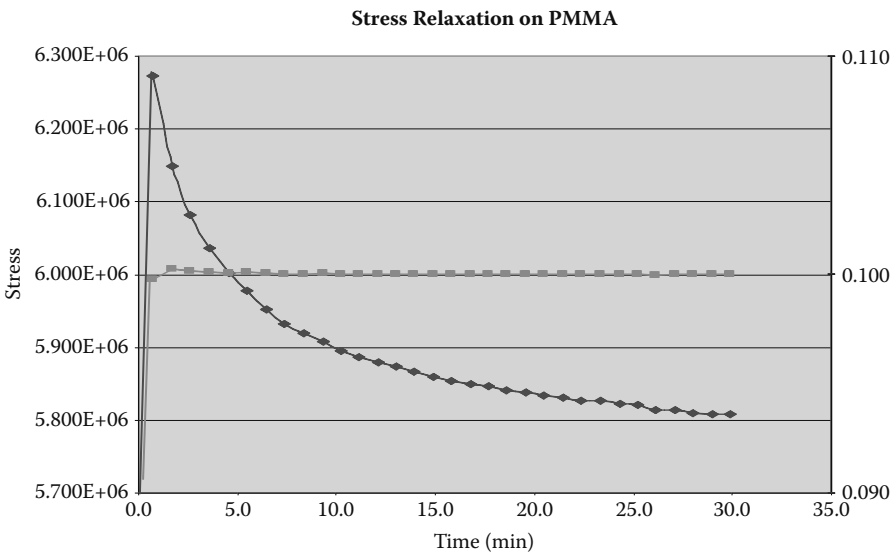


FIGURE 3.11 Stress relaxation experiments. Analysis of a classical stress relaxation experiment where the sample is held at length, l , and the stress changes are recorded. In this case, a sample of PMMA was deformed 0.1mm ($\sim 0.25\%$) and held for 30 minutes. It ran on a PerkinElmer DMA 8000 using the advanced stress relaxation software and used with the permission of Triton Technologies, Inc.

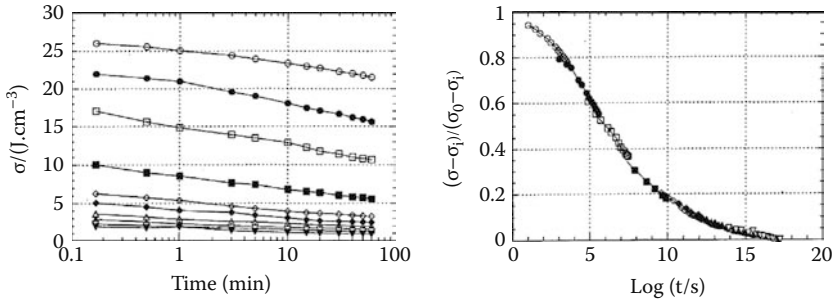


FIGURE 3.12 Superposition of stress relaxation data using data from W. Brostow’s lab at the University of North Texas and used with permission. (a) Stress relaxation data at various temperatures and (b) its superposition. See note 17 for details.

amount and the force need to hold it there tracked. From this, we can calculate a relaxation modulus

$$E_r(t_s, T) = \sigma_t / \gamma_c \quad (3.6)$$

where σ_t is the stress at time, t , and γ is the constant strain. The same models applied to creep can be applied here. For the Maxwell model, a simple spring and dashpot, one defines the relaxation time for the system as simply the viscosity of the dashpot divided by the modulus of the spring. More information on models can be found in the literature.²⁸

Stress relaxation tests are of interest because they generate some very useful data about a polymer’s real-world behavior. Think of tightening a nut down onto a gasket. The gasket flows and reforms in its new position. The data from a true stress relaxation test provides some very useful information that complements the more commonly available creep data. Creep data and stress relaxation data can be treated as mainly reciprocal²⁹ and roughly related as

$$(\epsilon_t / \epsilon_0)_{\text{creep}} \approx (\sigma_0 / \sigma_t)_{\text{stress relax}} \quad (3.7)$$

Practically, stress relaxation experiments give us information about the strain dependence of the polymer,³⁰ its molecular weight,³¹ its internal defects,³² degree of crosslinking³³ and crystallinity,³⁴ aging,³⁵ and the presence of crazing.³⁶ Similar trends are seen in creep. Unlike creep, which is mainly used with solid samples, stress relaxation experiments are also run on fluids and melts. Examples in the literature for all kinds of materials can be found including dough,³⁷ dental materials,³⁸ fibers,³⁹ adhesives and sealants,⁴⁰ gaskets and rubbers,⁴¹ and metals⁴² to mention just a few. One interesting application of the stress relaxation experiment exploits the relationship that the area under the stress relaxation curve plotted as $E(t)$ versus t is the viscosity, η_0 . Doing experiments at very low strain, this allows us to measure the viscosity of a colloid without destroying its structure.⁴³

As mentioned earlier, this data can also be superpositioned and Shaw⁴⁴ is an excellent lead reference for that. Brostow⁴⁵ has done the superposition for stress

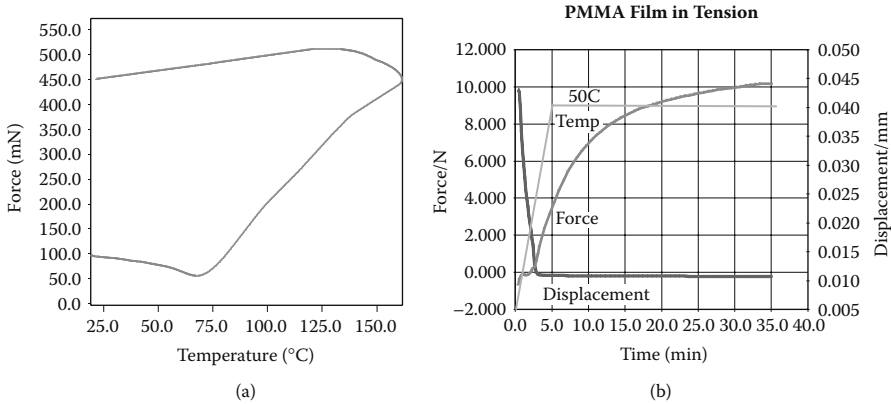


FIGURE 3.13 Constant gauge length data for (a) a fiber sample showing the change in force at constant length through a heating and cooling cycle generated on a DMA 7e and (b) for film heated to 50°C on the DMA 8000.

relaxation runs on PLC as shown in Figure 3.13. This work also looks at merging creep and stress relaxation data into one data set to cover very wide ranges of measurement exploiting the relationship in Equation 3.7. We'll see the addition of data from different types of tests again in Chapter 8. More commonly with DMA, mostly due to the instrumental limitation mentioned above, is a constant-strain variable temperature test called constant gauge length.

3.11 CONSTANT GAUGE LENGTH TESTS

Normally in a DMA, one runs a type of stress relaxation experiment where the sample is held at constant length and slowly heated or cooled. This type of experiment, shown in Figure 3.13a, is more precisely called a constant gauge length test and has wide industry applications.⁴⁶ A sample is held at a set length with a set stress and then the temperature is increased. As the material responds to the temperature changes, the stress exerted by it is measured. The shrinkage or expansion force of the material is recorded. The experiment may be done with thermal cycles to determine if the same behavior is seen during each cycle. The shrinkage of leather as it dries, shown in 3.13b, is a classic example.

One variation of this test is traditionally done in the rubber industry in much simpler form as a compression set test.⁴⁷ Clamp a piece of rubber so it is compressed to a known amount, normally 90% of its original thickness. The rubber sample is then heated to evaluated temperatures, held for a certain time, and cooled back to room temperature. The restraining force is then removed and the thickness measured. The amount the rubber doesn't recover is the compression set. This tells us how much the material has crosslinked and lost elasticity in the heating cycle. The advantage of running this in a DMA is that the change over multiple cycles is tracked. Any type of seal, gasket, or washer that experiences heating and cooling cycles can be adversely affected by the loss of elasticity that comes with aging in most polymers. Materials

that do set cause problems like leaking pipes, motors, and so forth. Several leaks in oil pipes lines over the years have been tracked to this problem.

Obviously, this type of testing is not limited to just compression. Any material that is expected to hold its shape under a deformation is vulnerable to these problems. Exposure to both humidity and to UV can also induce changes in the material that allow it to relax or set in the new position leading to product failure. For example, a piece of paper held in extension will change stresses as the local humidity is increased and decreased.

NOTES

1. J. Sosa, University of Houston short course on polymer analysis, Houston, Texas, May 5, 1994.
2. W. Andrew, *The Effect of Creep and Other Time Related Factors on Plastics*, Vols. 1 and 2, Plastic Design Library, New York, 1991.
3. M. Tirrell, Linear viscoelasticity at the 21st short course on rheometry, University of Minnesota, Minneapolis, 1996.
4. C. Macosko, *Rheology Principles, Measurements, and Applications*, VCH, New York, 1994, pp. 119–121. L. Kasehagen, Constant stress experiments at 21st short course on rheometry, University of Minnesota, Minneapolis, 1996.
5. T. Fox et al., in *Rheology*, Vol. 1, F. Eirich, Ed., Academic Press, New York, 1956, ch. 12.
6. For a more detailed discussion of these models and their use, please refer to C. Macosko, *Rheology Principles, Measurements, and Applications*, VCH, New York, 1994. L. Neilsen et al., *Mechanical Properties of Polymers and Composites*, 3rd ed., Marcel Dekker, New York, 1994. S. Rosen, *Fundamental Principles of Polymeric Materials*, Wiley, New York, 1993.
7. N. Tschoegl, *The Phenomenological Theory of Linear Viscoelasticity*, Springer-Verlag, Berlin, 1989.
8. C. Shoemaker et al., Society of rheology short course on food rheology, Society of Rheology, Boston, 1993.
9. J. Ellis, Society of rheology short course on food rheology, Society of Rheology, Boston, 1993.
10. While J is used in much of the literature for creep compliance, D is also used. I will be using J here for consistency.
11. J. Ferry, *Viscoelastic Properties of Polymers*, 3rd ed., Wiley, New York, 1980. N. Tschoegl, *The Phenomenological Theory of Linear Viscoelasticity*, Springer-Verlag, Berlin, 1989. C. Macosko, *Rheology Principles, Measurements, and Applications*, VCH, New York, 1994. J. Skrzypek, *Plasticity and Creep*, CRC Press, Boca Raton, FL, 1993.
12. L. H. Sperling, *Introduction to Physical Polymer Science*, 2nd ed., John Wiley, New York, 1992, pp. 458–497.
13. R. Ewoltdt and G. McKinley, *Rheol. Bull.*, 76, 4, 2007.
14. The ASTM can be reached at ASTM Committee on Standards, 1916 Race Street, Philadelphia, PA 19103. Standards are republished yearly.
15. We are not going to address the Boltzmann principle in detail as it is beyond the scope of this book. Interested readers are referred to Ferry, op. cit.
16. W. K. Goertzen and M. R. Kessler, *Mater. Sci. Eng.: A*, 421(1-2), 217, 2006.
17. W. Brostow, N. D'Sousa, J. Kubat, and R. Maksimov, *Int. J. Polym. Mater.*, 43, 233, 1999.

18. A. Akinay, W. Brostow, and R. Maksimov, *Polym. Eng. Sci.*, 41, 6, 2001.
19. W. Brostow, J. Mano, J. Lopes, and R. Silva, *Polymer*, 44, 4293, 2003.
20. A. Tobolsky, *Properties and Structure of Polymers*, Wiley, New York, 1964. J. Honerkamp and J. Weese, *Rheologica Acta*, 32, 65, 1993. N. Orbey and J. Dealy, *J. Rheol.*, 35(6), 1035, 1991. L. Nielsen et al., *Mechanical Properties of Polymers and Composites*, 3rd ed., Marcel Dekker, New York, 1994.
21. J. Ferry, *Viscoelastic Properties of Polymers*, 3rd ed., Wiley, New York, 1980. N. Tschoegl, *The Phenomenological Theory of Linear Viscoelasticity*, Springer-Verlag, Berlin, 1989.
22. J. Kaschta and F. Schwarzl, *Rheologica Acta*, 33, 17, 1994. J. Kaschta and F. Schwarzl, *Rheologica Acta*, 33, 530, 1994. I. Emri and N. Tschoegl, *Rheologica Acta*, 32, 311, 1993. I. Emri and N. Tschoegl, *Rheologica Acta*, 33, 60, 1994.
23. Most data on creep are well known, although work continues on specialized problems and new systems. The following is summarized from J. Ferry, *Viscoelastic Properties of Polymers*, 3rd ed., Wiley, New York, 1980. N. Tschoegl, *The Phenomenological Theory of Linear Viscoelasticity*, Springer-Verlag, Berlin, 1989. C. Macosko, *Rheology Principles, Measurements, and Applications*, VCH, New York, 1994. J. Skrzypek, *Plasticity and Creep*, CRC Press, Boca Raton, FL, 1993. J. Mark et al., *Physical Properties of Polymers*, ACS, Washington D.C., 1984. N. McCrum et al., *Principles of Polymer Engineering*, Oxford University Press, New York, 1990. W. Brostow and R. Corneliusen, *Failure of Plastics*, Hanser-Gardner, New York, 1989.
24. L. Nielsen and R. Landel, *Mechanical Properties of Polymers and Composites*, 2nd ed., Marcel Dekker, New York, 1994, pp. 89–120. J. Wu et al., *J. Rheol.*, 23, 231, 1979. N. Brown et al., *J. Polym. Sci. (Phys.)*, 16, 1085, 1978. C. Bucknall et al., *J. Mater. Sci.*, 7, 202, 1972.
25. F. Bueche, *J. Chem. Phys.*, 40, 484, 1964.
26. R. Chartoff and B. Maxwell, *J. Polym. Sci. A2*, 1970, 8, 455.
27. A. Tobolosky et al., *Polym. Eng. Sci.*, 10, 1, 1970.
28. C. Macosko, *Rheology Principles, Measurements, and Applications*, VCH, New York, 1994, pp. 119–121. L. Kasehagen, Constant stress experiments at 21st short course on rheometry, University of Minnesota, Minneapolis, 1996. C. Macosko, *Rheology Principles, Measurements, and Applications*, VCH, New York, 1994. L. Nielsen et al., *Mechanical Properties of Polymers and Composites*, 3rd ed., Marcel Dekker, New York, 1994. S. Rosen, *Fundamental Principles of Polymeric Materials*, Wiley, New York, 1993. J. Ferry, *Viscoelastic Properties of Polymers*, 3rd ed., Wiley, New York, 1980. N. Tschoegl, *The Phenomenological Theory of Linear Viscoelasticity*, Springer-Verlag, Berlin, 1989. C. Macosko, *Rheology Principles, Measurements, and Applications*, VCH, New York, 1994. J. Skrzypek, *Plasticity and Creep*, CRC Press, Boca Raton, FL, 1993. L. Nielsen and R. Landel, *Mechanical Properties of Polymers and Composites*, 2nd ed., Marcel Dekker, New York, 1994, pp. 89–120. J. Wu et al., *J. Rheol.*, 23, 231, 1979. N. Brown et al., *J. Polym. Sci. (Phys.)*, 16, 1085, 1978. C. Bucknall et al., *J. Mater. Sci.*, 7, 202, 1972.
29. L. Nielsen, *Mechanical Properties of Polymers and Composites*, Vol. 1, Marcel Dekker, New York, 1974.
30. R. Bird, R. Armstrong, and O. Hassager, *Dynamics of Polymer Liquids*, V1, Wiley, New York, 1987. E. Passaglia and H. Koppehele, *J. Polym. Sci.*, 33, 126, 2003.
31. L. Nielsen and R. Landel, *Mechanical Properties of Polymers and Composites*, 3rd ed., Dekker, New York, 1994, pp. 90–93.
32. R. de Baptist and A. Callen, *Physica Stat. Solidi (A)*, 21, 591, 2006. W. Brostow, J. Kubat, and M. Kubat, *Mech. Comp. Mater.*, 31, 591, 1995.

33. H. Fricker, *Proc. Royal Soc.(A) Math Phys. Sci.*, 335, 289, 1973. C. Macosko, *Rheology*, VCH, New York, 1994, 117–119.
34. A. Tobolsky, Stress relaxation studies, in *Rheology*, V2, F. Erich, Ed., Academic Press, New York, 1958, chap. 2. G.-H. Hsiue et al., *J. Applied Polym. Sci.*, 35, 995, 2003. A. Ajji et al., *Polymer*, 41, 7139, 2000.
35. F. Maurer et al., *Rheologica Acta*, 24, 1435, 1985. G. McKenna and A. Lee, *J. Polym. Sci. B: Polym. Phys.*, 35, 1167, 1998. M. Patel et al., *Polym. Degradation and Stability*, 87, 201, 2005. L. Nielsen and R. Landel, *Mechanical Properties of Polymers and Composites*, 3rd ed., Dekker, New York, 87, 1994. G. McKenna et al., *Polym. Eng. Sci.*, 37, 1429, 1997.
36. J. Wu and N. Brown, *J. Rheol.*, 23, 231, 1979. M. Delins and G. McKenna, *Mech. Time-Dependent Mater.*, 4, 1385, 2000.
37. P. Sherman, *Food Texture and Rheology*, Academic Press, London, 1979, p. 291.
38. H. Lu, J. Stansbury, and C. Bowman, *Dent. Mater.*, 20, 979, 2003. N. Katakura, S. Rikogaku Zasshi, 18, 118, 1977. S. Zufall and R. Kusy, *Eur. J. Orthod.*, 22, 1, 2000.
39. J. Van Miltenburg, *Text. Res. J.*, 61, 363, 1991.
40. R. Simha et al., *Polym. Eng. Sci.*, 29, 622, 2004.
41. R. Hahn et al., *Int. J. Pressure Vessels and Piping*, 79, 45, 2002. L. Kowalczyk, *Determination of Stress Relaxation in Non-metallic Gaskets*, DTIC #ADD461130, Defense Technical Information Center, Washington D.C., 1964. R. Pazur, J. Bielby, and U. Dingles, *Rubber World*, 2, 16, 2004. R. Scavuzzo, *J. Pressure Vessels Tech.*, 122, 386, 2000.
42. R. Rohde and J. Swearengen, *Metal Deformation Modeling SAND-78-0164*, Sandia National Labs, Sandia, NM, 1978. P. Ho et al., *J. Mater. Res.*, 21, 1512, 2006.
43. M. Tirrell, Linear viscoelasticity at the 21st short course on rheometry, University of Minnesota, Minneapolis, 1996.
44. M. Shaw and W. MacKnight, *Introduction to Polymer Viscoelasticity*, Wiley, New York, 2005, pp. 114–116.
45. W. Brostow, N. D'Sousa, J. Kubat, and R. Maksimov, *J. Chem. Phys.*, 110, 9706, 1999. A. Akinay, W. Brostow, V. Castano, R. Maksimov, and P. Olszynski, *Polymer*, 43, 3593, 2002.
46. C. Daley and K. Menard, *NATAS Notes*, 26(2), 56, 1994.
47. ASTM International, *Annual Book of Standards*, Rubber, West Conshohocken, PA, 2006, ASTM D395–Compression set.

4 Thermomechanical Analysis

One could argue that the standard type of thermomechanical analysis (TMA) tests, in which a very small load is applied to a sample, is really a subset of creep testing. However, TMA really needs to be addressed on its own for several reasons. First, the load applied for the classic TMA experiment, the measure of expansion, is really just enough to assure constant contact of the probe. Second, TMA looks not at the sample's response to the load in an expansion study but the material's response to changing temperature in terms of dimensional changes and the transitions that occur in the material. Also thermomechanical analyzers tend to be a different type of instrument, smaller and with better temperature control than the instruments used for measuring qualities like Young's modulus, viscosity, and creep, although the newer DMAs are now capable of these measurements.¹ Because of its convenient size and more precise temperature control associated with its smaller sample size, the TMA is a common instrument in many thermal laboratories and is the first mechanical analyzer used by many chemists. One could even suggest that all rheology and traditional mechanical tests should be included in this classification. In its purest form, TMA records changes in a material's dimensions under minimal load and these are used as an indicator of the changes in the material's free volume. This data allows the calculation of a material's expansivity or coefficient of thermal expansion (CTE; sometimes written LCTE for linear coefficient of thermal expansion to differentiate it from the volumetric expansion) as well as detection of transitions in the material. TMA on inorganic glass was the first measurement of the glass transition and it still remains the preferred technique for that measurement in many applications. It is often said to be more sensitive to the glass transition than differential scanning calorimetry (DSC) by an order of magnitude. However, its greatest advantage is obtaining the CTE value as part of the data.

4.1 THEORY OF THERMOMECHANICAL ANALYSIS

The basis of TMA is the change in the dimensions of a sample as a function of temperature. A simple way of looking at TMA is as a very sensitive micrometer. TMA is believed to have developed from hardness or penetration tests and first reported as being used on polymers in 1948. Subsequently, it has developed into a powerful tool in the analytical laboratory. TMA² measurements record changes caused by changes in the free volume of a polymer.³ Changes in free volume, v^f , can be monitored as the volumetric change in the polymer, the absorption or release of heat associated with that change, the loss of stiffness, increased flow, or the change in relaxation time. The free volume of a polymer, v^f , is known to be related to viscoelasticity,⁴ aging,⁵ penetration by solvents,⁶ and impact properties.⁷ Defined as the space a molecule has

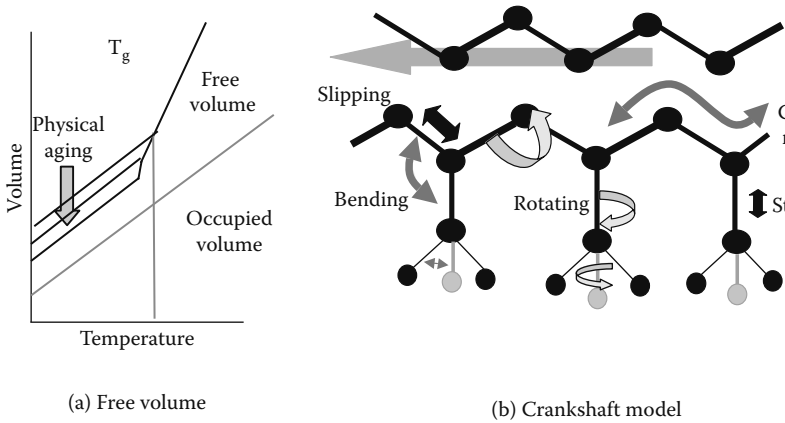


FIGURE 4.1 Free volume, v^f , in polymers: (a) the relationship of free volume to transitions, and (b) a schematic example of free volume and the crankshaft model. Below the T_g in (a) various paths with different free volumes exist depending on heat history and processing of the polymer, where the path with the least free volume is the most relaxed. (b) shows the various motions of a polymer chain. Unless enough free volume exists, the motions cannot occur.

for internal movement, it is schematically shown in Figure 4.1a. As the space available for the chains to move increases, larger and larger segments may move, giving rise to thermal transitions. This is often called the crankshaft model and is shown in Figure 4.1b.

The T_g in a polymer corresponds to the expansion of the free volume allowing greater chain mobility above this transition and in TMA this is what we measure by thermal expansion (Figure 4.2). Real life does not show as sharp a T_g as shown here.

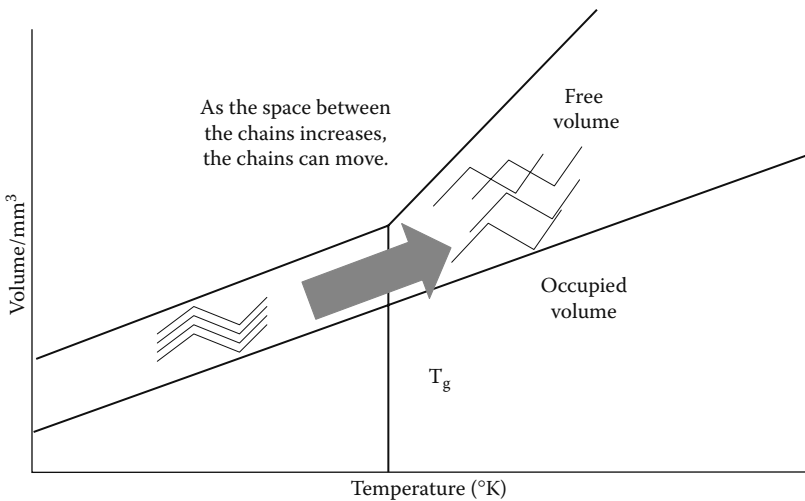


FIGURE 4.2 The increase in free volume is caused by increased energy absorbed in the chains and this increased free volume permits the various types of chain movement to occur.

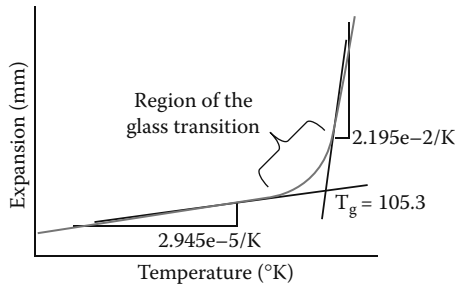


FIGURE 4.3 The T_g is a region, shown here between the points where the tangents depart from the curve. The T_g , by convention, is taken as the intersection of those two tangents.

Seen as an inflection or bend in the thermal expansion curve, this change in the TMA can be seen to cover a temperature range due to the distribution of molecular weights and relaxations times in a polymer. What we call a glass transition temperature or T_g is an indication of this range calculated by an agreed upon method (Figure 4.3). This fact seems to be forgotten by inexperienced users, who often worry why perfect agreement isn't seen in the value of the T_g when comparing different methods. The width of the T_g can be as important an indicator of changes in the material as the actual temperature.

4.2 EXPERIMENTAL CONSIDERATIONS WITH TMA SAMPLES

Experimentally, TMA consists of an analytical train that allows precise measurement of position and can be calibrated against known standards. A temperature control system of a furnace, heat sink, and temperature measuring device (most commonly a thermocouple) surrounds the samples (Figure 4.4a). Fixtures to hold the sample during the run are normally made out of quartz because of its low CTE, although ceramics and invar steels may also be used. Fixtures are commercially available for expansion, three-point bending or flexure, parallel plate, and penetration tests (Figure 4.4b), but specialized fixtures are common. Sample preparation varies with the method. Samples for CTE are the most difficult to prepare as ideally they are rectangular samples, with parallel and flat top and bottom sides. For anisotropic material, a cube is preferred with all sides parallel and squared. As large a sample as can be evenly heated should be prepared as this increases the accuracy of the CTE measurement. For glasses, samples of 2–5 inches in length are often used. Other geometries are more forgiving; in flexure tests of composites, a sliver of material taken off the edge of the sample with a blade is often used.

TMA applications are in many ways the simplest of the thermal techniques. We are just measuring the change in the size or position of a sample. However, they are also incredibly important in supplying information needed to design and process everything from chips to food products to engines. A sampling of ASTM methods

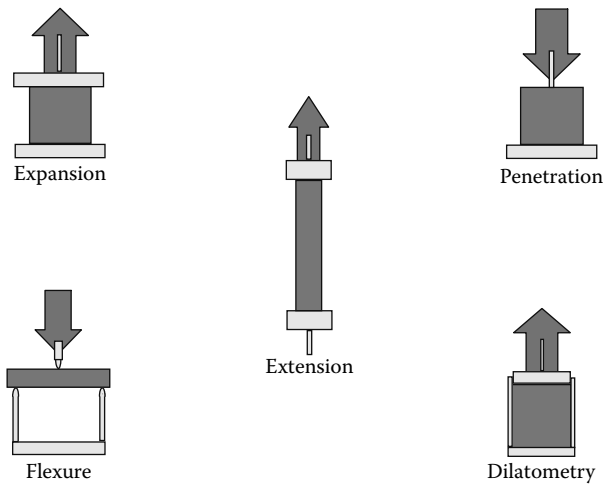


FIGURE 4.4 Testing geometries used for TMA measurements. Fixtures are often traditionally made in low expansion materials, like quartz glass or ceramics. Modern instruments and software allow correction for the fixture expansion and this permits the use of more robust materials like steel and titanium to also be used.

TABLE 4.1
ASTM Methods for TMA

- D4065-06 Standard Practice for Plastics: Dynamic Mechanical Properties: Determination and Report of Procedures
 - D4092-01 Standard Terminology: Plastics: Dynamic Mechanical Properties
 - E1363-03 Standard Test Method for Temperature Calibration of TMA
 - E1545-05 Standard Test Method for Assignment of the Glass Transition Temperature by TMA
 - E1953-07 Standard Practice for Description of Thermal Analysis and Rheology Apparatus
 - E2092-04 Standard Test Method for Distortion Temperature in Three-Point Bending by TMA
 - E2113-04 Standard Test Method for Length Change Calibration of TMA
 - E2206-06 Standard Test Method for Force Calibration of TMA
 - E2347-05 Standard Test Method for Indentation Softening Temperature by TMA
 - E831-06 Standard Test Method for Linear Thermal Expansion of Solid Materials by TMA
 - WK4278 Standard Test Method for Length Change Calibration of TMA
 - WK4747 Standard Test Method for Coefficient of Linear Thermal Expansion of Electrical Insulating Materials
 - WK5117 Standard Practice for Description of Thermal Analysis Apparatus
 - WK7944 Standard Test Method for Coefficient of Linear Thermal Expansion of Electrical Insulating Materials
 - WK9075 Standard Method for Force Calibration of TMA
-

for TMA is shown in Table 4.1. Because of the sensitivity of the modern TMA, it is often used to measure T_g 's that are difficult to obtain by DSC, such as those of highly crosslinked thermosets.

4.3 EXPANSION AND CTE

TMA allows the calculation of the thermal expansivity⁸ from the same data set used to calculate the T_g . Since many materials are used in contact with a dissimilar material in the final product, knowing the rate and amount of thermal expansion helps in designing around mismatches that can cause failure in the final product. This data is only available when the T_g is collected by thermal expansion, not by the flexure or penetration method. This is in many ways the simplest or most essential form of TMA measurement. A sample is prepared with parallel top and bottom surfaces and the sample is allowed to expand under minimal load (normally 5 mN or less, ideally it would be 0 mN) as it is slowly heated and cooled. Samples range down to micron-thick films but as thick a sample as possible should be used to minimize errors. For polymers, 5 mm tall blocks are common. Heating rates are normally kept low to allow equilibration of the sample to the furnace temperature. CTE is calculated by

$$\alpha_l = 1/l_0 (\delta l/\delta T)F \quad (4.1)$$

where α_l is the linear coefficient of thermal expansion, l_0 is the original length, δl is the change in length, and δT is the change in temperature. The F indicates this is done under constant force. Once this value is obtained, it can be used to compare the other materials used in the same produce. Large differences in the CTE can lead to motors binding, solder joints failing, composites splitting on bond lines, or internal stress build up. The T_g is obtained from the same data by measuring the inflection point in changes of slope of the baseline. As a material's CTE changes dramatically at T_g , one would expect this to be an easily detected transition. It can be but for highly crosslinked materials, the T_g can be so broad and the change in CTE so slight as to be undetectable. Other approaches, like flexure testing, are therefore used. Different T_g values will be seen for each mode of testing⁹ (Figure 4.5) and it is necessary to report the method one used to get the T_g by TMA. Values on CTE vary greatly from quartz (~0.5 ppm) to stainless stain (11 ppm) to high polymers (~25 ppm). In tension, where metal fixtures are often used, it is common to subtract the baseline signal from the data (Figure 4.5c).

If the material is heterogeneous or anisotropic, it will have different thermal expansions depending on the direction in which they have been measured. For example, a composite of graphite fibers and epoxy will show three distinct thermal expansions corresponding to the x, y, and z direction. Blends of liquid crystals and polyesters show a significant enough difference between directions that the orientation of the crystals can be determined by TMA.¹⁰ Similarly, oriented fibers and films have a different thermal expansivity in the direction of orientation than in the

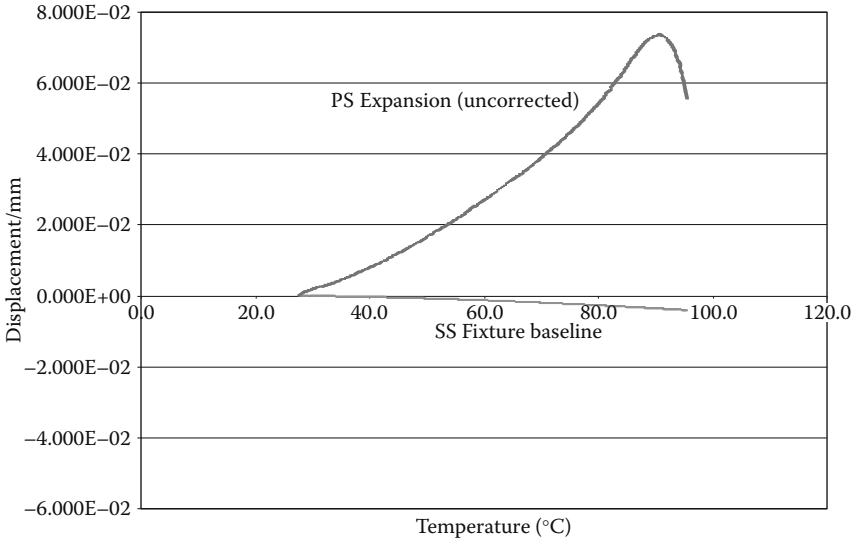
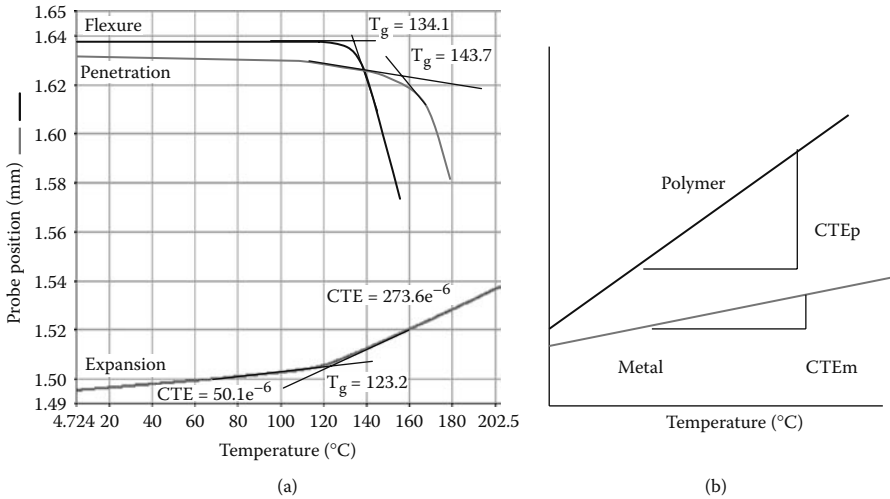


FIGURE 4.5 Different methods of measuring the T_g in TMA give different values as shown in (a) the overlay of the penetration, flexure, and expansion runs; (b) the comparison of a polymer to a metal CTE run; (c) the baseline and uncorrected sample expansion for polystyrene. For an accurate CTE value, one must subtract the baseline from the data. Note that at the T_g , the material has softened enough that it collapses and begins to contract.

unoriented direction. This is normally addressed by recording the CTE in the x, y, and z directions (Figure 4.6a). Bulk measurements or volumetric expansion can be made by dilatometry as shown in Figure 4.6b and this is discussed in detail in Section 4.5.

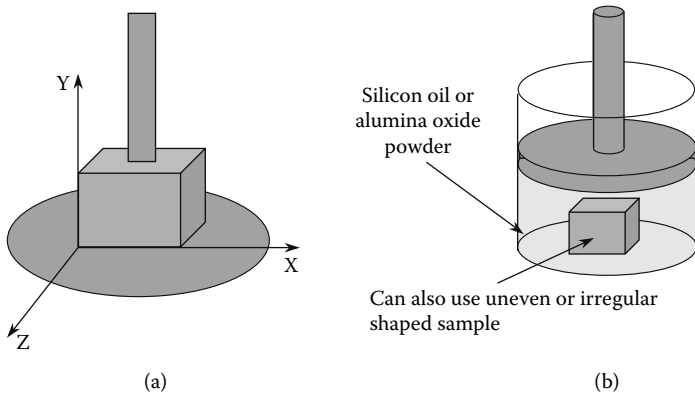


FIGURE 4.6 Heterogeneous samples require the CTE to be determined in (a) the x, y, and z planes or (b) in bulk to obtain a volumetric expansion in the dilatometer.

Expansion studies can also be run on samples immersed in solvents to measure the swelling of a polymer. This test is commonly used with rubbers to measure the crosslink density of the rubber.¹¹ As crosslinking increases, the amount of swelling will decrease. Special fixtures are commercially available for this or standard fixtures may be used in a lined furnace. A sample is immersed in oil and the degree of swelling measured. Figure 4.7 shows results from a rubber swelling study as an instrument set up in an immersion bath to allow this type of testing.

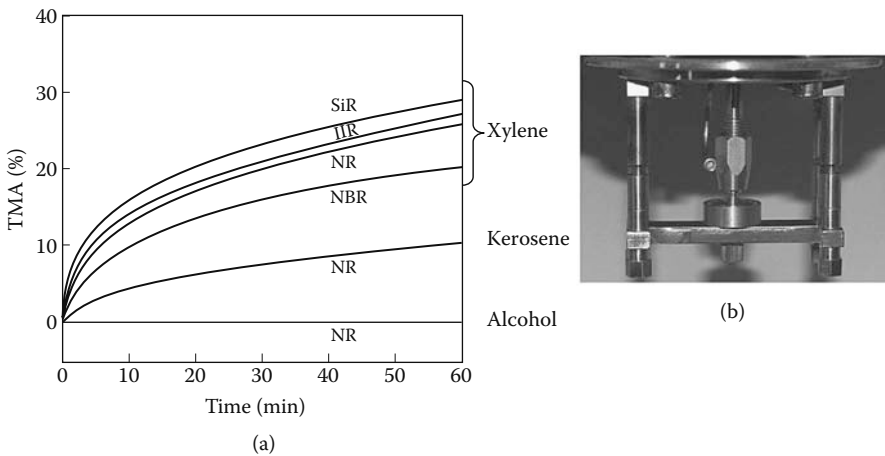


FIGURE 4.7 (a) Swelling of rubber samples in organic solvents measured in the Diamond TMA. NR = natural rubber, NBR = nitrile butyl rubber, SiR = silicon rubber, and IIR = isobutyl rubber. (b) The PerkinElmer DMA 8000 is the only instrument designed with an integrated fluid bath for this kind of work. Used with the permission of the PerkinElmer Instruments LAS, Shelton, Connecticut.

4.4 FLEXURE AND PENETRATION

TMA methods are used in geometries more commonly associated with traditional mechanical testing to increase sensitivity or to mimic other tests. The most common of these are the flexural and penetration modes.

Flexure studies involve loading a thin beam, often a splinter of material with a constant load of 100 mN or more, and heating it until the sample deflects. This is similar to a heat distortion test and is often used for quality control as it gives clear, easily detected transitions. Samples, being small, can be heated at moderate rates and 5°C/min is often used. The lower platform can be as small as 3 mm and may be made out of quartz or steel.

Thin coatings are often better handled by penetration tests, when a small quartz or steel probe (1 mm or less) is used to penetrate into the sample. This technique involves moderate forces and allows one to measure the transitions of a material as thin as 10 microns. It is often used for polymers mimicking some of the mechanical tests developed in that industry.¹² Baseline subtraction is often used to remove any effects from the substrate's thermal expansion during the test. An example of a penetration run is shown in Figure 4.8. As mentioned earlier, these methods often give different values for the T_g and O'Neal, et al. did a fairly extensive study on how the method of testing affected the T_g .¹³ Their work reports that the expansion method gives the lowest value for T_g by TMA. The flexure method tends to give a T_g that is 5°C higher. By the penetration method, the T_g was 10°C higher than what the expansion method reports. While this was specific to an epoxy-graphite composite, similar trends have been seen in other polymers. Despite the slightly higher values for transitions, the penetration method is often preferred as the expansion method is notorious for giving results that require a large amount of skill to interpret. Both the flexure and penetration methods are much easier to interpret and minimize the influence of the operator.

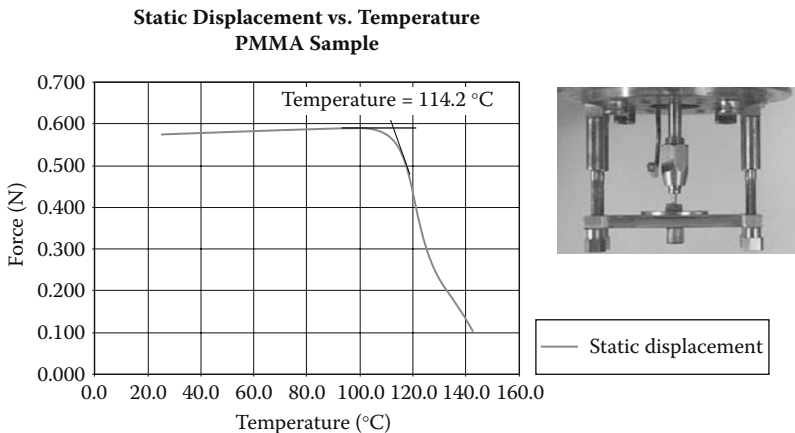


FIGURE 4.8 Data from a penetration run on PMMA using a PerkinElmer DMA 8000 and the show penetration accessory. Data collected by the author.

4.5 DILATOMETRY AND BULK MEASUREMENTS

Another approach to anisotropic materials instead of the testing in all three directions as discussed earlier is to measure the bulk expansion of the material using dilatometry (Figure 4.6b). The technique itself is fairly old and was commonly used with glass dilatometers, where one followed very precisely the change in the level of a liquid. It was used extensively to study initial rates of reaction for bulk styrene polymerization in the 1940s,¹⁴ an experiment that the author has used in his thermal analysis class on the TMA. By immersing the sample in a fluid (normally silicon oil) or powder (normally Al_2O_3) in the dilatometer, the expansions in all directions are converted to a vertical movement, which is measured by the TMA. This technique has enjoyed a renaissance in the last few years because modern TMAs make it easier to perform than previously. It has been particularly useful for studying the contraction of a thermoset during its cure.^{15,16} The technique itself is rather simple: a sample is immersed in either a fluid like silicone oil or buried in alumina oxide in the dilatometry and run through the temperature cycle. If an actual dilatometer is used, the plunger is inserted and rests on the medium. For powdered samples, it is common to place them in a dish and put a quartz disk on top. The probe itself normally has too small a surface area to cover the sample. While quartz is preferred for its low expansion, other materials are used. If a pure liquid or a monomer is used, the dilatometer is filled with that liquid instead of the silicon oil or alumina oxide. A coefficient of thermal expansion can be determined and Speyer reports that as well as discusses the technique in detail.¹⁷ Conceptually, it is not a hard technique; however, practically it can be tricky. I find it necessary to run a baseline of the system in most cases and care in loading the dilatometer is essential. As with any expansion measurement, the more sample you use, the better data you can get. You have to scan more slowly to allow for even heating but often the improvement in the data is worth it.

Recently, dilatometry in TMA has also been used to obtain both the glass transitions¹⁸ and CTE¹⁹ of lyophilized materials. These materials are normally powders and traditional mechanical tests do not easily support testing them. Dilatometry is a surprisingly simple way to test these materials to gain confirming data for high ramp-rate DSC studies as shown in Figure 4.9.²⁰ In addition, dilatometry on the sugar solutions freeze-dried to make the above materials has been reported.²¹ This requires floating a polyethylene disk on the surface in place of the quartz disk or plunger normally used.

4.6 MECHANICAL TESTS

A wide variety of tests are performed in TMA that are adapted from physical tests that were used before the instrument became commonly available.²² These tests may also be modeled or mimicked in TMA, like heat distortion (Figure 4.10) and Vicat,²³ film softening,²⁴ and softening points.²⁵ Methods to obtain the modulus,²⁶ compressive viscosity,²⁷ and penetrative viscosity²⁸ have been developed. Many of these methods, like ASTM D648 for example, will specify the stress the sample needs to be exposed to during the run. In D648 for example, a sample is tested at 66 and 264 psi. Most TMAs on the market today have software available that allows them

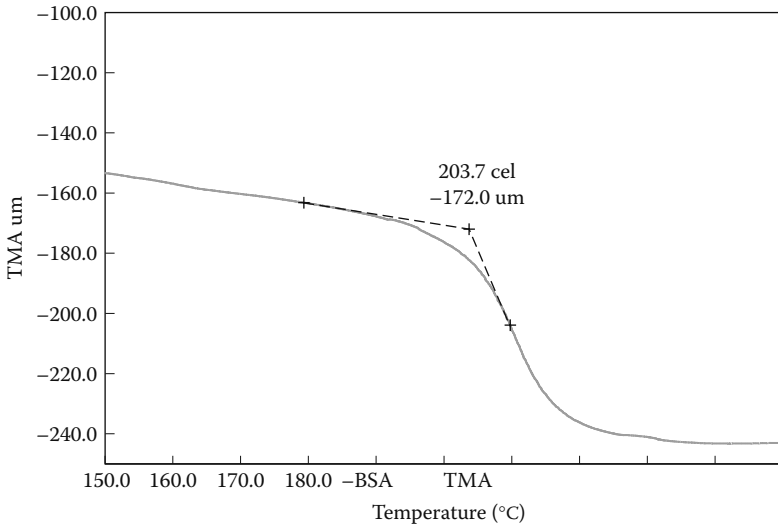


FIGURE 4.9 Dilatometry on a sample of bovine serum albumin run using a modified dilatometry approach. Fifty mN of force was used on a sample in a 5 mm quartz dilatometer. As the Tg is approached, the sample collapses and the Tg appears as drop in the probe position.

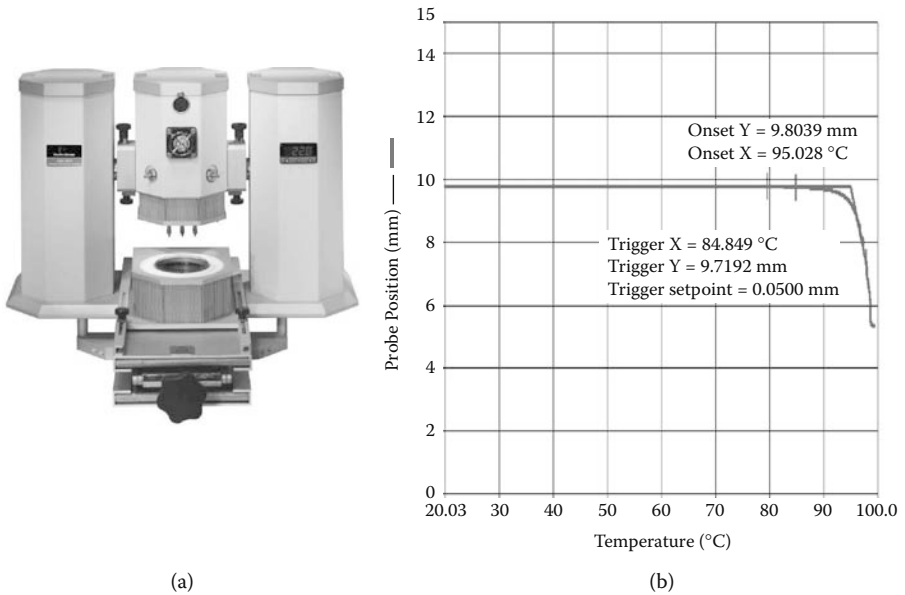


FIGURE 4.10 Heat distortion tests (HDT), can be run in TMA or DMA with a fluid bath as shown in (a). The above (b) shows the results of the HDT runs. Vicat testing is also done and gives similar results.

to generate stress–strain curves and to run creep–recovery experiments.²⁹ Some are also capable of limited types of stress relaxation studies (for example, a constant gauge length test).³⁰

4.7 PVT RELATIONSHIP STUDIES

The temperature of a polymer's melting, its glass transition, its crystallization, and its solid state annealing are all known to have pressure dependencies.³¹ High-pressure instruments, such as the Gnomix, have been developed to study pressure–volume–temperature (PVT) relationships in polymers. In these experiments, the sample is placed in an incompressible fluid and then the desired pressure is applied. Full details of this technique as well as a collection of PVT relationships for a wide range of polymers up to 200 MPa (~30,000 psi) and 400°C have recently been published.³² This data has been mainly collected isothermally to report the effects of pressure and temperature on the volume of the polymer and to monitor the respective changes in melt and glass transitions. For example, data on polymer liquid crystals have been obtained as a function of the concentration of the liquid crystal (rigid) constituent in a series of copolymers.³³

The measurement of the volume of the polymer above and below the glass transition under high pressure is an attempt to determine the occupied volume of the polymer. As the pressure is increased, the glass transition, which occurs in the free volume, becomes generally greater and broader (Figure 4.11) as the material changes between two different types of glasses before the T_g is reached. This pressure

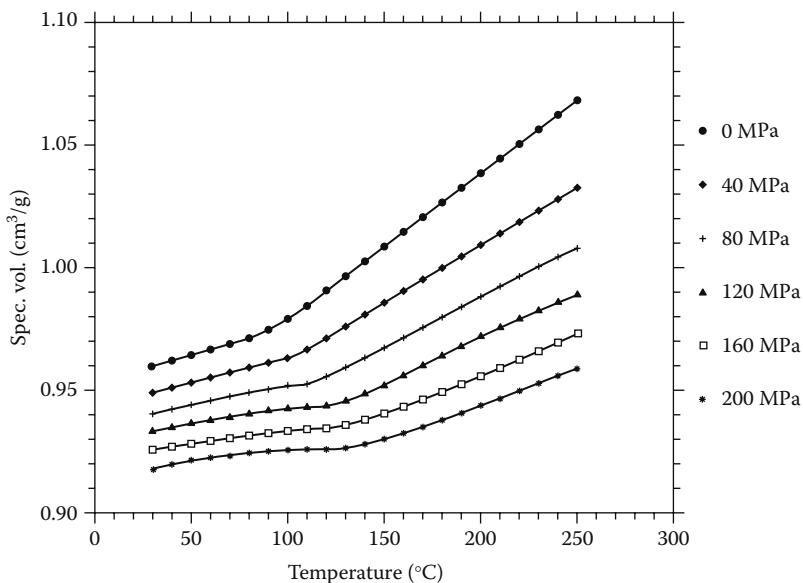


FIGURE 4.11 The effect of pressure of the T_g of a polystyrene ($M \sim 1.1e5$, $D \sim 1.06$) from Zoller's *Standard Pressure–Volume–Temperature Data for Polymers*. Used with the permission of the Technomics Publishing Company, Inc.

sensitivity can be useful information for determining processing conditions. While the Gnomix can apply pressures that greatly exceed any high pressure differential scanning calorimeter (HP DSC), the experimental times are long and DSC may be more useful for studies up to ~6.8 MPa (~1000 psi). The agreement between these techniques is quite good³⁴ and hence HP DSC, within its limits, is a suitable alternative in a number of cases to a PVT instrument.

NOTES

1. J. Duncan, Principles and applications of mechanical thermal analysis, in *Principles and Applications of Thermal Analysis*, P. Gabbot, Ed., Blackwell, Oxford, 2007.
2. V. Kargin et al., *Dokl. Akad. Nauk SSSR*, 62, 239, 1948.
3. R. Bird, C. Curtis, R. Armstrong, and O. Hassenger, *Dynamics of Polymer Fluids*, 2nd ed., Wiley, New York, 1987.
4. J.D. Ferry, *Viscoelastic Properties of Polymers*, 3rd ed., Wiley, New York, 1980. M. Shaw and W. MacKnight, *Introduction to Polymer Viscoelasticity*, 3rd ed., Wiley, New York, 2005.
5. L.C.E. Struik, *Physical Aging in Amorphous Polymers and Other Materials*, Elsevier, New York, 1978. L.C.E. Struik, *Failure of Plastics*, W. Brostow and R.D. Corneliusen, Eds., Hanser, New York, 1986. S. Matsuoka, *Failure of Plastics*, W. Brostow and R.D. Corneliusen, Eds., Hanser, New York, 1986. S. Matsuoka, *Relaxation Phenomena in Polymers*, Hanser, New York, 1992.
6. J.D. Vrentas, J.L. Duda, and J.W. Huang, *Macromolecules*, 19, 1718, 1986.
7. W. Brostow and M.A. Macip, *Macromolecules*, 22(6), 2761, 1989.
8. Thermal expansivity is often referred to as the coefficient of thermal expansion or CTE by polymer scientists and in the older literature. The terms are used interchangeably in this paper.
9. G. Curran, J. Rogers, H. O'Neal, S. Welch, and K. Menard, *J. Adv. Mater.*, 26(3), 49, 1995.
10. W. Brostow, A. Arkinay, H. Ertepinar, and B. Lopez, *POLYCHAR-3 Proc.*, 3, 46, 1993.
11. J. Mark, Ed., *Physical Properties of Polymers Handbook*, American Institute of Physics, Woodbury, NY, 1996. A. Beerblower and J. Dickey, *Am. Soc. Lubr. Eng. Trans.*, 12, 1, 1969.
12. A. Riga, *Polym. Eng. Sci.*, 14, 764, 2004. T. Ozawa, *J. Therm. Anal. Calorimetry*, 40, 1388, 1993. V. Shah, *Handbook of Polymer Analysis*, Wiley, New York, 1984. A. Riga and M. Neag, *Materials Characterization by Thermomechanical Analysis, ASTM STP 1136, ASTM*, Barr Harbor, 1991.
13. H. O'Neal, G. Curran, J. Rogers, S. Welch, and K. Menard, *J. Adv. Mater.*, 26(3), 49, 1995.
14. R. Boundy, R. Boyer, and S. Stoesser, Eds., *Styrene, Its Polymers, Copolymers, and Derivatives*, Reinhold, New York, 1952.
15. A. Snow and J. Armistead, *J. Appl. Polym. Sci.*, 52, 401, 1994.
16. B. Bilyeu and K. Menard, *POLYCHAR-6 Proceedings*, 1998. B. Bilyeu, W. Brostow, and K. Menard, *Polimetry*, 46, 794, 2001.
17. R. Speyer, *Thermal Analysis of Materials*, Marcel Dekker, New York, 1993, p. 165. This book has chapters on many of the less common techniques like dilatometry, interferometry, thermal conductivity, and pyrometry as well as the more standard ones.

18. D. Katayma, J. Carpenter, M. Manning, T. Rundolph, P. Setlow, and K. Menard, *J. Pharm. Sci.*, in press. J. Carpenter, W. Chonkaew, L. Liu, and K. Menard, Thermomechanical methods of measuring the Tg of protein-exciipient mixtures, *Protein Stability Conference*, 2007, p. 57.
19. J. Magoshi et al., *J. Appl. Polym. Sci.*, 45, 2043, 1992. T. Chen and D. Oakley, *Thermochimica Acta*, 248, 229, 1995. S. Yokoto et al. *Int. J. Pharm.*, 286, 53, 2004.
20. D. Katayma, J. Carpenter, M. Manning, T. Rundolph, P. Setlow, and K. Menard, *J. Pharm. Sci.*, in press. J. Carpenter, W. Chonkaew, L. Liu, and K. Menard, Thermomechanical methods of measuring the Tg of protein-exciipient mixtures, *Protein Stability Conference*, 2007, p. 57.
21. J. Rose, Rose Consulting, Half Moon Bay, CA. Private communication.
22. R. Cassel and R. Fyans, *Industrial Research*, August 1977, p. 44. R. Cassel, *Thermal Application Study*, 1977, p. 20.
23. A. Riga, *Polym. Eng. Sci.*, 14, 764, 2004. T. Ozawa, *J. Therm. Anal. Calorimetry*, 40, 1388, 1993. V. Shah, *Handbook of Polymer Analysis*, Wiley, New York, 1984. A. Riga and M. Neag, *Materials Characterization by Thermomechanical Analysis*, ASTM STP 1136, ASTM, Conshohocken, PA, 1991. O. Carter, *Thermochimica Acta*, 4, 199, 1972.
24. Testing method for softening temperature of film by TMA, *JIS K 7196:1991*, Japan Standards Association, Tokyo, 1991. An ASTM method is currently in development.
25. R. Cassel and R. Fyans, *Industrial Research*, August 1977, p. 44. R. Cassel, *Thermal Application Study*, 1977, p. 20.
26. R. Cassel and R. Fyans, *Industrial Research*, August 1977, p. 44. R. Cassel, *Thermal Application Study*, 1977, p. 20.
27. P. Webber and J. Savage, *J. Mater. Sci.*, 23, 783, 1983. H. Tong and G. Appleby-Hougham, *J. Appl. Polym. Sci.*, 31, 2509, 1986.
28. M. McLin and A. Angell, *Polymer*, 37, 4703, 1996.
29. See, for example, the product literature for PerkinElmer's Diamond 8000 and the older TMAs run in PYRIS™ software. The thermomechanical analyzer and the dynamic mechanical analyzer can both be used for running simple mechanical tests like stress-strain curves, creep-recovery, heat set, and stress relaxation. Other vendors have similar packages.
30. C. Daley and K. Menard, *North American Thermal Analysis Society Notes*, 26 (1), 56, 1994.
31. P. Zoller and Y. Fakhreddine, *Thermochimica Acta*, 238, 397, 1994.
32. P. Zoller and D. Walsh, *Standard Pressure-Volume-Temperature Data for Polymers*, Technomic Publishing, Lancaster, PA, 1995.
33. J. Berry, W. Brostow, M. Hess, and E. Jacobs, *Polymers*, 39, 243, 1998.
34. J. Berry, W. Brostow, M. Hess, and E. Jacobs, *Polymers*, 39, 243, 1998.

5 Dynamic Testing and Instrumentation

In this chapter, we will address the use of a dynamic force to deform a sample. We have already looked at how a polymer exhibits both elastic (spring-like) and viscous (dashpot-like) behavior and that combination of these elements allows us to devise simple models of polymer behavior. We have seen that polymers have a time-dependent form of behavior and a “memory.” Finally, we saw that free volume of polymers is a function of temperature. This last point will become very important in explaining dynamic mechanical analysis (DMA) data.

In this chapter we shall begin by discussing the application of a dynamic force to a polymeric material. We will take a look at instrumentation, its calibration, and the fixtures used. In the following chapters, we will address the question of scanning temperature (Chapters 6 and 7), and varying frequency (Chapter 8). We will also look at melts and fluids (Chapter 8) and some less traditional applications (Chapter 9).

5.1 APPLYING A DYNAMIC STRESS TO A SAMPLE

If we take a sample at constant load and start a sinusoidal oscillation of the applied stress (Figure 5.1), the sample will deform sinusoidally. This will be reproducible if we keep the material within its linear viscoelastic region. For any one point on the curve, we can determine the stress applied as

$$\sigma = \sigma_0 \sin \omega t \quad (5.1)$$

where σ is the stress at time t , σ_0 is the maximum stress, and ω is the frequency of oscillation. The resulting strain wave shape will depend on how much viscous behavior the sample has as well as how much elastic behavior. In addition, we can write a term for the rate of stress by taking the derivative of Equation 5.2 in terms of time

$$d\sigma/dt = \omega\sigma_0 \cos \omega t \quad (5.2)$$

We can look at the two extremes of the materials behavior, elastic and viscous, to give us the limiting extremes that will sum to give us the strain wave. Let's start by treating the material as each of the two extremes discussed in Chapter 2. The material at the spring-like or Hookean limit will respond elastically with the oscillating stress. The strain at any time can be written as

$$\epsilon(t) = E \sigma_0 \sin (\omega t) \quad (5.3)$$

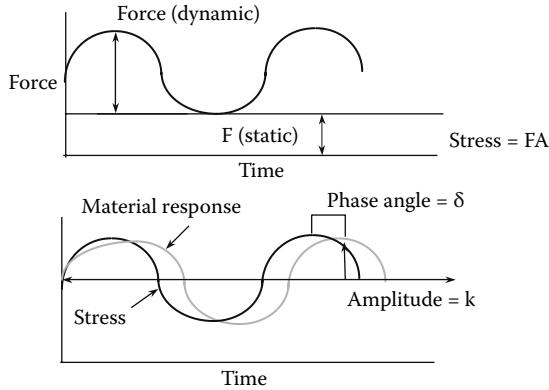


FIGURE 5.1 When a sample is subjected to a sinusoidal oscillating stress, it responds in a similar strain wave provided the material stays within its elastic limits.

where $\epsilon(t)$ is the strain at time t , E is the modulus, σ_0 is the maximum stress at the peak of the sine wave, and ω is the frequency. Since in the linear region σ and ϵ are linearly related by E , we can also write that

$$\epsilon(t) = \epsilon_0 \sin(\omega t) \quad (5.4)$$

where ϵ_0 is the strain at the maximum stress. This curve, shown in Figure 5.2a, has no phase lag (or no time difference from the stress curve) and is called the in-phase portion of the curve.

The viscous limit was expressed as the stress being proportional to the strain rate, which is the first derivative of the strain. So if we take the dashpot we discussed before, we can write a term for the viscous response in terms of strain rate as

$$\epsilon(t) = \eta d\sigma_0/dt = \eta\omega\sigma_0 \cos(\omega t) \quad (5.5)$$

or

$$\epsilon(t) = \eta\omega\sigma_0 \sin(\omega t + \pi/2) \quad (5.6)$$

where the terms are as above and η is the viscosity. We can also replace terms as above to write this as

$$\epsilon(t) = \omega\epsilon_0 \cos(\omega t) = \omega\epsilon_0 \sin(\omega t + \pi/2) \quad (5.7)$$

This curve is shown in Figure 5.2b. Now, let's take the behavior of the material that lies between these two limits. That curve is shown in Figure 5.2c and is intermediate between the above cases. The difference between the applied stress and the

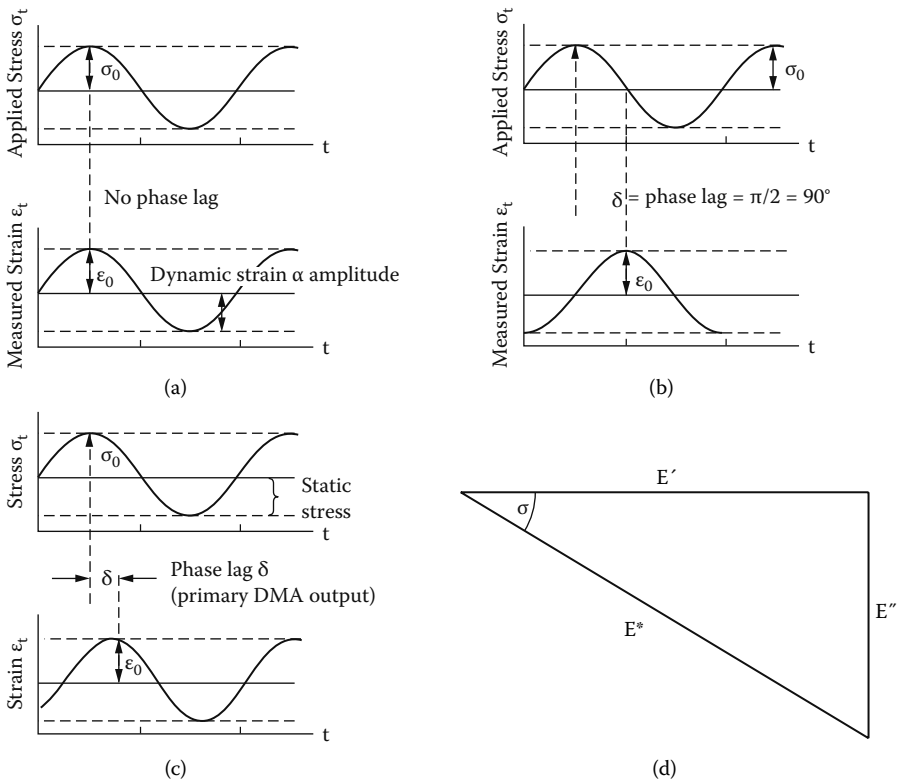


FIGURE 5.2 (a) When the material response to the applied wave perfectly elastic, an in-phase response is seen, while (b) a viscous response gives an out-of-phase response. (c) Viscoelastic materials fall in between these two lines. (d) The relationship between the phase angle, E^* , E' , and E'' is graphically shown. Used with the permission of the PerkinElmer Corporation, Life and Analytical Sciences (LAS), Norwalk, Connecticut.

resultant strain is an angle, δ , and this must be added to equations. So the elastic response at any time can now be written as

$$\epsilon(t) = \epsilon_0 \sin(\omega t + \delta) \tag{5.8}$$

From this we can go back to our old trigonometry book and rewrite this as

$$\epsilon(t) = \epsilon_0 [\sin(\omega t) \cos \delta + \cos(\omega t) \sin \delta] \tag{5.9}$$

We can now break this equation, corresponding to the curve in Figure 5.2c, into the in-phase and out-of-phase strains that correspond to curves like those in Figure 5.2a and b, respectively. These sum to the curve in 5.2c and are

$$\epsilon' = \epsilon_0 \sin(\delta) \tag{5.10}$$

$$\epsilon'' = \epsilon_0 \cos(\delta) \tag{5.11}$$

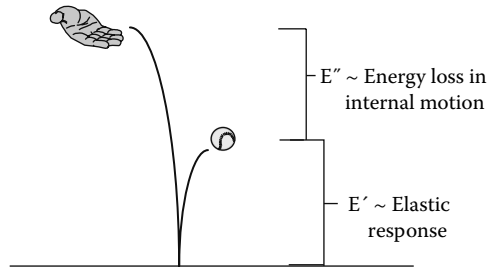


FIGURE 5.3 When a ball is bounced, the energy initially put is divided into two parts, a recovered part (how high it bounced) that can be described as E' and the energy lost to friction and internal motions (the difference between the height dropped from and the bounce) called E'' .

and the vector sum of these two components gives us the overall or complex strain on the sample

$$\epsilon^* = \epsilon' + i\epsilon'' \quad (5.12)$$

This relationship can be seen as the triangle shown in Figure 5.2d and makes sense mathematically.¹ But what does it mean physically in terms of analyzing the polymer behavior?

Basically, this approach allows us to “break” a single modulus (or viscosity or compliance) into two terms: one related to the storage of energy and another related to the loss of energy. This can be seen schematically in the bouncing ball in Figure 5.3. One term lets us see how elastic the polymer is (its spring-like nature) while the other lets us see its viscous behavior (the dashpot). In addition, because all this requires is one sinusoidal oscillation of the polymer, we can get this information quickly rather than through modulus mapping or capillary flow studies.

5.2 CALCULATING VARIOUS DYNAMIC PROPERTIES

Based on our earlier discussion, a material that is under sinusoidal stress has some amount of strain at the peak of the sine wave and an angle defining the lag between the stress sine wave and the strain sine wave. All of the other properties for the DMA are calculated from these data.² We can first calculate the storage or elastic modulus, E' . This value is a measure of how elastic the material is and ideally is equivalent to Young’s modulus. This is not true in the real world for several reasons. First, Young’s modulus is normally calculated over a range of stresses and strains as it is the slope of a line while the E' comes from what can be considered a point on the line. Second, the tests are very different as in the stress–strain test, one material is constantly stretched, whereas it is oscillated in the dynamic test.

5.2.1 CALCULATION FROM DEFORMATION AND PHASE LAG

If we were to bounce a ball as shown in Figure 5.3, the storage modulus (also called the elastic modulus, the in-phase modulus, and the real modulus) would be related to the amount of energy the ball gives back (how high it bounces). E' is calculated as

$$E' = (\sigma^\circ/\epsilon^\circ) \cos \delta = (f_0/bk) \cos \delta \quad (5.13)$$

where δ is the phase angle, b is the sample geometry term, f_0 is the force applied at the peak of the sine wave, and k is the sample displacement at peak. The full details of developing this equation and the basic treatment of how DMA equations are derived is in Ferry.³ Similarly, Duncan gives a similar result developed from a stiffness approach, which we will look at later.⁴

The amount the ball doesn't recover is the energy lost to friction and internal motions. This is expressed as the loss modulus, E'' , also called the viscous or imaginary modulus. It is calculated from the phase lag between the two sine waves as

$$E'' = (\sigma^\circ/\epsilon^\circ) \sin \delta = (f_0/bk) \sin \delta \quad (5.14)$$

where δ is the phase angle, b is the sample geometry term, f_0 is the force applied at the peak of the sine wave, and k is the sample displacement at the peak.

The tangent of the phase angle is one of the most basic properties measured in DMA. Some earlier instruments only recorded phase angle and consequently the early literature uses the $\tan \delta$ as the measure for many properties. This property is also called the damping and is an indicator of how efficiently the material loses energy to molecular rearrangements and internal friction. It is also the ratio of the loss to the storage modulus and therefore is independent of geometry affects. It is defined as

$$\tan \delta = E''/E' = \eta'/\eta'' = \epsilon''/\epsilon' \quad (5.15)$$

where η' is the energy loss portion of the viscosity and η'' the storage portion. Because it is independent of geometry (the sample dimensions cancel out above), $\tan \delta$ can be used as a check on the possibility of measurement errors in a test. For example, if the sample size is changed and the forces are not adjusted to keep the stresses the same, the E' and E'' will be different (because modulus is a function of the stress; see Equations 5.13 and 5.14), but the $\tan \delta$ will be unchanged. A change in modulus with no change in the $\tan \delta$ should lead one to check the applied stresses to see if they are different.

Once we have calculated the basic properties all the other properties are calculated from them. Table 5.1 shows the calculation of the remaining properties from DMA. Note that complex viscosity has a dependence on the frequency in the denominator so that at 1 Hz, complex viscosity will overlap the complex modulus. Also note that converting E into G or the reverse requires the use of Poisson's ratio, ν . Out of these remaining properties, the most commonly used is the complex viscosity, η^* . The reasons for this are discussed in Chapter 8. The biggest reason is that data from

TABLE 5.1
Calculations of Material Properties by DMA

Damping	$\text{Tan } \delta = E''/E'$
Complex modulus	$E^* = E' + iE'' = \text{SQRT}(E'^2 + E''^2)$
Complex shear modulus	$G^* = E^*/2(1 + \nu)$
Complex viscosity	$\eta^* = 3G^*/\omega = \eta' - i\eta''$
Complex compliance	$J^* = 1/G^*$

frequency scans give a viscosity versus shear rate (or frequency) curve that can be obtained much faster than by other methods. The complex viscosity is given by

$$\eta^* = G^*/\omega = E^*/2(1 + \nu) \quad (5.16)$$

where G^* is the complex shear modulus. Like other complex properties, it can be divided into an in-phase and out-of-phase component

$$\eta^* = \eta' - i\eta'' \quad (5.17)$$

where η' is a measure of energy loss and η'' is a measure of stored energy. Unlike the difficulties that sometimes exist with E' and Young's modulus, the complex viscosity usually agrees fairly well with the steady shear viscosity. One applies the Gleiselle's mirror relationship, which is

$$\eta(d\gamma/dt) = \eta^+(t)|_{\tau = 1/(d\gamma/dt)} \quad (5.18)$$

where $\eta^+(t)$ is the limiting value of the viscosity as $d\gamma/dt$ approaches zero.⁵ Another option, the well-known Cox–Mertz Rule, is discussed in Chapter 8. The agreement of both is normally within $\pm 10\%$. The relationship between steady shear viscosity, normal forces, and dynamic viscosity is discussed in more detail in Chapter 8.

5.2.2 CALCULATING PROPERTIES FROM A MEASURED STIFFNESS

Another approach, discussed briefly in Chapter 2, is to calculate a stiffness for the sample, the deformation caused by a certain load. This can then be converted to a modulus using the equations and geometry factors.

5.3 INSTRUMENTATION FOR DMA TESTS

5.3.1 FORCED RESONANCE ANALYZERS

The most common analyzers on the market today are forced resonance analyzers. These are designed to force the sample to oscillate at a fixed frequency and are ideally suited for scanning material performance across a temperature range. The analyzers consist of several parts for controlling the deformation, the temperature, the sample

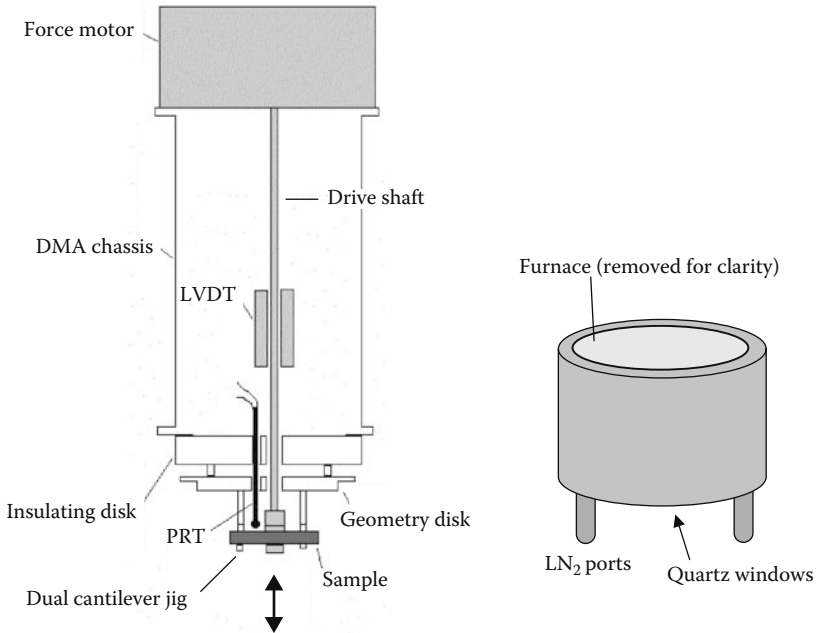


FIGURE 5.4 Schematic of the PerkinElmer DMA 8000 showing the motor, Linear Vertical Displacement Transducer (LVDT), sample compartment, furnace, and heat sink. Used with the permission of the PerkinElmer LAS, Shelton, Connecticut.

geometry, and the sample environment. Figure 5.4 shows an example. Obviously, various choices can be made for all of the components, each with their own advantages and disadvantages. For example, furnaces come in a wide variety of materials and types and each has its pros and cons. A ceramic covered, wire wound furnace gives a very fast temperature response over a wide range and is very inert, but it is more fragile than other types. Other choices could be a Peltier heater, a forced air furnace, a recirculation bath (the most stable for isothermal work), or a resistance type. The instrument shown in Figure 5.4 uses several types of heating depending on its configuration. More important than the exact type of furnace is that the temperature control be accurate and reproducible. Similarly, the measurement of the probe position can be done by using several techniques, including a linear vertical displacement transducer, an optical encoder, or an eddy current detector. There are advantages and disadvantages to each type but again the important point is that they are designed properly to allow accurate and reproducible measurements. The fact is most commercial DMAs do the job and emphasis on this is usually a sales tactic.

5.3.2 STRESS AND STRAIN CONTROL

One of the main choices made in selecting a DMA experiment is to decide whether to choose stress (force) or strain (displacement) control for applying the deforming load to the sample (Figure 5.5a and b). Strain-controlled analyzers, whether for

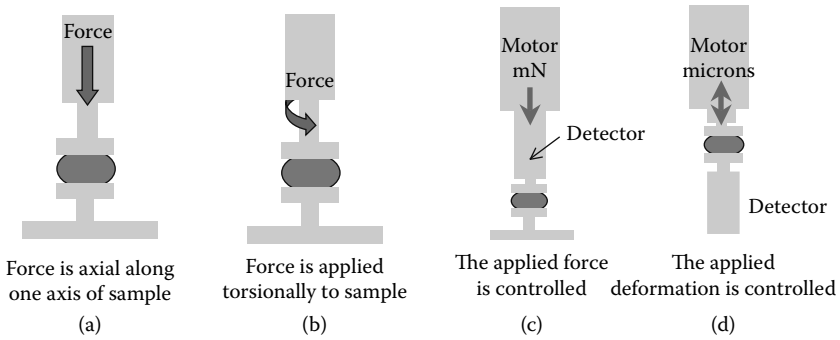


FIGURE 5.5 Types of dynamic mechanical analyzers: (a) axial, (b) torsional, (c) controlled stress, and (d) controlled strain.

simple static testing or for DMA, move the probe a set distance and use a force balance transducer or load cell to measure the stress. These parts are typically located on different shafts. The simplest version of this is a screw-driven tester, where the sample is pulled one turn. This requires very large motors so the available force always exceeds what is needed. Strain-controlled analyzers normally have better short-time response for low viscosity materials and can normally perform stress relaxation experiments easily. They also usually can measure normal forces if they are also torsional analyzers. A major disadvantage is their transducers may drift at long times or with low signals.

Stress-controlled analyzers are cheaper to make because there is only one shaft but somewhat trickier to use. Many of the difficulties have been alleviated by software and many strain-controlled analyzers on the market are really stress-controlled instruments with feedback loops making them act as if they were strain controlled. In stress control, a set force is applied to the sample. As temperature, time, or frequency varies, the applied force remains the same. This may or may not be the same stress; in extension, for example, the stretching and necking of a sample will change the applied stress seen during the run. However, this constant stress is a more natural situation in many cases and it may be more sensitive to material changes. Good low-force control means stress-controlled analyzers are less likely to destroy any structure in the sample. Long relaxation times or long creep studies are more easily performed on these instruments. Their biggest disadvantage is that their short time responses are limited by inertia with low viscosity samples. Hence one of the major design concerns in these is trying to reduce the measurement system mass or otherwise compensate for the inertia. The vast majority of DMAs available for solid samples are stress-controlled analyzers that are designed to mimic strain control.

Since most DMA experiments are run at very low strains ($\sim 5\%$ maximum) to stay well within a polymer's linear region, it has been reported that the both analyzers give the same results. However, when one gets to the nonlinear region, the difference becomes significant as stress and strain are no longer linearly related. Stress control can be said to duplicate real-life conditions more accurately since most applications of polymers involve resisting a load.

5.3.3 AXIAL AND TORSIONAL DEFORMATION

Dynamic mechanical analyzers are normally built to apply the stress or strain in two ways (Figure 5.5c and d). One can apply force in a twisting motion so one is testing the sample in torsion. This type of instrument is the dynamic analog of the constant shear spinning disk rheometers. Although mainly used for liquids and melts, solid samples may also be tested by twisting a bar of the material. Torsional analyzers normally also permit continuous shear and normal force measurements. Most of these analyzers can also do creep–recovery, stress relaxation, and stress–strain experiments.

Axial analyzers are normally designed for solid and semisolid materials and apply a linear force to the sample. These analyzers are usually associated with flexure, tensile, and compression testing but they can be adapted to do shear and some liquid specimens by proper choice of fixtures. Sometimes the instrument’s design makes this inadvisable however. (For example, working with a very fluid material in a system where the motor is underneath the sample has the potential for damage to the instrument if the sample spills into the motor.) These analyzers can normally test higher modulus materials than torsional analyzers and can sometimes run thermomechanical analysis (TMA) studies in addition to creep–recovery, stress relaxation, and stress–strain experiments.

Despite the traditional selection of torsional instruments for melts and liquids and axial instruments for solids, there is really considerable overlap between the types of instruments. With the proper choice of sample geometry and good fixtures, both types can handle similar samples, as shown by the use of both types to study the curing of neat resins (see the data in Chapter 7 for examples of this). Axial analyzers cannot normally handle fluid samples below about 500 Pa/sec and torsional instruments will top out with the harder samples (the exact modulus depending on the size of the motor and/or load cell). Because of this considerable overlap, I will not be separating the applications by analyzer type in the following discussions.

5.3.4 FREE RESONANCE ANALYZERS

Some of the earlier instruments used free resonance analyzers, but I am discussing it second because it requires a little more sophistication than the conceptually simpler forced resonance analyzers. If we suspend a sample in it to swing freely, it will oscillate like a harp or guitar string until the oscillations gradually come to a stop. The naturally occurring damping of the material controls the decay of the oscillations. This gives us a wave, shown in Figure 5.6a, which is a series of sine waves decreasing in amplitude and frequency. Several methods exist to analyze these waves and are covered in the review by Gillham.⁶ These methods have also been successfully applied to the recovery portion of a creep–recovery curve where the sample goes into free resonance on removal of the creep force.⁷

From the decay curve, we need to calculate or collect the period, T , and the logarithmic decrement, Λ , from the decay curve. Several methods exist for both manual and digital processing. Fuller details of the following may be found in McCrum et al. and Gillham.⁸ Basically we begin by looking at the decay of the amplitude over as many swings as possible to reduce error

$$\Lambda = 1/j \ln(A_n/A_{(n+j)}) \quad (5.19)$$

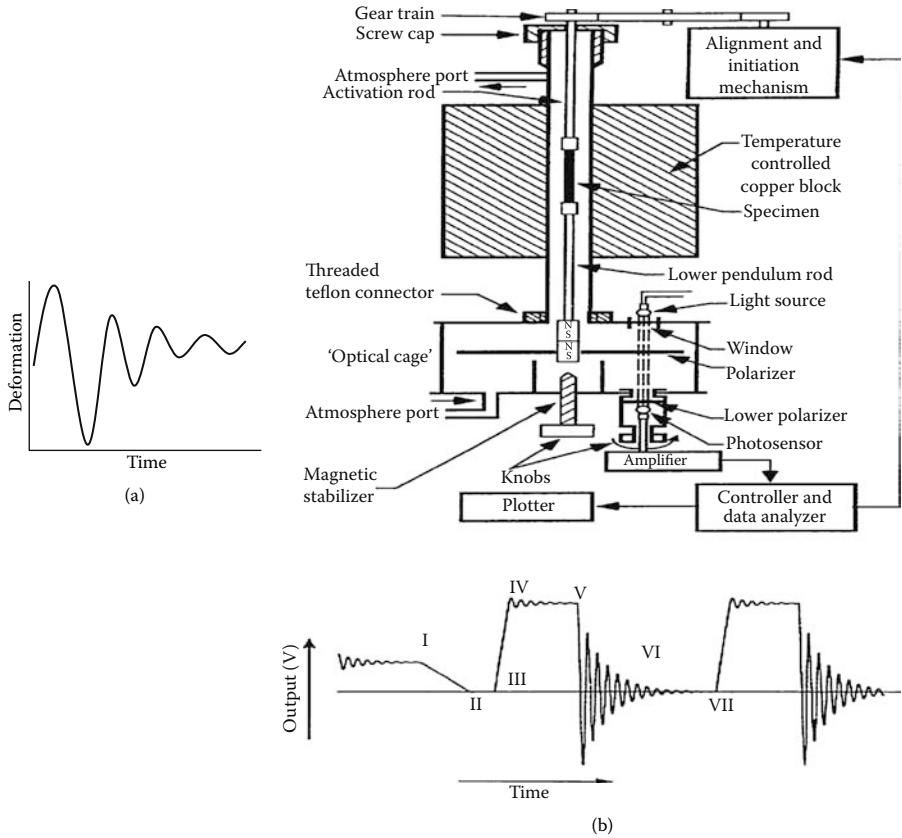


FIGURE 5.6 Free resonance analyzer. (a) The decay wave from free resonance and (b) a schematic of a torsional braid analyzer. Reprinted from J.K. Gillham and J.B. Enns, On the cure and properties of thermosetting polymers using torsional braid analysis, *Trends in Polymer Science*, 2(12), 406–419, 1994, with permission from Elsevier Science.

where j is the number of swings and A_n is the amplitude of the n th swing. For one swing, where $j = 1$, the equation becomes

$$\Lambda = \ln(A_n/A_{(n+j)}) \quad (5.20)$$

If for a low value of Λ where A_n/A_{n+1} is approximately one, we can rewrite the equation as

$$\Lambda \approx \frac{1}{2} \left(\frac{A_n^2 - A_{n+1}^2}{A_n^2} \right) \quad (5.21)$$

From this, since the square of the amplitude is proportional to the stored energy, $\Delta W/W_{st}$, and the stored energy can be expressed as $2\pi \tan \delta$, the equation becomes

$$\Lambda \approx \frac{1}{2} (\Delta W/W_{st}) = \pi \tan \delta \quad (5.22)$$

which gives us the phase angle, δ . The time of the oscillations, the period T , can be found using the following equation

$$T = 2\pi \sqrt{\frac{M}{\Gamma_1}} \sqrt{\frac{1 + \Lambda^2}{4\pi^2}} \quad (5.23)$$

where Γ_1 is the torque for one cycle and M is the moment of inertia around the central axis. Alternatively we could calculate the T directly from the plotted decay curve as

$$T = (2/n)(t_n - t_0) \quad (5.24)$$

where n is the number of cycles and t is time. From this, we can now calculate the shear modulus, G , which for rod of length, L , and radius, r , is

$$G = \left(\frac{4\pi^2 ML}{NT^2} \right) \left(1 + \frac{\Lambda^2}{4\pi^2} \right) - \left(\frac{mgr}{12N} \right) \quad (5.25)$$

where m is the mass of the sample, g is the gravitational constant, and N is a geometric factor. In the same system, the storage modulus, G' , can be calculated as

$$G' = (1/T^2)(8\pi ML/r^4) \quad (5.26)$$

where I is the moment of inertia for the system. Having the storage modulus and the tangent of the phase angle, we can now calculate the remaining dynamic properties.

Free resonance analyzers normally are limited to rod or rectangular samples or materials that can be impregnated onto a braid. This last approach is how the curing studies on epoxy and other resin systems were done in torsion and gives these instruments the name of torsional braid analyzers (TBAs). A schematic of a TBA is shown in Figure 5.6b.

Ringing can be induced in a creep measurement under certain conditions and this data can be analyzed using the approach of a free resonance system. Zolzer and Eicke have reported using this approach with creep data on stress-controlled instruments and developed a method to extract data from the ringing.⁹ McKinley and Ewoldt review different approaches to using the data from creep ringing and suggest a couple of different approaches.¹⁰

5.4 FIXTURES OR TESTING GEOMETRIES

We are now going to take a quick look at the commonly used fixtures for the DMA. It is important to be familiar with the effect the sample geometry has on stress and strain values because small dimensional changes often have large consequences. When measuring the temperature of transitions alone, a great deal of inaccuracy can be tolerated in the sample dimensions. This is not true for modulus values. Each of the following geometries discussed has a different set of equations for calculating stress and strain from force and deformation. One way of handling this is the use of a geometry factor, b , used to calculate E' and E'' in Equations 5.13 and 5.14. The equations for these geometric factors are given in Table 5.2. One practical use of these

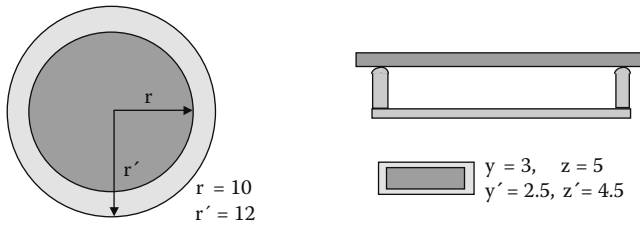
TABLE 5.2
Geometric Factors for Fixtures

	Axial		Torsion
3 pt. Bending (bar)	$4z_s y_s^3 / x_s^3$	Parallel Plate	$2\pi r_s^2 / y_s$
(rod)	$12\pi r^4 / x^3$	Cone and Plate	$2\pi r_s^3 / 3\Theta$
Single Cantilever	$z_s y_s^3 / 4x_s^3$	Coaxial Cylinders	$\frac{4\pi L(R_1)^2}{1/R_1^2 - 1/R_2^2}$
Dual Cantilever	$16z_s y_s^3 / x_s^3$	Torsion Bar (rectangular)	$\frac{3 + 8(z_s / x_s)^2}{x_s z_s^3 / y_s (1 - 0.378)(z_s / x_s)^2}$
Extension	$x_s z_s / y_s$		
Parallel Plates	$2\pi r_s^2 / y_s$		
Shear Sandwich	$y_{1s} / 2\pi r_{1s}^2 + y_{2s} / 2\pi r_{2s}^2$		
Coaxial Cylinders	$\frac{2\pi L / \ln(r_2 / r_1) \text{ or } 2\pi L}{(\ln(r_2 / r_1) - ((r_2 / r_1)^2 - 1) / ((r_2 / r_1)^2 + 1))}$		

Note: These factors are used to convert the load and the amount of deformation into stress and strain by using the dimensions of the sample. The letters refer to dimensions as drawn in Figures 5.7–5.12. The dimensions for rectangular samples are width (x), height (y), and depth (z) as drawn in the respective fixture. For a sample with a circular cross-section (i.e., a disk, plate, bar, or fiber), r_s is the sample radius, x becomes the length, and y is again the height. Θ is the cone angle in a cone-and-plate fixture. For the coaxial or Couette fixture, R_1 and R_2 refer to the inner and outer cylinder diameters respectively, while L refers to the length of the inner cylinder. Thanks to Dr. Kunigal N. Shivakumar of North Carolina A&T State University for checking my math.

equations is estimating the amount of error in the modulus expected due to the inaccuracies of measuring the sample. For example, if the accuracy of the dimensional measurement is 5%, the error in the applied stress can be calculated. Since many of these factors involve squared and cubed terms, small errors in dimensions can generate surprisingly large errors in the modulus. Figure 5.7 shows how small changes can have very large effects even in the liner region.

Two other issues need to be mentioned: those of inertia effects and of shear heating. Inertia is the tendency of an object to stay in its current state, whether moving or at rest. When a DMA probe is oscillated, this must be overcome and as the frequency increases, the effect of the instrument inertia becomes more troublesome. The simplest approach to controlling this is to keep the mass of the moving parts as low as possible. Inertia is greatest at high frequencies (Figure 5.8). Shear heating occurs when the mechanical energy supplied to the sample is converted to heat by the friction and changes the sample temperature. This is a problem mostly in testing of fluids and melts in torsion.



The difference between r and r' is 2.0 mm, but the difference in the geometric factor is 31%. So the stress is very different on samples of the same height.

Here the difference is 40%!

FIGURE 5.7 Errors in modulus values are commonly caused by mismeasurement of the sample. As shown, this can be a nontrivial error.

5.4.1 AXIAL

Axial analyzers allow a great deal of flexibility in the choice of fixtures, which allows for the testing of a wide range of materials. Ease of exporting data is also important in these analyzers as they are often adapted to run very specialized tests. For example, some contact lens manufacturers test samples on spherical plates, and tubing manufacturers will use fixtures that test the tubing in its original shape. With easy access to the raw data, one can go to *Roark's* and look up the stress and strain formulas for the appropriate geometry.¹¹

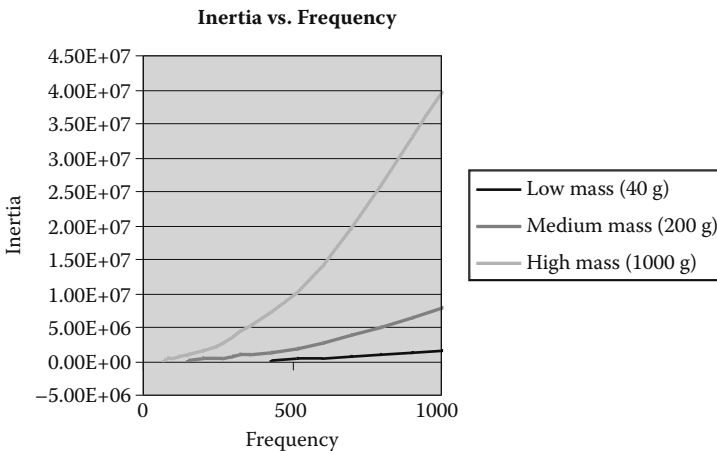


FIGURE 5.8 Inertia effects have serious implications in DMA. As frequency increases, the effect of mass on inertia becomes significant. This is a major concern in torsional analyzers but also can be a problem in axial ones. It is important to keep the mass of the analytical train as light as possible to minimize it. Mathematical corrections for inertia are also applied.

5.4.1.1 Three-Point and Four-Point Bending

There are four types of bending or flexure fixtures commonly used. The simplest and most straight forward of these is the three-point bending fixture shown in Figure 5.9a. No flexure mode is a pure deformation as they can all be looked at as a combination of an extension and compressive strain. Three-point bending depends on the specimen being a freely moving beam and the sample should be about 10% longer on each end than the span. The four sides of the span should be true, that is, parallel to the opposite side and perpendicular of the neighboring sides. There should be no nicks or narrow parts. Rods should be of uniform diameter. Throughout the experiment the beam should be freely pivoting. This is checked after the run by examining the sample to see if there are any indentations in the specimen. If there are, this suggests that a restrained beam has been tested, which gives a higher apparent modulus. The sample is loaded so the three edges of the bending fixture are perpendicular to the long axis of the sample.

Four-point bending replaces the single edge on top with a pair of edges as shown in Figure 5.9b. The applied stress is spread over a greater area than in three-point bending as the load is applied on two points rather than one. The mathematics remains the same, as the flexing of the beam is unchanged. One can use either knife-edged or round-edged fixtures and, in some cases, a ball probe is used to replace the center knife-edge of the three-point bending fixture to simplify alignment. As long

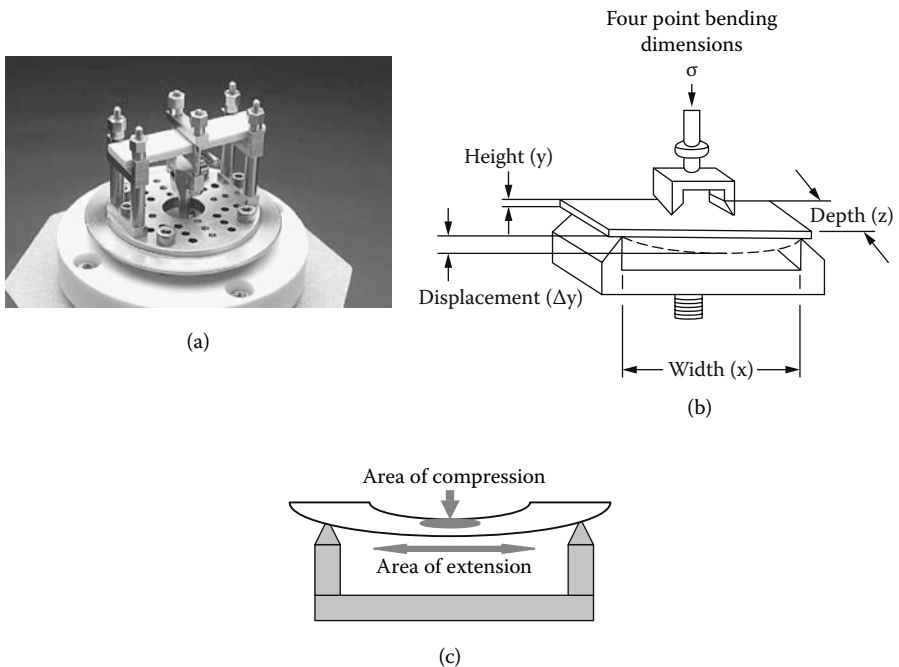


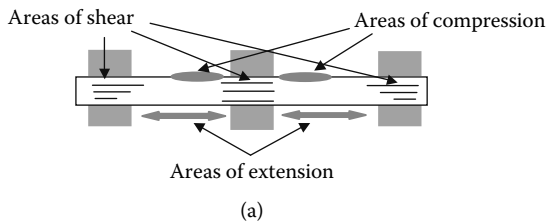
FIGURE 5.9 Flexure test fixtures I; (a) three-point bending, (b) four-point bending, and (c) compressive and tensile strains in a three-point bending specimen. Used with the permission of the PerkinElmer LAS, Shelton, Connecticut.

as the specimen shows the required even deflection, these are all acceptable. Sample alignment and deformation are shown in Figure 5.9c.

5.4.1.2 Dual and Single Cantilever

Cantilever fixtures clamp the ends of the specimen in place, introducing a shearing component to the distortion (Figure 5.10a) and increasing the stress required for a set displacement. Two types of cantilever fixtures are used: dual cantilever shown in Figure 5.10b and single cantilever shown in Figure 5.10c. Both cantilever geometries require the specimen to be true as described earlier and to be loaded with the clamps perpendicular to the long axis of the sample. In addition, care must be taken to clamp the specimen evenly, with similar forces, and to not introduce a twisting or distortion in clamping. Moduli from dual cantilever fixtures tend to run 10%–30% different than the same material measured in three-point bending at best. This is due to shearing strain induced by clamping the specimen in place at the ends and center, which makes the sample more difficult to deform.

For example, a sample of mild steel has a modulus of about 210 GP (10^9 P) and normally a well-prepared and precisely measured specimen in three-point bending will give a value within 5% of that. However, using a single cantilever system, one ends up 50% to 100% low. Now it is possible to do calibrations to correct for this and DMA designers come up with all sorts of techniques. The problem with that is you really would need to check your results for different materials against the results for three-point bending to be sure it's correct.



(b)



(c)

FIGURE 5.10 Flexure test fixtures II. (a) Strain in a dual cantilever specimen showing the shear regions, (b) dual cantilever, and (c) single cantilever. Used with the permission of the PerkinElmer LAS, Shelton, Connecticut.

Some software will introduce a shear correction to calculation. So the equations for single and dual cantilever become more elaborate.¹² The problem with this approach is equations for shear correction often work for either hard or soft materials, but not both. The argument for introducing these is that the standard equation doesn't correct for the compliance in the clamps. This can get a bit tricky as materials that yield, which includes aluminum, lead, and polyethylene, tend to be very different from hard elastic materials like steel, PMMA, and polycarbonate. One way to address this is to check the results at various lengths. The slope of a plot of length versus $\text{length}/(E)^{1/3}$ would yield an accurate modulus and the intercept would yield a length error (of the order of 1 to 2 mm). This length correction would then be the basis of modifying the data. It's a bit tricky though as its magnitude falls with decreasing stiffness, so once the sample is a rubber it becomes zero.

Another way to handle this is a shear correction based on Poisson's ratio. For example, a small shear correction can be applied to clamped, bending data by dividing the geometry factor by $1 + 2.9(y/x)^2$. This correction is based on an average Poisson's ratio of 0.33 for glassy polymers and 0.5 for rubbers, giving us 0.45.

5.4.1.3 Parallel Plate and Variants

Parallel plates (Figure 5.11a) in axial rheometers means testing in compression, and several variations of simple parallel plates exist for special cases (Figure 5.11b and c). Sintered or sandblasted plates are used for slippery samples; plates and trays for

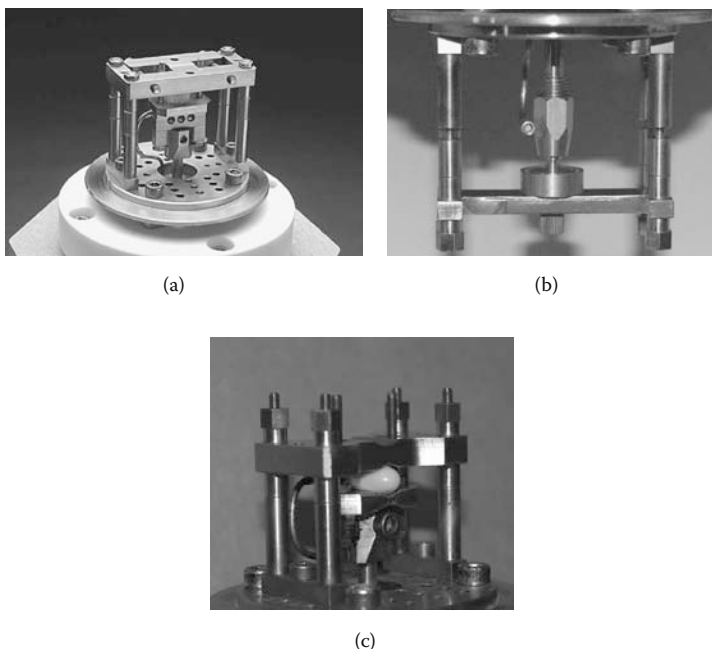


FIGURE 5.11 Parallel plate fixture for axial analyzers. (a) Standard parallel plates (b) cup and plate, and (c) tablet plates. (b) Is also used for bulk measurements. Used with the permission of the PerkinElmer LAS, Shelton, Connecticut.

samples that drip or need to be in contact with a solvent; and plates and cups for low viscosity materials. Photocuring materials can be studied with quartz fixtures. For samples in compression, circular plates are normally used because these are easily manufactured and the samples can be fabricated by die cutting films or sheets to size. Rectangular plates and samples are also used. Any type of plate needs to be checked after installation to make sure the plates are parallel. The easiest way to check the alignment is by bringing the plates together and seeing if they are touching each other with no spaces or gaps. Samples should be the same size as the plates with the edges even or flush, having no dips or bulges. On compressing, it should deform by bowing outward slightly in an even, uniform bulge.

5.4.1.4 Bulk

If we run a sample in a dilatometer-like fixture (Figure 5.11b) where it is restrained on all sides, we measure the bulk modulus of the material. This can be done in a specialized pressure–volume–temperature (PVT) instrument with very high loads (up to 200 MPa of applied pressure) to study the free volume of the material.¹³ In this geometry, alignment is critical, as the fit between the top plate and the walls of the cup must be very tight to prevent the material from escaping. The cup and plate/plunger system must still be able to move freely without binding.

5.4.1.5 Extension/Tensile

Extension or tensile analysis (Figure 5.12a) is done on samples of all types and is one of the more commonly done experiments. This geometry is more sensitive to loading and positioning of the sample than most other geometries. Any damage or distress to the edges of the sample as well will cause inaccuracies in the measurements. A nick in the edge will also often cause early failure as it acts as a stress concentrator. After loading a film or fiber in extension, it is important to adjust it so that there are not any twists, the sides are perpendicular to the bottom, and there are no crinkles.

5.4.1.6 Shear Plates and Sandwiches

Figure 5.12b shows one of the two approaches to measuring shear in an axial analyzer. Shear measurements are done by a sliding plate moving between two samples.

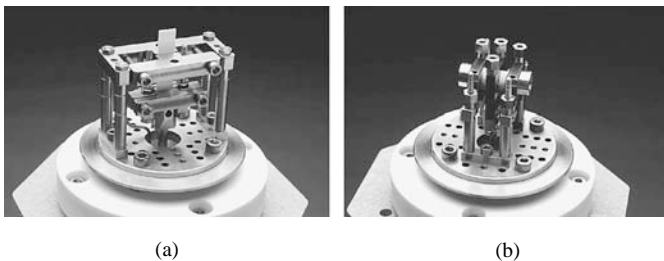


FIGURE 5.12 Extension and sliding shear fixtures. (a) An extension fixture for thin films or fibers and (b) a sliding plate shear fixture using two round samples. Used with the permission of the PerkinElmer LAS, Shelton Connecticut.

This is the common approach today. Another older approach is to use a single sample, but this requires a very rigid analyzer. Again, sample size and shape must be controlled tightly for modulus data to be fully meaningful. It is very important in the shear sandwich fixtures to make sure both samples are as close to identical as possible. This technique can be difficult to run over wide temperature ranges as the thermal expansion of the fixture can cause the clamping force to vary greatly.

5.4.2 TORSIONAL

Samples run in torsional analyzers tend to be of lower viscosity and modulus than those run in axial instruments. Torsional instruments can be made to handle a wide variety of materials ranging from very low viscosity liquids to bars of composite. Inertia affects tend to be more of a problem with these instruments and very sophisticated approaches have been developed to address them.¹⁴ Most torsional rheometers can also perform continuous shear experiments and also measure normal forces.

5.4.2.1 Parallel Plates

The simplest geometry in torsional shear is two parallel plates run at a set gap height. This is shown in Figure 5.13a. Note that the important dimensions are the same as in Figure 5.12a. The height or gap here is determined by the viscosity of the sample. We want enough space between the plates to obtain decent flow behavior, but not so much that the material flies out of the instrument. The edge of the sample should be spherical without fraying or rippling. These plates have an uneven strain field across them; the material at the center of the plate is strained very little as it barely moves. At the edge, the same degree of turning corresponds to a much larger movement. So the measured strain is an average value and the real strain is inhomogeneous. The thrust against the plates can be used to calculate the normal stress difference in steady shear runs.

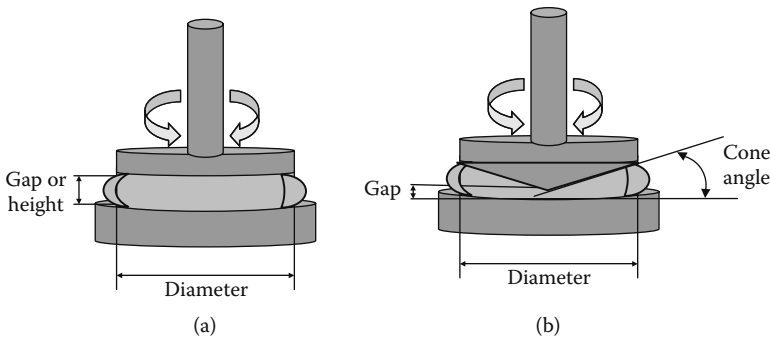


FIGURE 5.13 Plate geometries for torsion. (a) Parallel plates, which are measured the same way as in Figure 5.11, and (b) cone and plates.

5.4.2.2 Cone-and-Plate

The cone-and-plate geometry uses a cone of known angle instead of a top plate. When this cone angle is very small, the system generates an even, homogeneous strain across the sample. Shown in Figure 5.13b, the gap is set to a specific value, normally supplied by the manufacturer. This value corresponds to the truncation of the cone. The cone-and-plate system is probably the most common geometry used today for studying non-Newtonian fluids. As earlier, at very high shear rate, the material reaches a critical edge velocity and fails. This geometry is discussed extensively by Macosko, along with other geometries for testing fluids.¹⁵

5.4.2.3 Couette

Some materials are of such a low viscosity that testing them in a cone-and-plate or parallel plate fixture is inadvisable. When this occurs, one of the Couette geometries can be used. Also called concentric or coaxial cylinders, the geometry is shown in Figure 5.14a with the recessed bottom style of bob (inner cylinder). This shape is used to eliminate or reduce end effects. Other choices might be a conicylinder, where the cylinder has a cone-shaped (pointed) end, or a double Couette, where a thin sheet of material has solution around it. The recessed end traps air, which transfers no force to the fluid, and seems to be the one most commonly used today. This fixture requires tight tolerances and the side gap is fixed by the design. The bottom gap is also tightly controlled and the tops of the cylinders must be flush. The fluid level must come close, say within 5 mm of the top of the fixture, but not overflow it. Both inertia effects and shear heating are concerns that must be addressed.

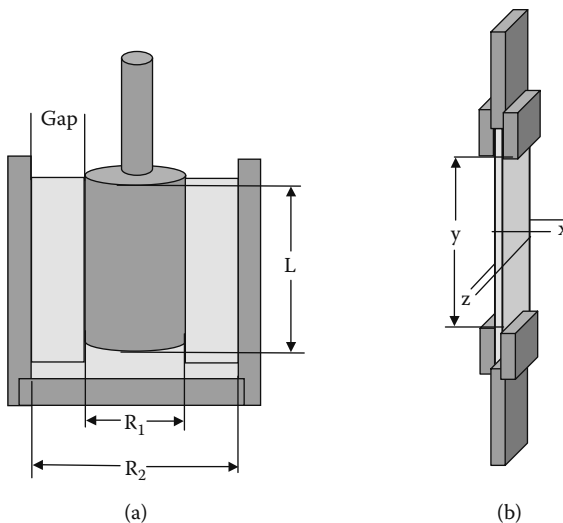


FIGURE 5.14 Couette and torsion bar geometries. (a) Couette fixture and (b) torsion bar showing a rod shaped specimen.

5.4.2.4 Torsional Beam and Braid

Stiff, solid samples in a torsional analyzer are tested as bars or rods that are twisted about their long axis. This geometry is shown in Figure 5.14b. The bar needs to be prepared as precisely as those discussed earlier. Another variation is the use of a braid of material impregnated with resin for curing studies. This can be a tricky approach as even nondrying oils appear to increase in viscosity or cure (crosslinked) as they heat up (their viscosity drops and the fibers start rubbing together so that the measured viscosity appears to increase as if the material had cured).

5.5 SAMPLE HANDLING ISSUES

So far we have basically talked about nice homogenous samples. Before we move on, we should discuss the effects on nonhomogeneous samples. Some of this is really common sense. The vast majority of fiber-reinforced composites are run in modes where the load is applied to the length of the fiber. Pulling one in tension is going to measure the modulus of the fiber, not the composite. Similarly in shear or compression a very hard material laminated to a soft material (I am assuming the lamination line runs parallel to the plate here), we will only see the softer modulus as the harder material will act as another plate (Figure 5.15). That's what we exploit when we use Superglue™ to anchor a silicon rubber sample to the shear plates so it doesn't slide out during the run. The dried glue's modulus is so high that it doesn't show up at all.

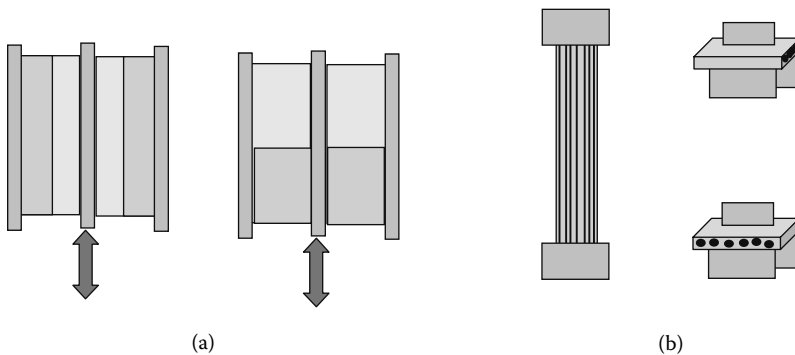


FIGURE 5.15 Sample orientation in nonhomogeneous samples. What you measure depends on how you arrange the samples. In (a), we see that in shear we would expect different moduli from the two types of orientation. The first arrangement, with the hard material next to the plate, is similar to gluing rubber samples to the parallel plates. In those cases, the glues used are so much harder than the rubber they act as if they are invisible. In (b), the modulus in tension will be that of the fibers, whereas in the flexure modes it will be the resin. In the lower figure, some contribution of the fiber may occur depending on how flexible the fiber is.

5.6 CALIBRATION ISSUES

Calibration may be one of the most misunderstood concerns in operating a DMA. All of the systems in a DMA need to be tied back to some standard for the collected data to have meaning. Figure 5.16 shows the PerkinElmer DMA 8000, as an example, with the calibrations needed to standardize the performance of each part of the instrument. All instruments require this and normally these procedures are described in the operation manual. Temperature calibration is especially critical as material properties are strongly influenced by it.

The calibrations shown in Figure 5.16 cover the major types used. Force, height or position, and temperature calibrations relate the instrument's signal to a known standard of performance. This should ideally be traceable to a primary source. For temperature, NIST traceable materials, like indium or tin, are preferred.

All instruments have some sort of movement, as none are ideally rigid. Therefore, some measure of the instrument's rigidity or self-deformation is needed. Various approaches are used, but as harder and stiffer samples are run, the amount of deformation in the instrument becomes more important. With very stiff samples, the deformation in the analyzer could become greater than the sample and inaccurate results are obtained. Similarly, if the analyzer is too stiff, then very soft samples may not be detected. In addition, inertia needs to be addressed for the system. Frequency response, phase lag, and time constants for the analytical train also need to be set.

Finally, some sort of control over the furnace's performance is needed. Whether a control thermocouple or a voltage table, the furnace needs to be tuned so that its operation is in agreement with the measured temperature of the thermocouple.

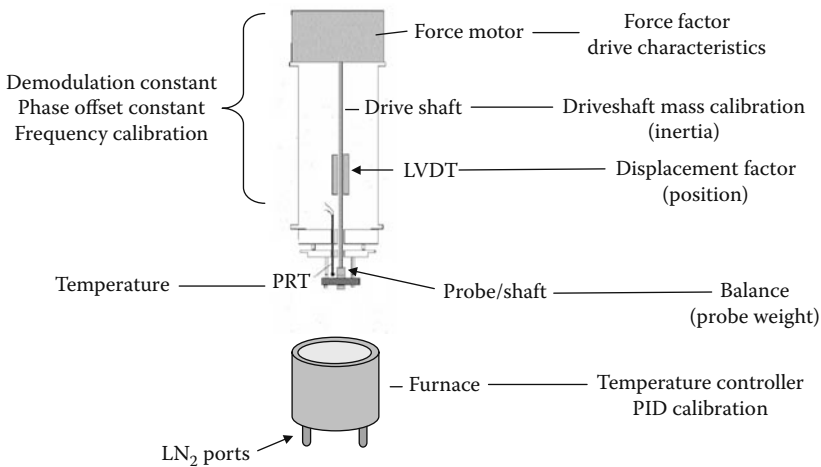


FIGURE 5.16 A schematic showing the interrelationship of calibration and analyzer systems. Used with the permission of the PerkinElmer LAS, Shelton, Connecticut.

The approach of the furnace to the set temperature should be tuned to give the desired response (i.e., degree of overshoot). This is done by using proportional, integral, and derivative control (PID) files in many cases. This approach has the advantage of a great detail of control in tuning the furnace. It is important that these calibrations be done under the same cooling system as the instrument will be operated. For long-term isothermal conditions, nothing matches the control of a good recirculation bath.

5.7 DYNAMIC EXPERIMENTS

DMA experiments can be classed as temperature–time studies, frequency studies, and dynamic stress–strain curves. Temperature–time scans hold the frequency constant as the temperature or time at temperature changes. These are discussed in Chapters 6 and 7. Frequency scans vary the frequency at a set temperature and are discussed in Chapter 8. Finally, the dynamic force can be constantly increased at a fixed rate and a dynamic stress–strain curve can be generated.

This last technique is commonly used as a method of tuning the DMA and selecting the proper operating range for a sample. It is done by increasing the amplitude of the sine wave analogously to the increased stress in a stress–strain experiment. This is shown in Figure 5.17. It is often necessary to also continually increase the static force to maintain constant tension on the sample. Because this experiment is a series of larger and larger sine waves, we cannot only plot dynamic stress versus dynamic strain but also get E' , E'' , E^* , $\tan \delta$, η^* , and other dynamic properties for each cycle. This allows us to plot those properties as a function of dynamic stress, too. Besides providing insight into the material behavior, this method makes an excellent method of quality control. As stated earlier, each sine wave can be solved for the full range of dynamic properties, allowing very detailed comparisons in very short times. Figure 5.18 shows dynamic stress–dynamic strain and $\tan \delta$ –dynamic strain plots on two rubbers.

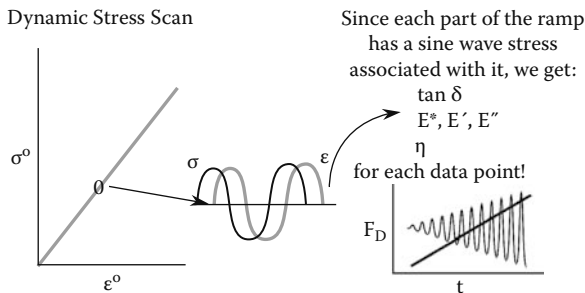


FIGURE 5.17 Dynamic stress–strain curves involved the application of a dynamic stress ramp to a specimen so each data point measures a different sine wave.

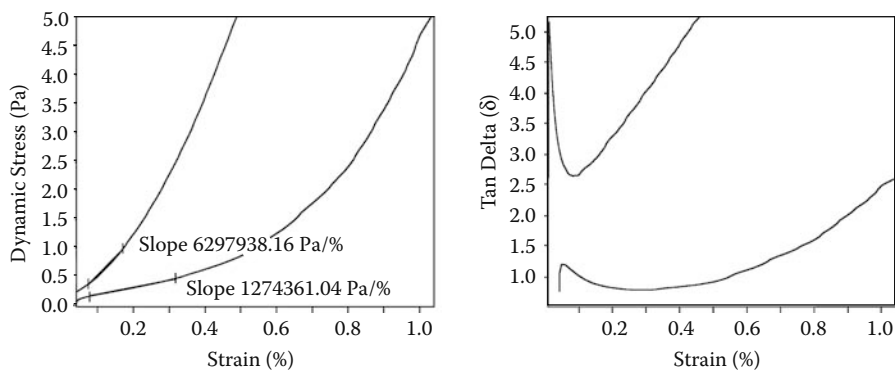


FIGURE 5.18 Results from dynamic stress–strain curves showing (a) the relationship between dynamic stress and strain and (b) $\tan \delta$ versus dynamic strain for two materials.

NOTES

1. This explanation was developed in terms of stress control and tensile stress, instead of the shear strain and strain control normally used. For more detailed development, see one of the following: L. Sperling, *Introduction to Physical Polymer Science*, 2nd ed., Wiley, New York, 1996. L. Nielsen et al., *Mechanical Properties of Polymers and Composites*, Marcel-Dekker, New York, 1996. J. Ferry, *Viscoelastic Properties of Polymers*, Wiley, New York, 1980. The nice thing is that software does all this today and you just need to understand how it works so you realize exactly what you are doing.
2. B. Read and J. Duncan, *Polymer Testing*, 2(1), 135, 1981.
3. J. Ferry, *Viscoelastic Properties of Polymers*, Wiley, New York, 1980, ch. 5–7.
4. J. Duncan, Dynamic mechanical analysis, in *Principles and Applications of Thermal Analysis*, P. Gabbott, Ed., Blackwell Publishing, Oxford, 2007.
5. R. Armstrong, B. Bird, and O. Hassager, *Dynamics of Polymer Fluids, Volume I: Fluid Mechanics*, 2nd ed., Wiley, New York, 1987, pp. 151–153.
6. J. Gillham, in *Developments in Polymer Characterizations*, Vol. 3, J. Dworkins, Ed., Applied Science Publisher, Princeton, NJ, 1982, pp. 159–227. J. Gillham and J. Enns, *TRIP*, 2(12), 406, 1994.
7. U. Zolzer and H.-F. Eicke, *Rheologica Acta*, 32, 104, 1993.
8. N. McCrum et al., *Anelastic and Dielectric Properties of Polymeric Solids*, Dover, New York, pp. 192–200, 1992. J. Gillham in *Developments in Polymer Characterizations*, Vol. 3, J. Dworkins, Ed., Applied Science Publisher, Princeton, NJ, 1982, pp. 159–227. J. Gillham and J. Enns, *TRIP*, 2(12), 406, 1994.
9. U. Zolzer and H.-F. Eicke, *Rheologica Acta*, 32, 104, 1993.
10. R. Ewoldt and G. McKinley, *Rheol. Bull.*, 76(1), 4, 2007.
11. W. Young, *Roark's Formulas for Stress and Strain*, McGraw-Hill, New York, 1989.
12. Thanks to Dr. John Duncan of Triton Technologies for his help with this discussion.
13. P. Zoller and Y. Fakhreddine, *Thermochimica Acta*, 238, 397, 1994. P. Zoller and D. Walsh, *Standard Pressure–Volume–Temperature Data for Polymers*, Technomic Publishing, Lancaster, PA, 1995.
14. See, for example, the instrument manuals written by Rheometric Sciences of Piscataway, New Jersey, where inertia affects are discussed at length.
15. C. Macosko, *Rheology*, VCH Publishers, New York, 1994, ch. 5.

6 Time and Temperature Scans Part I

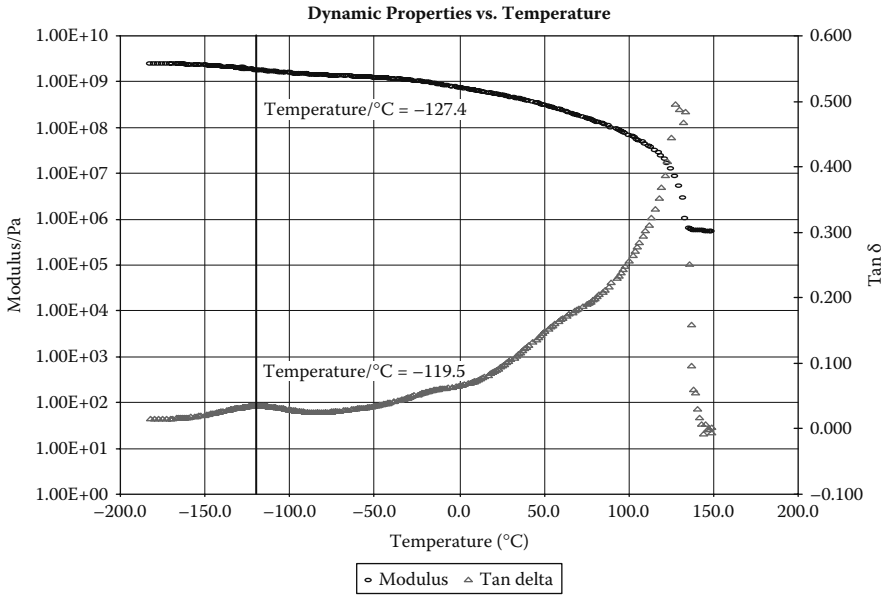
Transitions in Polymers

One of most common uses of the DMA for users from a thermal analysis background is the measurement of the various transitions in a polymer. A lot of users exploit the greater sensitivity of the DMA to measure T_g s undetectable by the differential scanning calorimeter (DSC) or the differential thermal analyzer (DTA). For more sophisticated users, DMA temperature scanning techniques let you investigate the relaxation processes of a polymer. In this chapter, we will look at how time and temperature can be used to study the properties of polymers. We will address curing studies in Chapter 7.

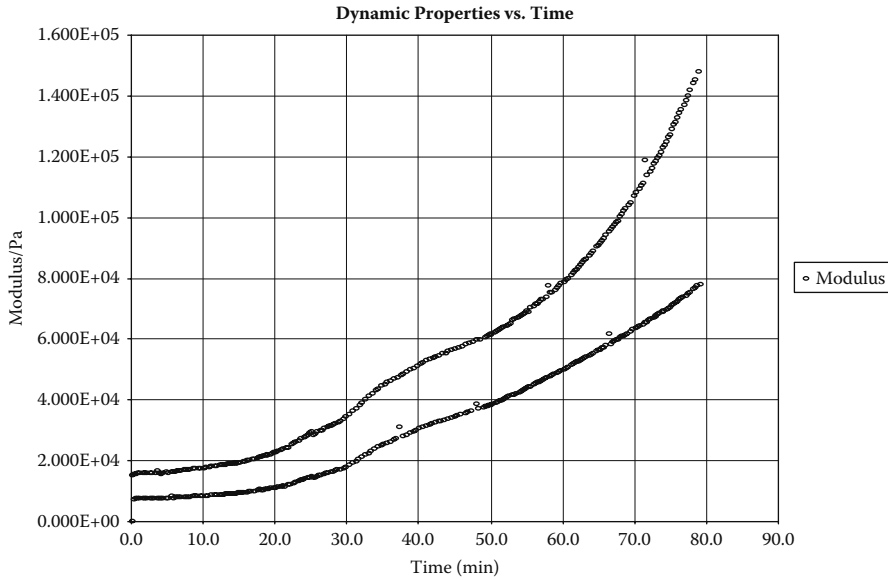
6.1 TIME AND TEMPERATURE SCANNING IN THE DMA

If we start with a polymer at very low temperature and oscillate it at a set frequency while increasing the temperature, we are performing a temperature scan (Figure 6.1a). This is what most thermal analysts think of as a DMA run. Similarly, we could also hold the material at a set temperature and see how its properties change over time (Figure 6.1b).

Experimentally we need to be concerned with the temperature accuracy and the thermal control of the system as shown in Figure 6.2. This is one of the most commonly overlooked areas experimentally as poor temperature control is often accepted to maintain large sample size. A large sample means that there will be a temperature difference across the specimen, which can result in anomalies such as dual glass transitions in a homopolymer.¹ Bird describes in his polymer fluids short course an experiment where measuring the temperature at various points in a large parallel plate showed a 15°C difference from the plate edge to the center.² Similarly, Chodak et al. report that equilibration times are long in both plates and tension experiments, although tension specimens respond quicker.³ Large samples require very slow heating rates and hide local differences. This is especially true in postcure studies. A smaller sample permits a smaller furnace, which is inherently more controllable. Also, smaller sample size allows the sectioning of specimens to see how properties vary across a specimen. Figure 6.2d schematically shows the affect of doubling a sample size. As Duncan discusses, temperature calibration is a contentious issue in DMA.⁴ The best discussion of temperature in the DMA comes from the National Physics Laboratory and that report gives excellence recommendations for assuring the accuracy of the measured values.⁵



(a)



(b)

FIGURE 6.1 Time–temperature studies in the DMA. We can (a) vary temperature at a set rate and scan across the various transitions and regions of a material’s behavior as shown here for LDPE or (b) hold temperature constant and watch properties change as a function of time, gas changes, and so forth. In this case, paint dries at room temperature.

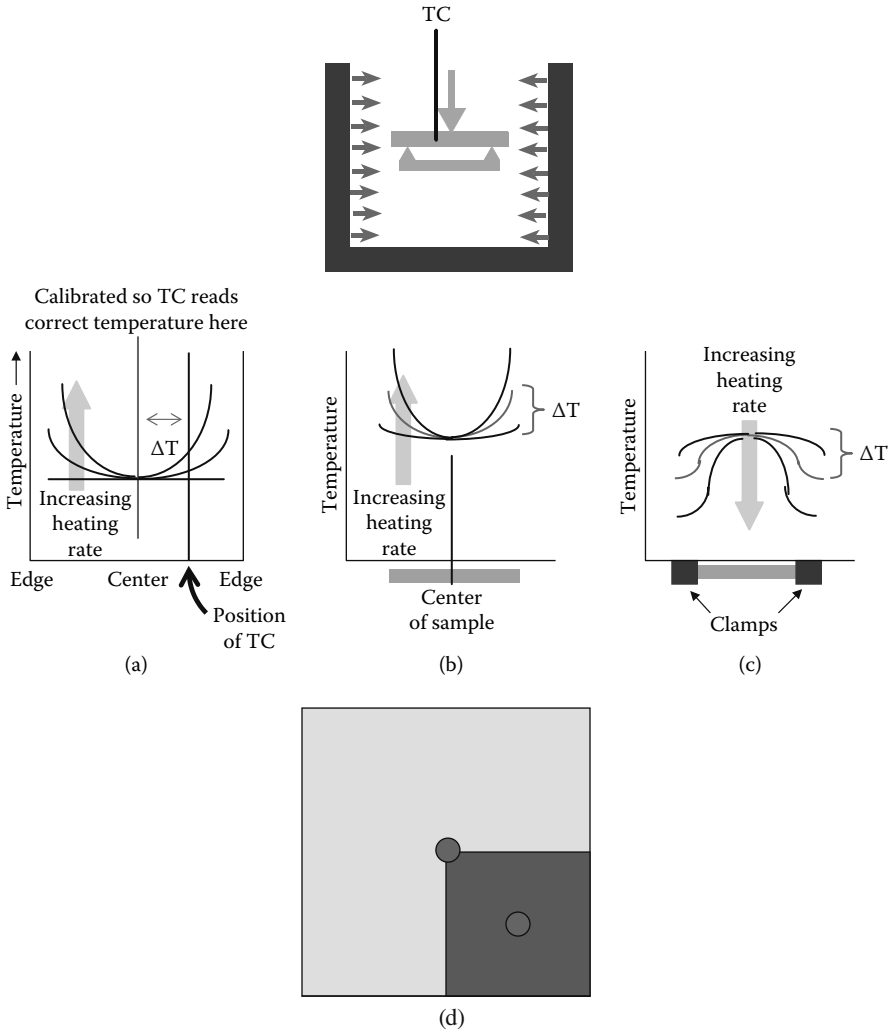


FIGURE 6.2 Temperature control in a DMA sample; a schematic representation of the problems of temperature control in a DMA for a solid sample. Similar problems exist for melts. (a) The problem of thermal lag between the sample and the furnace, which is normally handled by calibration. (b) The lag across a sample under heating due to the thermal conductivity of the sample. (c) The effect of heavy clamps on sample temperature. (d) Doubling the side dimensions as we did above increases the cross-sectional area by four times. This means we have four times the mass to heat, greatly increasing the possibility of thermal lag in the sample. To get the sample to heat evenly, the small circles are the same temperature as the right edge the larger gray box will require a much slower heating rate than the smaller one.

It is often very difficult to examine one specimen across the whole range of interest with only one experiment or one geometry. Materials are very stiff and brittle at low temperatures and soft near the melt, so very different conditions and fixtures may be required. Some analyzers use sophisticated control loops to address this problem,⁶ but often it is best handled doing multiple runs.

6.2 TRANSITIONS IN POLYMERS: OVERVIEW

The thermal transitions in polymers can be described in terms of either free volume changes⁷ or relaxation times.⁸ While the latter tends to be preferred by engineers and rheologists, in contrast to chemist and polymer physicists who lean toward the former, both descriptions are equivalent. Changes in free volume, v_f , can be monitored as a volumetric change in the polymer, the absorption or release of heat associated with that change, the loss of stiffness, increased flow, or the change in relaxation time.

The free volume of a polymer, v_f , is known to be related to viscoelasticity,⁹ aging,¹⁰ penetration by solvents,¹¹ and impact properties.¹² Defined as the space a molecule has for internal movement, it is schematically shown in Figure 6.3a. A simple approach to looking at free volume is the crankshaft mechanism, where the molecule is imagined as a series of jointed segments.¹³ From this model, we can simply describe the various transitions seen in a polymer. Other models exist that allow for more precision in describing behavior; the best seems to be the Doi–Edwards model.¹⁴ Shaw and MacKnight¹⁵ give a good summary of the available models, as do Rohn¹⁶ and Ward and Sweeney.¹⁷

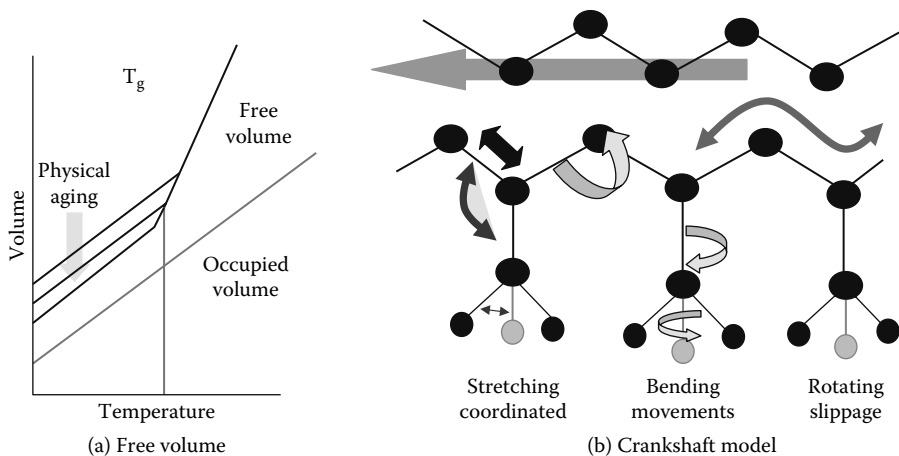


FIGURE 6.3 Free volume, v_f , in polymers. (a) The relationship of free volume to transitions and (b) a schematic example of free volume and the crankshaft model. Below the T_g in (a), various paths with different free volumes exist depending on heat history and processing of the polymer, where the path with the least free volume is the most relaxed. (b) Shows the various motions of a polymer chain. Unless enough free volume exists, the motions cannot occur.

The crankshaft model treats the molecule as a collection of mobile segments that have some degree of free movement. This is a very simplistic approach, yet very useful for explaining behavior. As the free volume of the chain segment increases, its ability to move in various directions also increases (Figure 6.3b). This increased mobility in either side chains or small groups of adjacent backbone atoms results in a greater compliance (lower modulus) of the molecule. These movements have been studied and Heijboer classified β and γ transitions by their type of motion.¹⁸ The specific temperature and frequency of this softening help drive the end use of the material.

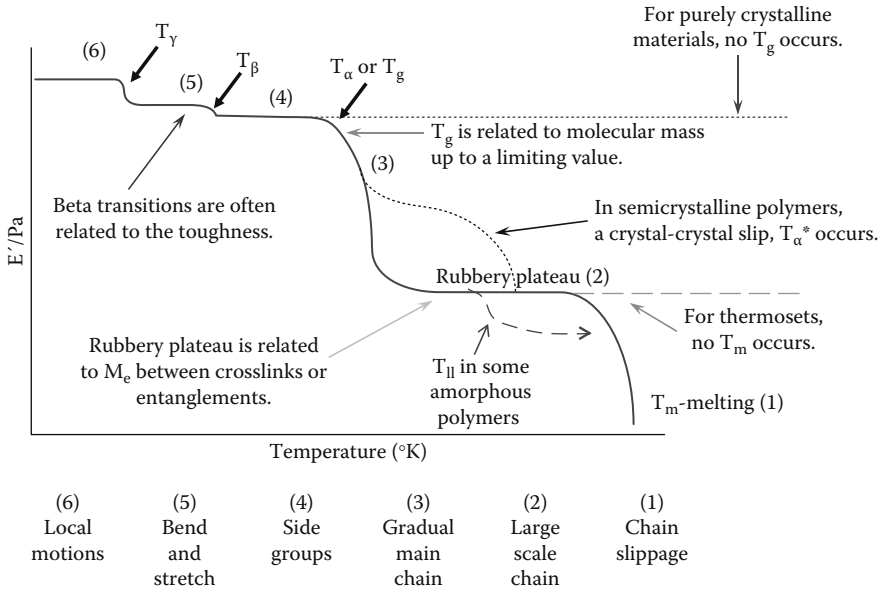
As we move from a very low temperature, where the molecule is tightly compressed, we first pass through the solid-state transitions. This process is shown in Figure 6.4. As the material warms and expands, the free volume increases so that localized bond movements (bending and stretching) and side chain movements can occur. This is the gamma transition, T_γ , which may also involve associations with water.¹⁹ As the temperature and the free volume continue to increase, the whole side chains and localized groups of four to eight backbone atoms begin to have enough space to move and the material starts to develop some toughness.²⁰ This transition, called the beta transition (T_β), is not always as clearly defined as we are describing here. Often it is the T_g of a secondary component in a blend or of a specific block in a block copolymer. However, a correlation with toughness is seen empirically.²¹ Recently, a definition of brittleness²² has also been developed using the DMA in conjunction with the ultimate strength of the material measured as the strain at breaking

$$B = 1/(\epsilon_b E') \quad (6.1)$$

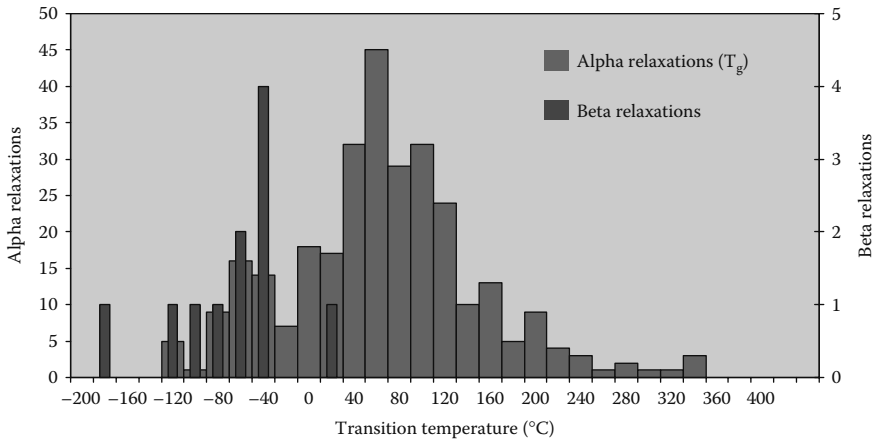
where B is brittleness, ϵ_b is the strain at break, and E' is the storage modulus at the temperature of testing.

As heating continues, we reach the T_g , or glass transition, where the chains in the amorphous regions begin to coordinate large-scale motions. One classical description of this region is that the amorphous regions have begun to melt. Since the T_g only occurs in amorphous material, in a 100% crystalline material we would not see a T_g . Continued heating bring us to the T_α^* and T_{11} . The former occurs in crystalline or semicrystalline polymer and is a slippage of the crystallites past each other. The latter is a movement of coordinated segments in the amorphous phase that relates to reduced viscosity. Everyone does not accept these two transitions and their existence is still a matter of some disagreement. Finally, we reach the melt where large-scale chain slippage occurs and the material flows. This is the melting temperature, T_m . For a cured thermoset, nothing happens after the T_g until the sample begins to burn and degrade because the crosslinks prevent the chains from slipping past one another.

This quick overview gives us an idea of how an idealized polymer responds. Now let us go over these transitions in more detail with some examples of their applications. The best general collection of this information is still McCrum's 1967 text, which characterizes the transitions of many commercial polymers.²³ Figure 6.4b shows the temperature range of the T_g or T_α and the T_b for a range of materials.



(a)



(b)

FIGURE 6.4 Idealized temperature scan of a polymer. Starting at a low temperature, the modulus decreases as the molecules gain more free volume resulting in more molecular motion. (a) This shows the main curve divided into six regions that corresponds to: (6) local motions, (5) bond bending and stretching, (4) movements in the side chain or adjacent atoms in the main chain, (3) the region of the T_g , (2) coordinated movements in the amorphous portion of the chain, (1) and the melting region. (b) T_g (alpha) and T_β transitions for approximately 300 polymers. While low temperature performance is needed, for polymer work one never goes over $400^{\circ}C$.

6.3 SUB- T_g TRANSITIONS

The area of sub- T_g or higher order transitions has been heavily studied as these transitions have been associated with mechanical properties.²⁴ These transitions can sometimes be seen by DSC and TMA (thermomechanical analysis), but they are normally too weak or too broad for determination by these methods. DMA, DEA (dielectric analysis), and similar techniques are usually required.²⁵ Some authors have also called these types of transitions second-order transitions to differentiate them from the primary transitions of T_m and T_g , which involve large sections of the main chains.²⁶ Boyer reviewed the T_β in 1968 and pointed out that while a correlation often exists, the T_β is not always an indicator of toughness.²⁷ Bershtein and Egorov reported that this transition can be considered the “activation barrier” for solid-phase reactions, deformation, flow or creep, acoustic damping, physical aging changes, and gas diffusion into polymers, as the activation energies for the transition and these processes are usually similar.²⁸ The strength of these transitions is related to how strongly a polymer responds to those processes. These sub- T_g transitions are associated with the materials properties in the glassy state. In paints, for example, peel strength (adhesion) can be estimated from the strength and frequency dependence of the subambient beta transition.²⁹ Nylon 6,6 shows a decreasing toughness, measured as impact resistance, with declining area under the T_β peak in the $\tan \delta$ curve. Figure 6.5 shows the relative differences in the T_β compared to the T_g for a high impact and low impact nylon. It has been shown, particularly in cured thermosets, that increased freedom of movement in side chains increases the strength of the transition. Cheng reports that in rigid rod polyimides that the beta transition is caused by the noncoordinated movement of the diamine groups, although the link to physical properties was not investigated.³⁰ Johari has reported in both

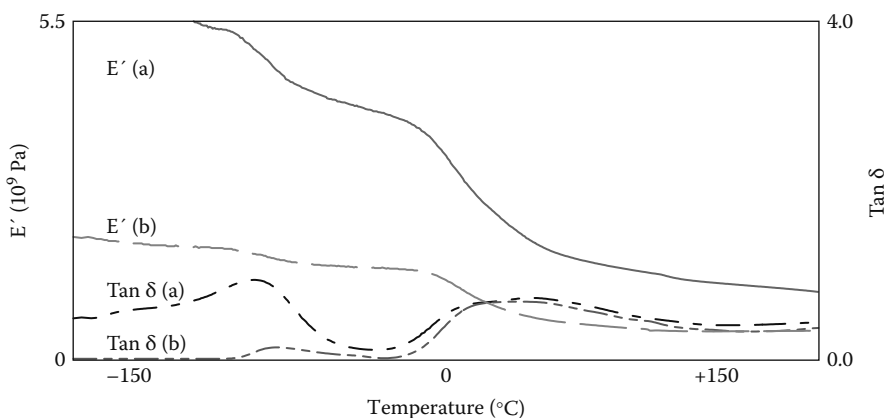


FIGURE 6.5 High and low impact nylon samples showing how the beta transition is related to sample toughness as measured by impact testing. The (a) lines show a material with good impact strength by the falling dart test and the (b) lines shows one with poor values by the same test.

mechanical³¹ and dielectric studies³² that both the β and γ transitions in bisphenol-A-based thermosets depend on the side chains and unreacted ends, and that both are affected by physical aging and postcure. Nelson has reported that these transitions can be related to vibration damping.³³ This is also true for acoustical damping.³⁴ In both of these cases, the strength of the beta transition is taken as a measurement of how effectively a polymer will absorb vibrations. Similarly in molded polyethylenes, beta transitions were found to relate to temperature-dependent impact tests.³⁵ A wide range of molecular weights³⁶ show this affect as does PVC,³⁷ polyesters,³⁸ PPO,³⁹ and acrylics.⁴⁰ There is some frequency dependence involved in this, which will be discussed later in Section 6.7, but modeling based on that seems to only approximate the response.⁴¹

Boyer⁴² and Heijober⁴³ showed that this information needs to be considered with care as not all beta transitions correlate with toughness or other properties. This can be due to misidentification of the transition or the transition not sufficiently dispersing energy. A working rule of thumb is that the beta transition must be related to either localized movement in the main chain or very large side chain movement to sufficiently absorb enough energy.⁴⁴ The relationship of large side chain movement and toughness has been extensively studied in polycarbonate by Yee and Smith,⁴⁵ as well as in many other tough glassy polymers.⁴⁶

Less use is made of the T_γ transitions (Figure 6.6) and they are mainly studied to understand the movements occurring in polymers. Wendorff and Schartel⁴⁷ report that this transition in polyarylates is limited to inter- and intramolecular motions within the scale of a single repeat unit. Both McCrum⁴⁸ and Boyd⁴⁹ similarly limited the T_γ and T_δ to very small motions either within the molecule or with bound water. The use of what is called 2D-IR, which couples either a Raman or Fourier Transform Infrared Spectrometer (FTIR) and a DMA to study these motions, is a topic of current interest.⁵⁰

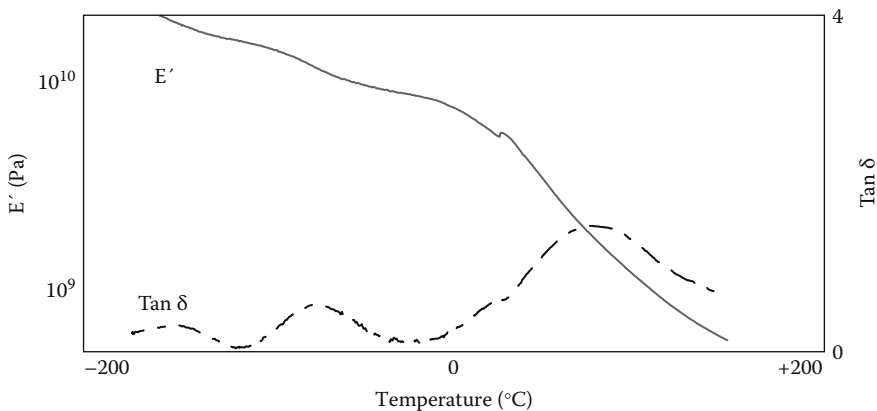


FIGURE 6.6 Transitions at temperatures below the T_g as seen in a sample of nylon 6. Data generated by B. Cassell of PerkinElmer LAS and used with permission.

6.4 THE GLASS TRANSITION (T_g OR T_α)

As the free volume continues to increase with increasing temperature, we reach the glass transition, T_g , where large segments of the chain start moving. This transition is also called the alpha transition, T_α . The T_g is very dependent on the degree of polymerization up to a value known as the critical T_g or the critical molecular weight. Above this value, the T_g typically becomes independent of molecular weight.⁵¹ The T_g represents a major transition for many polymers, as physical properties change drastically as the material goes from a hard glassy to a rubbery state. It defines one end of the temperature range over which the polymer can be used, often called the operating range of the polymer and examples of this range are shown in Figure 6.7. For where strength and stiffness are needed, it is normally the upper limit for use. In rubbers and some semicrystalline materials like polyethylene and polypropylene, it is the lower operating temperature. Changes in the temperature of the T_g are commonly used to monitor changes in the polymer such as plasticizing by environmental solvents and increased crosslinking from thermal or UV aging (Figure 6.8).

The T_g of cured materials or thin coatings is often difficult to measure by other methods and more often than not the initial cost justification for a DMA is measuring a hard to find T_g . While estimates of the relative sensitivity of a DMA to a DSC or a DTA vary, it appears that DMA is 10 to 100 times more sensitive to the changes occurring at the T_g . The T_g in highly crosslinked materials can easily be seen long after the T_g has become too flat and diffuse to be seen in the DSC (Figure 6.9a). A highly crosslinked molding resin used for chip encapsulation was run by both methods and the DMA is able to detect the transition after it is undetectable in the DSC. This is also a known problem with certain materials like medical grade urethanes and very highly crystalline polyethylenes. Kessler reports on the relation of postcure and $\tan \delta$; in the DMA these weak transitions are easy to see and this has generated tremendous interest from the pharmaceutical industry despite the sample handling difficulties.⁵²

The method of determining the T_g in the DMA can be a manner for disagreement as at least five ways are in current use (Figure 6.9b). This is not unusual as DSC has multiple methods, too (Figure 6.9c). Depending on the industry standards or background of the operator, the peak or onset of the $\tan \delta$ curve, the onset of the E' drop, or the onset or peak of the E'' curve may be used. The values obtained from these methods can differ up to 25°C from one another on the same run. In addition, a 10°C–20°C difference from the DSC is also seen in many materials. In practice, it is important to specify exactly how the T_g should be determined. For DMA, this means defining the heating rate, applied stresses (or strains), the frequency used, and the method of determining the T_g . For example, the sample will be run at 10°C/min under 0.05% strain at 1 Hz in nitrogen purge (20 cc/min) and the T_g determined from peak of the $\tan \delta$ curve. Notice we are not even discussing the affect of prestain and frequency on the values. This also changes the values^{53,54} of the glass transition as well as the $\tan \delta$.⁵⁵

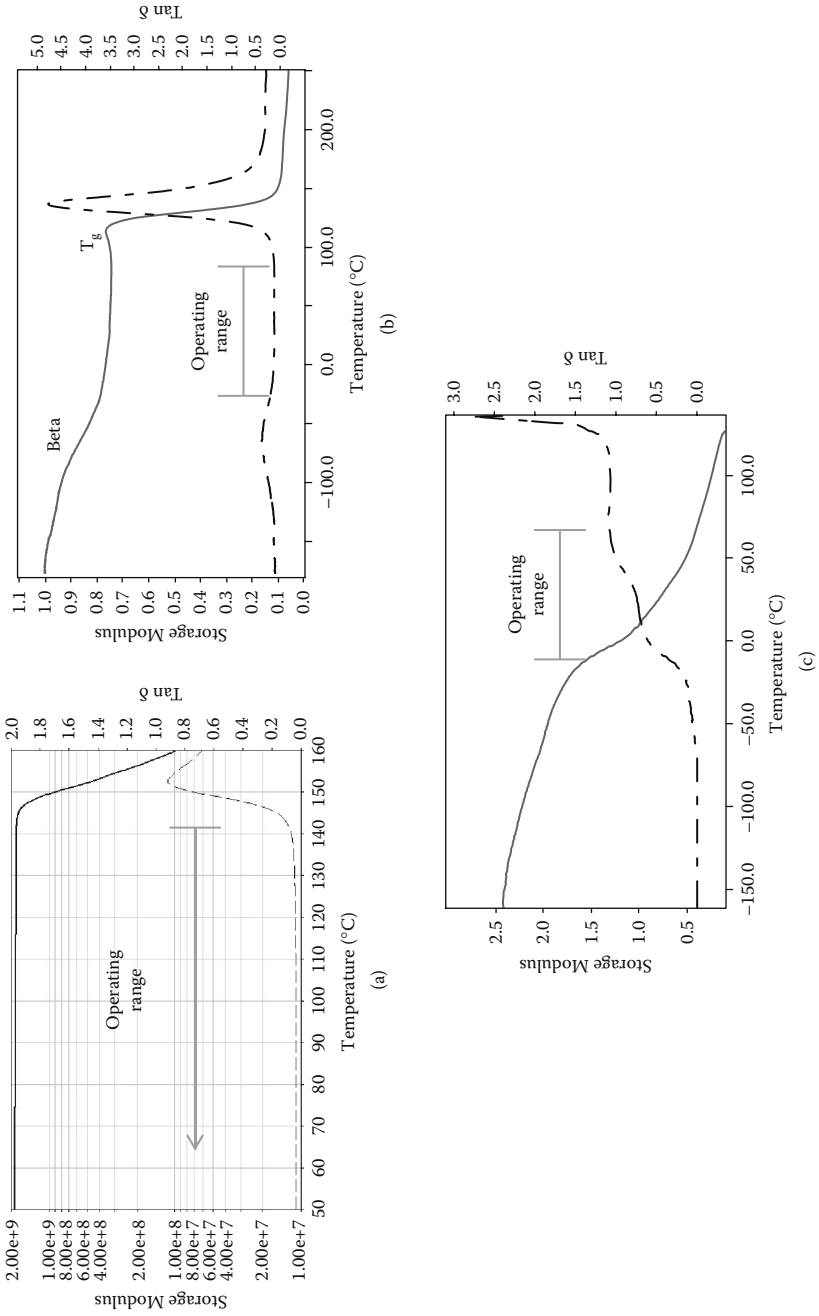


FIGURE 6.7 Definition of an operating range based on position of T_g in (a) polycarbonate, (b) epoxy, and (c) polypropylene.

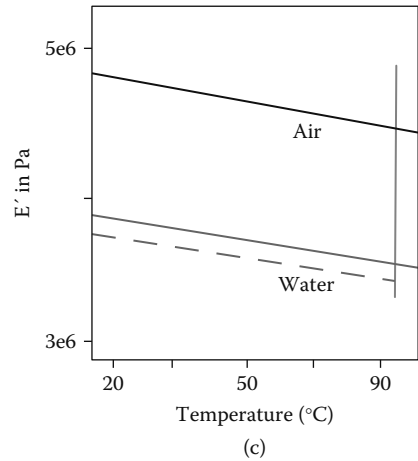
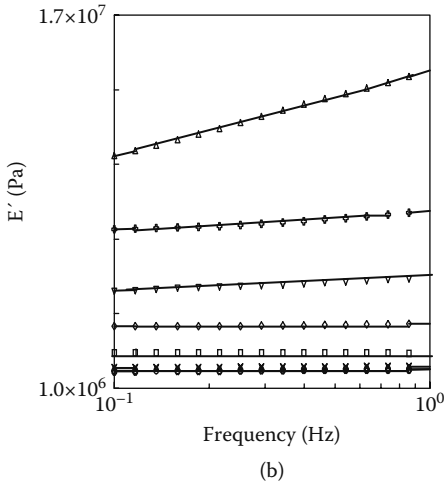
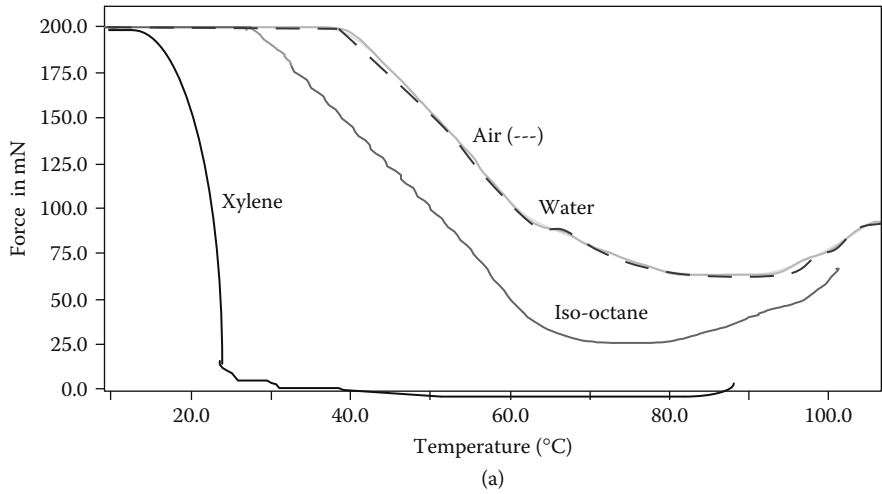


FIGURE 6.8 Effects of various environmental conditions on the T_g . (a) The effect of various solvents on polypropylene fibers in air, water, iso-octane, and xylene. Note that the air and water curves overlay exactly proving there is no effect like buoyancy or drag caused by the presence of liquid supporting the probe. (b) The swelling of rubber in MEK and (c) the effect of a 10-minute immersion in saline solution on medical grade polyurethane.

It is not unusual to see a peak or hump on the storage modulus directly preceding the drop that corresponds to the T_g . This is shown in Figure 6.10. This is also seen in the DSC and DTA and corresponds to a rearrangement in the molecule to relieve stresses frozen in below the T_g by the processing method. These stresses are trapped in the material until enough mobility is obtained at the T_g to allow the chains to move to a lower energy state. Often a material will be annealed by heating it above the T_g

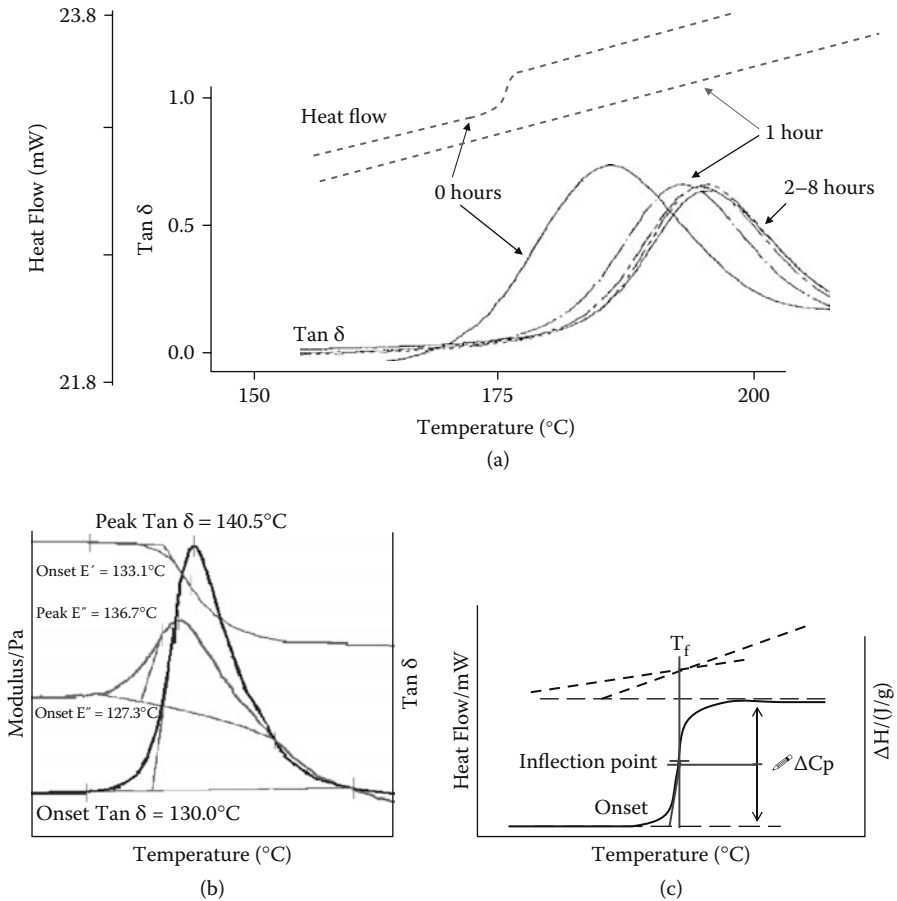


FIGURE 6.9 Measurement of the T_g by DMA and DSC. (a) The T_g of a chip encapsulation material was measured by DSC and DMA as a function of postcure time. (b) Multiple methods of determining the T_g are shown for the DMA. The temperature of the T_g varies up to $10^{\circ}C$ in this example depending on the value chosen. Differences as great as $25^{\circ}C$ have been reported. (c) Four of the methods used to determine the T_g in DSC are shown. The half-height and half-width methods are not included.

and slowly cooling it to remove this affect. For similar reasons, some experimenters will run a material twice or use a heat-cool-heat cycle to eliminate processing effects.

6.5 THE RUBBERY PLATEAU, T_{α}^* AND T_{II}

The area above the T_g and below the melt is known as the rubbery plateau, and the length of it as well as its viscosity is dependent on the molecular weight between entanglements (M_e)⁵⁶ or crosslinks. The molecular weight between entanglements is normally calculated during a stress relaxation experiment, but similar behavior

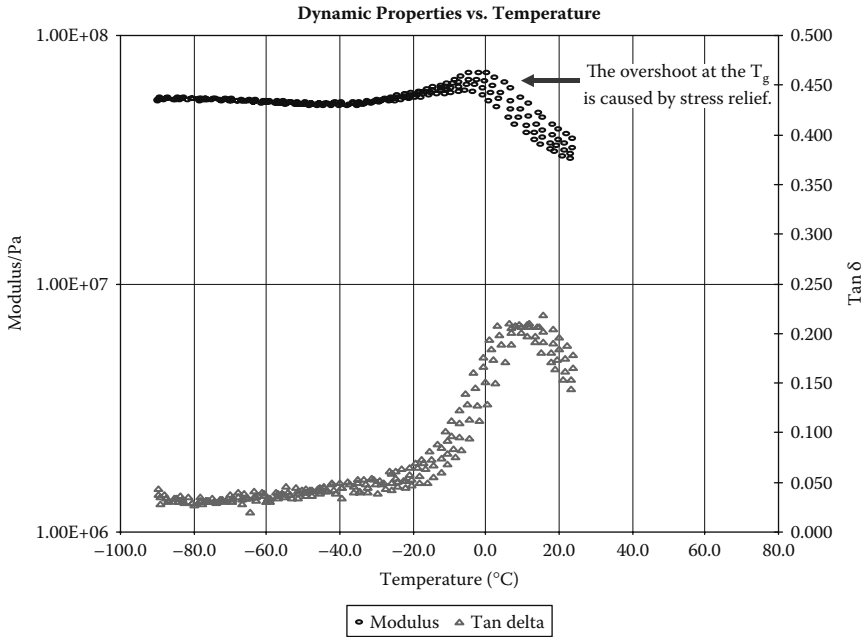


FIGURE 6.10 Stress relief at the T_g in the DMA. The overshoot is similar to that seen in the DSC and is caused by molecular rearrangements that occur due to the increased free volume at the transition.

is observed in the DMA (Figure 6.11). The modulus in the plateau region is proportional to either the number of crosslinks or the chain length between entanglements. This is often expressed in shear as

$$G' \cong (\rho RT)/M_e \tag{6.2}$$

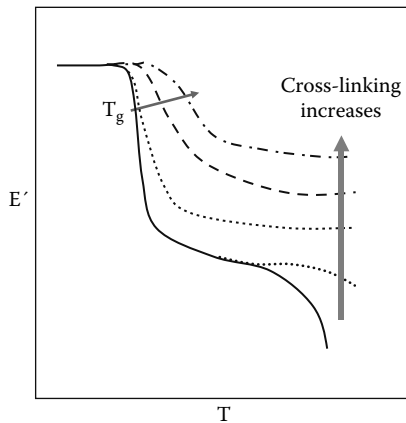


FIGURE 6.11 DMA results indicating increased crosslinking by increasing T_g temperature and increasing modulus above the T_g .

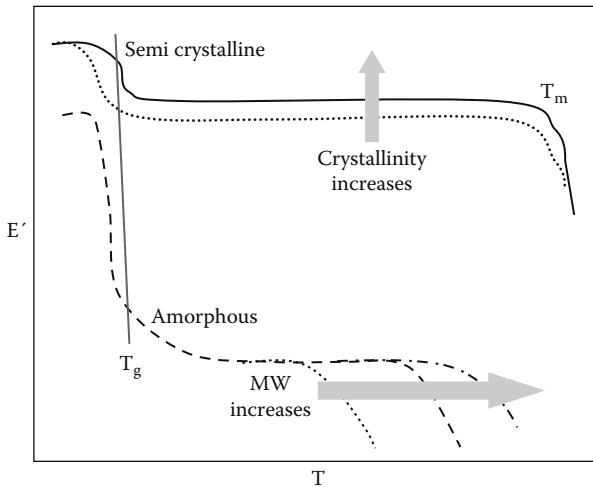


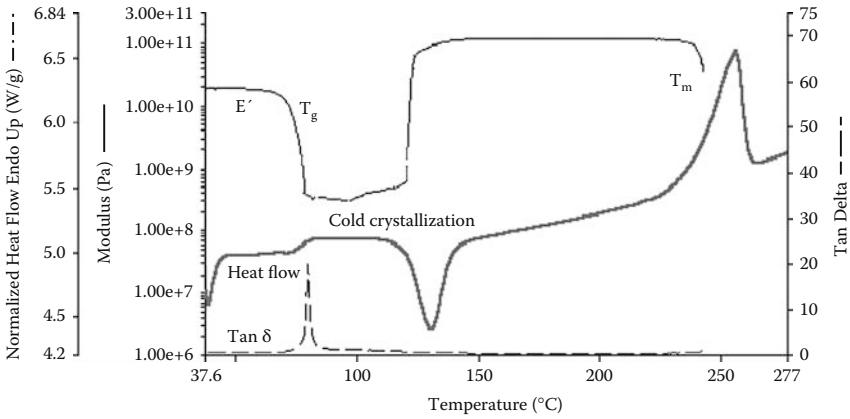
FIGURE 6.12 Effects of crystallinity and M_w on the DMA curves.

where G' is the modulus of the plateau region at a specific temperature, ρ is the polymer density, and M_e is the molecular weight between entanglements. In practice, the relative modulus of the plateau region tells us about the relative changes in M_e or the number of crosslinks compared to a standard material.

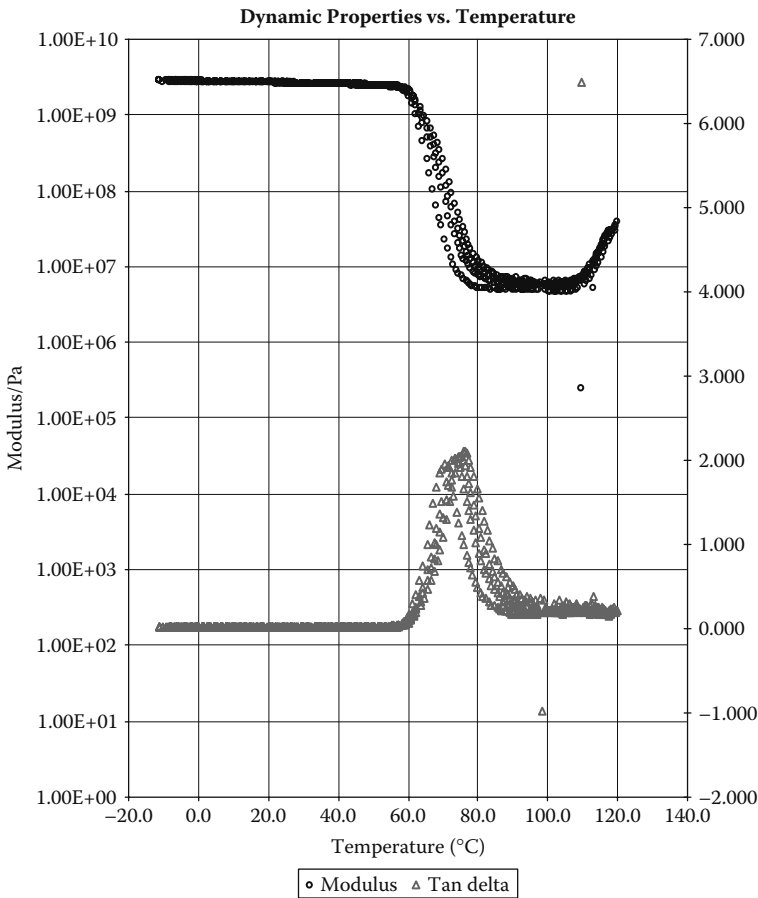
The rubbery plateau is also related to the degree of crystallinity in a material, although DSC is a better method for characterizing crystallinity than DMA.⁵⁷ This is shown in Figure 6.12. Also as in the DSC, we can see evidence of cold crystallization in the temperature range above the T_g (Figure 6.13). That is one of several transitions that can be seen in the rubbery plateau region. This crystallization occurs when the polymer chains have been quenched (quickly cooled) into a highly disordered state. On heating above the T_g these chains gain enough mobility to rearrange into crystallites, which causes a sometimes dramatic increase in modulus (Figure 6.13). DSC or a modulated temperature technique, like StepScan DSC can be used to confirm this.⁵⁸

The alpha star transition (T_{α}^*), the liquid–liquid transition (T_{ll}), the heat set temperature, and the cold crystallization peak are all transitions that can appear on the rubbery plateau. In some crystalline and semicrystalline polymers, a transition is seen called the T_{α}^* .⁵⁹ Figure 6.14 shows this in a sample of polypropylene. The alpha star transition is associated with the slippage between crystallites and helps extend the operating range of a material above the T_g . This transition is very susceptible to processing induced changes and can be enlarged or decreased by the applied heat history, processing conditions, and physical aging.⁶⁰ The T_{α}^* has been used by fiber manufacturers to optimize properties in their materials.

In amorphous polymers, we instead see the T_{ll} , a liquid–liquid transition associated with increased chain mobility and segment–segment associations.⁶¹ This order is lost when the T_{ll} is exceeded and regained on cooling from the melt. Boyer reports



(a)



(b)

FIGURE 6.13 (a) Cold crystallization in PET caused a large increase in the storage modulus, E' , above the T_g . A DSC scan of the same material is included. (b) Same effect in PLA.

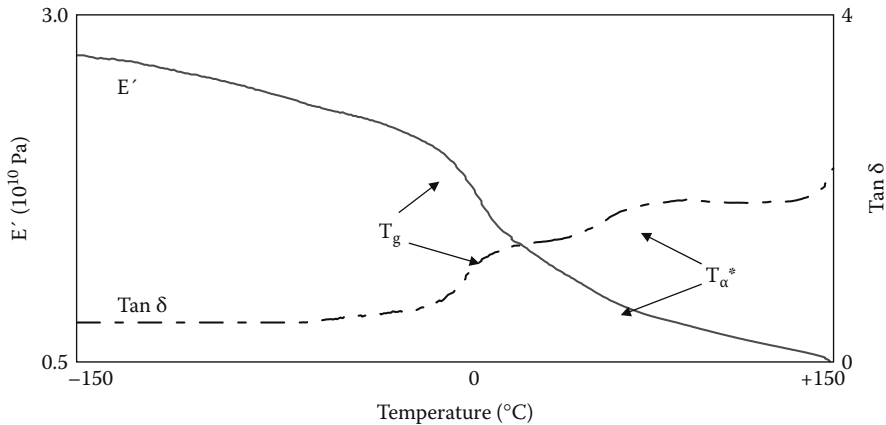


FIGURE 6.14 The alpha star transition, T_{α}^* , in polypropylene corresponding to a crystal-crystal slip in the polymer.

that, like the T_g , the appearance of the T_{II} is affected by the heat history.⁶² The T_{II} is also dependent on the number average molecular weight, M_n , but not on the weight average molecular weight, M_w . Bershtein et al. suggest that this may be considered as quasimelting on heating or the formation of stable associates of segments on cooling.⁶³ While this transition is reversible, it is not always easy to see and Boyer spent many years trying to prove it was real.⁶⁴ Not everyone accepts the existence of this transition. This transition may be similar to some of the data from temperature modulated DSC experiments showing a recrystallization at the start of the melt.⁶⁵ In both cases, some subtle changes in structure are sometimes detected at the start of melting. Following this transition, a material enters the terminal or melting region.

Depending on its strength, the heat set temperature can also be seen in the DMA. While it is normally seen in either a TMA or a constant gauge length (CGL) experiment (Figure 6.15), it will sometimes appear as either a sharp drop in modulus (E') or an abrupt change in probe position. Heat set is the temperature at which some strain or distortion is induced into polymeric fibers to change their properties, such as to prevent a nylon rug from feeling like fishing line. Since heating above this temperature will erase the texture, and you must heat polyesters above the T_g to dye them, it is of critical importance to the fabric industry. Many final properties of polymeric products depend on changes induced in processing.⁶⁶

6.6 THE TERMINAL REGION

On continued heating, the melting point, T_m , is reached. The melting point is where the free volume has increased so the chains can slide past each other and the material flows. This is also called the terminal region. In the molten state, this ability to flow is dependent on the molecular weight of the polymer (Figure 6.16). The melt of a polymer material will often show changes in temperature of melting, width of the melting peak, and enthalpy as the material changes⁶⁷ resulting from changes in the polymer molecular weight and crystallinity.

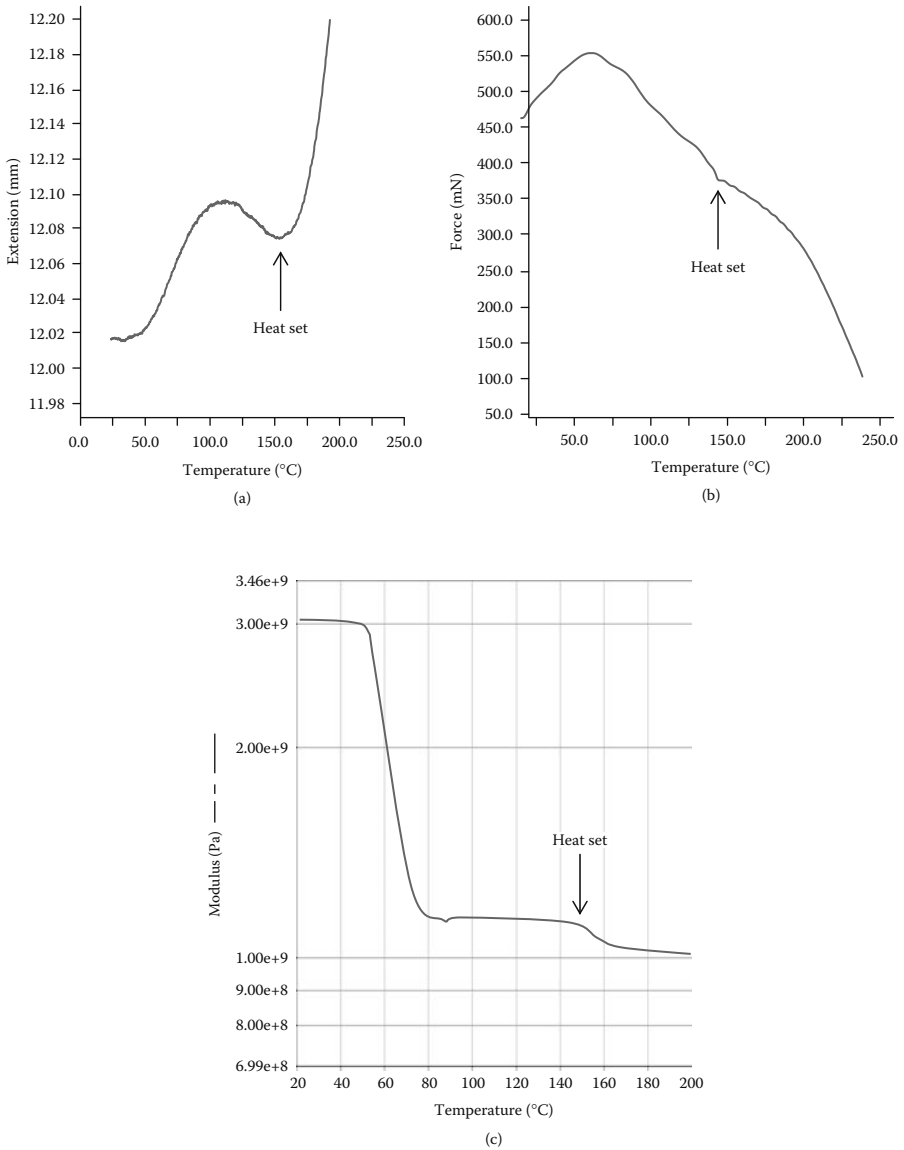


FIGURE 6.15 The heat set temperature by (a) TMA, (b) CGL, and (c) DMA.

Degradation, polymer structure, and environmental effects all influence what changes occur. Polymers that degrade by crosslinking will look very different from those that exhibit chain scissoring. Very highly crosslinked polymers will not melt as they are unable to flow.

The study of polymer melts, and especially their elasticity, was one of the areas that drove the development of commercial DMAs. Although we see a decrease in the

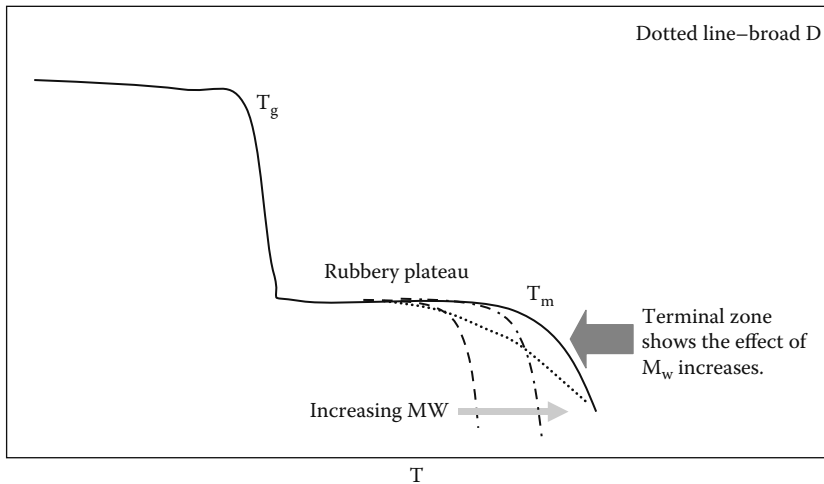


FIGURE 6.16 The terminal zone or melting region follows the rubbery plateau and is sensitive to the M_w of the polymer.

melt viscosity as temperature increases, the DMA is most commonly used to measure the frequency dependence of the molten polymer as well as its elasticity. The latter property, especially when expressed as the normal forces, is very important in polymer processing. These topics will be discussed in detail in Chapter 8.

6.7 FREQUENCY DEPENDENCIES IN TRANSITION STUDIES

We have neglected to discuss either the choice of a testing frequency or its effect on the resulting data. While most of our discussion on frequency will be in a later chapter, a short discussion of how frequencies are chosen and how they affect the measurement of transitions is in order. If we consider that higher frequencies induce more elastic-like behavior, we can see that there is some concern a material will act stiffer than it really is at high test frequencies. Frequencies for testing are normally chosen by one of three methods.

The most scientific method would be to use the frequency of the stress or strain that the material is exposed to in the real world. However, this is often outside of the range of the available instrumentation. In some cases, the test method or the industry standard sets a certain frequency and this frequency is used. Ideally, a standard method like this is chosen so that the data collected on various commercial instruments can be shown to be compatible. Some of the ASTM methods for DMA are listed in Table 5.1. Many industries have their own standards so it is important to know whether the data is expected to match a military-specification (Mil-spec), an ASTM standard, or a specific industrial test. Finally, one can arbitrarily pick a frequency. This is done more often than not, so that 1 Hz and 10 rad/sec are often used. As long as the data are run under the proper conditions, they can be compared to

TABLE 6.1
ASTM Tests for the DMA

- D4065-06 Standard Practice for Plastics: Dynamic Mechanical Properties: Determination and Report of Procedures
 - D6456-99 (2004) Standard Specification for Finished Parts Made from Polyimide Resin
 - E1640-04 Standard Test Method for Assignment of the Glass Transition Temperature by Dynamic Mechanical Analysis
 - E1867-01 Standard Test Method for Temperature Calibration of Dynamic Mechanical Analyzers
 - E1867-06 Standard Test Method for Temperature Calibration of Dynamic Mechanical Analyzers
 - E1953-07 Standard Practice for Description of Thermal Analysis and Rheology Apparatus
 - E2254-03 Standard Test Method for Storage Modulus Calibration of Dynamic Mechanical Analyzers
 - E2425-05 Standard Test Method for Loss Modulus Conformance of Dynamic Mechanical Analyzers
 - WK278 New Test Method for Glass Transition Temperature (T_g) DMA of Polymer Matrix Composites
 - WK3113 Loss Modulus Calibration or Conformance of DMAs
 - WK3645 Standard Test Method for Temperature Calibration of DMAs
 - WK10344 Standard Terminology: Plastics: Dynamic Mechanical Properties
-

highlight material differences. This requires that frequency, stresses, and the thermal program to be the same for all samples in the data set.

Most DMAs today can collect data on multiple frequencies in a single temperature scan. This can often be anywhere from 2 to 10 scanned as the temperature changes. Now, obviously we want to avoid things like 0.001 Hz where the data takes a long time to collect. Normally one picks a couple of frequencies a decade apart. This allows one to get an indication of the frequency response while still collecting at reasonable rates. Normally if one uses frequencies like 1, 5, 10, and 50, one can still heat at 2–3 degrees a minute and get good data. Frequencies lower than one require to very slow ramp rates; data points at .01 Hz take 100 sec to collect.

So what is the effect of frequency on transitions? Briefly, lowering the frequency shifts the temperature of a transition to a lower temperature (Figure 6.17). At one time, it was suggested that multiple frequencies could be used and the T_g should then be determined by extrapolation to zero hertz. This was never really accepted as it represented a fair amount of work for a small improvement in accuracy. However, one will still occasionally see this done, especially when a very close match to DSC data is being sought. For most polymer systems, for very precise measurements, one uses a DSC. This isn't always possible due to the weakness of some transitions and we are seeing more and more testing on pharmaceutical materials with amorphous content being done in the DMA.⁶⁸ Some techniques for handling tests will be discussed in Chapter 9.

Different types of transitions also have different frequency dependencies. McCrum et al. listed many of these.⁶⁹ If one looks at the slope of the temperature dependence of transitions against frequency, one sees that in many cases the primary transitions like T_m and T_g are less dependent than the secondary transitions. However, a perusal of McCrum et al.'s data shows this isn't always true.

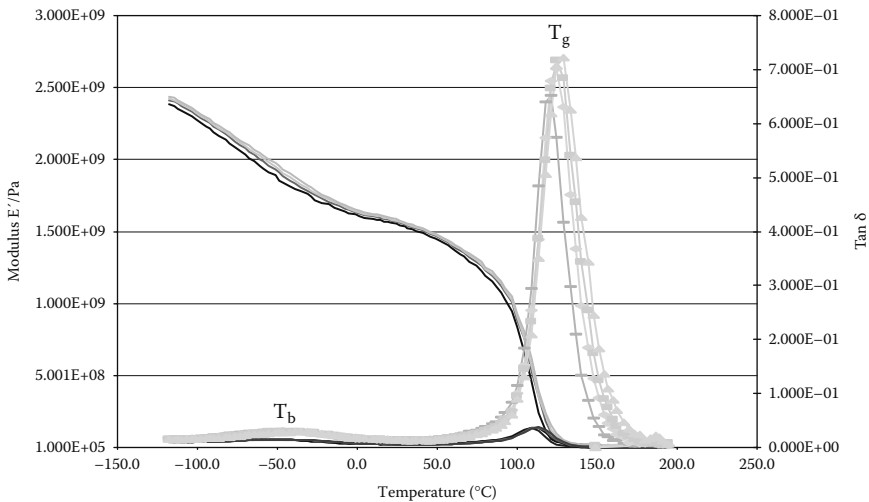


FIGURE 6.17 Frequency dependence of transitions. T_b and T_g at three different frequencies in PLC.

6.8 APPLICATIONS

In the previous sections, we have been staying mainly with either a homopolymer or with a material such as a fiber-filled composite where the filler does not show transitions. Actual commercial formulations and systems tend to be a bit messier and I would like to address some of those issues here.

Many commercial polymers contain modifiers and fillers,⁷⁰ which are blended with the polymer to improve properties or to reduce costs. The concentration and presence of these additives is often best studied by other methods, but DMA lets us examine their effects on the bulk properties of the polymers. These may show up as small drops in the storage modulus curve. More likely, the effects are seen as changes to the strength and temperature of the bulk polymer. For example, changing the amount of filler or the amount of oil in peanut butter makes noticeable changes in the DMA scan as shown in Figure 6.18. Adding more filler to a rubber increases its modulus and improves the material's resistance to abrasion (Figure 6.18a). Adding oil to peanut butter softens it and makes it easier to spread (Figure 6.18b). Rigid PVC is made flexible to improve its resistance to breakage and to make the tubing made from it easier to use (Figure 6.18c). Some of these effects are best seen in frequency scans and will be discussed in Chapter 8. Sometimes the polymer is added as a binder to an inorganic material, like the magnetic particles used to make the magnetic coating on a videotape. This is then coated on a polymer film. The overlapping transitions are difficult to see and the uncoated PET film's data was subtracted from the coated film to allow detection of the transitions of the binder (Figure 6.18d).

Many polymers contain a second or third polymer as either a blend (a physical mixture of materials) or as a copolymer (a chemical mixture). This is done to toughen a hard brittle material by adding a quantity of a rubbery material to it. The study of "rubber-toughened" or just "toughened plastics" is a large and sophisticated

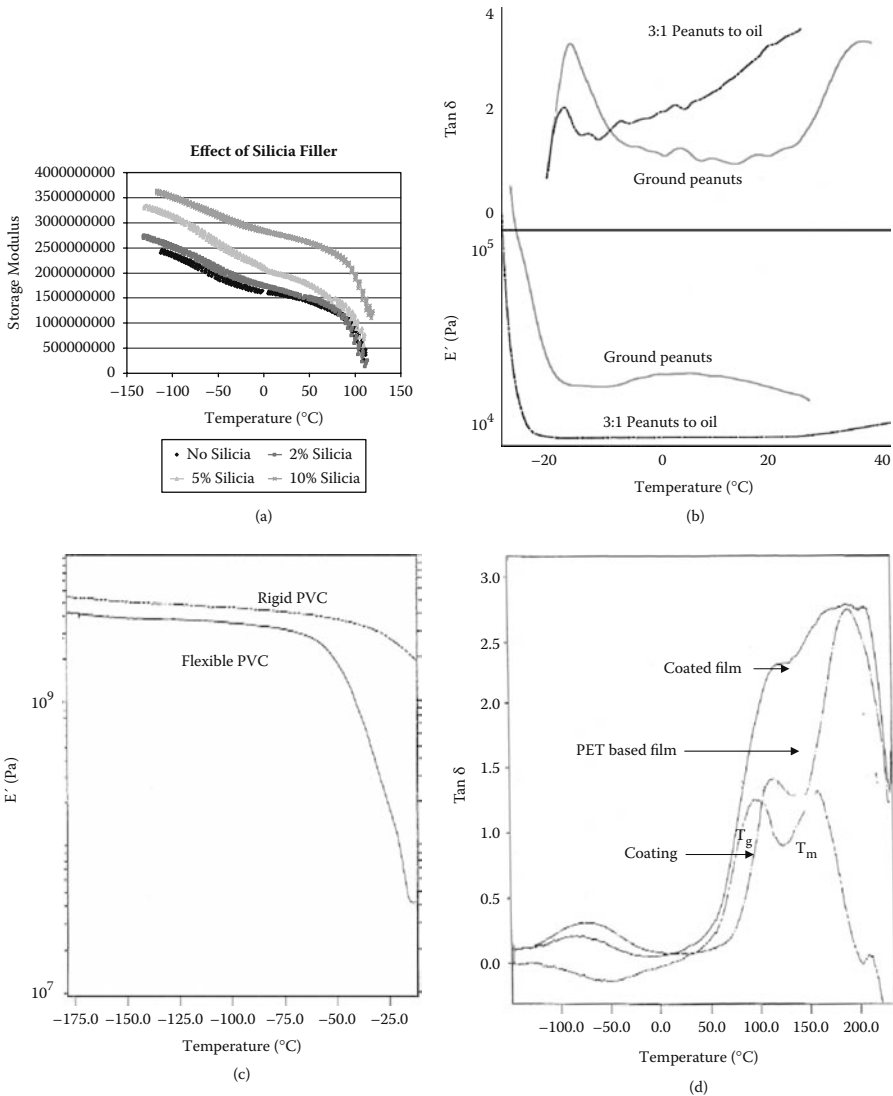


FIGURE 6.18 Effects of additives, fillers, and coatings on polymers. (a) The effect of increasing silica content on a cured epoxy, which increases the storage modulus. (b) The effect of adding oil to peanut butter to soften it and increase its spreadability. Data taken by Dr. Farrell Summers and used with his permission. (c) Rigid and flexible PVC where additives decrease the stiffness of the material. (d) Coatings are used to give materials special properties like the magnetic coating applied to PET. The curve for the coating is obtained by subtracting the PET curve from the coated curve.

area of research.⁷¹ In the DMA scan, it is often possible to see the transitions of both the main polymer and the toughening agent. One can use DMA to look for the degree of phase separation in polymer blends like epoxy-propylene⁷² and relate this to toughness.

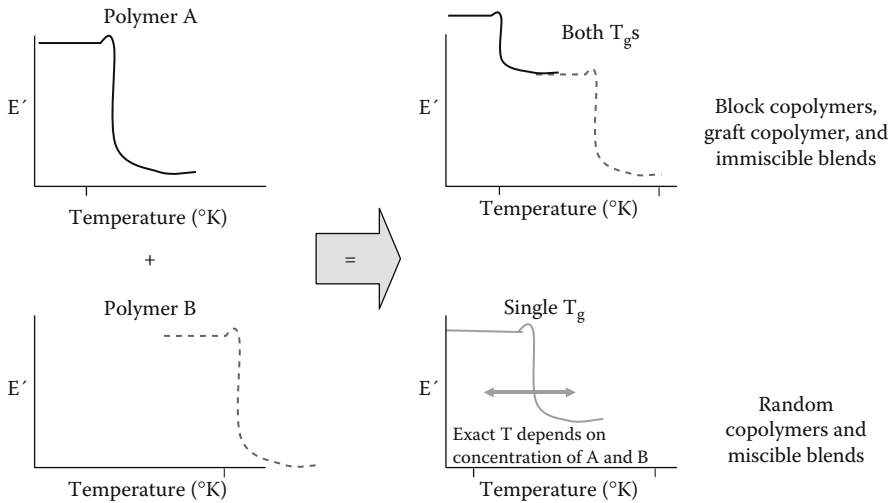


FIGURE 6.19 Blends and copolymers. How polymer blending affects the T_g is shown schematically.

For copolymers in the DMA,⁷³ one sees effects like the T_g of the copolymer moving between the extremes of the two homopolymers in relation to the molecular concentration of the components.⁷⁴ These effects are summarized in Figure 6.19, which shows how copolymers and blends change the T_g . There is a morphological component here, too, as block copolymers will appear to be blends if the blocks are large enough. One can use DMA to look for grafting in polymers⁷⁵ and rates of polymerization⁷⁶ as well as decomposition.⁷⁷

Certain materials like foams represent other areas of special study. Because the bulk properties of a foam depend not only on the bulk properties of the matrix but also on the size and spacing of the air pockets (cells), characterization is tricky. DMA allows measurement of the matrix T_g as well as allowing characterization of the expanded foam. Macosko reports good results in studying foams in the DMA⁷⁸ and Bessette has shown good agreement between DMA and the more traditional test methods.⁷⁹

Although we are dealing mainly with polymers, it should be mentioned that DMA is also used to study the properties of metals, particularly those with considerable amorphous content.⁸⁰ As mentioned in Chapter 1, the initial development of DMA was to look at wires, and today there is a lot of interest in the properties of wires used in orthodontics⁸¹ and aerospace applications. In looking at amorphous metals, or perhaps better called metallic glasses, one finds both glass transitions and memory effects much more like one associates with polymers than traditional metals. Some of the effects are quite extreme as seen with metals that remember their shape after deformation. Electronic materials such as those used in electronic cooling devices also exhibit interesting behavior in the DMA with different transitions being seen when current is applied.⁸²

Finally, because DMA can give an almost instantaneous measurement of modulus, it can be used for a quick one-minute test of a material to see its modulus and

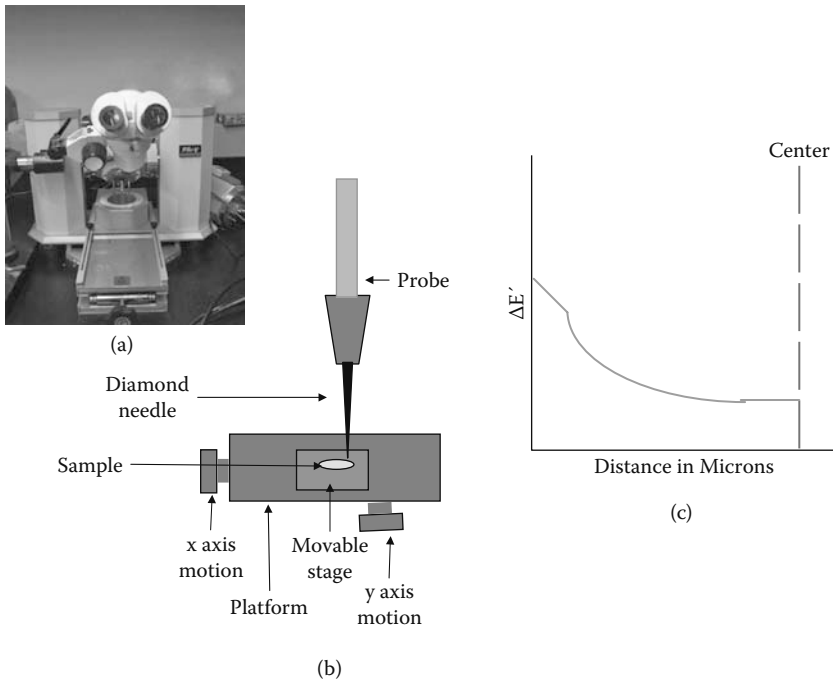


FIGURE 6.20 Micro-DMA. (a) A PerkinElmer DMA 8000 adapted to allow use of a microscope for micro-DMA. (b) Schematic of the movable stage and diamond needle under the scope and (c) results of mapping the modulus across the thickness of a part.

$\tan \delta$. This is often used as a quick quality control tool on incoming materials or suspect products. However, it can also be used to map the modulus of a specimen to look for surface oxidation or localized embrittlement. Figure 6.20a shows a picture of a DMA system adapted to using a microprobe (a diamond phonograph needle) to map the modulus of polyethylene parts across their wall thickness.⁸³ The results are shown in Figure 6.20c.

6.9 TIME-BASED STUDIES

The other part of time–temperature effects is studying how a material responds when held at constant temperature for set periods of time. This is most commonly seen in curing and postcuring studies, which will be discussed in Chapter 7. However, there are several applications where a sample will be held at a set temperature under oscillatory stress for long periods of time. Some early work using this approach was reported by Ferry where samples were run for long periods of time at varying temperatures for superposition to study age life.⁸⁴

However, this is not a common use of the DMA and it is more common to hold material under constant dynamic stress at a set temperature under some special conditions. The condition can simply be elevated temperature where degradation occurs or it can be a special environment, like UV light, solvents, humidity, or corrosive gases.

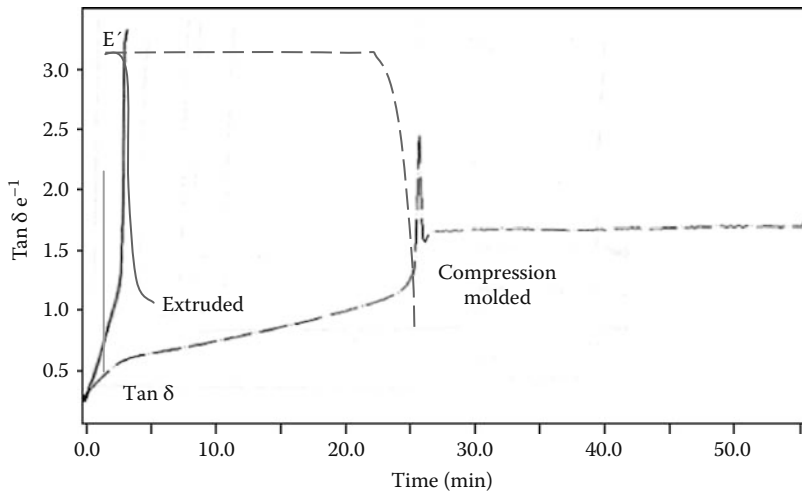


FIGURE 6.21 Degradation of High Impact Polystyrene (HIPS) in food oils by DMA. A comparison of compression molded parts and extruded sheets. Failure is seen in both the $\tan \delta$ and in the E' curves. Both samples were made from the same batch of HIPS.

These conditions are normally chosen to accelerate the degradation or changes seen in the final use of the material. Figure 6.21 shows the effect of elevated temperature and a cottonseed–olive oil mixture at 70°C on high impact polystyrene. Other examples include medical grade polyurethane in saline or Rykker's solution, fibers in organic solvents, oil filters in oil, Teflon® piping gaskets and valves at elevated temperatures in crude oil, soft contact lenses in saline under UV, thermoset composites in high humidity, geotextile fabrics in highly acidic media, coatings in corrosive gases like H₂S, human hair coated with hair sprays at elevated temperature, and photocuring adhesives in UV. The ability to get failure data in these diverse conditions while exploring the changes in modulus, viscosity, and damping during the tests is a unique, useful strength of DMA and we'll talk about that in Chapter 9.

6.10 CONCLUSIONS

We have intentionally not extensively covered the effects of blends, morphology, and additives in order to limit the scope of this chapter to basic topics. Nor are we going to discuss relaxation spectra or other more advanced topics. In Chapter 10, we will discuss where you can go for more specialized information. What is important to realize is that by performing time or temperature studies in the DMA on thermoplastics or cured thermosets allows one to probe the transitions that define their properties. This is not to suggest you should throw out your impact or Izod tester as the promise of DMA does not always come through. It is to suggest that more transitions than the T_g are important in describing behavior in the solid state. DMA allows you to easily collect data that is difficult or costly by other means. Now, we need to consider thermosets and their study in the DMA.

NOTES

1. A. Sircar et al., *Assignment of the Glass Transition*, R. Seyler, Ed., ASTM, Philadelphia, 1994, p. 293.
2. This is a fairly serious concern of a lot of users in practice, though it does not get discussed in the literature frequently. See for example: R. Armstrong, *Short Course in Polymeric Fluids Rheology*, MIT, Cambridge, MA, 1990. R. De le Garza, *Measurement of Viscoelastic Properties by Dynamic Mechanical Analysis*, University of Texas at Austin, Master's thesis, 1994. R. Hagan, *Polym. Test.*, 13, 113, 1994.
3. I. Chodak et al., *Polym. Test.*, 19, 755, 2000.
4. J. Duncan, *Principles and Applications of Thermal Analysis*, Blackwell, Oxford, 2007, ch. 4.
5. D. Mulligan, S. Gnaniah, and G. Simms, *Thermal Analysis Techniques for Composites and Adhesives*, 2nd ed., NPL Measurement Good Practice Guide No. 62, 2003.
6. S. Goodkowski and B. Twombly, *Thermal Application Notes*, PerkinElmer, Norwalk, 1994, p. 56.
7. P. Flory, *Principles of Polymer Chemistry*, Cornell University Press, Ithaca, NY, 1953.
8. R. Bird, C. Curtis, R. Armstrong, and O. Hassenger, *Dynamics of Polymer Fluids*, Vols. 1 and 2, 2nd ed., Wiley, New York, 1987.
9. J.D. Ferry, *Viscoelastic Properties of Polymers*, 3rd ed., Wiley, New York, 1980. J.J. Aklonis and W.J. MacKnight, *Introduction to Polymer Viscoelasticity*, 2nd ed., Wiley, New York, 1983.
10. L.C.E. Struik, *Physical Aging in Amorphous Polymers and Other Materials*, Elsevier, New York, 1978. L.C.E. Struik, in *Failure of Plastics*, W. Brostow and R.D. Corneliusen, Eds., Hanser, New York, 1986, ch. 11. S. Matsuoka, in *Failure of Plastics*, W. Brostow and R.D. Corneliusen, Eds., Hanser, New York, 1986, ch. 3. S. Matsuoka, *Relaxation Phenomena in Polymers*, Hanser, New York, 1992.
11. J.D. Vrentas, J.L. Duda, and J.W. Huang, *Macromolecules*, 19, 1718, 1986.
12. W. Brostow and M.A. Macip, *Macromolecules*, 22(6), 2761, 1989.
13. N. McCrum, G. Williams, and B. Read, *Anelastic and Dielectric Effects in Polymeric Solids*, Dover, New York, 1967.
14. M. Doi and S. Edwards, *The Dynamics of Polymer Chains*, Oxford University Press, New York, 1986.
15. M. Shaw and J. MacKnight, *Introduction to Viscoelasticity*, 3rd ed., Wiley, New York, 2005.
16. C.L. Rohn, *Analytical Polymer Rheology*, Hanser-Gardner, New York, 1995.
17. I. Ward and J. Sweeney, *The Mechanical Properties of Solid Polymers*, Wiley, New York, 2004.
18. J. Heijboer, *Int. J. Polym. Mater.*, 6, 11, 1977.
19. N. McCrum, G. Williams, B. Read, *Anelastic and Dielectric Effects in Polymeric Solids*, Dover, New York, 1967.
20. R.F. Boyer, *Polym. Eng. Sci.*, 8(3), 161, 1968.
21. C.L. Rohn, *Analytical Polymer Rheology*, Hanser-Gardner, New York, 1995, pp. 279–283.
22. W. Brostow, H. Hagg Lobland, and M. Narkis, *J. Mater. Res.*, 21, 2422, 2006.
23. N. McCrum, G. Williams, and B. Read, *Anelastic and Dielectric Effects in Polymeric Solids*, Dover, New York, 1967.
24. J. Heijboer, *Int. J. Polym. Mater.*, 6, 11, 1977. M. Mangion and G. Johari, *J. Polym. Sci. Part B: Polym. Phys.*, 29, 437, 1991. G. Johari, G. Mikolajczak, and J. Cavaille, *Polymer*, 28, 2023, 1987. S. Cheng et al., *Polym. Sci. Eng.*, 33, 21, 1993. G. Johari,

- Lect. Notes Phys.*, 277, 90, 1987. R. Daiz-Calleja and E. Riande, *Rheologica Acta*, 34, 58, 1995. R. Boyd, *Polymer*, 26, 323, 1985. V. Bershtein, V. Egorov, L. Egorova, and V. Ryzhov, *Thermochimica Acta*, 238, 41, 1994.
25. B. Twombly, *NATAS Proc.*, 20, 63, 1991.
 26. C.L. Rohn, *Analytical Polymer Rheology*, Hanser-Gardner, New York, 1995. J. Heijboer, *Int. J. Polym. Mater.*, 6, 11, 1977.
 27. R. Boyer, *Polym. Eng. Sci.*, 8(3), 161, 1968.
 28. V. Bershtein and V. Egorov, *Differential Scanning Calorimetry in the Physical Chemistry of Polymers*, Ellis Horwood, Chichester, 1993.
 29. B. Coxton, private communication. Also see the sections on coatings in the *SAMPE Proceedings* for 1995 and 1996.
 30. S. Cheng et al., *Polym. Sci. Eng.*, 33, 21, 1993.
 31. G. Johari, G. Mikoljaczak, J. Cavaille, *Polymer*, 28, 2023, 1987.
 32. M. Mangion and G. Johari, *J. Polym. Sci. Part B: Polym. Phys.*, 29, 437, 1991.
 33. F.C. Nelson, *Shock and Vibration Digest*, 26(2), 11, 1994. F.C. Nelson, *Shock and Vibration Digest*, 26(2), 24, 1994.
 34. W. Brostow, private communication.
 35. L. Pick and E. Harkin-Jones, *Polym. Eng. Sci.*, 43, 905, 2003.
 36. R. Benson and L. Mandelkern, *J. Poly. Sci.*, 1984, 22, 407. M. Mateev et al., *Int. J. Mater.*, 10, 85, 1995.
 37. K. Tanaka et al., *Kobunshi Ronbonshu*, 36, 321, 1979.
 38. J. Guzman et al., *J. Polym. Sci.*, 24, 337, 1986.
 39. K. Adachi et al., *Polymer*, 25, 625, 1984.
 40. P. Frontini et al., *Polym. Int.*, 43, 260, 1997.
 41. R. Duckett et al., *Polymer*, 25, 1392, 1984.
 42. R. Boyer, *Polym. Eng. Sci.*, 8(3), 161, 1968.
 43. J. Heijboer, *Int. J. Polym. Mater.*, 6, 11, 1977.
 44. G. Johari, *Lecture Notes in Physics*, 277, 90, 1987. J. Heijboer, *Int. J. Polym. Mater.*, 6, 11, 1977. J. Heijboer et al., *Physics of Non-Crystalline Solids*, J. Prins, Ed., Interscience, New York, 1965. J. Heijboer, *J. Polym. Sci.*, C16, 3755, 1968. L. Nielsen et al., *J. Macromol. Sci. Phys.*, 9, 239, 1974.
 45. A. Yee and S. Smith, *Macromolecules*, 14, 54, 1981.
 46. G. Gordon, *J. Polym. Sci. A2*, 9, 1693, 1984.
 47. J. Wendorff and B. Schartel, B., *Polymers*, 36(5), 899, 1995.
 48. N. McCrum, G. Williams, and B. Read, *Anelastic and Dielectric Effects in Polymeric Solids*, Dover, New York, 1967.
 49. R. H. Boyd, *Polymer*, 26, 323, 1985.
 50. I. Noda, *Appl. Spectroscopy*, 44(4), 550, 1990. V. Kien, *Proc. 6th Symp. Radiat. Chem.*, 6(2), 463, 1987.
 51. L.H. Sperling, *Introduction to Physical Polymer Science*, 2nd ed., Wiley, New York, 1992.
 52. This will be discussed more in Chapter 9, but see, for example, K. Menard, et al., *Protein Stability Conference Proceedings*, 2007, p. 57. D. Katayama et al., *J. Pharma. Sci.*, in press or K. Menard et al., *Journal of Thermal Analysis and Calorimetry* in press.
 53. Y. Leong, *J. Appl. Polym. Sci.*, 88, 2118, 2003. J. Sullivan, *J. Appl. Polym. Sci.*, 1983, 23, 1993. C. Anton et al., *Polymer*, 33, 3635, 1992.
 54. G. Bussu and A. Lazzeri, *J. Mater. Sci.*, 41, 6072, 2006.
 55. M. Kessler and R. Palakodeti, *Mater. Lett.*, 60, 3437, 2006.
 56. C. Macosko, *Rheology*, VCH, New York, 1994.

57. F. Quinn et al., *Thermal Analysis*, Wiley, New York, 1994. B. Wunderlich, *Thermal Analysis*, Academic Press, New York, 1990.
58. J. Schawe, *Thermochimica Acta*, 261, 183, 1995. J. Schawe, *Thermochimica Acta*, 260, 1, 1995. J. Schawe, *Thermochimica Acta*, 271, 1, 1995. B. Wunderlich et al., *J. Thermal Anal.*, 42, 949, 1994. G. Hohne et al., *Differential Scanning Calorimetry*, Springer, Berlin, 2005.
59. R.H. Boyd, *Polymer*, 26, 323, 1985. R.H. Boyd, *Polymer*, 26, 1123, 1985.
60. S. Godber, private communication. M. Ahmed, *Polypropylene Fiber: Science and Technology*, Elsevier, New York, 1982.
61. A. Lobanov et al., *Polym. Sci. USSR*, 22, 1150, 1980.
62. R.J. Boyer, *Polym. Sci. Part B: Polym. Phys.*, 30, 1177, 1992. J.K. Gillham et al., *J. Appl. Polym. Sci.*, 20, 1245, 1976. J.B. Enns and R. Boyer, *Encyc. of Polym. Sci.* Vol. 17, 1989, pp. 23–47.
63. V. Bershtein, V. Egorov, L. Egorova, and V. Ryzhov, *Thermochimica Acta*, 238, 41, 1994.
64. C.M. Warner, *Evaluation of the DSC for Observation of the Liquid-Liquid Transition*, Central Michigan State University, master's thesis, 1988.
65. B. Cassel et al., *PETAN #69 DDSC*, PerkinElmer, Norwalk, 1995. W. Sichina, *NATAS Proc.*, 23, 137, 1994. B. Wunderlich, A. Boller, and Y. Jin, *J. Thermal. Anal.*, 42, 307, 1994. B. Wunderlich, *Modulated DSC*, University of Tennessee, Knoxville, 1994.
66. J. Dealy et al., *Melt Rheology and Its Role in Plastic Processing*, Van Nostrand Reinhold, Toronto, 1990. N. Cheremisinoff, *An Introduction to Polymer Rheology and Processing*, CRC Press, Boca Raton, FL, 1993.
67. E. Turi, Ed., *Thermal Characterization of Polymeric Materials*, Academic Press, Boston, 1981. E. Turi, Ed., *Thermal Analysis in Polymer Characterization*, Heydon, London, 1981.
68. P. Royall et al., *Int. J. Pharma.*, 301, 181, 2005.
69. N. McCrum, G. Williams, and B. Read, *Anelastic and Dielectric Effects in Polymeric Solids*, Dover, New York, 1967.
70. Fillers can be quite interesting. See for example: S.K. De et al., *J. Appl. Polym. Sci.*, 48, 1089, 1993.
71. C.B. Bucknall, *Toughened Plastics*, Applied Science Publishers, London, 1977. R. Deanin et al., *Toughness and Brittleness of Plastics*, ACS, Washington D.C., 1976.
72. A. Taylor et al., *Polymer*, 46, 7352, 2005.
73. S. Turley et al., *J. Polym. Sci.: Part C*, 1, 101, 1963. H. Keskkula, *Polym. Letters*, 7, 697, 1969. Y. Lipatov et al., *J. Appl. Polym. Sci.*, 47, 941, 1993. J.H. An, *J. Appl. Polym. Sci.*, 47, 305, 1993. B. Kim et al., *J. Appl. Polym. Sci.*, 47, 295, 1993. M. Wyzgoski, *J. Appl. Polym. Sci.*, 25, 1443, 1980.
74. N.G. McCrum et al., *Principles of Polymer Engineering*, Oxford University Press, New York, 1990. L.H. Sperling, *Introduction to Physical Polymer Science*, 2nd ed., Wiley, New York, 1992.
75. K. De Santos et al., *Int. J. Pharm.*, 310, 36, 2006.
76. M. Gil et al., *Eur. Polym. J.*, 42, 2313, 2006.
77. P. Gupta and A. Bansa, *AAPS Pharm. Sci. Tech.*, 6, E223, 2005.
78. C. Macosko et al., *NATAS Proc.*, 18, 271, 1989.
79. M. Bessette et al., *Polym. Proc. Eng.*, 3, 25, 1985.
80. N.J. Grant and B.C. Giessen, Eds., *Rapidly Quenched Metals*, MIT Press, 1970. B. Giessen et al., *Mater. Sci. Eng.*, 23, 83, 1976. T. Taylor et al., *J. Mater. Sci.*, 23, 2613, 1998. R. Vaidyanathan, M.A.M. Bourke, and D.C. Dunand, *Met. Mat. Trans. A*, 32A, 777, 2001.

81. L. Jordan and P. Garrec, *Angle Orthodontist*, 74, 691, 2004. M. Epple et al., *Mater. Sci. Eng. A*, 378, 110, 2004. M. Epple et al., *Biomaterials*, 26, 5801, 2005.
82. W. Brostow, K. Menard, and J. White, *e-Polymers*, 4, 45, 2004. W. Brostow, K. Menard, and J. White, *POLYCHAR World Forum on Advanced Materials Proceedings II*, 2003, Denton, Texas. W. Brostow, K. Menard, and J. White, *Mater. Res. Soc. Symp.*, 692, G94, 2002. W. Brostow, K. Menard, and J. White, in *Thermoelectric Materials 2001: Research and Applications*, G. Nolas, Ed., MRS, Boston, 691, 425, 2001.
83. B. Gohill and K. Menard, unpublished results.
84. J.D. Ferry, *Viscoelastic Properties of Polymers*, 3rd ed., Wiley, New York, 1980.

7 Time and Temperature Scans Part II

Thermosets

This chapter will concentrate on the study of curing systems in the DMA. The fully cured material was covered in Chapter 6, as the concerns there are the same as for thermoplastics. However, the interest in studying curing behavior and curing materials may be even greater. The high sensitivity of the DMA and its ability to measure viscosity quickly make it one of the most valuable tools for studying curing systems. I personally have found it more useful even than the differential scanning calorimeter (DSC), although characterizing a thermoset without having both techniques available would be inefficient at best. In examining the applications of the DMA to thermosets, we will discuss fingerprinting materials, curing kinetics, methods of characterization like the Gillham–Enns diagram, postcure studies, and decomposition studies. This chapter, like Chapter 6, will concentrate on methods that mainly involve the variation of time and temperature, although a few digressions will occur.

7.1 THERMOSETTING MATERIALS: A REVIEW

Thermosets are materials that change chemically on heating. This can occur in one step or in several, and those multiple steps do not need to be immediately sequential. In addition, many processes not normally considered chemical are studied the same way. Cakes, cookies, eggs, and meat gels (e.g., hot dog batter) are all curing systems.¹ Figure 7.1a shows the DMA scan of a commercial angel food cake batter and Figure 7.1b shows an acrylate resin used as a dental material. Despite the great difference in materials, both curves show similar features and can be analyzed by the same approach. The same DMA techniques applied to traditional chemical studies can be applied to problems considered very different from those areas. In fact, the general shape of a curve is consistent for either thermal cures or photocures as seen in Figure 7.1c. The materials can even be in powdered form as shown in Figure 7.1d instead of solid disks or liquids. Whereas Figure 7.1d shows a cup run in compression, in Figure 7.1e a similar cure is down in a material pocket and lacks the compression set. So when we discuss the cure profile, it should be remembered that this applies to epoxies, foods, paints, coatings, and adhesives in a variety of forms. In all cases, the material goes to a stiffer, higher modulus state as the cure continues. The cure is not necessarily complete at the end of a cure cycle and subsequent heatings may show an increase in the T_g as shown in Figure 7.1e.

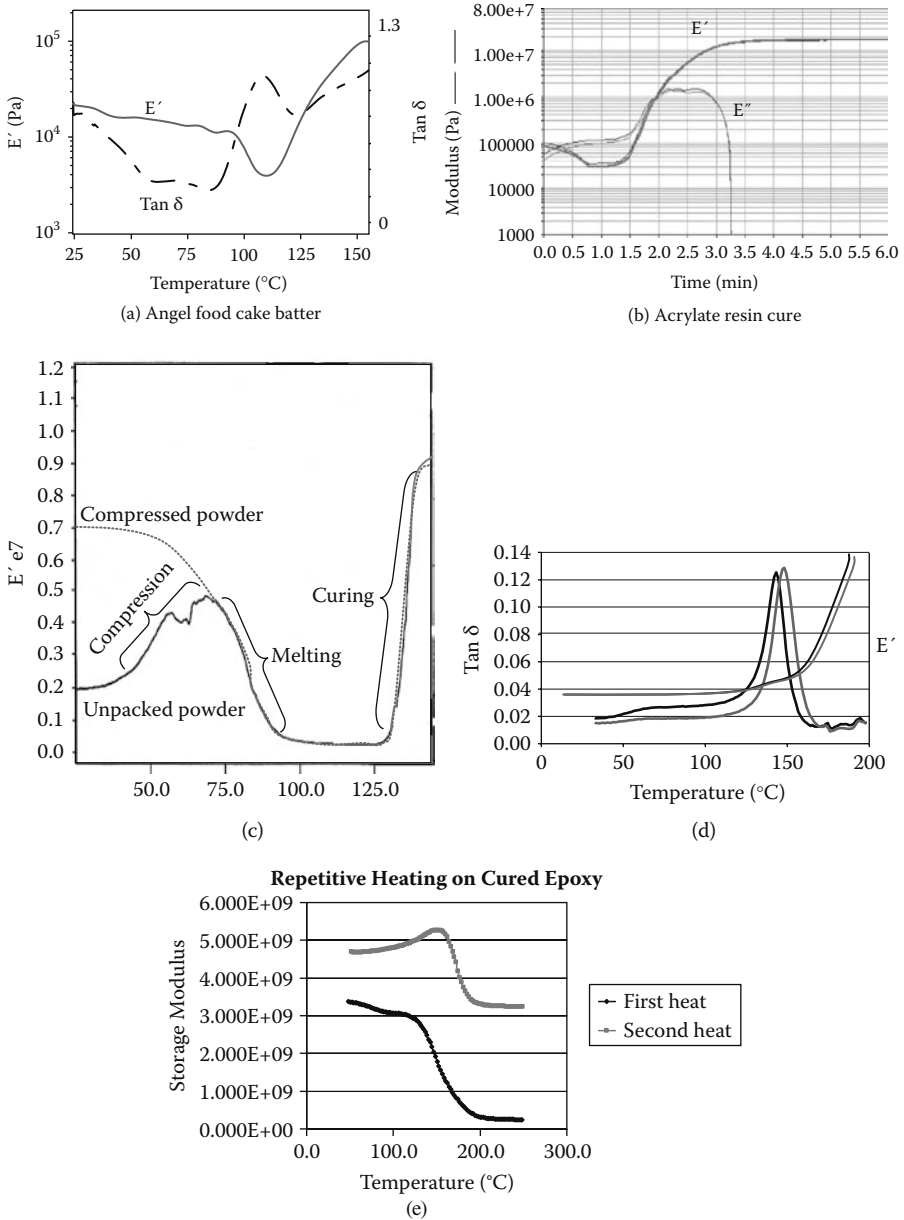


FIGURE 7.1 (a) DMA scan of commercial angel food cake batter in a DMA under the conditions specified on the box. Compare this with (b) an acrylate resin cure to see the similar behavior of very different systems. (c) A thermosetting resin in powdered and patty (compressed) forms show the same general behavior as other samples. The initial part of the cure is dependent on the sample preparation as shown. After the material has started melting, the runs are identical. (d) Same material run in a material pocket. E' values are not shown as the influence of the pocket skews them. (e) Repeat scanning of a thermoset gives different results, as the material is seldom 100% cured and the process of temperature scanning changes it.

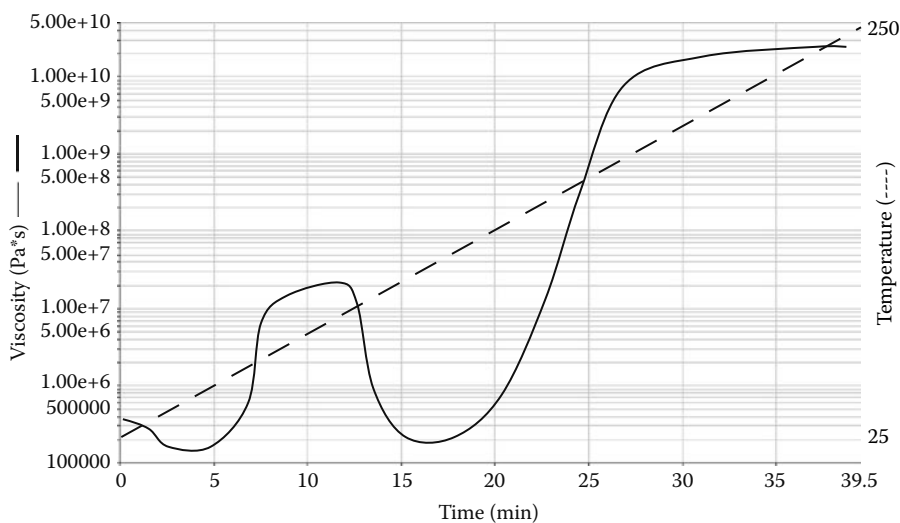


FIGURE 7.2 Cure of a two-stage condensation resin of a polyimide in the DMA. The second cure is associated with crosslinking.

Thermosetting reactions can be classed by their reactions into those that involve the loss of a molecule upon reacting, the condensation reactions; and those that join “mers” together without changes in the repeat structure, the addition reactions.² This classification is based on the reaction mechanism of the polymers and is manifested in very different kinetics. Figure 7.2 shows the curing of a resin that releases water in the first stage of its cure and doesn’t lose a part of the molecule in the second stage. The first valley will often show noise, which appears as a very jagged curve, due to loss of water, while the material in the second valley undergoes chain growth. This noise is often smoothed out in practice and can be related to the kinetics on a mole basis. TGA, TG/IR, or TG/MS³ normally is used to collect data on the amount of water lost. I am simplifying this somewhat and for a full development one should refer to a specialized text on polymer synthesis.⁴

Many of these curing processes are done as multistep cures and that gives you a lot of flexibility in processing the material. A common practice is to cure the material to a given point, often to where crosslinking has just barely started and then shape or layup the “ α - or β -staged” resin to the final form. The alpha or beta staging refers to how long the material is cured before shipping. Beta staging is roughly twice as cured as alpha staging. This layup is then cured into one piece.⁵ Obviously different processes will require different degrees of staging as staging affects the viscosity of the prepreg (an uncured resin that is impregnated onto the matrix) as shown in Figure 7.3. After the material is cured to a degree where it can support its own weight (often taken as $1 \cdot 10^6$ Pa sec), the item is removed from its mold or form and postcured. Postcuring involves heating the freestanding piece in an oven until full mechanical strength is developed.

Figure 7.4 shows an idealized relationship of degree of cure to T_g .⁶ Initially the material in region one is a monomer and as it begins to cure continues to act

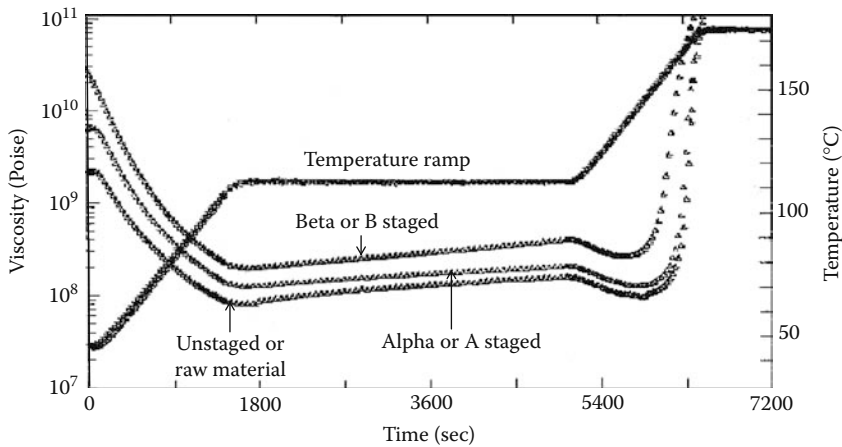


FIGURE 7.3 Affect of staging on the curing of resins. Staging is done to improve handling properties during layup but also changes the cure profile.

monomer-like. This continues up to about 35% of cure when it begins to start developing polymeric properties. After a transition zone, the relationship levels off and T_g tracks well with degree of cure. The point at which the curve levels off to this slope is sometimes referred to critical glass transition temperature, T_g^c , and is where the material shows the properties of a high polymer. At some point, normally at less than 100% as measured by residual cure energy in the DSC, the T_g greatly slows or stops increasing and the material has full mechanical strength. Many physical properties follow this shape of curve when plotted against molecular weight or degree of cure.⁷

For example, in some epoxy-based systems, the cure reaches a point where increased postcure time causes little to no increase in either the modulus or T_g . At

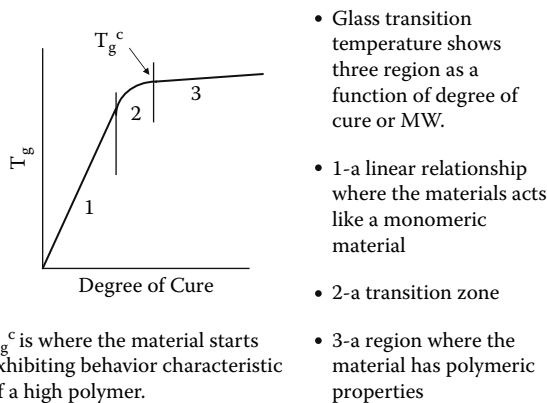


FIGURE 7.4 Relationship of T_g to cure time and the stages of a cure. Note that for thermosets, it is often difficult to impossible to see the T_g by DSC in the latter half of the third region.

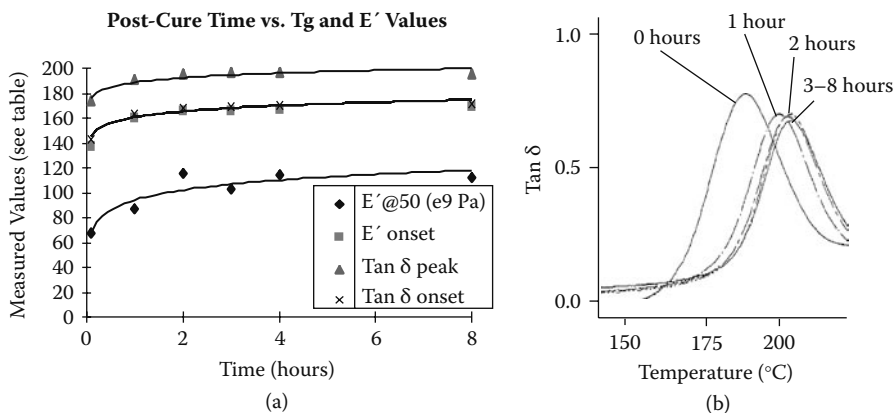


FIGURE 7.5 (a) Data collected by DMA on chip encapsulation material plotted as time of postcure versus measured values listed in the table. T_g was measured as the peak of the $\tan \delta$, the onset of $\tan \delta$, and the onset of the drop in E' . Storage modulus was measured at 50 $^{\circ}C$ and is reported as e⁹ Pa. (b) The measurement of T_g by $\tan \delta$ peak values for the data in (a) is shown. All the T_g s except the zero hour of postcure T_g were undetectable by DSC.

this point, increased postcuring gives no advantage and only wastes money and time.⁸ In some systems, this occurs at 94% of complete cure when measured by the residue enthalpy of cure in the DSC. Being aware of this value and of where full mechanical strength is developed is necessary for cost-efficient process design. If we can develop full mechanical strength at 4 hours for the material shown in Figure 7.5, postcuring for 8 hours would only mean lost profit. As can be seen, both the T_g and the storage modulus (measured at 50 $^{\circ}C$) level out and do not increase anymore after 3 to 4 hours of postcure. This might not be true of another property, such as solvent resistance or aging, and that should be checked separately. The relationships of heating rate, time, and frequency on the T_g need to be well defined. Similar work has been reported on carbon-epoxy composites⁹ and cyanate esters.¹⁰

7.2 STUDYING CURING BEHAVIOR IN THE DMA: CURE PROFILES

The DMA's ability to give viscosity and modulus values for each point in a temperature scan allows us to estimate kinetic behavior as a function of viscosity. This has the advantage of telling us how fluid the material is at any given time, so we can determine the best time to apply pressure, what design of tooling to use, and when we can remove the material from the mold. The simplest way to analyze a resin system is to run a plain temperature ramp from ambient to some elevated temperature.¹¹ This "cure profile" allows us to collect several vital pieces of information.

Before we analyze the cure in Figure 7.6 in more detail, we should mention that in curing studies, all three types of commercial DMA's are used. The shape of the curve and the temperature of events follow the same pattern. The values for viscosity and modulus often greatly differ. Both types of forced resonance DMA's also use samples impregnated into fabrics in techniques that are referred to as "torsion

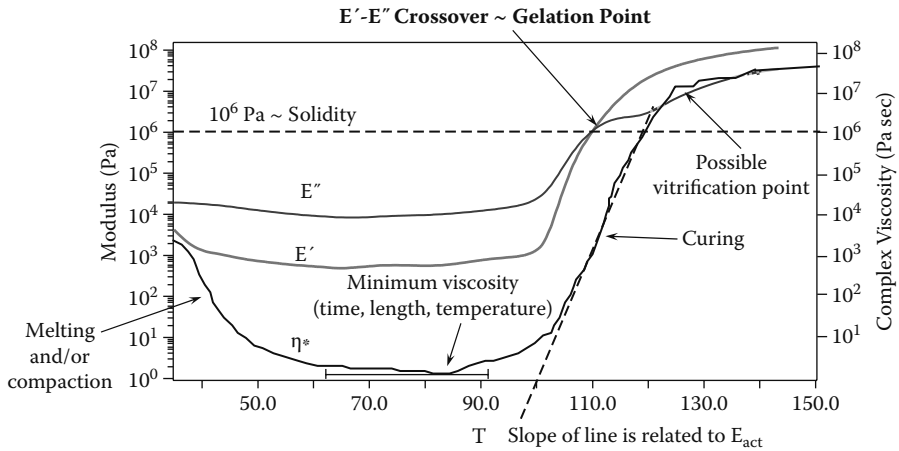


FIGURE 7.6 The DMA cure profile of a two-part epoxy showing the typical analysis for minimum viscosity, gel time, vitrification time, and estimation of the action energy. See the discussion in the text for details.

braid” in the torsional system and usually just “supported” in axial instruments. There are some problems with this technique as temperature increases will cause an apparent curing of nondrying oils as thermal expansion increases friction. However, the “soaking of resin into a shoelace,” as this technique has been called, allows one to handle difficult specimens under conditions where the pure resin is impossible to run in bulk (due to viscosity or evolved volatiles). In practice, you can also use a material pocket to support the resin, a metal shim, a cotton ball, or a piece of paper soaked in the resin. Composite materials like graphite-epoxy composites are sometimes studied in industrial situations as the composite rather than the “neat” or pure resin because of the concern that the kinetics may be significantly different. In terms of ease of handling and sample, the composite is often easier to work with. In those cases, DSC becomes especially difficult as the material may only be 30% resin and the DMA’s higher sensitivity is a must.

Another special area of concern is paints¹² and coatings¹³ where the material is used in a thin layer. This can be addressed experimentally by either a braid or coating the material on a thin sheet of metal. The metal is often run first and its scan subtracted from the coated sheet’s scan to leave only the scan of the coating. This is also done with thin films and adhesive coatings. Other approaches are to soak pieces of stiff paper in the resin or to use a scaffolding of metal mesh (a fancy way of saying a piece of stainless steel screen). Because many of these materials actually dry or lose solvent as opposed to react, a thin layer on the surface works better. Paint inside a material pocket would dry first at the end and seal the rest of the material off so it never dried. Examples of these kinds of experiments are shown in Figure 7.7.

A sample cure profile for a commercial two-part epoxy resin is shown in Figure 7.6. From this scan, we can determine the minimum viscosity (η^*_{\min}), the time to η^*_{\min} and the length of time it stays there, the onset of cure, the point of gelation where

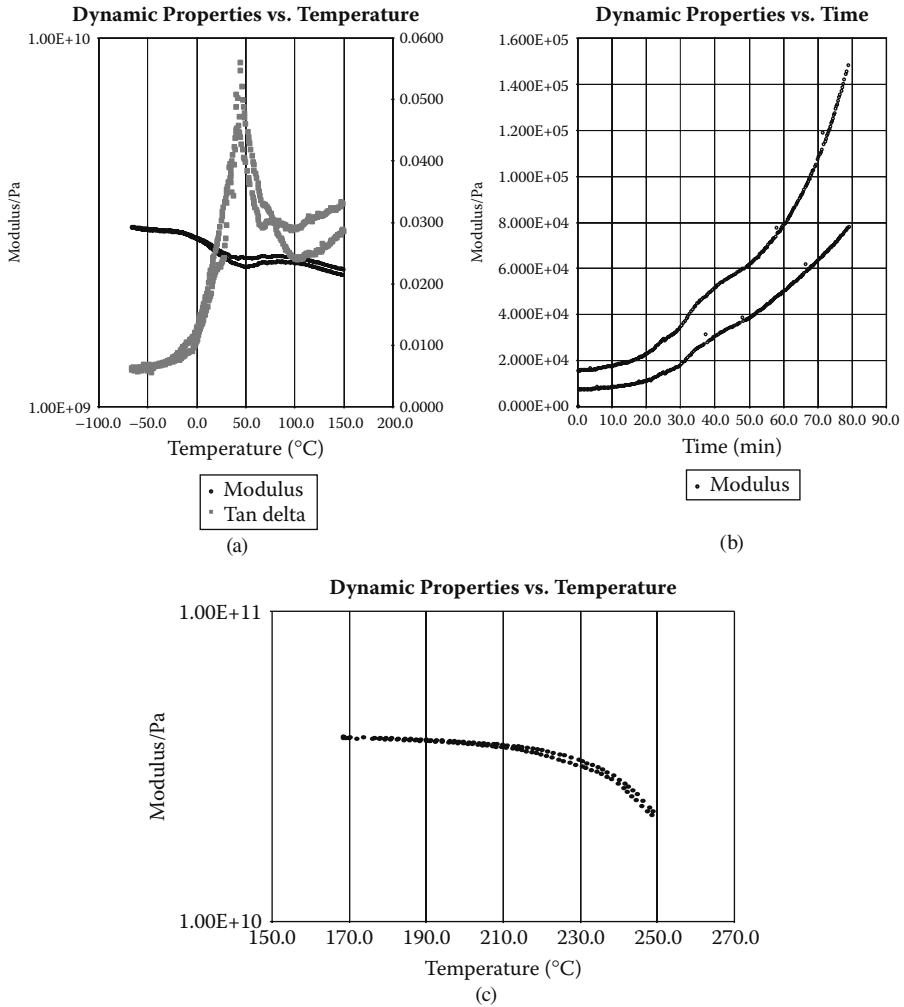


FIGURE 7.7 “Supported” runs in the DMA. (a) Paint coated on a metal shim, dried, and then run in the DMA 8000 for the T_g . (b) Solvent-based adhesive soaked into a piece of cotton support (aka shoelace) and allowed to dry in the DMA at $40^{\circ}C$. (c) A lyophilized sample of bovine serum albumin powder run in a material pocket.

the material changes from a viscous liquid to a viscoelastic solid, and the beginning of vitrification. The minimum viscosity is seen in the complex viscosity curve and is where the resin viscosity is the lowest. A given resin’s minimum viscosity is determined by the resin’s chemistry, the previous heat history of the resin, the rate at which the temperature is increased, the testing frequency, and the amount of stress or strain applied. Increasing the rate of the temperature ramp is known to decrease the η^*_{min} , the time to η^*_{min} , and the gel time. The resin gets softer faster, but also cures faster. The degree of flow limits the type of mold design and when, as well as how much, pressure can be applied to the sample. The time spent at the minimum

viscosity plateau is the result of a competitive relationship between the softening or melting as it heats and the rate of curing. At some point, the material begins curing faster than it softens, and that is where we see the viscosity start to increase.

So far we have assumed that the material will soften to some degree before curing. This is the more complicated case where a solid or semisolid starting material is used. Obviously this isn't always the case. Many materials start out at low viscosity and increase from there during the cure as we saw in Figure 7.1.

As the viscosity begins to climb, we see an inversion of the E'' and E' values as the material becomes more solid-like. This crossover point also corresponds to where the $\tan \delta$ equals one (since $E' = E''$ at the crossover). This is taken to be the gel point,¹⁴ where the crosslinks have progressed to forming an "infinitely" long network across the specimen. At this point, the sample will no longer dissolve in solvent. Although the gel point correlates fairly often with this crossover, it doesn't always. For example, for low initiator levels in chain addition thermosets, the gel point precedes the modulus crossover.¹⁵ Some temperature dependence for the presence of the crossover has also been reported.¹⁶ In some cases, when powder compacts and melts before curing, there may be several crossovers.¹⁷ Then, the one following the η^*_{\min} is usually the one of interest. Another approach is based on the frequency dependence of the modulus values during the cure.¹⁸ This is done by applying multiple frequencies to the sample during the cure. At the gel point, the frequency dependence disappears (see Figure 7.8).¹⁹ During this rapid climb of viscosity in the cure, the slope for η^* increase can be used to calculate an estimated E_{act} (activation energy).²⁰ We will discuss this later, but the fact that the slope of the curve here is a function of E_{act} is important. Above the gel temperature, one can estimate the molecular weight, M_c , between crosslinks as

$$G' = RT\rho/M_c \quad (6.1)$$

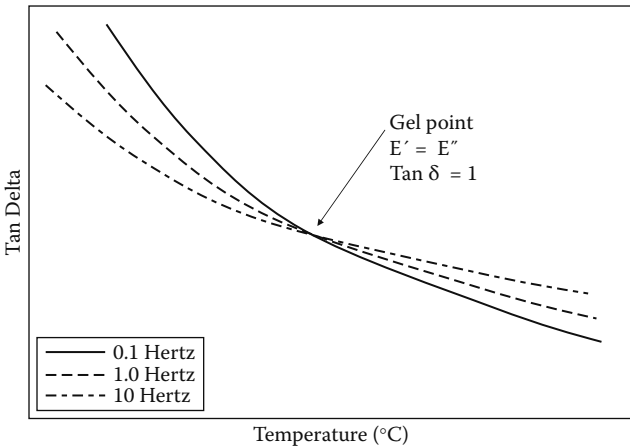
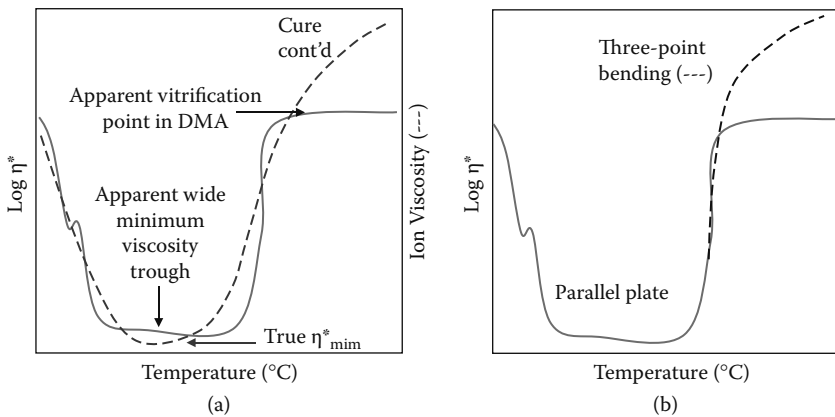


FIGURE 7.8 Collapse of curves run at different frequencies to a single point at the gel point.

where R is the gas constant, T is the temperature in Kelvin, and ρ is the density. At some point the curve begins to level off and this is often taken as the vitrification point, T_{vf} .

The vitrification point is where the cure rate slows because the material has become so viscous that the bulk reaction has stopped. At this point, the rate of cure slows significantly. The apparent T_{vf} , however, is not always real; any analyzer in the world has an upper force limit. When that force limit is reached, the “topping out” of the analyzer can pass as the T_{vf} . Use of a combined technique like DMA-DEA²¹ to see the higher viscosities; measuring by both DMA and IR²² (or Raman²³) to see degree of conversion; or the removal of a sample from a parallel plate and sectioning it into a flexure beam is often necessary to see the true vitrification point (Figure 7.9). A reaction can also completely cure without vitrifying and will level off the same



Step Scan DSC Heat Capacity

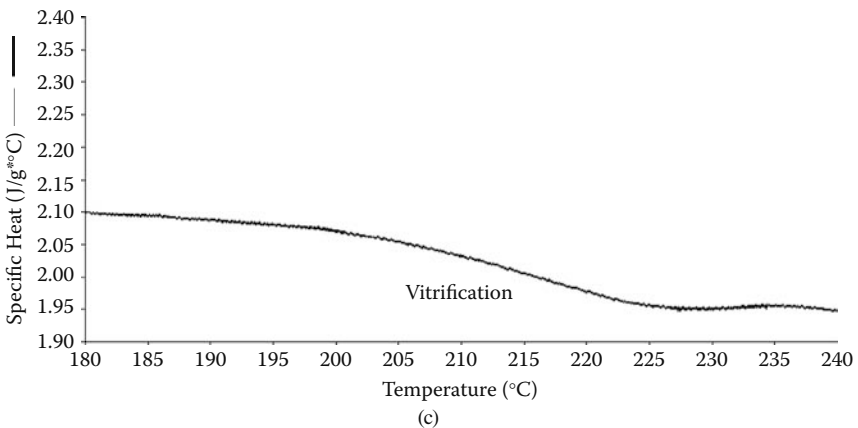


FIGURE 7.9 Masking of the vitrification point by instrument limits is shown by (a) DMA-DEA and (b) rerunning of a section of parallel plate specimen. (c) Vitrification can also be confirmed by StepScan.

TABLE 7.1
Viscosity of Common Materials

Water	0.00001 Pa s
Olive oil	0.1 Pa s
Honey at 20°C	100 Pa s
Molasses at 20°C	1000 Pa s
Molten polymers	10,000 Pa s
Asphalt	1e ⁸ Pa s
Solid glass	1e ⁴⁰ Pa s

way. One should be aware that reaching vitrification or complete cure too quickly can be as bad as reaching it too slowly. Often an overly aggressive cure cycle will cause a weaker material, as it does not allow for as much network development,²⁴ but gives a series of hard (highly crosslinked) areas among softer (lightly crosslinked) areas.

On the way to vitrification, I have marked a line at 10⁶ Pa sec. This is the viscosity of bitumen²⁵ and was often used as a rule of thumb for where a material is stiff enough to support its own weight. This is a rather arbitrary point, but is chosen to allow the removal of materials from a mold and the cure is then continued as a post-cure step. As an example, Table 7.1 gives the viscosities of common materials. As we shall see later, the postcure is often a vital part of the curing process.

The cure profile is both a good predictor of performance as well as a sensitive probe of processing conditions. We will discuss the former case in Section 7.4 and the latter as part of Section 7.8. A final note on cure profiles should be that a volume change occurs during the cure.²⁶ This shrinkage of the resin is important and can be studied by monitoring the probe position of a bulk sample on either DMA or TMA by dilatometry.

7.3 PHOTOCURING

A photocure in the DMA is run by applying a UV light source to a sample that is held at a specific temperature or subjected to a specific thermal cycle.²⁷ Photocuring is done for dental resin, contact adhesives, and contact lenses. UV exposure studies are also run on cured and thermoplastic samples by the same techniques as photocuring to study UV degradation. As shown in Figure 7.10, the cure profile of a photocure is very similar to that of a cake or epoxy cement. The same analysis is used and the same types of kinetics are developed as is done for thermal curing studies.²⁸

One normally had to adapt a commercial DMA to run these experiments. The PerkinElmer DMA-7e has been successfully adapted to use quartz fixtures, a home-made heating chamber, and commercial UV source triggered from the DMA's RS32 port.²⁹ Recently, commercial systems like the PerkinElmer DMA 8000 with a UV adapter have become available. We will discuss photocuring and degradations in Chapter 9.

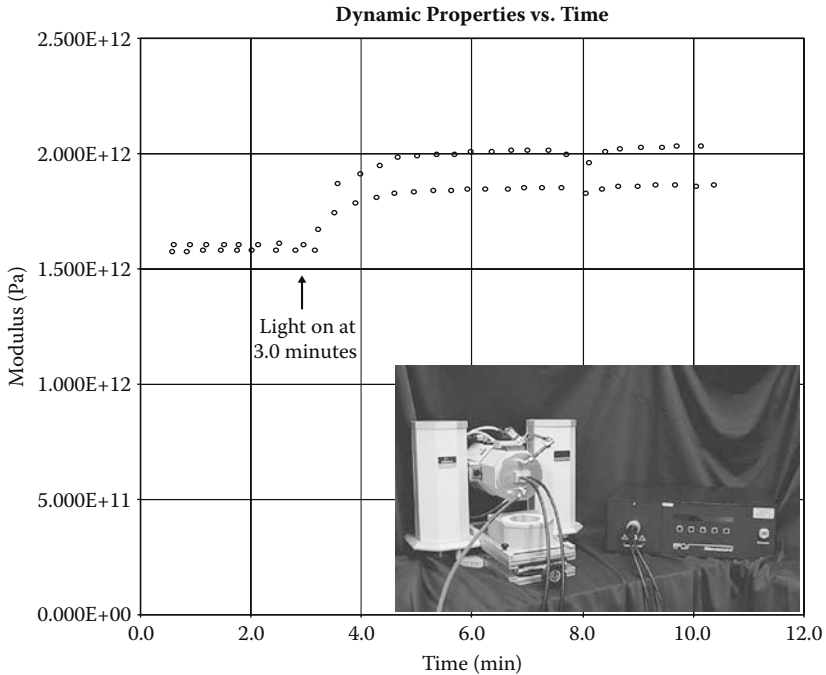


FIGURE 7.10 Photocure of an UV curing adhesive in the DMA. Note the similarity to the materials in Figure 7.1a and b.

7.4 MODELING CURE CYCLES

The discussions so far are based on using a simple temperature ramp to see how a material responds to heating. In actual use, many thermosets are cured using more complex cure cycles to optimize the tradeoff between the processing time and the final product's properties.³⁰ The use of two-stage cure cycles is known to develop stronger laminates in the aerospace industry. Exceptionally thick laminates often also require multiple stage cycles in order to develop strength without porosity. As thermosets shrink on curing, careful development of a proper cure cycle to prevent or minimize internal voids is necessary.

One reason for the use of multistage cures is to drive reactions to completion. Another is to extend the minimum viscosity range to allow greater control in forming or shaping the material. An example of a multistage cure cycle is shown in Figure 7.11. The development of a cure cycle with multiple ramps and holds would be very expensive if done with full-sized parts in production facilities. The use of the DMA gives a faster and cheaper way of optimizing the cure cycle to generate the most efficient and tolerant processing conditions.

7.5 ISOTHERMAL CURING STUDIES

Often curing is done at a constant temperature for a period of time.³¹ This is how the data needed for the kinetic models discussed in the next section are normally collected. It is also how rubber samples are crosslinked, how initiated reactions are run, and how

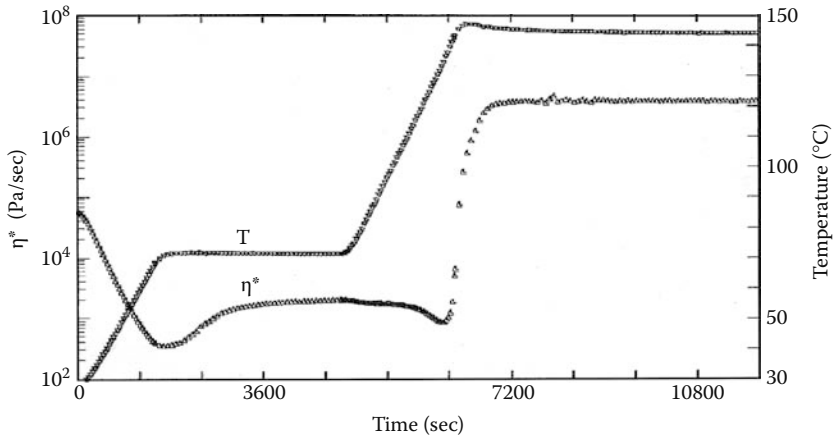


FIGURE 7.11 Multistep cure cycles. A multiple step cure cycle with two ramps, and two isothermal holds are used to model processing conditions. Run on an RDA 2 by the author.

bulk polymerizations are performed. Industrially, continuous processes, as opposed to batch, often use an isothermal approach. Figure 7.12 shows the isothermal cure of an epoxy system used in kinetic studies. UV light and other forms of nonthermal initiation also use isothermal studies for examining the cure at a constant temperature.

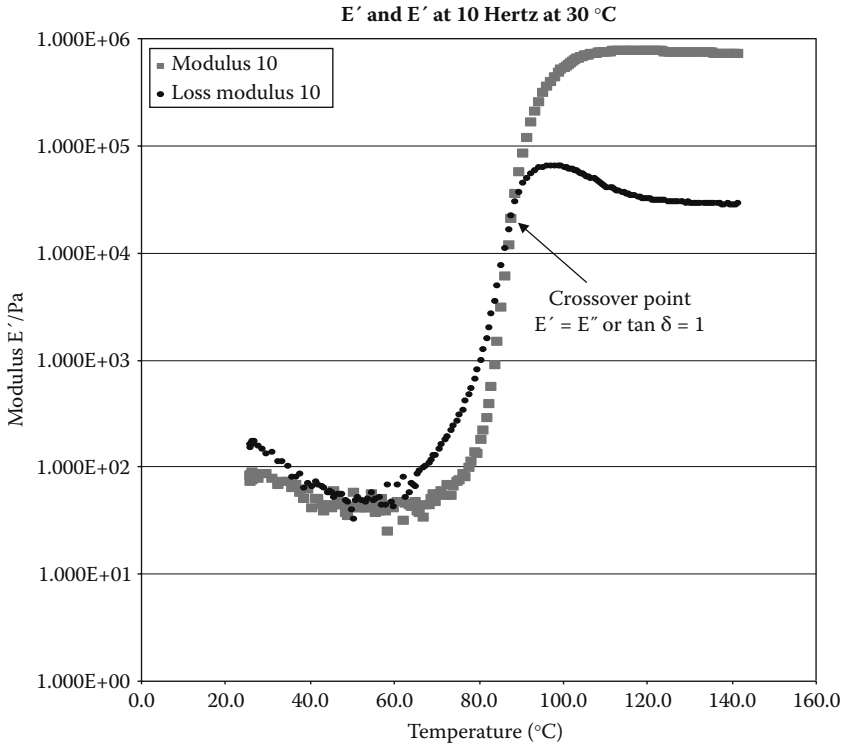
7.6 KINETICS BY DMA: THE ROLLER MODEL AND OTHER APPROACHES

Several approaches have been developed to study the chemorheology of thermosetting systems. Halley and MacKay (Table 7.2) recently reviewed chemorheology and the more common kinetic models.³² A fundamental method is the Williams–Landel–Ferry (WLF) model, which looks at the variation of T_g with degree of cure.³³ This has been used and modified extensively.³⁴ A common empirical model for curing has been proposed by Roller.³⁵ This method will be discussed in depth, as well as some of the variations on it.

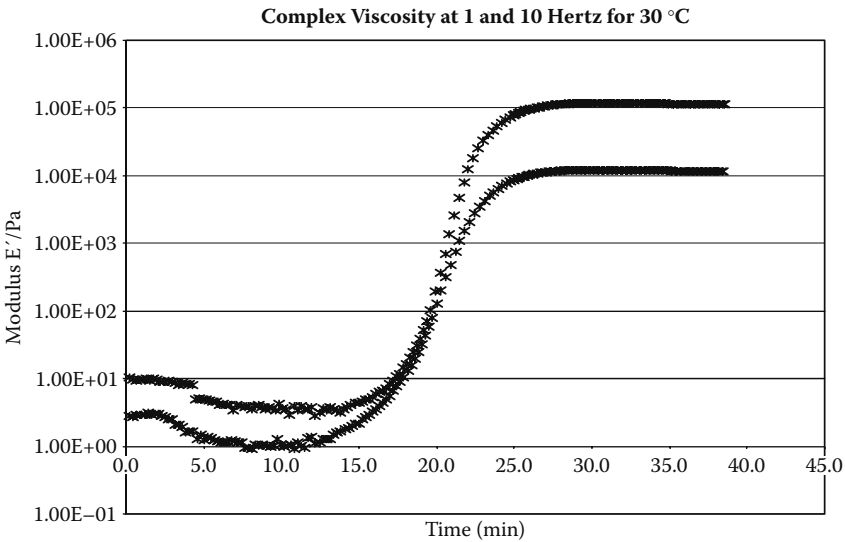
Samples of the thermoset are run isothermally as described earlier and the viscosity versus time data plotted as shown in Figure 7.12b. This is replotted in Figure 7.13 as $\log \eta^*$ versus time in seconds, where a change in slope is apparent in the curve. This break in the data indicates the sample is approaching the gel time. From these curves, we can determine the initial viscosity, η_0 and the apparent kinetic factor, k . By plotting the \log viscosity versus time for each isothermal run, we get the slope, k , and the viscosity at $t = 0$. The initial viscosity and k can be expressed as

$$\eta_0 = \eta_\infty e^{\Delta E_\eta/RT} \quad (7.2)$$

$$k = k_\infty e^{\Delta E_k/RT} \quad (7.3)$$



(a)



(b)

FIGURE 7.12 Isothermal curing studies. (a) An isothermal cure on a two-part epoxy showing the crossover point for E' and E'' and (b) the complex viscosity with the frequency collapse.

TABLE 7.2
Chemorheological Cure Models

Model	Polymer	Equation
Macosko	Epoxy, phenolic, EDPM	$1/t_1 = C \exp(-E/RT)$
First order Iso	Epoxy	$\eta = \eta_0 \exp(\Theta t)$
First order	Epoxy	$\eta_c = \eta(T) \exp(\phi kt)$
Empirical	Epoxy	$1 \ln \eta_c = 1 \ln \eta_v + E_v/RT + k\alpha + k\alpha$
	Polyurethane	$\eta_c/\eta^0 = [(1 + kt) / (1 - t/t^*)]^a$
Gel	Thermosets	$\eta_c/\eta^0 = [(\alpha^*/\alpha^* - \alpha)^A + B\alpha]$
Arrhenius -1st	Epoxy	$1 \ln \eta_c = 1 \ln \eta_v + E_v/RT + tk_k \exp E_k/RT$
-1st Iso	Epoxy	$1 \ln \eta_c = 1 \ln \eta_v + E_v/RT + k_k \int \exp(E_k/RT) dt$
-nth	Epoxy	$1 \ln \eta_c = 1 \ln \eta_v + E_v/RT + k_k \int (1 - \alpha)^n \exp(E_k/RT) dt$
Modified WLF	Epoxy	$\ln[\eta_c(T)/\eta_c(T_g)] = \{C_1(\alpha)[T - T_g(\alpha)] / C_2(\alpha) + T - T_g(\alpha)\}$

Source: Extracted and reprinted from P.J. Halley and M.E. MacKay, *Polymer Engineering and Science*, Vol. 36, No. 3, 1996, pp. 593–609, Table 3 with permission from the Society of Plastic Engineers. These models show the range of approaches used in trying to model the curing of various systems.

Combining these allows us to set up the equation for viscosity under isothermal conditions as

$$\ln \eta(t) = \ln \eta_\infty + \Delta E_\eta/RT + tk_\infty e^{\Delta E_k/RT} \tag{7.4}$$

By replacing the last term with an expression that treats temperature as a function of time, we can write

$$\ln \eta(T,t) = \ln \eta_\infty + \Delta E_\eta/RT + \int_0^t k_\infty e^{\Delta E_k/RT} dt \tag{7.5}$$

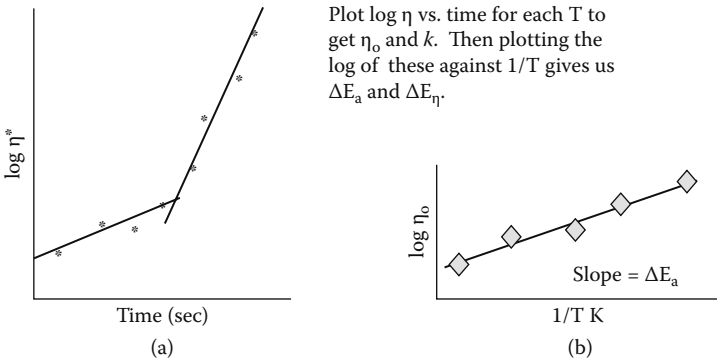


FIGURE 7.13 The steps in Roller's kinetic method. (a) Viscosity at $t = 0$ plotted against time, (b) \ln initial viscosity versus $1/T$, and (c) $\ln k$ versus $1/T$.

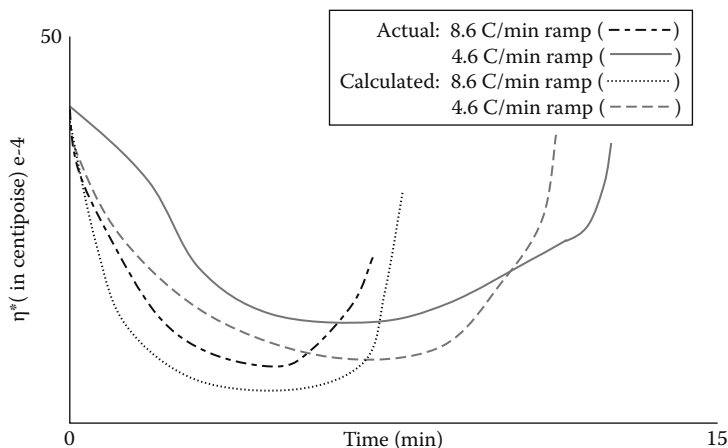


FIGURE 7.14 A comparison of Roller's predicted cure to the actual cure. Redrawn from M. Roller, *Polymer Engineering and Science*, Vol. 15, 1975, p. 406, with permission from the Society of Plastic Engineers.

This equation can be used to describe viscosity–time profiles for any run where the temperature can be expressed as a function of time. Returning to the data plotted in Figure 7.13, we can determine the activation energies we need as follows. The plots of the natural log of the initial viscosity (determined above) versus $1/T$ and the natural log of versus $1/T$ are used to give us the activation energies, ΔE_{η} and ΔE_k . Figure 7.14 shows a comparison between viscosity–time profiles from actual runs and calculated from this model. Comparison of these values to the k and ΔE to those calculated by DSC shows that this model gives larger values.³⁶ The DSC data is faster to obtain, but it does not include the needed viscosity information.

Several corrections have been proposed, addressing different orders of reaction³⁷ (the above assumes first order) and modifications to the equations.³⁸ Many of these adjustments are reported in Roller's 1986 review of curing kinetics.³⁹ It is noted that these equations do not work well above the gel temperature. These same equations have been successfully used to predict the degradation of properties in thermoplastics.⁴⁰

7.7 MAPPING THERMOSET BEHAVIOR: THE GILLHAM–ENNS DIAGRAM

Another approach to attempt to fully understand the behavior of a thermoset was developed by Gillham and is analogous to the phase diagrams used by metallurgists.⁴¹ The time–temperature–transition (TTT) diagram, or the Gillham–Enns diagram (named after its creators), is used to track the effects of temperature and time on the physical state of a thermosetting material. Figure 7.15 shows an example. These can be done by running isothermal studies of a resin at various temperatures and recording the changes as a function of time. One has to choose values for the various regions and Gillham has done an excellent job of detailing how one picks

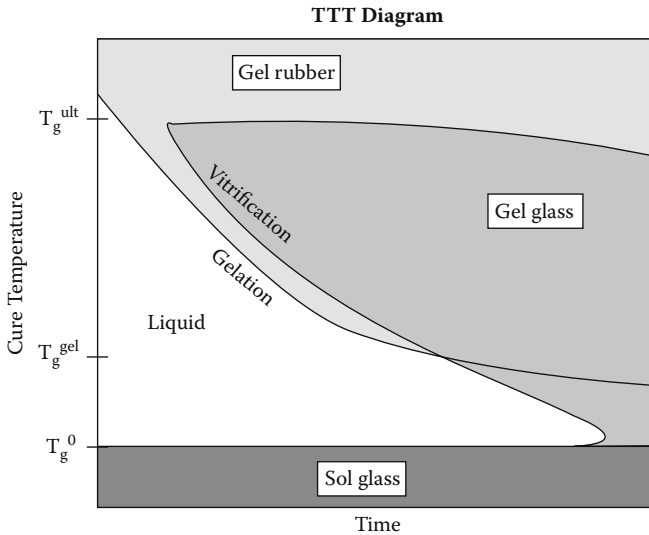


FIGURE 7.15 The Gillham–Enns or time–temperature–transition (TTT) diagram. The classical TTT diagram based on an epoxy amine. Taken from B. Bilyeu’s Ph.D. thesis and used with his permission.

the T_g , the glass, the gel, the rubbery, and the charring regions.⁴² These diagrams are also generated from DSC data,⁴³ and several variants,⁴⁴ like the continuous heating transformation and conversion–temperature–property diagrams, have been reported. Surprisingly easy to do, although a bit slow, they have not yet been accepted in industry despite their obvious utility. A review was done in 1994 that is still the definitive collection of this work.⁴⁵

7.8 QUALITY CONTROL APPROACHES TO THERMOSET CHARACTERIZATION

Quality control (QC) is still one of the biggest applications of the DMA in industry. For thermosets, this normally involves two approaches to examining incoming materials or checking product quality. First is the very simple approach of fingerprinting a resin. Figure 7.16 shows this for two adhesives; a simple heating run under standardized conditions allows one to compare the known good material with the questionable material. This can be done as simply as described or by measuring various quantities.

A second approach is to run the cure cycle that the material will be processed under in production and then checking the key properties for acceptable values. Figure 7.17 shows three materials run under the same cycle. Note the differences in the minimum viscosity, in the length and shape of the minimum viscosity plateau, the region of increasing viscosity associated with curing, and both the time required to exceed 1×10^6 Pa sec and to reach vitrification. These materials, sold for the same application, would require very different cure cycles to process. If we estimate the

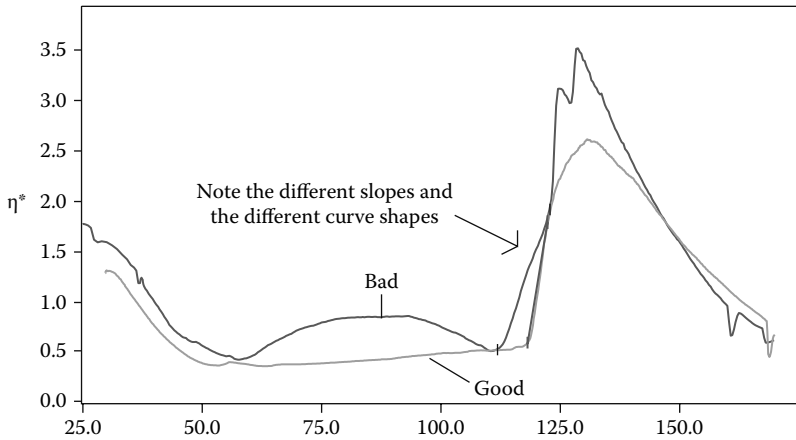


FIGURE 7.16 Fingerprinting of materials for QC is often done. Good and bad hot melt adhesives scanned using a constant heating rate cure profile.

activation energy, E_{act} , by taking the values of η^* at various temperatures and plotting them versus $1/T$, we get very different numbers. (This is a fast way of estimating the E_{act} , where we will assume the viscosity obtained from the temperature ramp is close to the initial viscosity of the Roller method. This is not a very accurate assumption but for materials cured under the same conditions, it works.) This indicates, as did the shape of the cures, different times are required to complete the cures. The differences in the minimum viscosity mean the material will have different flow characteristics and, for the same pressure cycle, give different thicknesses.

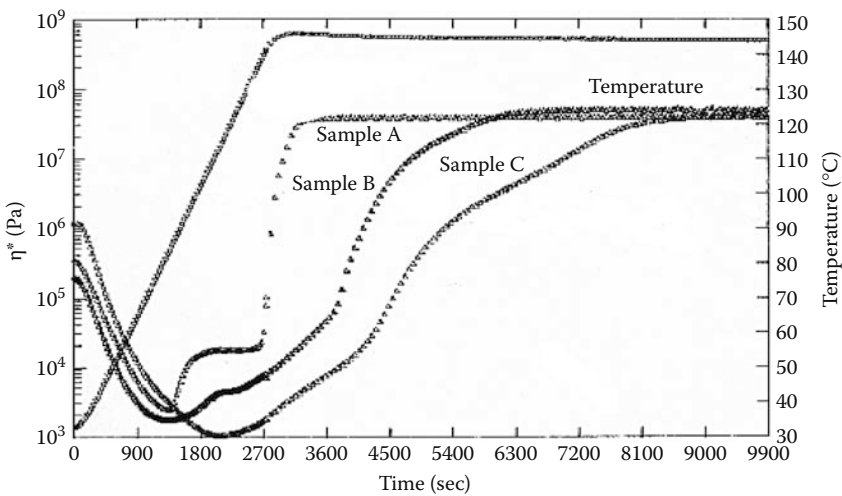


FIGURE 7.17 Comparison of materials using a standard cure cycle and analyzed as described in Figure 7.6.

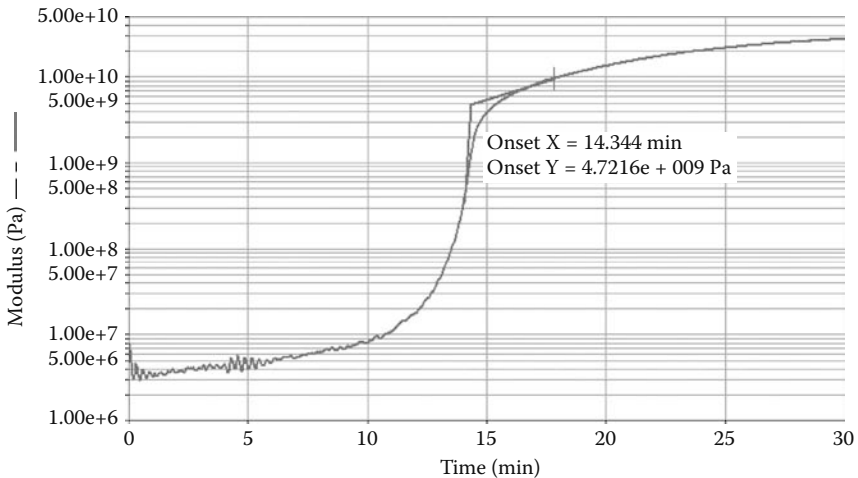


FIGURE 7.18 Results and analysis of a “gel” time test from a DMA run. Note the “gel time” here is really the time to vitrification, not gelation in the way the terms are used earlier. The industrial gel time test is a very simple test that involves poking a material until it resists movement and really measures when the material becomes glassy.

As different times are required to reach a viscosity equal to or exceeding 10^6 Pa sec, the materials will need to be held for different times before they are solid enough to hold their own weight. The overall message from this comparison is that these three materials are not interchangeable.

Another method is to convert the standard gel time test to operation in the DMA. The gel time test as done by the aerospace industry involves holding a resin sample at elevated temperature while poking it to see how long it takes to “gel.” Gel in this case, however, means harden and this “gel” point is not the same as the gelation point estimated for the $E'-E''$ crossover. It is similar to the point of vitrification or complete cure on the DMA and to the vitrification point measured by the dynamic differential scanning calorimeter (DDSC). This test is the basic resin quality test for a lot of plants and is very time consuming, as someone has to be there throughout the experiment. The same information is obtained by running an isothermal cure in the DMA. The instrument and fixtures are heated to a set temperature, often 171°C (340°F), and the run set up. The sample is then quickly loaded and a time scan done until vitrification occurs (Figure 7.18). Agreement between the DMA and manual methods is quite good ($<5\%$ in my experience) and the DMA method does not require constant monitoring.

7.9 POSTCURE STUDIES

After a material has been cured to a set level, it is often not at full strength. To allow the completion of the cure, the materials are often postcured by heating in an oven at atmospheric pressure outside of the mold or form. This frees up expensive mold space or press time while giving a stronger laminate. This sample is normally

Dynamic Properties vs. Temperature

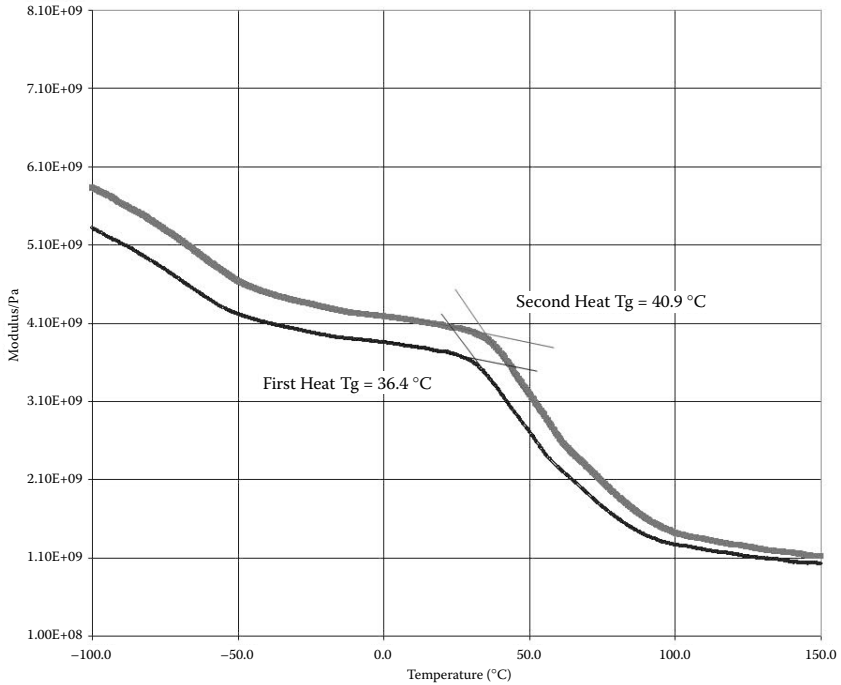


FIGURE 7.19 Shift in the glass transition of a specimen of cured epoxy on the second heating can be used as an indicator of how complete the cure. Large changes from heating the first to the second heating ramp are not good.

examined for residual cure (how close to 100% cured) by DSC and checked for T_g and other transition temperatures by DMA as described in Chapter 5. Figure 7.5 shows the effect of postcuring on T_g . Another approach is to measure the creep of a thermoset under actual-use stress as a function of postcure.⁴⁶

A standard approach in DMA to evaluating the sample after a postcure is to run the sample for the T_g and then rerun it under the same conditions. This is shown in Figure 7.19. If the two T_g are within a certain predetermined limit, say 5°C, the material is assumed to be fully cured.

7.10 CONCLUSIONS

We have seen how most curing systems can be handled by a similar approach in the DMA. The underlying similarity of the behavior of curing materials makes it fairly straightforward to investigate their behavior via the DMA. In the next chapter, we will look at the frequency dependence of materials, which can also give us insight into the effects of the cure.

NOTES

1. C.-Y. Ma, *Thermal Analysis of Foods*, Elsevier, New York, 1990. P. Sherman et al., *Food Texture and Rheology*, Academic Press, London, 1979. C. Shoemaker et al., *Food Rheology Short Course*, S. Rheology, Boston, 1993.
2. R.B. Cassel, *Thermal Analysis Application Study # 19*, PerkinElmer Corp., Norwalk, CT, 1977.
3. TGAs, or thermogravimetric analyzers, are used to track weight loss with temperature. They are often coupled to FTIR, called TG/IR, or a mass spectrometer (TG/MS) to perform evolved gas analysis (EGA) on the gases released or generated from the sample. See notes in Chapter 10.
4. G. Odian, *Polymer Synthesis*, Wiley, New York, 1992.
5. The area of thermoset curing and composite manufacture is very active. Some good lead references include: N.G. McCrum et al., *Principles of Polymer Engineering*, Oxford Science, Oxford, 1990. L. Carlsson et al., *Experimental Characterization of Advanced Composite Materials*, Prentice-Hall, New York, 1987. J.K. Gillham et al., Eds., *Rubber-Modified Thermoset Resins*, ACS, Washington D.C., 1984. B. Prime, in *Thermal Characterization of Polymeric Materials*, E. Turi, Ed., Academic Press, New York, 1998.
6. L. Sperling, *Introduction to Physical Polymer Science*, Wiley, New York, 1994.
7. R. Seymour and C. Carraher, *Polymer Chemistry*, Marcel Dekker, New York, 1981. R. Seymour and C. Carraher, *Structure Property Relationships in Polymers*, Plenum, New York, 1984.
8. H. Mallella et al., *ANTEC Proc.*, 40(2), 2276, 1994.
9. W. Goertzen and M. Kessler, *Composites: Part B*, 38, 1, 2007.
10. W. Goertzen and M. Kessler, *Composites: Part A*, in press.
11. G. Martin et al., in *Polymer Characterization*, ACS, Washington D.C., 1990, ch. 12. M. Ryan et al., *ANTEC Proc.*, 31, 187, 1973. C. Gramelt, *American Laboratory*, January, 1984, p. 26. S. Etoh et al., *SAMPE J.*, 3, 6, 1985. F. Hurwitz, *Polym. Composites*, 4(2), 89, 1983.
12. G. Spinks et al., *Prog. Org. Coat.*, 49, 95, 2007.
13. M. Roller, *Polym. Eng. Sci.*, 19, 692, 1979. M. Roller et al., *J. Coat. Tech.*, 50, 57, 1978.
14. M. Heise et al., *Polym. Eng. Sci.*, 30, 83, 1990. K. O'Driscoll et al., *J. Polym. Sci.: Polym. Chem.*, 17, 1891, 1979. O. Okay, *Polymer*, 35, 2613, 1994.
15. M. Hiese, G. Martin, and J. Gotro, *Polym. Eng. Sci.*, 30 (2), 83, 1990.
16. G. Martin et al., in *Polymer Characterization*, ACS, Washington D.C., 1990, ch. 12. M. Ryan et al., *ANTEC Proc.*, 31, 187, 1973. C. Gramelt, *American Laboratory*, January, 1984, p. 26. S. Etoh et al., *SAMPE J.*, 3, 6, 1985. F. Hurwitz, *Polym. Composites*, 4(2), 89, 1983.
17. K. Wissbrun et al., *J. Coat. Tech.*, 48, 42, 1976.
18. F. Champon et al., *J. Rheol.*, 31, 683, 1987. H. Winter, *Polym. Eng. Sci.*, 27, 1698, 1987. C. Michon et al., *Rheologica Acta*, 32, 94, 1993.
19. C. Michon et al., *Rheologica Acta*, 32, 94, 1993.
20. I. Kalnin et al., *Epoxy Resins*, ACS, Washington D.C., 1970. W. Goertzen and M. Kessler, *Composites: Part B*, 38, 1, 2007. W. Goertzen and M. Kessler, *Composites Part A*, in press.
21. DEA is dielectric analysis, where an oscillating electrical signal is applied to a sample. From this signal, the ion mobility can be calculated, which is then converted to a viscosity. See McCrum (op cit.) for details. DEA will measure to significantly higher viscosities than DMA.

22. S. Newman, University of Colorado Dental School, private communication. P. Steelman et al., *Macromolecules*, 37, 7001, 2004.
23. P. Musto, *Polymer*, 48, 3703, 2007.
24. W. Goertzen and M. Kessler, *Composites: Part A*, in press. R. Fan et al., *Polym. Test.*, 20, 925, 2001.
25. H. Barnes et al., *An Introduction to Rheology*, Elsevier, New York, 1989.
26. A.W. Snow et al., *J. Appl. Polym. Sci.*, 52, 401, 1994.
27. T. Renault et al., *NATAS Notes*, 25, 44, 1994. H.L. Xuan et al., *J. Polym. Sci.: Part A*, 31, 769, 1993. W. Shi et al., *J. Appl. Polym. Sci.*, 51, 1129, 1994.
28. V. Litvinov and A. Dias, *Macromolecules*, 34, 4051, 2001. N. Emami et al., *Dent. Mater.*, 21, 977, 2005. R. Johnson, *SPE ANTEC Proc. V2*, 43, 1886, 2003.
29. J. Enns, private communication.
30. R. Geimer et al., *J. Appl. Polym. Sci.*, 47, 1481, 1993. R. Roberts, *SAMPE J.*, 5, 28, 1987.
31. J. Lopez et al., *J. Appl. Polym. Sci.*, 83, 78, 2002. J. Cuevas et al., *J. Polym. Sci.: Part B*, 41, 1965, 2003. I. Muhtarogullari, *J. Appl. Polym. Sci.*, 74, 2971, 1999. W. Cook et al., *J. Appl. Polym. Sci.*, 93, 1348, 2004.
32. P.J. Halley and M.E. MacKay, *Polym. Eng. Sci.*, 36(5), 593, 1996.
33. J. Ferry, *Viscoelastic Properties of Polymers*, 3rd ed., Wiley, New York, 1980.
34. J. Mijovic et al., *J. Comp. Met.*, 23, 163, 1989. J. Mijovic et al., *SAMPE J.*, 23, 51, 1990.
35. M. Roller, *Met. Finish.*, 78, 28, 1980. M. Roller et al., *ANTEC Proc.*, 24, 9, 1978. J. Gillham, *ACS Symp. Ser.*, 78, 53, 1978. M. Roller et al., *ANTEC Proc.*, 21, 212, 1975. M. Roller, *Polym. Eng. Sci.*, 15, 406, 1975. M. Roller, *Polym. Eng. Sci.*, 26, 432, 1986.
36. M. Roller, *Polym. Eng. Sci.*, 19, 692, 1979. M. Roller et al., *J. Coat. Tech.*, 50, 57, 1978.
37. C. Rohn, *Problem Solving for Thermosetting Plastics*, Rheometrics, Austin, TX, 1989.
38. J. Seferis et al., *Chemorheology of Thermosetting Polymers*, ACS, Washington D.C., 1983, p. 301. R. Patel et al., *J. Thermal Anal.*, 39, 229, 1993.
39. M. Roller, *Polym. Eng. Sci.*, 26, 432, 1986.
40. M. Roller, private communication, 1998.
41. J. Gillham et al., *Polym. Composites*, 1, 97, 1980. J. Enns et al., *J. Appl. Polym. Sci.*, 28, 2567, 1983. L.C. Chan et al., *J. Appl. Polym. Sci.*, 29, 3307, 1984. J. Gillham, *Polym. Eng. Sci.*, 26, 1429, 1986. S. Simon et al., *J. Appl. Polym. Sci.*, 51, 1741, 1994. G. Palmese et al., *J. Appl. Polym. Sci.*, 34, 1925, 1987. J. Enns et al., in *Polymer Characterization*, C. Craver, Ed., ACS, Washington D.C., 1983, ch. 2.
42. J. Gillham et al., *J. Appl. Polym. Sci.*, 53, 709, 1994. J. Enns and J. Gillham, *Trends Polym. Sci.*, 2(12), 406, 1994.
43. A. Otero et al., *Thermochimica Acta*, 203, 379, 1992. K. Menard et al., *Mater. Innovations*, 10, 111, 2006. B. Bilyeu et al., *J. ASTM Int.*, 2(10), 1, 2005.
44. J. Gillham et al., *J. Appl. Polym. Sci.*, 42, 2453, 1991. B. Osinski, *Polymers*, 34, 752, 1993.
45. J. Enns and J. Gillham, *Trends Polym. Sci.*, 2(12), 406, 1994. B. Bilyeu et al., *Polym. Composites*, 23, 1111, 2002.
46. R.C. Allen, Proc. 35th Tech. Conf. Reinforced Plastics and Composites, 35(26C), 1, 1980.

8 Frequency Scans

Frequency scans are the most commonly used method to study melt behavior in DMA and, at the same time, the most neglected experiment for many users. DMA users from a rheological or polymer engineering background depend on the DMA to answer all sorts of questions about polymer melts. For many chemists and thermal analysts using DMA, the frequency scan is an ill-defined technique associated with a magical predictive method called time–temperature superposition. In this chapter, we will attempt to clear away some of the confusion and explain why the frequency dependence of a polymer is important and how we can use it to expand our understanding of materials. We'll also look at the biggest area of use for frequency scans, polymer melts, solutions, and suspensions.

8.1 METHODS OF PERFORMING A FREQUENCY SCAN

Frequency effects can be studied in various ways of changing the frequency: scanning or sweeping across a frequency range, applying a selection of frequencies to a sample, applying a complex wave form to the sample and solving its resultant strain wave, or by free resonance techniques (Figure 8.1). Special techniques are also used to obtain collections of frequency data as a function of temperature for developing master curves and for studying the effect of frequency on temperature-driven changes in the material.

To collect frequency data, the simplest approach is to hold the temperature constant and scan several frequencies as you scan temperature. As long as the frequencies are fairly high, say 0.1 Hz and above, and the heating rate is low, the temperature should be mostly constant for the data collection. This statement does assume that the same mass is not so large as to exhibit large thermal lags. One can sample a set collection of frequencies, normally limited by the instrument to some number that gives a good overview of the frequency response for a couple decades on a logarithmic graph, for example, in PerkinElmer's DMA 8000 it is 10. One could choose 0.1, 0.2, 0.5, 1, 2, 5, 10, 20, 50, 100, and heat at 1 or 2 degrees a minute. However, two variables are changing at the same time and one needs to be concerned. If you are worried about thermal transfer, you probably need to use the other common approach with isotherm holds. This is done by applying a number of frequencies to the sample while it is held at a series of isotherms to obtain a multiplex of curves. A greater number of frequencies can be sampled this way, up to 100 in the PerkinElmer's DMA 8000, and because we let the instrument stabilize at a temperature and soak, the lower frequencies are limited only by your instrument and your patience.

The initial response to the idea of low frequencies is "I'm patient. How low does this thing go?" However, the first time one tries a run and realizes that taking three data points at .0001 Hz and averaging them is going to take about 8 hours for the

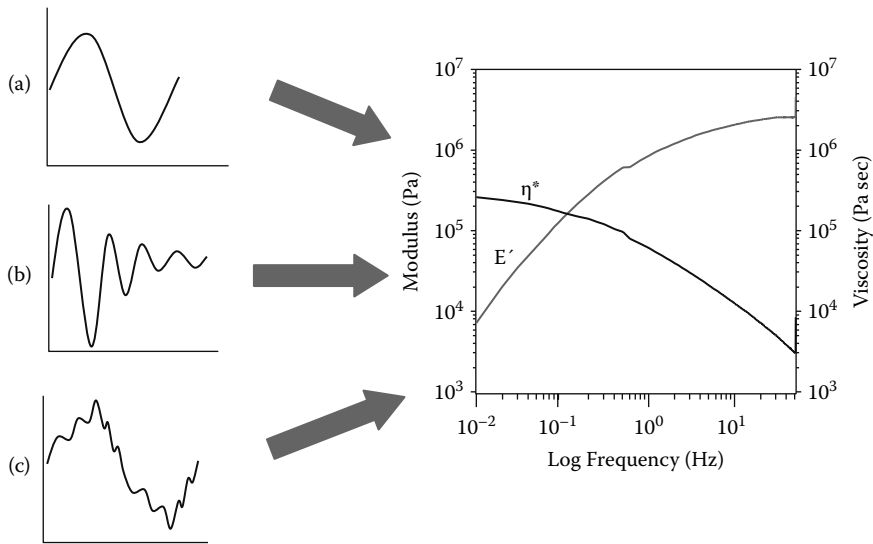


FIGURE 8.1 Methods of obtaining frequency information include: (a) sequential forced frequency runs, (b) free resonance decay, and (c) complex waveforms. All can be used to generate the same types of plots.

first data point, one reconsiders. To give an example, a run from -70°C to 70°C , taking 14 data points logarithmically spread across a frequency range of .01 to 215 Hz was set up using a 0.6 mm thick piece of a plastic. Three data points were collected at each frequency and averaged. Only a 3 minute soak was used with the isotherms being 10°C apart. The experiment took 13 hours. Notice the points were spaced logarithmically not linearly. I used a similar arrangement with the 1, 2, 5 spacing. On a log scale, this prevents the points from clumping together and frequency data is analyzed on a log scale. Evenly dividing the points into the decade linearly gives an odd looking graph.

The application of a complex waveform allows very fast collection of data. By combining a set of sine waves into one wave, data can be taken for multiple frequencies in less than 30 seconds. Several approaches are used and have been reviewed by Dealy and Nelson.¹ The user should be concerned that the test is confined to the region where the Boltzmann superposition principle holds for the material.² This unfortunately limits its application. From my experience, the time saving does not seem to be worth it. Free resonance techniques, discussed in Chapter 5, can also be used.³ Creep ringing is sometimes used this way intentionally as opposed to our discussion in Chapter 3 where we were trying to save something from bad data.

To extend the range of frequency studies to very low or high frequencies outside the instrument's scanning range, data are often added from either creep or free resonance experiments. Creep data provide results at very low rates of deformation, whereas free resonance or stress relaxation will provide results at the higher rates of deformation. The former can be obtained in a stress-controlled rheometer in a

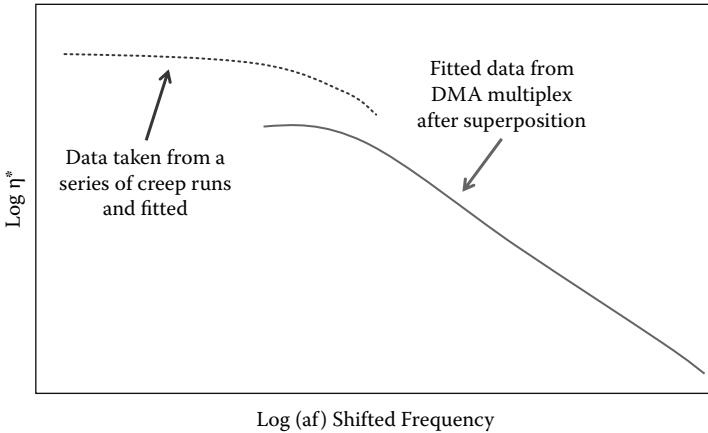
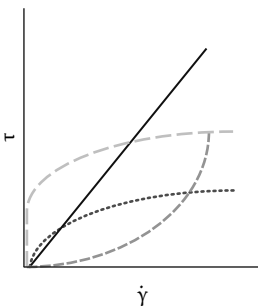


FIGURE 8.2 Frequency data from both a creep test and a DMA frequency scan for a medical grade polyurethane. Note that the creep data does not lie on the same curve as the frequency data obtained from a DMA run.

recovery experiment⁴ or from a specialized free resonance instrument.⁵ The data from these experiments can only be added if the material acts similarly in these tests as it does in a dynamic scan. This is not always true as shown in Figure 8.2 for polyurethane. However, often the nature of the material is simple enough that this does work.

8.2 FREQUENCY EFFECTS ON MATERIALS

In Chapter 2, we discussed how a fluid or polymer melt response is a result of strain rate (Figure 8.3) rather than to the amount of stress applied. The viscosity is the one of the main reasons why people run frequency scans. As the stress-strain curves and the creep recovery runs show (Figure 8.4), viscoelastic materials exhibit some



- Newtonian behavior (—) is linear and the viscosity is independent of rate.
- Pseudoplastic(-----) fluids get thinner as shear increases.
- Dilatant Fluids (- - -) increase their viscosity as shear rates increase.
- Plastic Fluids (— —) have a yield point with pseudoplastic behavior.
- Thixotropic and rheopectic fluids show viscosity-time nonlinear behavior. For example, the former shear thin and then reform its gel structure.

FIGURE 8.3 The response of a fluid to strain rate. Polymeric fluids and melts normally show deviations from Newtonian behavior.

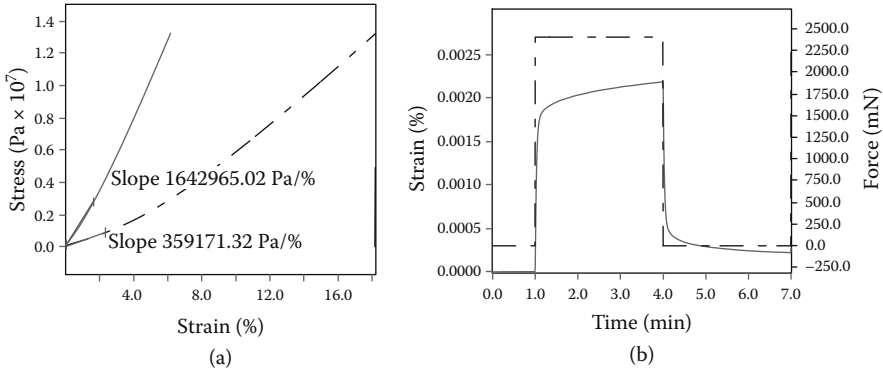


FIGURE 8.4 The effect of the viscous nature of polymers on the stress–strain and creep behavior of polymeric solids. Note both cases show nonlinearities caused by the viscoelastic, rather than elastic, nature of the materials. For (a), elastic behavior would show a flat line instead of the curved one seen. While in (b), a purely elastic material would show a square wave like the stress wave.

degree of flow or unrecoverable deformation. The effect is strongest in melts and liquids where frequency versus viscosity plots are the major application of DMA.

Figure 8.5 shows a frequency scan on a viscoelastic material. In this example, the sample is a rubber above the T_g in three-point bending, but the trends and principles we discuss will apply to both solids and melts. We have plotted the storage modulus and complex viscosity on log scales against the log of frequency. Let’s examine the curve and see what it tells us. First, we should note that in analyzing the frequency scans we will be looking at trends and changes in the data, not for specific peaks or transitions as we did in earlier chapters.

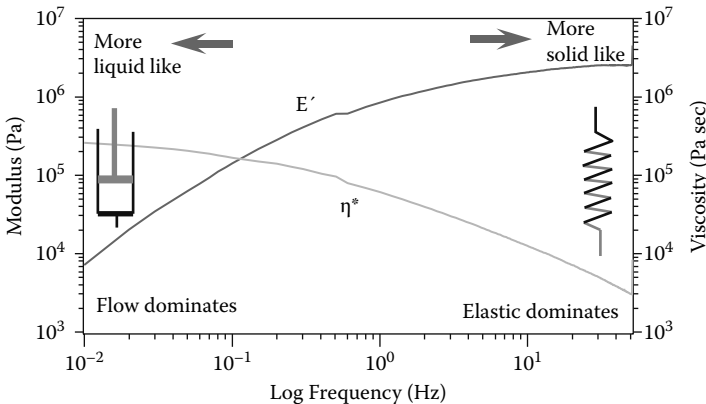


FIGURE 8.5 An example of a frequency scan showing the change in a material’s behavior as frequency varies. Low frequencies allow the material time to relax and respond, hence, flow dominates. High frequencies do not and elastic behavior dominates.

Starting with the viscosity curve, η^* , we see at low frequency a fairly flat region called the zero-shear plateau.⁶ This is where the polymer exhibits Newtonian behavior and its viscosity is dependent on M_w , not the strain rate. The viscosity of this plateau has been experimentally shown to relate to the molecular weight for Newtonian fluid

$$\eta \propto cM_v^1 \quad (8.1)$$

for cases where the molecular weight, M_v , is less than the entanglement molecular weight, M_e . For cases where M_v is greater than M_e

$$\eta \propto cM_v^{3.4} \quad (8.2)$$

where η is the viscosity of the initial Newtonian plateau, c is a material constant, and M_v is the viscosity average molecular weight. The relationship can also be written in general as replacing the exponential term with the Mark–Houwink constant, a . Similar relationships have been found for solids using different constants. This approach is used as a simple method of approximating the molecular weight of a polymer. The value obtained is closest to the viscosity average molecular obtained by osmometry.⁷ In comparison with the weight average data obtained by gel permeation chromatography (GPC), the viscosity average molecular weight would be between the number average and weight average molecular weights, but closer to the latter.⁸ We will discuss this again in Section 8.10.

This relationship was originally developed for continuous shear measurements, not dynamic measurements and the question arises if we can apply it to DMA data. Since we said in earlier chapters that E' is not exactly Young's modulus and that you should not expect the dynamic modulus to equal the static modulus to equal the creep modulus, the question arises if η^* is equal to η . Cox and Mertz found that an empirical relationship exists between complex viscosity and steady shear viscosity when the shear rates are the same.⁹ The Cox–Mertz rule is

$$|\eta^*(\omega)| = \eta(\dot{\gamma})|_{\dot{\gamma}=\omega} \quad (8.3)$$

where η is the constant shear viscosity, η^* is the complex viscosity, ω is the frequency of the dynamic test, and $\dot{\gamma}$ is the shear rate of the constant shear test. This rule of thumb seems to hold for most materials to within about $\pm 10\%$. Another approach, which we discussed in Chapter 5, is the Gleiselle mirror relationship¹⁰ that states

$$\eta\dot{\gamma} = \eta^+(t)|_{t=1/\dot{\gamma}} \quad (8.4)$$

when $\eta^+(t)$ is the limiting value of the viscosity as the shear rate, $\dot{\gamma}$, approaches zero.

The low frequency range is where viscous or liquid-like behavior predominates. If a material is stressed over long enough times, some flow occurs. As time is the inverse of frequency, this means we can expect materials to flow more at low frequency. As the frequency increases, the material will act in a more and more elastic

fashion. Silly Putty™, the children's toy, shows this clearly. At low frequency, Silly Putty™ flows like a liquid while at high frequency it bounces like a rubber ball.

This behavior is also similar to what happens with temperature changes. Remember that a polymer becomes softer and more fluid as it is heated and it goes through transitions that increase the available space for molecular motions. Over long enough time periods, or small enough frequencies, similar changes occur. This means one can move a polymer across a transition by changing the frequency. This relationship is also expressed as the idea of time–temperature equivalence.¹¹ Often stated as low temperature is equivalent to short times or high frequency, it is a fundamental rule of thumb in understanding polymer behavior.

As we increase the frequency in the frequency scan, we leave the Newtonian region and begin to see a relationship between the rate of strain, or the frequency, and the viscosity of the material. This region is often called the power law zone and can be modeled by

$$\eta^* \equiv \eta(\dot{\gamma}) = c\dot{\gamma}^{n-1} \quad (8.5)$$

where η^* is the complex viscosity, $\dot{\gamma}$ is the shear rate, and the exponent term n is determined by the fit of the data. The can also be written as

$$\sigma \equiv \eta(\dot{\gamma}) = c\dot{\gamma}^n \quad (8.6)$$

where σ is the stress and η is the viscosity. Other models exist and some are given in Table 8.1. The exponential relationship is why we traditionally plot viscosity versus frequency on a log scale. With modern curve fitting programs, the use of log–log plots has declined and is a bit anachronistic. The power law region of polymers shows the shear thickening or thinning behavior discussed in Chapter 2. This is also the region in which we find the $E' - \eta^*$ or the $E' - E''$ crossover point. As frequency increases and shear thinning occurs, the viscosity (η^*) decreases. At the same time,

TABLE 8.1
Flow Models

Newtonian	$f = \eta(\dot{\gamma})$
Viscoplastic	$f - f_o = \eta(\dot{\gamma})$
Power Law	$f = k(\dot{\gamma})^n$
Power Law with Yield Stress	$f - f_o = k(\dot{\gamma})^n$
Williamson	$\eta - \eta_\infty = (\eta_o - \eta_\infty) / (1 + f / f_m)$
Cross	$\eta - \eta_\infty = (\eta_o - \eta_\infty) / (1 + \alpha(\dot{\gamma})^n)$
Carreau	$\eta - \eta_\infty = (\eta_o - \eta_\infty) / (1 + (\lambda\dot{\gamma})^a)^{(n-1)/a}$

Note: Where f_o is the yield stress, η_o the low shear rate viscosity, η_∞ the high shear rate viscosity, and α and n are constants.

increasing the frequency increases the elasticity (E'). This is shown in Figure 8.5. The $E' - \eta^*$ crossover point is used as an indicator of the molecular weight and molecular weight distribution.¹² Changes in its position are used as a quick method of detecting changes in the molecular weight and distribution of a material. After the power law region, we reach another plateau, the infinite shear plateau.

This second Newtonian region corresponds to where the shear rate is so high that the polymer no longer shows a response to increases in the shear rate. At the very high shear rates associated with this region, the polymer chains are no longer entangled. This region is seldom seen in DMA experiments and usually avoided because of the damage done to the chains. It can be reached in commercial extruders and causes degradation of the polymer, product failures, and discoloration.

As the curve in Figure 8.5 shows, the modulus also varies as a function of the frequency. A material exhibits more elastic-like behavior as the testing frequency increases and the storage modulus tends to slope upward toward higher frequency. The storage modulus's change with frequency depends on the transitions involved. Above the T_g , the storage modulus tends to be fairly flat with a slight increase with increasing frequency as it is on the rubbery plateau. The change in the region of a transition is greater. If one can generate a modulus scan over a wide enough frequency range (Figure 8.6), the plot of storage modulus versus frequency appears like the reverse of a temperature scan. The same time–temperature equivalence discussed earlier also applies to modulus, as well as compliance, $\tan \delta$, and other properties.

The frequency scan is used for several purposes that will be discussed in this chapter. One very important use that is very straightforward is to survey the material's response over various shear rates. This is important because many materials are used under different conditions. For example, adhesives, whether tape, Band-Aids®, or hot melts, are normally applied under conditions of low frequency and this property is referred to as tack (Figure 8.7). When adhesives are removed, the removal often occurs under conditions of high frequency called peel. Different properties are required at these regimes and to optimize one property may require chemical changes that harm the other. Similarly, changes in polymer structure can show these

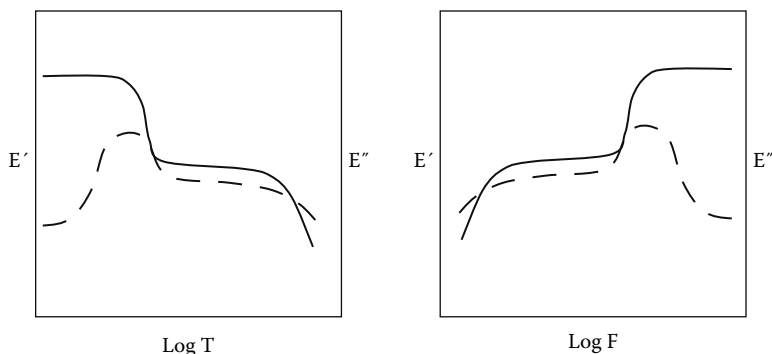


FIGURE 8.6 Comparison of a modulus scan taken by scanning at various frequencies and by varying temperature. This relationship is called time–temperature equivalency and is discussed later in the chapter.

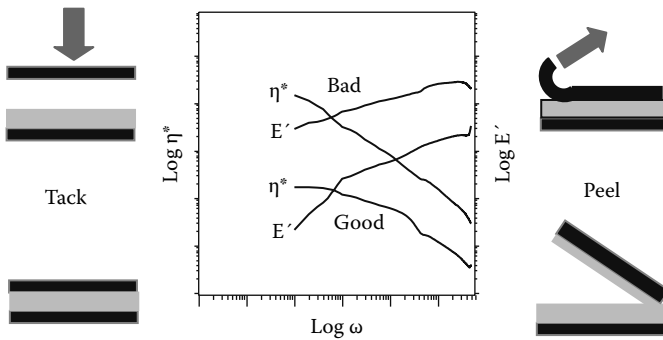


FIGURE 8.7 Tack and peel represent two properties that depend on opposite frequency ranges. (a) Tack is a very low frequency response involving the settling of the material into position. (b) Peel, on the other hand, is very high frequency.

kinds of differences in the frequency scan. Branching affects different frequencies differently as shown in Figure 8.8.

For example, in a contact adhesive, we desire sufficient flow under pressure at low frequency to fill the pores of the material to obtain a good mechanical bond. When the laminate is later subjected to peel, we want the material to be very elastic so it will not pull out of the pores.¹³ The frequency scan allows us to measure these properties in one scan so we can be sure that tuning one property does not degrade another. This type of testing is not limited to adhesives as many materials see multiple frequencies in actual use. Viscosity versus frequency scans are used extensively to study how changes in polymer structures or formulations affect the behavior of the melt. A list of common products and the frequency of use are shown in Table 8.2. Figure 8.9 shows frequency scans on some common materials.

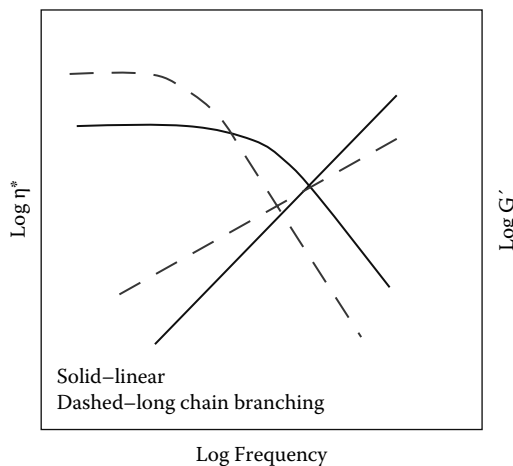


FIGURE 8.8 Comparing data for a long branched and a short branched polymer by DMA.

TABLE 8.2
Common Products and Their Use Frequencies

Paint leveling	0.01 Hz
Heart valves	1.2 Hz
Latex gloves and condoms	2 Hz
Plastic hip joints	4 Hz
Chewing, dental fillings	10 Hz
Contact lenses	16 Hz
Airbag openings	10,000 Hz

Another good example of why frequency scans are used is in the layup of graphite-epoxies composites (Figure 8.10). Composites are often laid up by hand and by mechanical tape layers in the same plant. The purchased material is designed to meet the operating requirements of both processes. However, as the material ages it becomes unsuitable for one process or the other depending on whether it was exposed to room temperature for too long or stored in freezers too long. The frequency scan checks both conditions in one experiment.

We need also to mention here that since we are scanning a material across a frequency range, we occasionally find conditions where the material-instrument system acts like a guitar string and begins to resonate when certain frequencies are reached. These frequencies are either the natural resonance frequency of the sample-instrument system or one of its harmonics. This is shown in Figure 8.11. Under this set of experimental conditions, the sample-instrument system is oscillating like a guitar string and the desired information about the sample is obscured.

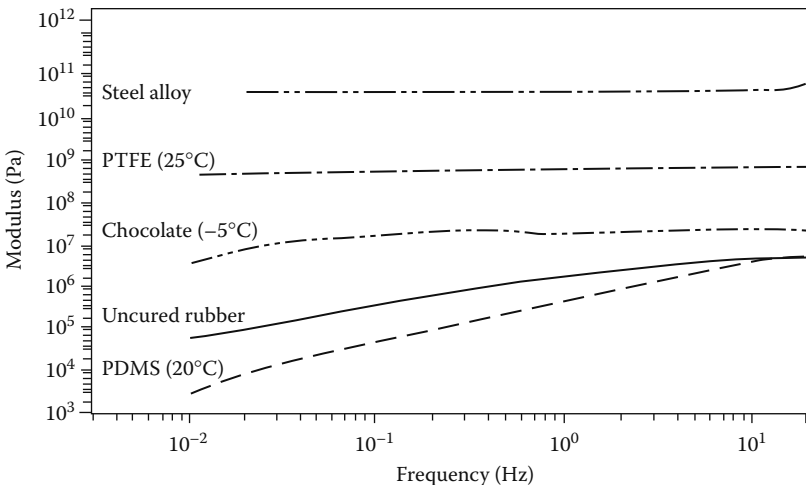


FIGURE 8.9 Frequency scans on common materials show that the modulus changes as a function of frequency more in viscoelastic materials than in elastic ones. Used with the permission of the PerkinElmer Corporation, Norwalk, Connecticut.

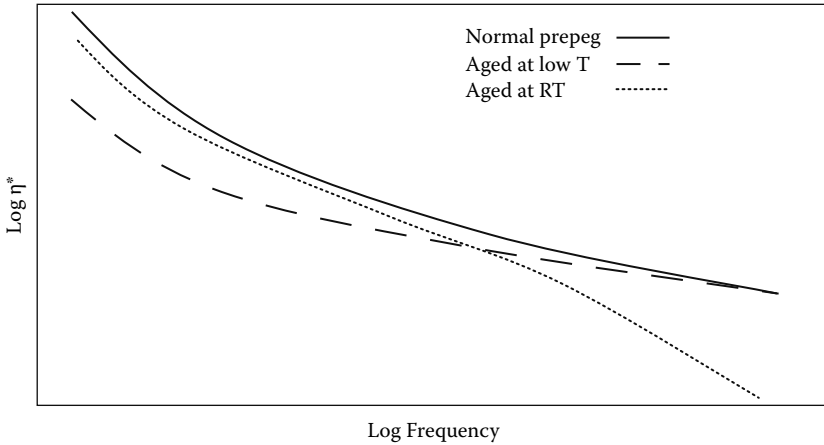


FIGURE 8.10 Frequency scans on three epoxy-graphite composite prepegs. Notice that different conditions show up as differences at different parts of the curve. Low frequency responses affect tack and therefore hand layup, whereas high frequency changes affect performance in the automatic tape winders.

Since there is no way to change this resonance response as it is a function of the system (in fact, in a free resonance analyzer we use the same effect), we will then need to redesign the experiment by changing sample dimensions or geometry to escape the problem. Using a sample with much different dimensions, which changes the mass, or changing from extension to three-point bending geometry changes the natural oscillation frequency of the sample and hopefully solves this problem. One should note a well-designed instrument will go through the resonance and continue to collect data on the other. The existence of resonance limits high frequency testing and most materials exhibit it before one reaches 300 Hz.

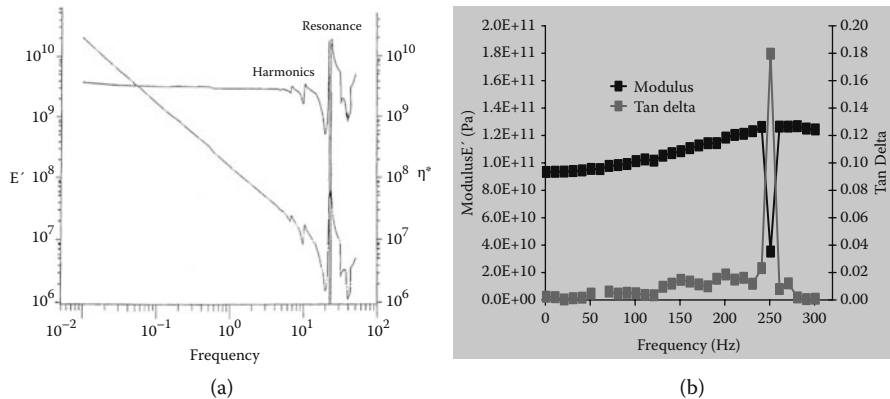


FIGURE 8.11 Free resonance occurs during a frequency scan in the (a) DMA 7e and (b) DMA 8000. Used with the permission of PerkinElmer Life and Analytical Sciences, Shelton, Connecticut.

8.3 THE DEBORAH NUMBER

Dimensionless numbers are used to allow the comparison of material behavior from many different situations. One such number used in DMA studies is the Deborah number and is defined as

$$D_e = \lambda/t = \tau_r/t_d \quad (8.7)$$

where the λ is the time scale of the material's response, and t is the time scale of the measurement process, which for DMA is the inverse of the frequency of measurement. Rosen points out that the quick estimate of λ is the relaxation time taken from a creep–recovery experiment as described in Chapter 3, where the time required for the material to recover to 1/e of the initial stress is defined as the relaxation time.¹⁴ Determination of an exact relaxation time for a polymer can be tricky and it is not uncommon to plot E' versus E'' in a variation of the Cole–Cole or Wicket plot to see if the polymer can really be treated as having a single relaxation time.^{15,16} This is a necessity for understanding whether a time–temperature superposition is valid and is discussed in Section 8.8. The τ_r is the polymer's relaxation time, often taken as one, the crossover frequency in radians/second, and t_d is the deformation time. The Deborah number is used in calculations to predict polymer behavior. If

$D_e \ll 1$, the material is viscous

$D_e \gg 1$, the material is elastic

$D_e \cong 1$, the material will act viscoelastically

One use of the Deborah number is to understand how the process will affect the polymer's relaxation time. One can calculate the deformation time from the process and then see how elastic or viscous the polymer will be. By going through a process and calculating the Deborah number for each step of the process with a certain material, one can highlight areas where problems can occur.

Reiner describes how the name of the Deborah number was selected in reference to a verse from the book of Judges in the Old Testament.¹⁷ There, in the song of Deborah, mountains are said to “flow before the Lord.” The implication was that just as on our time scale Silly Putty™ flows and rock is solid, on God's time scale rock flows.

8.4 FREQUENCY EFFECTS ON SOLID POLYMERS

Both solid thermoplastics and cured thermosets are studied by various frequency methods for several reasons. First, we may be interested to see how additives or modifications affect the material over a range of frequencies. For examples, adding oils and extenders to a rubber is done to adjust properties and reduce costs. As shown in Figure 8.12, sometimes the advantage is only gained in one frequency region. By using a frequency scan, we can see if the effect occurs at frequency of actual use.

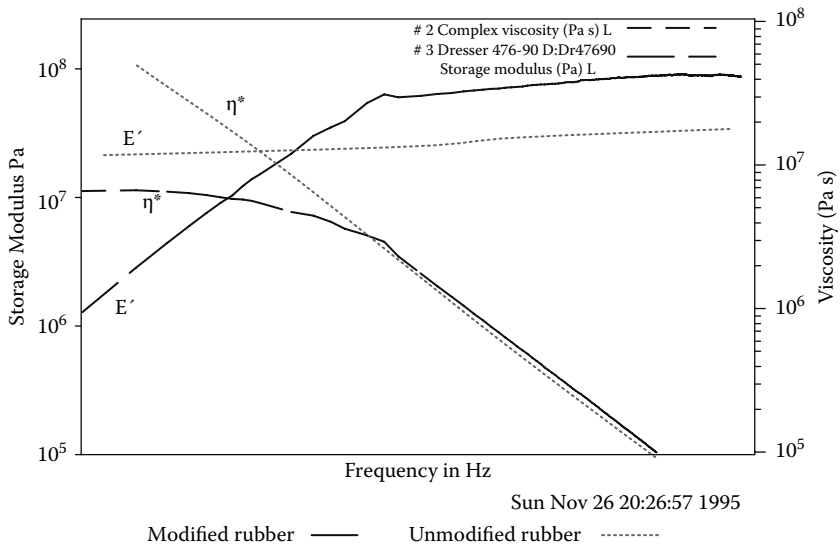


FIGURE 8.12 The effect of adding an oil modifier to a highly crosslinked rubber. Note that above a certain frequency, no effect of the additive is seen.

When analyzing a solid polymer, we are often looking at its transitions as a function of temperature. The frequency at which the temperature scan is run will affect the temperature of the transition. Figure 8.13a shows temperature scans run at different frequencies across a T_g . The general trend is that transitions like the glass transition move to lower temperatures as frequency decreases. In addition, the dependency of the transition on frequency is often related to the nature of the transition.¹⁸ The sub- T_g transitions (T_β , T_γ , T_δ) are not coordinated whereas the T_g requires the coordinated movement of multiple chains. Plotting the inverse of the temperature of these transitions against the log of the frequency will give different slopes for coordinated transitions than for uncoordinated ones. This is shown in Figure 8.13b. This can be exploited when investigating a polymer product for competitive analysis. By plotting the log of the frequency dependence against $1/T$ in Kelvin one can estimate the activation energy of the transition. Since a T_g activation energy is about 300 to 400 kJ/g and a beta transition has an E_{act} of about 20 to 30 kJ/g, one can make an educated guess if the beta peak is another polymer added as a toughening agent or a side chain movement.

This dependency of transition temperature on frequency also has another implication that sometimes goes unnoticed. By changing the frequency, you can move a material through a transition, as shown in Figure 8.14. This is another reason why we need to know both the frequencies to which the material will be exposed to in use and the frequency dependence of the material. This is why many workers will run a sample in a simple temperature scan at 1 and 10 Hz, to get a feeling for whether the material exhibits unusual frequency dependencies.

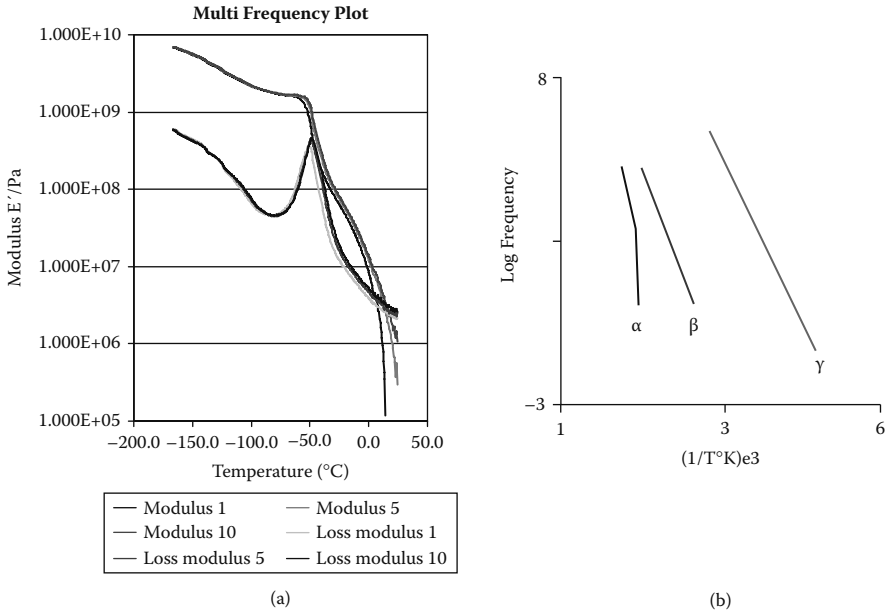


FIGURE 8.13 Effect of frequency on transitions. (a) The dependence of the T_g in Santoprene™ rubber on frequency. (b) Plots of the frequency dependence for polycarbonate. Redrawn with permission from N.G. McCrum, B.E. Read, and G. Williams, *Anelastic and Dielectric Effects in Polymeric Solids*, 1991, Dover Publications Inc.

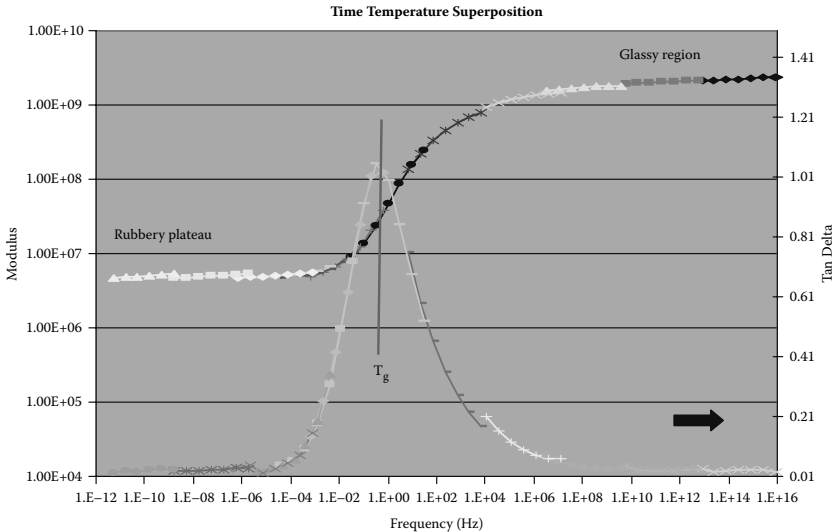


FIGURE 8.14 The moving of a material through its transitions, such as the T_g , can be done by varying the frequency. This can be an important consideration in materials like airbag liners where the use frequency is close to 10,000 Hz.

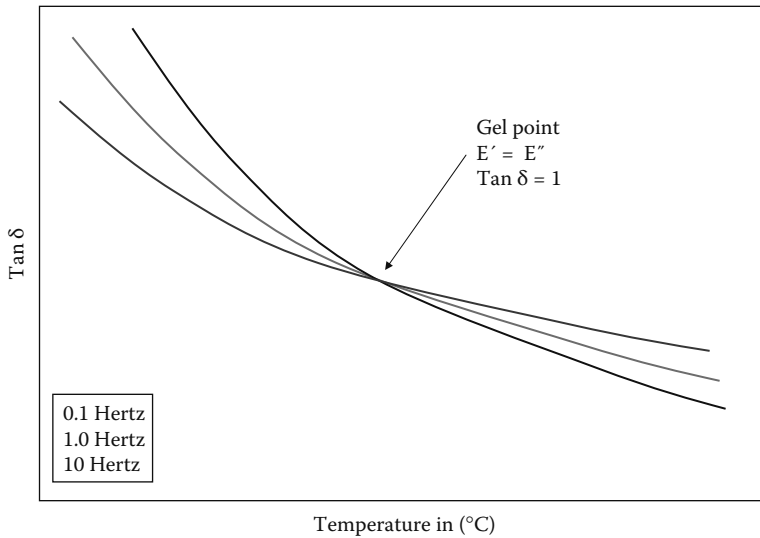


FIGURE 8.15 The collapse of viscosity curves run at various frequencies to one point at the gelation point.

8.5 FREQUENCY EFFECTS DURING CURING STUDIES

Cure studies are normally run at a frequency selected to allow good data to be collected or at a frequency matching that applied during the test. The application of pressure, or its increase, at various times during the minimum viscosity plateau is known to affect the final thickness of a part. Since we know that viscosity is dependent on frequency over a very wide range, the frequency at which this force is applied is also important.

By using one of the faster techniques of collecting frequency data, one can also look at the frequency dependence of the curing system. As shown in Figure 8.15, the frequency dependence reduces to zero at one point. This is taken as the point of gelation, where the network of crosslinks has formed across the material.¹⁹ (Note the discussion in Chapter 7 where it is pointed out that the classical “gel time” test does not measure what is commonly gelation in DMA studies.) The loose network acts as a very efficient damping system at this point and the frequency curves collapse into one.

8.6 FREQUENCY STUDIES ON POLYMER MELTS

The study of polymer melts by DMA is a large enough topic to be a text in itself. In this section, we will discuss the basics and refer the reader to more advanced texts on the topic. Since almost all of the processing techniques for polymers involve the melting of these materials, this is one of the most important topics in general

rheology. Dealy and Wissbrum have written a book on melt rheology and other good texts are available.²⁰ Graduate and short courses are offered that deal exclusively with this topic.²¹

The concerns of melt rheology for the DMA operator are normally the frequency dependence of viscosity, the elasticity or normal forces associated with the shearing of the melt, and the determination of molecular weight and distribution. The frequency dependence of a molten polymer's modulus and elasticity is determined by running a series of frequency scans as described in Section 8.1. This is done at a series of temperatures since the viscosity will have both frequency and temperature dependencies. These data are often combined into a master curve as discussed in Section 8.8. At some point increasing temperature or frequency will begin to irreversibly degrade the polymer by actually breaking chains. Since extrusion, injection molding, film blowing, and so on are influenced by the viscosity and modulus of the polymer for the amount of force needed to process it as well as the strength of the molten film and so forth, these data are vital to a processor.

8.7 NORMAL FORCES AND ELASTICITY

One of the interesting effects in polymer extrusion is the die swell.²² When a polymer is processed, it springs out of the extruder and visually swells. Die swell is the term used to describe how much a polymer melt expands when leaving the die and is critically important in die design. The swelling can be between 200% and 400% of the die diameter for polymers. Because of this swell, the die for extruding a square tube is slightly concave on the sides. The same effect can be easily seen in capillary rheometer studies. This requires designing dies with dimensions that are different from those of the desired product. Early work on rheology reports the concern with these values.²³ Similarly, if we stir a polymer melt or solution at high speed we see not the expected rise of the solution at the walls (caused by the centrifugal force throwing the material outwards) but the solution instead climbs the stirrer. All of these effects are caused by the elasticity of the melt or solution.

So when we shear a material in Figure 8.16, the entanglements of the chains cause the material to push and pull in directions normal (perpendicular) to the applied stress. This is called the normal force or the normal stresses. Normal force can be determined in certain shear rheometers by measuring how hard the polymer pushes against the top and bottom plates while sheared. One usually discusses this in terms of the normal stresses coefficients. One calculates the normal stress for each direction and then looks at the first and second normal stress coefficients. For a cubic sample where the normal stress can be called σ_x , σ_y , and σ_z , we can define the normal stress coefficients as

$$\Psi_1 = (\sigma_x - \sigma_y)/(d\gamma/dt)^2 \quad (8.8)$$

$$\Psi_2 = (\sigma_y - \sigma_z)/(d\gamma/dt)^2 \quad (8.9)$$

The second value, Ψ_2 , is normally small and negative so most of the concern is on the first normal stress coefficients, Ψ_1 .

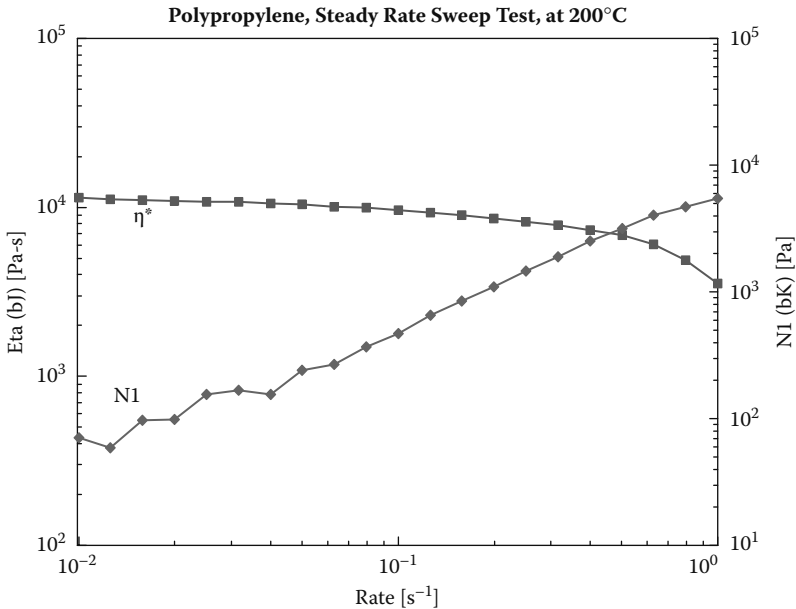


FIGURE 8.16 The existence of the normal force in a polymer melt under shear. When sheared the entanglements of the polymer chains cause a force to be generated to the direction of shear. Normal force can be measured in a constant shear or in a dynamic shear experiment. Data collected by the author.

One can measure the normal stress coefficients by combining the results of two continuous shear experiments.²⁴ Experimentally this is done by measuring the total thrust, F , on the lower plate in a cone-and-plate fixture and solving

$$\Psi_1 = 2F/(\pi R^2)(d\gamma/dt)^2 \quad (8.10)$$

where R is the radius of the plate. Then one can perform another run using parallel plates and get the difference between the normal stress coefficients as

$$\Psi_1 - \Psi_2 = [1/(d\gamma/dt)_R](F/\pi R^2)[2 + d\ln(F/\pi R^2)/d\ln(d\gamma/dt)_R] \quad (8.11)$$

where R is the radius, $(d\gamma/dt)_R$ is the shear rate at the rim of the plate, and F is the normal force (thrust against the plate). So in two experiments, we get both coefficients.²⁵

Armstrong has reported that the shape of the normal force curve tracks the storage modulus shape closely and the information collected from the E' or G' curve is often adequate to study a material's elasticity.²⁶ The ability of DMA to give a measurement of elasticity has, to some degree, lowered the interest in direct measurement of Ψ_1 and Ψ_2 . The storage shear modulus, G' , can be used to estimate Ψ_1 . Under conditions where the Cox–Mertz rule applies, we can assume

$$G'(\omega)/\omega^2|_{\omega \rightarrow 0} = N_1(\gamma)/2\gamma^2|_{\gamma \rightarrow 0} = \Psi_1(\gamma)/2|_{\gamma \rightarrow 0} \quad (8.12)$$

where G' is the shear storage modulus, N_1 the first normal force, and Ψ_1 the first normal force coefficient. More simply put, the first normal stress difference can be expressed as

$$\Psi_1 = (\sigma_x - \sigma_y) = 2G' \quad (8.13)$$

under conditions where the frequency is very low. One can also estimate the first normal stress different from η' and η'' . Laun's²⁷ rule is similar to the Cox–Mertz rule and states

$$\Psi_1 (d\gamma/dt) = \{2\eta''(\omega)/\omega\} [1 + (\eta''/\eta')^2]^{0.7} \Big|_{\omega = d\gamma/dt} \quad (8.14)$$

A mirror relation has also been proposed by Gleiselle²⁸

$$\Psi_1 (d\gamma/dt) = \Psi_1^+(t) \Big|_{t = k/(d\gamma/dt)} \quad (8.15)$$

where k is a constant between 2.5 and 3 for many polymer fluids. Another area of interest is the dependence of the first normal stress difference on molecular weight, which is reported to be quite large.²⁹

8.8 MASTER CURVES AND TIME–TEMPERATURE SUPERPOSITION

As previously discussed, the problem with performing frequency scans is that all instruments have a limited range and often one wants data outside of the available range. In addition, sometimes we want to estimate behavior at times that are inconvenient or impossible to measure experimentally. There are a couple of approaches to addressing these problems. Experimentally one can add data collected from creep experiments at very low rates of strain (frequencies;³⁰ see Figure 8.17b). This is done by calculating the rate of strain of a material during its equilibrium or steady-state plateau and using the corresponding viscosity and modulus measured at those conditions. Very low frequencies can be reached by this method and added to the data collected by frequency scans. However, as creep is not the same as dynamic tests, sometimes the data are not even similar as shown for the polyurethane in Figure 8.2. Due to the hard and soft segments of this polyurethane, the polymer has very different behavior under creep and DMA conditions. One can also use the results of free resonance studies to obtain higher frequencies using either a free resonance instrument³¹ or by performing a recovery experiment in a stress-controlled rheometer.³² This was discussed in Chapter 5. These data can also be added to the frequency scan.

These approaches are relatively underused compared to the concept of time–temperature superposition. Time–temperature superposition was described by Ferry as a “method of reduced variables.”³³ Shifting a series of multiplexed frequency scans relative to a reference curve performs the superposition. This is shown in Figure 8.17a. After shifting the curves, the resultant master curve (Figure 8.17b) covers a range much greater than that of the original data.

As mentioned, materials were studied by various techniques to obtain a series of curves often referred to as a multiplex. This is normally done to develop the master

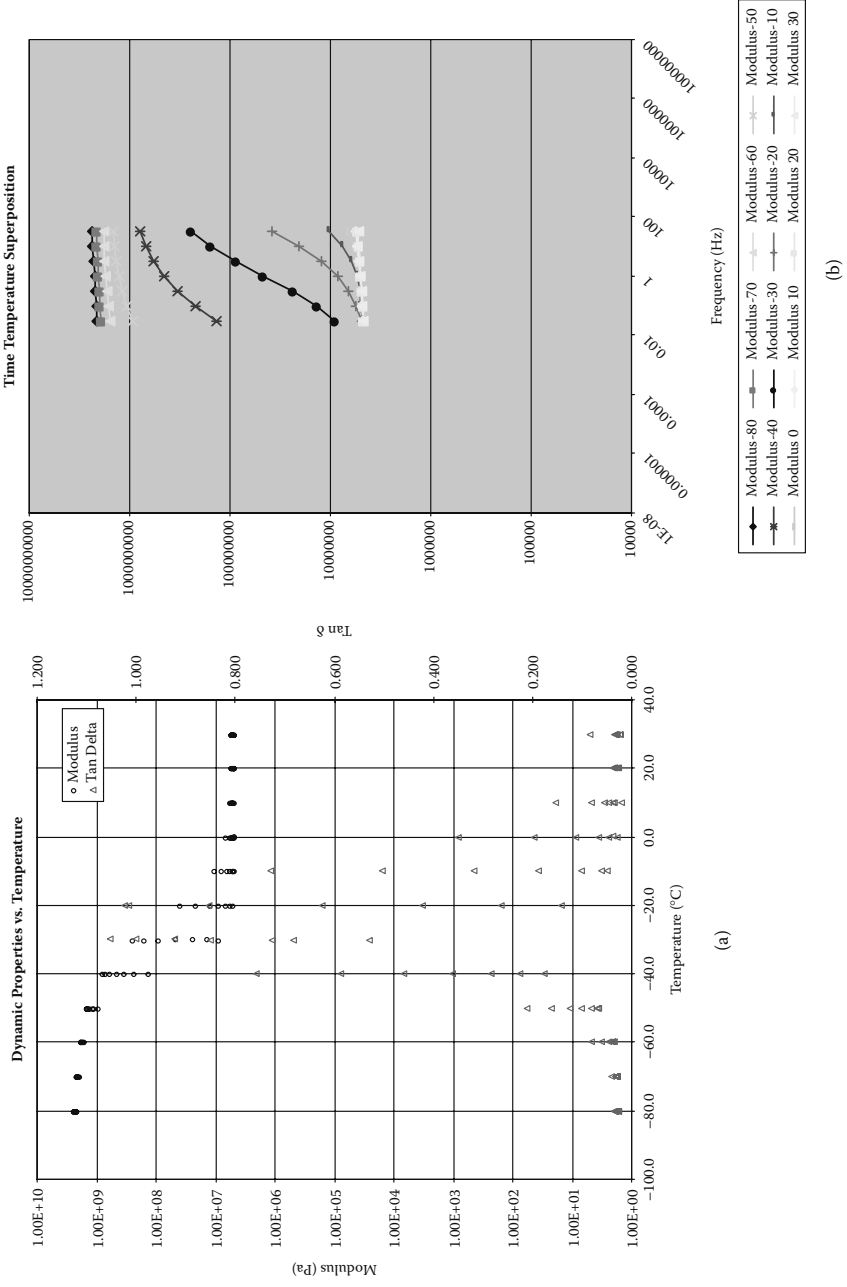


FIGURE 8.17 From a series of frequency scans, the complex viscosity curve was collected at (a) different temperatures and then (b) added together to (c) get a master curve.

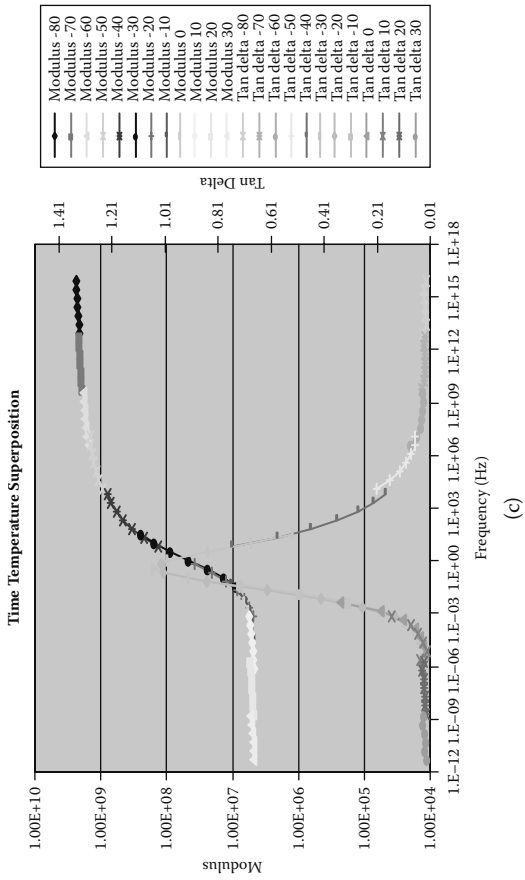


FIGURE 8.17 Contd.

curve, which is a collection of data that have been treated so they are displayed as one curve against an axis of shifted values. This has traditionally been done using a frequency scale for the x axis and temperature as the variable to create the multiplex of curves. Using the idea of time–temperature equivalence, we can assume that the changes seen by altering the temperature are similar to those caused by frequency changes. Therefore, the data can then be superpositioned to generate one curve.

Unfortunately, current use of this technique seems to be limited to mainly time–temperature superposition. As shown by Ferry³⁴ and Goldman,³⁵ this approach can be used for a wide range of variables including humidity, degree of cure, and strain. Goldman's tour de force gives many examples of the application of this technique to many properties of polymers. We will limit our discussion to the most commonly used approach, that of time–temperature superposition, but it is important to realize the principles can be applied to many other variables. For example, other workers have looked at the idea of superpositioning stress,³⁶ strain,³⁷ or aging time.³⁸

Various models have been developed for the shift. The most commonly used and the best known is the Williams–Landel–Ferry (WLF) model.³⁹ The WLF model for the shift factors is given as

$$\text{Log } a_T = \log (\eta/\eta_r) = -C_1(T - T_r)/C_2 + (T - T_r) \quad (8.16)$$

where a_T is the shift factor, T is the temperature in Kelvin, T_r is the reference temperature in Kelvin, and C_1 and C_2 are material constants. The reference temperature is the temperature of the curve the data is shifted to. This is normally assumed to be valid from the T_g to 100K above the T_g . Occasionally a vertical shift is applied to compensate for the density change of the polymer with temperature

$$a_v = T_g \rho_g / T \rho \quad (8.17)$$

where ρ is the density of the polymer at a temperature, T .⁴⁰ After the curves are shifted, the combined curves, the master curve, can be used to predict behavior over a wide range of frequencies.

If we consider a Newtonian fluid, we can state the viscosity in terms of a flow activation energy

$$\eta = Ae^{(E/RT)} \quad (8.18)$$

where E is the activation energy, R is the universal gas constant, and T is the temperature in Kelvin. If we combine this with Equation 8.16, the shift factor can be written as

$$\log a_t = \log (\eta/\eta_r) = (0.434E_{act}/R)(1/T - 1/T_r) \quad (8.19)$$

where E is the activation energy for the change in viscosity (called the flow activation energy), R is the universal gas constant, T is the temperature in Kelvin of the shifted curve, and T_r is the temperature in Kelvin of the reference curve. Plotting the $\log a_t$

against $(1/T - 1/T_r)$ will allow us to calculate E from the slope.⁴¹ As these values depend on the molecular parameters of the polymer, they can be used as a probe of changes in a polymer's structure. For example, changes in molar ratio of a series of copolymers will have a corresponding change in E_{act} .⁴²

Another approach to shifting curves based on free volume has been developed by Brostow and reduces to the WLF equation under certain assumptions. This equation is less limited by temperature and is

$$\ln a_r = A + B/(v_r - 1) \quad (8.20)$$

where v_r is the reduced volume of the material, calculated by dividing the molecular volume (volume per segment of polymer) of the material by a characteristic parameter called the hard core volume.⁴³

Not all materials can be shifted and the term rheologically simple or rheological simplicity is applied to materials that can be superpositioned. Chemical simplicity is not enough. Both polyethylene and polystyrene⁴⁴ are reported as failing to superposition. Other materials, like natural and synthetic rubbers, are known to work quite well.

After the master curve has been generated, it can be used to predict behavior, used as the basis for further manipulations to obtain relaxation or retardation spectra,⁴⁵ or used to estimate the molecular weight distribution (see Section 8.10). The most common uses are the prediction of behavior at a shifted frequency or as a prediction of aging. To predict the aging or long-term properties of a material, one uses the fact that frequency is measured in hertz with units of reciprocal seconds. By inverting the curve, one can see the data against time (Figure 8.18a). Note that it is the low temperature–low frequency data that gives the longest times after the inversion of the frequency scan. This explains the interest in measuring as low a frequency as possible. Creep data are especially valuable in this case.

If you are trying to extend the frequency range of the analyzer, the temperature chosen is normally the one at which the material will be used. It is an unfortunately common practice to ignore the theory and to shift the curves to maximize the variable you wish to study. So to obtain long times when the curve is inverted, everything is shifted to lower frequencies to obtain long times. This is done without regard to the reference temperature or the limits of the superposition model. Shifting is often done empirically and the lines are moved up and down or straightened as necessary.

Many authors have warned that superposition does not always work and is often wrong. Dealy and Wissbrum give a good discussion on this, including the warning that “this assumes that all relaxation times are equally affected by temperature. This assumption is known to often be invalid.”⁴⁶ Plazek recently reviewed the approach of time–temperature superposition and pointed out that the same difficulties and failures exist today as did 20 years ago in applying this approach to various systems.⁴⁷ Some implicit assumptions exist about the mechanism of change within the sample (degradation, depolymerization, crosslinking, etc.) being the same at all temperatures. Also one assumes that different mechanisms do not occur on different sides of

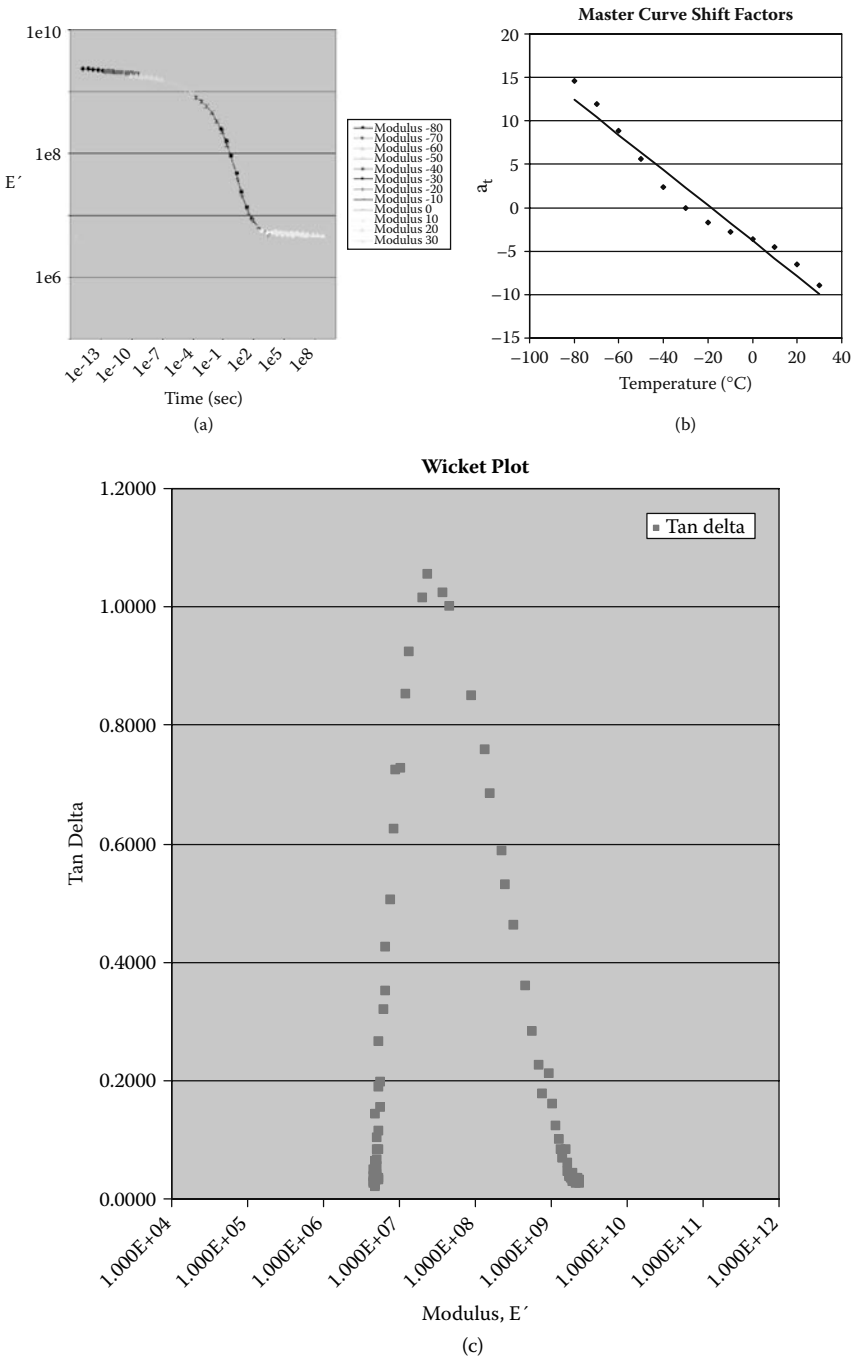


FIGURE 8.18 (a) The data from Figure 8.17 can then converted to a time scale to predict aging. (b) The shift factors can be plotted against a model. (c) A Wicket plot checks the assumption of one relaxation time. (d) An unsuccessful time–temperature superposition (TTS) for Santoprene™ with its Wicket plot is shown.

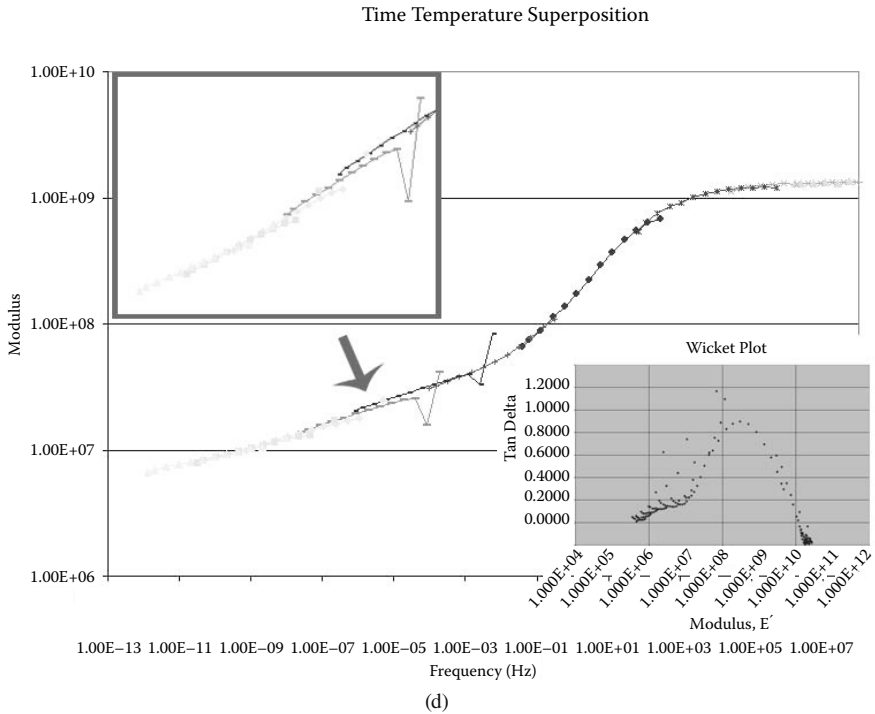


FIGURE 8.18 (Contd.)

transitions and all rates are relatively unaffected by temperature. These are untrue for a lot of situations and the literature on accelerated aging studies is full of case studies showing the dangers of simplistic assumptions. Although this technique is a powerful tool when it works, it has been presented as a panacea and care must be taken in its use. At a minimum, one should generate a Wicket or Cole–Cole plot (Figure 8.18b) and a plot of the shift factor. A curve looking like an arc or a croquette wicket should result from the Cole–Cole plot and a straight line should be seen through the shift factors. If not, then the assumptions of the WLF are not met and one should proceed with caution, if at all.

We are not going into the free volume models or the other non-WLF approaches at this time. Those interested can check the references discussed earlier for more information. As no commercial packages yet exist for these nor do they exist for nonlinear studies, it is beyond the scope of this book.

8.9 TRANSFORMATIONS OF DATA

One of the advantages of frequency data is that it is possible to transform it into other forms to allow better probing of a polymer’s characteristics. We have mainly used viscosity plots as examples because the frequency data give linear plots on a log–log plot. (Log–log plots are offered on all commercial DMAs but this should

not be taken to mean that this is the best way to handle the data.) However, the same shift factors also work for E' and E'' as all the values are calculated from the same data set. Having these data, we can generate data for master curves that would take much longer to obtain experimentally.⁴⁸ For example, we can use Ferry's method⁴⁹ to approximately calculate the equivalent stress relaxation master curve

$$E(t) = E'(\omega) - 0.4(E'')(\omega) + 0.014(E'')(10\omega) \quad (8.21)$$

where $E(t)$ is the stress relaxation modulus, E' is the storage modulus from the dynamic experiment, ω is the dynamic test frequency, and E'' is the dynamic loss modulus. A similar equation exists for the compliance, J . This data can then be converted to a creep compliance master curve by

$$\int_0^t E(t)J(t - \tau)d\tau = t \quad (8.22)$$

and similarly for compliance. One can also convert these data to discrete viscoelastic functions, such as the retardation spectra, $L(\ln \tau)$, and relaxation spectra, $H(\ln \tau)$, for the material. Figure 7.19 shows the interconversion of data. While this is beyond the scope of this book, several good references exist. These conversions, like those discussed earlier, are also available in software packages from instrument vendors and other sources.⁵⁰

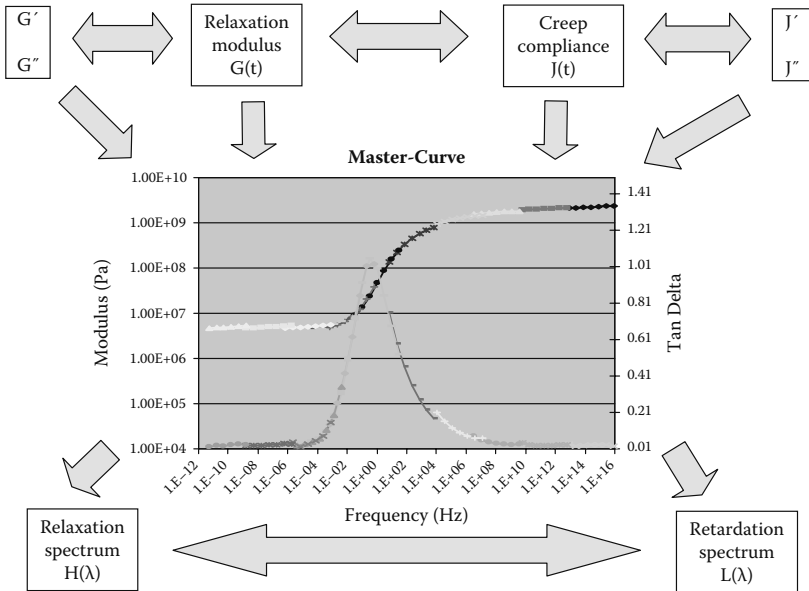


FIGURE 8.19 The interconversion of frequency scan data to different types of data.

8.10 MOLECULAR WEIGHT AND MOLECULAR WEIGHT DISTRIBUTIONS

It has long been known that molecular weights could be related to the polymer viscosity in the Newtonian region.⁵¹ This was discussed earlier and is still used as a way to obtain the viscosity average molecular weight, M_v . The viscosity average molecular is larger than the number average molecular weight but slightly smaller than the weight average molecular. The viscosity average molecular weight is close enough to the latter that it responds similarly to changes in the polymer structure. The viscosity of this plateau can be related to the molecular weight for a melt by

$$\log \eta_0 = cM_v^\alpha \quad (8.23)$$

where η_0 is the viscosity of the initial Newtonian plateau, c is a material constant, α is the Mark–Houwink exponent, and M_v is the viscosity average molecular weight. Above the entanglement or critical molecular weight, M_e , the value of α for melts and highly concentrated solutions is 3.4. Below that value, molecular weight is linearly related to the viscosity by a factor of one. This is shown in Figure 8.20b. Similar relationships have been found for polymeric solids using different constants and different exponentials. If the shear rate is not in the Newtonian region, the constant changes and at infinite shear becomes one. This approach is often used as a simple method of approximating the molecular weight of a polymer.

A more qualitative approach has also been used as an indicator of the relative difference in molecular weight and molecular weight distribution in polymers. Known as a rule of thumb for years, Rahalkar showed that it could be developed from the Doi–Edwards theory.⁵² The crossover point between E' and E'' or between E' and η^* moves with changes in both properties (Figure 8.21a). Both points work equally well, but the theory was developed for the E' – E'' crossover. As molecular weight increases, the viscosity also increases, and the crossover moves upward

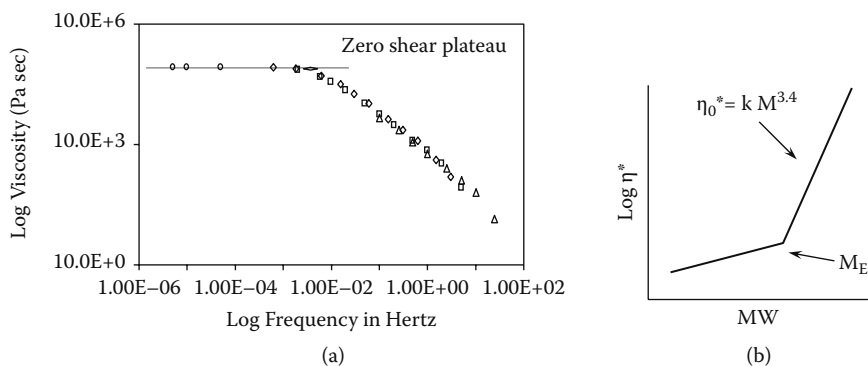


FIGURE 8.20 The zero-shear plateau is shown in (a) and the molecular weight for a polymer melt is (b).

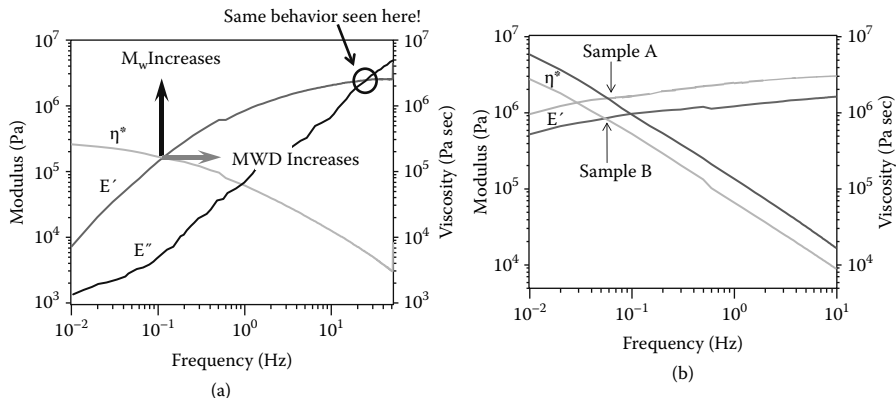


FIGURE 8.21 The crossover point (a) between either E' and E'' or between E' and η^* for a series of materials corresponds to the relative molecular weight and molecular weight distribution. (b) This is shown for real samples.

(toward higher viscosity). As the distribution increases, the frequency at which the material starts acting elastic increases and the point moves toward higher frequency. An example is shown in 8.20b for a pair of materials. My own experience is that this approach is much more responsive to molecular weight changes than to distribution.

The difficulty in measuring the distribution is not limited to just this approach. Measurement of the molecular weight distribution by DMA or rheology is currently a topic of discussion at many technical meeting. The Society of Plastic Engineers has had full sessions devoted to the use of rheology for quality control,⁵³ and these were heavily weighted toward molecular weight and molecular weight distribution measurement. Bonilla-Rios has a good overview with a detailed application in his thesis.⁵⁴ Other works are also excellent lead references in this area.⁵⁵ Software to perform this calculation is commercially available using an assumed normal distribution.⁵⁶ Recently, work has been published using a nonnormal distribution.⁵⁷ This is of great interest because many polymer distributions are skewed or tailed rather than normal. In fact, knowledge of how the polymer was made will often be enough to suggest whether it is high or low tailed.

The basic approach starts with the frequency shifted master curve. We now need a mixing rule. A mixing rule is a quantitative relationship that relates the observed mechanical properties of a polydisperse melt and the underlying polymer structure. This can be a relatively simple mathematical approximation to a more complex molecular theory of polydispersity and is normally supplied by the software. For example, a double reptation mixing rule, such as

$$G(t) = G_N \left[\int_0^\infty F^{\frac{1}{2}}(M, t) W(M) dM \right]^2 \quad (8.24)$$

is used in one commercial package. $G(t)$ is the relaxation modulus, which can be determined from experiments as discussed earlier, and $F^{1/2}(M,t)$ is the monodisperse relaxation function, which represents the time dependent fractional stress relaxation of a monodisperse polymer following a small step strain. $W(M)$ is the weight-based molecular weight distribution. Physically, all components of the molecular weight distribution will contribute to the modulus to some extent. The magnitude of each component's contribution to the stress will depend on the details of the interaction with the other molecules in the molecular weight distribution. One normally needs to supply the plateau modulus (G_n) and $F^{1/2}(M,t)$ in addition to the above. While the plateau modulus can be obtained from the literature, some form of the relaxation function must be assumed. For example, a form like

$$F^{1/2}(M,t) = \exp\left\{\frac{-t}{2\lambda(M)}\right\} \quad (8.25)$$

and

$$\lambda(M) = K(T)M^x \quad (8.26)$$

where $\lambda(M)$ is the characteristic relaxation time for the monodisperse system, $K(T)$ is a coefficient that depends on temperature, and the exponent x is ~ 3.4 for flexible polymers.

One then grinds through the mathematics, or allows the software package to do so. For many commercially manufactured polymers, where a normal distribution is a valid assumption, good results can be obtained.

8.11 CONCLUSIONS

Frequency scans and frequency dependencies are probably the least used and the most powerful techniques in DMA. While well known among people working with melts, the average user who comes from the thermal analysis or chemistry background normally ignores them. Frequency scans and frequency dependencies represent a powerful probe of material properties that should be in any testing laboratory.

NOTES

1. J. Dealy and B. Nelson, in *Techniques in Rheological Measurement*, A. Collyer, Ed., Chapman & Hall, New York, 1993, ch. 7.
2. I. M. Ward and D.W. Hadley, *Introduction to the Mechanical Properties of Solid Polymers*, Wiley, New York, 1993, pp. 51–54.
3. J. Enns and J. Gillham, in *Polymer Characterization: Spectroscopic, Chromatographic, and Physical Instrumental Methods*, C. Craver, Ed., ACS, Washington D.C., 1983, p. 27.
4. U. Zolzer and H.-F. Eicke, *Rheologica Acta*, 32, 104, 1993.
5. J. Enns and J. Gillham, in *Polymer Characterization: Spectroscopic, Chromatographic, and Physical Instrumental Methods*, C. Craver, Ed., ACS, Washington D.C., 1983, p. 27.

6. C. Rohn, *Analytical Polymer Rheology*, Hanser, New York, 1995.
7. M. Miller, *The Structure of Polymers*, Reinhold, New York, 1966, pp. 611–612.
8. S. Rosen, *Fundamental Principles of Polymeric Materials*, Wiley Interscience, New York, 1993, pp. 53–77, 258–259.
9. W. Cox and E. Mertz, *J. Polym. Sci.*, 28, 619, 1958. P. Leblans et al., *J. Polym. Sci.*, 21, 1703, 1983.
10. W. Gleissle, in *Rheology*, Vol. 2, G. Astarita et al., Eds., Plenum Press, New York, 1980, p. 457.
11. D.W. Van Krevelin, *Properties of Polymers*, Elsevier, New York, 1987, p. 289.
12. C. Macosko, *Rheology*, VCH Publishers, New York, 1996, p. 120–127.
13. This is a very simplified version of adhesion. The reader is referred to the following for a detailed discussion: L.-H. Lee, Ed., *Adhesive Bonding*, Plenum Press, New York, 1991. L.-H. Lee, Ed., *Fundamentals of Adhesion*, Plenum Press, New York, 1991.
14. S. Rosen, *Fundamental Principles of Polymeric Materials*, 2nd ed., Wiley, New York, 1993.
15. S. Havriliak and S.J. Havriliak, *Dielectric and Mechanical Relaxations in Materials*, Hanser, New York, 1997.
16. M. Reiner, *Twelve Lectures on Rheology*, North Holland, Amsterdam, 1949.
17. M. Reiner, *Twelve Lectures on Rheology*, North Holland, Amsterdam, 1949.
18. N. McCrum, B. Read, and G. Williams, *Anelastic and Dielectric Effects in Polymeric Solids*, Dover, New York, 1995, ch. 5, 7–14.
19. F. Champon et al., *J. Rheol.*, 31, 683, 1987. H. Winter, *Polym. Eng. Sci.*, 27, 1698, 1987. C. Michon et al., *Rheologica Acta*, 32, 94, 1993.
20. J. Dealy and K. Wissbrum, *Melt Rheology and Its Role in Polymer Processing*, Van Nostrand Reinhold, Toronto, 1990.
21. Both the University of Minnesota and the Massachusetts Institute of Technology offer weeklong courses.
22. R. Racin and D. Bogue, *J. Rheol.*, 23, 263, 1979. B. Bagley and H. Schreiber, in *Rheology*, Vol. 5, R. Eirich, Ed., Academic Press, New York, 1969, p. 93.
23. J. Dealy and K. Wissbrum, *Melt Rheology and Its Role in Polymer Processing*, Van Nostrand Reinhold, Toronto, 1990.
24. R. Bird, R. Armstrong, and O. Hassager, *Dynamics of Polymeric Liquids*, Vol. 1, Wiley, New York, 1987, p. 521–529.
25. C. Macosko, *Rheology*, VCH Publishers, New York, 1994, pp. 205–229.
26. R. Armstrong et al., *Rheologica Acta*, 20, 163, 1981.
27. H. Laun, *J. Rheol.*, 30, 459, 1986.
28. W. Gleissle, in *Rheology*, Vol. 2, G. Astarita et al., Eds., Plenum Press, New York, 1980, 457.
29. G. Vinogradov et al., *Rheology of Polymers*, Springer-Verlag, New York, 1980, p. 338.
30. L. Sperling, *Introduction to Physical Polymer Science*, 2nd ed., Wiley, New York, 1994, pp. 458–502.
31. J. Enns and J. Gillham, in *Polymer Characterization: Spectroscopic, Chromatographic, and Physical Instrumental Methods*, C. Craver, Ed., ACS, Washington D.C., 1983, p. 27.
32. U. Zolzer and H.-F. Eicke, *Rheologica Acta*, 32, 104, 1993.
33. J.D. Ferry, *Viscoelastic Properties of Polymers*, 3rd ed., Wiley, New York, 1980.
34. J.D. Ferry, *Viscoelastic Properties of Polymers*, 3rd ed., Wiley, New York, 1980.
35. A. Ya Goldman, *Prediction of the Deformation Properties of Polymeric and Composite Materials*, ACS, Washington D.C., 1994.

36. W. Brostow, N. D'Sousa, J. Kubat, and R. Maksimov, *J. Chem. Phys.*, 110, 9706, 1999. A. Akinay, W. Brostow, V. Castano, R. Maksimov, and P. Olszynski, *Polymer*, 43, 3593, 2002.
37. P. O'Connell and G. McKenna, *Polym. Eng. Sci.*, 37, 1485, 1997.
38. P. O'Connell and G. McKenna, in *Handbook of Polycarbonate Science and Technology*, D.G. LeGrand and J.T. Bendler, Eds., Marcel Dekker, New York, 1999, chap. 10.
39. M. L. Williams, R.F. Landel, J.D. Ferry, *J. Amer. Chem. Soc.*, 77, 3701, 1955.
40. J. Kubat and M. Rigdahl, in *Failure of Plastics*, W. Brostow and R. Corneliussen, Eds., Hanser, New York, 1986, ch. 4.
41. R. Tanner, *Engineering Rheology*, Oxford Science Publishers, Oxford, 1985, pp. 352–353.
42. N. D'Sousa, in preparation.
43. W. Brostow, in *Failure of Plastics*, W. Brostow and R. Corneliussen, Eds., Hanser, New York, 1986, ch. 10.
44. D. Plazek, *J. Rheol.*, 40(6), 987, 1996.
45. M. Baumgarertel and H. Winter, *Rheologica Acta*, 28, 511, 1989. N. Orbey and J. Dealy, *J. Rheol.*, 35, 1035, 1991.
46. J. Dealy and K. Wissbrum, *Melt Rheology and Its Role in Polymer Processing*, Van Nostrand Reinhold, Toronto, 1990, pp. 86–100.
47. D. Plazek, *J. Rheol.*, 40(6), 987, 1996.
48. A good introduction to the manipulation of DMA data can be found in H. Hopfe and C. Hwang, *Computer Aided Analysis of Stress-Strain Response of High Polymers*, Technomics, Lancaster, 1993. This book gives a fuller development of what is discussed here.
49. J. Ferry and K. Ninomiya, *J. Colloid Sci.*, 14, 36, 1959.
50. My favorite is the Isis program from Professor Winters at University of Massachusetts–Amherst. Simpler packages can be found in H. Hopfe and C. Hwang, *Computer Aided Analysis of Stress-Strain Response of High Polymers*, Technomics, Lancaster, 1993, and in G. Gordon and M. Shaw, *Computer Programs for Rheologists*, Hanser, New York, 1994. What is available changes yearly and I am sure there are some good packages out there I am unaware of.
51. R. Bird, R. Armstrong, and O. Hassager, *Dynamics of Polymeric Liquids*, Vol. 1, Wiley, New York, 1987, pp. 143–150. R. Nunes et al., *Polym. Eng. Sci.*, 22, 205, 1982. G. Pearson et al., *Polym. Eng. Sci.*, 18, 583, 1978.
52. R.R. Rahalkar, *Rheologica Acta*, 28, 166, 1989. R. Rahalkar and H. Tang, *Rubber Chem. Technol.*, 61(5), 812, 1988.
53. See the *Proceeding of the Annual Technical Conference* of the Society of Plastic Engineers #53, 54, and 55, for example.
54. J. Bonilla-Rios, Ph.D. thesis, Texas A&M University, College Station, 1996.
55. S. Wu, *Polym. Eng. Sci.*, 25, 122, 1985. A. Letton and W. Tuminello, *ANTEC Proc.*, 45, 997, 1987. W. Tuminello and N. Cudre-Mauroux, *Polym. Eng. Sci.*, 31, 1496, 1991.
56. Rheometrics Science. Discussion taken from information supplied by K.L. Lavanga.
57. Y. Liu and M. Shaw, *J. Rheol.*, 42(2), 267, 1998.

9 Unusual Conditions and Specialized Tests

Despite my expectations when I wrote the last edition of this book, the process in DMA has not moved to analyzers for nonlinear analysis. What has changed dramatically is the ability to handle nonstandard samples like powders and gels, and the ability to manipulate the environment of the sample by applying UV light or humidity, or immersing the sample in solvent. What were once specialized tests that required you to rebuild your instrument are now fairly routine applications. In addition, hyphenated techniques like DMA-FTIR and DMA-MS (mass spectrometry) have become more than just isolated curiosities and although they are not yet common, they are moving that way. In this chapter, we will take a look at these oddities that didn't really fit into the earlier chapters.

9.1 UV STUDIES

In Chapter 7, we mentioned that curing can be driven by irradiation as well as heat. Anyone who has had a cavity filled has seen an example of this. In DMA, it is very easy to track the development of mechanical strength during a cure, although one should not assume that the degree of cure tracks perfectly with that. Work by Stanbury and Newman suggests in some systems that direct monitoring of the cure by FTIR or Raman is also needed.¹ Photoreactions are not limited to curing and photodegradations can also be studied in the DMA. This is normally done as an accelerated aging test, with very high light intensities to minimize the instrument time needed.

When considering the study of photoreactions, we need to consider several variables outside of those of the DMA experiment. Depending on the exact DMA system you use, your choices of geometry may be limited. In the DMA 8000, for example, if you irradiate from the quartz viewing window in the standard furnace you can directly irradiate samples in the flexure modes and compression (if a custom quartz base is used). Tension and shear geometries will only get exposure to reflected light this way and gets only reflect light and a special transverse furnace is needed for them. Shear also requires special quartz fixtures. Whatever geometry is selected, one has to be concerned with the amount of energy that actually reaches the sample. This is a very easy task in a differential scanning calorimeter (DSC),² where a graphite target allows direct measurement of the energy in the pan. In DMA, one has to build a jig the holds a sensor to measure light intensity in the same location as the sample. Relative work can be done without this but a true measure of light intensity is needed to do kinetics.

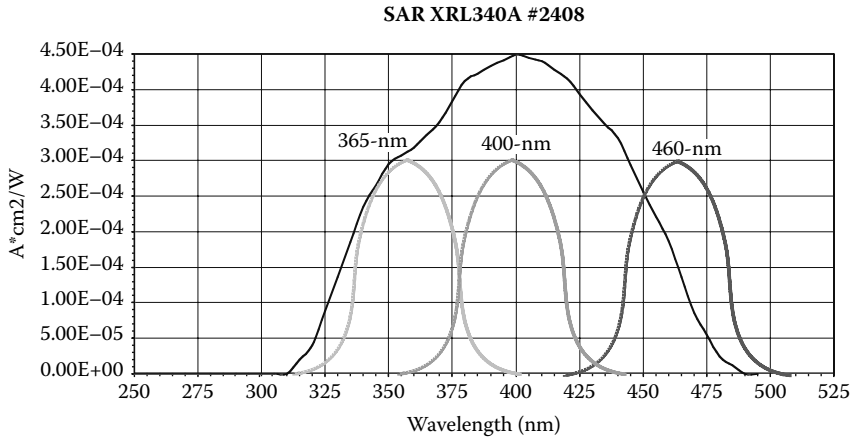


FIGURE 9.1 Spectral spread of three LED sources compared to a mercury lamp source. Used with the permission of Digital Light Labs, Knoxville, Tennessee.

Most people doing DMA work are not experts in spectroscopy and often neglect concerns we can call “quality of the light” issues. (Those of you who are, please stop shuddering and bear with me.) A beam of light has certain properties like breadth of frequencies around the stated frequency, intensity per frequency, how much it spreads out over a distance, and so on. These affect the delivered energy in various ways. For example, Figure 9.1 shows the spectra characteristics of some LED sources compared to a lamp. Note that none of the beams are purely the labeled frequency. There’s a range of light. Years ago I ran into a problem where a light source used with a photocuring reaction was changed and the reaction rate dropped dramatically. The original source had a wide frequency range around the nominal value and the new system, using filters, had a narrow bandwidth and cut off the frequency actually driving the cure. This is one reason many people prefer to test using the same type of system they use in production.

Another side effect of dumping light into a sample is that you also get heating. This is a much bigger effect than many realize. In photocalorimetry, the cooling systems are normally run all the time and hence the heating effect is compensated for. In DMA, especially near room temperature, this isn’t always true. Figure 9.2 shows the effect of UV irradiation on the temperature of a sample. This degree of heating actually causes a small dip in the modulus values due to the increase in temperature. Some sort of cooling system is needed whenever a DMA sample is irradiated. In addition, heat will be generated by the exothermic reaction of cooling. In degradation studies, where high intensity light is supplied for long times, it is vital to have enough cooling to keep the sample temperature stable.

Many samples used in photocuring require a supporting medium. In some cases, say quartz shear fixtures in the transverse furnace discussed earlier, it may not be needed but in many cases the material is painted onto or soaked into a carrier. This can affect the kinetics of the reaction. If painted on a metal shim for example, some localized heating can occur. One also has to consider the possibility of catalysis by the metal.

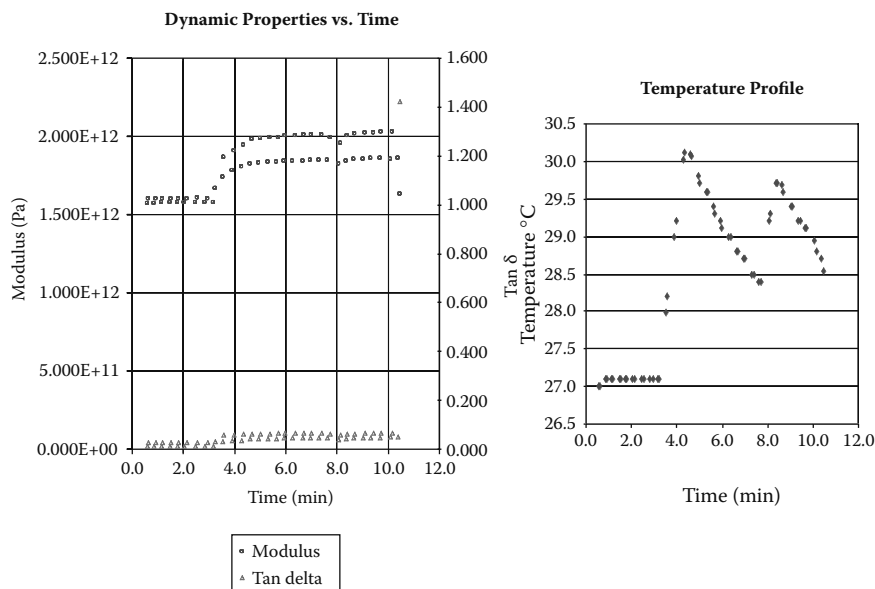


FIGURE 9.2 In photocuring, heat is generated by the lamp and can adversely affect data. The modulus data shows a drop where the light is pulsed for a second time. The temperature data shows spikes corresponding to the lamp being on. Note that recovery from the spike is slow. Efficient cooling is necessary in these runs.

Impregnating samples can also cause changes in the response due to either blocking some of the light, interactions with the curing system, and so forth. Normally this isn't always a problem but one needs to consider it lest you get unpleasantly surprised.

9.1.1 UV PHOTOCURES

Like thermal curing, photoexperiments can be run several ways: irradiation for a set period of time, a series of pulses of light, or a program of varying intensity. In addition, we can mix both photo and thermal programs so we vary both conditions. The classical photo-DMA experiment is a simple isothermal irradiation of the sample at one intensity and frequency at a fixed temperature.³ This is the experiment shown in Figure 9.3, where a sample of optically curing adhesive was coated on a metal strip and exposure to 50,000 mW of light for 5 seconds at 30°C. The sample cured completely. We can check that by either pulsing the light again for another 5 seconds and observing any change or by running a thermal cycle on the material and looking at the glass transition temperature. Under conditions where we use less intense light, we can see that more curing happens with more exposure as shown in Figure 9.4. With modern systems, it is possible to vary the intensity and time of the light during the cure. This allows the same type of control of the cure that temperature cure cycles do. One is able to reach a desired degree of cure with minimal residue stress in the product.⁴ This is important in a wide range of products as the residue stresses can cause distortion and/or brittleness in the cured material.

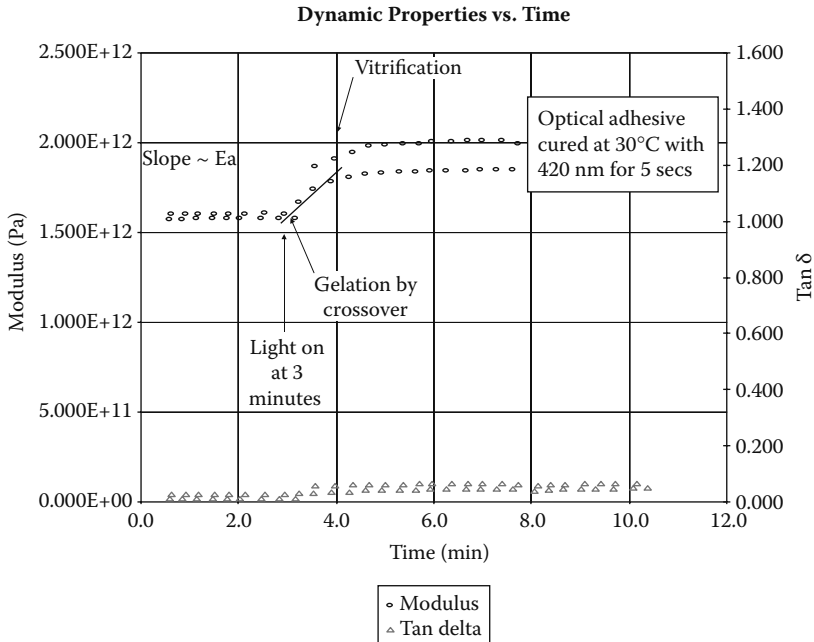


FIGURE 9.3 Photocure of an optical adhesive painted on a metal shim. The metal raises the modulus considerably.

One needs to remember the supporting media will have a large effect on the data in many cases. For example, in Figure 9.3, the modulus is never really low because the modulus of the steel support the adhesive was put on. In Figure 9.5, a similar material is cured under the same conditions but impregnated on a piece of paper. As can be seen, the modulus values are quite different starting with wet paper and ending with a solid. For the same sample, the gel and vitrification times are similar. Obviously the ideal conditions for kinetic studies would be an unsupported material. This can be done in shear using quartz fixtures using specially designed furnaces to allow transmission of the light. However, very reasonable results are obtained from supported materials and this is often much easier to run. The same analysis is used and the same types of kinetics developed as is done for thermal curing studies.⁵

9.1.2 UV PHOTODEGRADATIONS

One use of DMA has always been accelerated aging testing, normally using time-temperature superposition to estimate material properties to long times. Photo-DMA gives us the opportunity to monitor the modulus under the effects of light. Traditionally these studies were done using a sample exposed in a light chamber and then tested in DMA.⁶ Recently, adaptations of various analyzers to UV have allowed the entire experiment to be run in the instrument and this has been reported for High Impact Polystyrene (HIPS).⁷ These tend to be longer runs than curing studies, but the intensity of the UV available for various units is high enough we can see effects

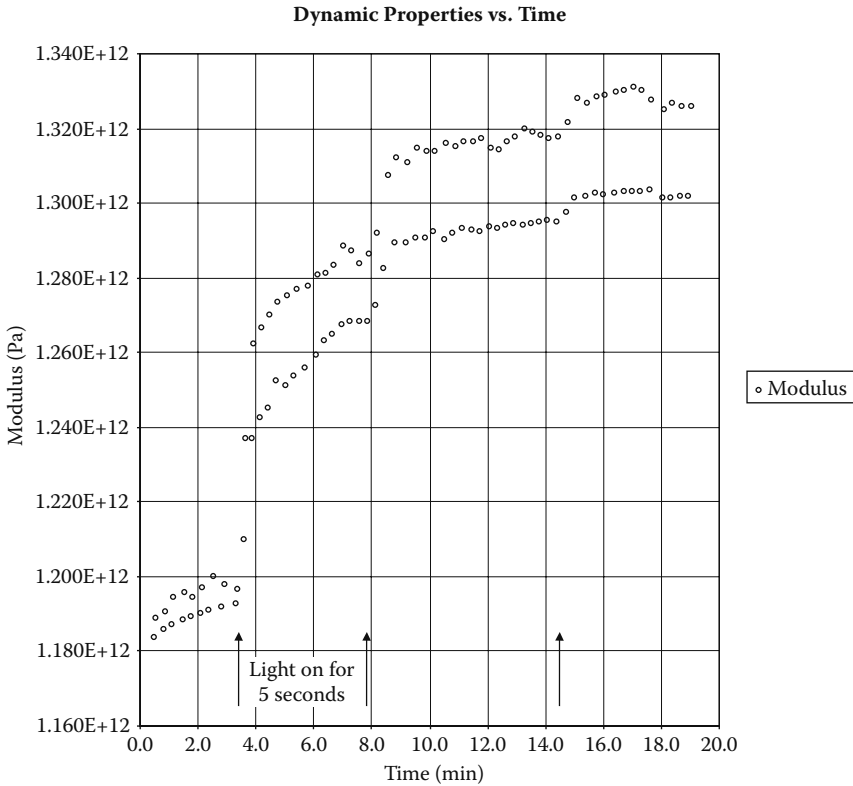


FIGURE 9.4 Lower light intensities may require multiple exposures to get full cures. This sample was run at 20% the intensity of the one in Figure 9.3. Three pulses were required to obtain a full cure. This is sometimes advantageous as it helps limit stress development in a sample.

in reasonable amounts of time. This has the advantage of letting us see how the changes occur and not just the results of UV exposure, as you would get if you aged the samples in a light chamber and then ran DMA. By using the combined approach, for example, we can see if the UV inhibitor fails slowly or all at once when exposed to long-term UV radiation.

9.2 HUMIDITY STUDIES

The effects of changes in the relative humidity on a sample can be quite pronounced. Hence, there is considerable interest in testing materials under controlled humidity. However, not all humidity generators are equal and it is important to consider some of the intricacies of the humidity system in setting up an experiment.

One of the most important of these is the location of the humidity sensor. Older humidity systems generated a gas of known relative humidity in a chamber and pumped it over to the DMA's sample chamber. If everything worked right, all of the

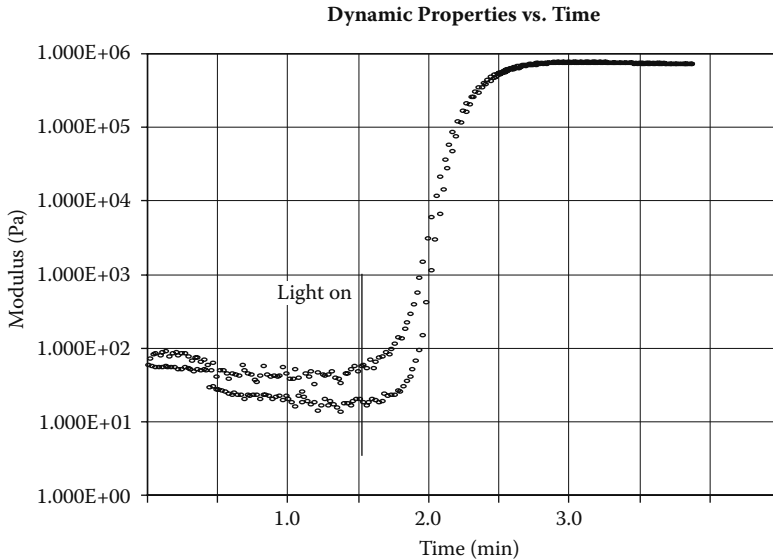


FIGURE 9.5 Optical adhesive soaked onto a piece of paper and then irradiated as in Figure 9.3. Notice the difference in the modulus values from the values in Figure 9.3.

temperatures matched, that is, you had the sample exposed to the right humidity. However, if something didn't work—for example the transfer line had a hot or cold spot, the sample chamber temperature was exactly the same, or there was variation in the chamber, the humidity can be very different from what you expect it to be. Even worse, you don't know the problem exists. The development of sensors that sit near the sample area and systems that control to the sensor's reading solved many of these issues.

These were fairly serious problems. We attempted to monitor the humidity in a DMA chamber at various points in a system where the humidity was generated in a chamber and pumped into the instrument. We did this by drilling holes into the lid and placing a humidity sensor at various points. We found considerable variation from the set relative humidity at the entrance and that the humidity varied across the chamber. Relative humidity has a strong temperature dependence and variations or drift in temperature can cause large changes in humidity as change heating too fast (Figure 9.6).

All this does assume that your relative humidity values are valid and that requires you to calibrate your sensors by some method. One method is using saturated solutions of various salts. By allowing the sensor to sit in a closed container over the solution in the vapor, one can then calibrate the sensor with two or more data points. Triton Technologies uses NaCl and MgCl salt solutions to calibrate their systems' sensors.⁸ Because of interest in desorption and adsorption studies, the ASTM has standards for generating constant humidity⁹ and a working group looking at humidity generation for thermogravimetric analyzer (TGA) studies.¹⁰

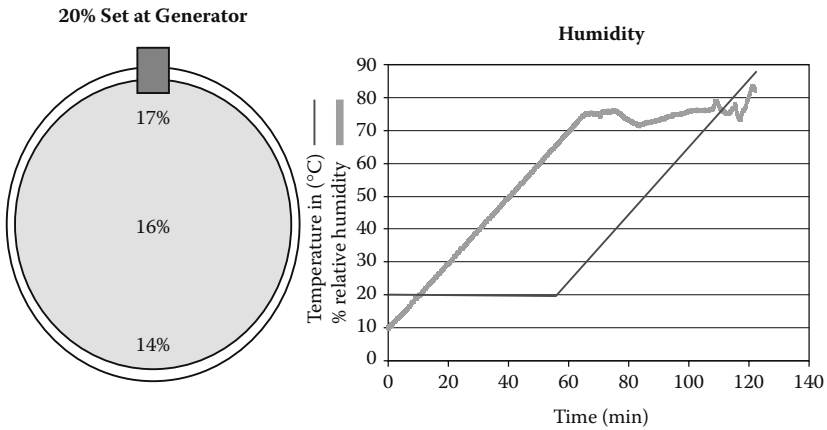


FIGURE 9.6 Humidity in a DMA furnace can vary substantially as is shown in schematic, and hence monitoring it directly at the sample is preferred. Temperature greatly affects the humidity and if temperature is ramped too quickly as shown here, the humidity generator may not be able to control it precisely.

9.2.1 EQUILIBRATION TIMES

Previously, we discussed that samples in the DMA need time to equilibrate with the furnace temperature internally. This normally limits both sample size and heating rate in the DMA. Similarly, equilibration is required in humidity levels and this is a slow process. It is important to allow long enough times for the sample to reach equilibrium. Figure 9.7 shows a sample of paper loaded in the DMA and its modulus tracked.

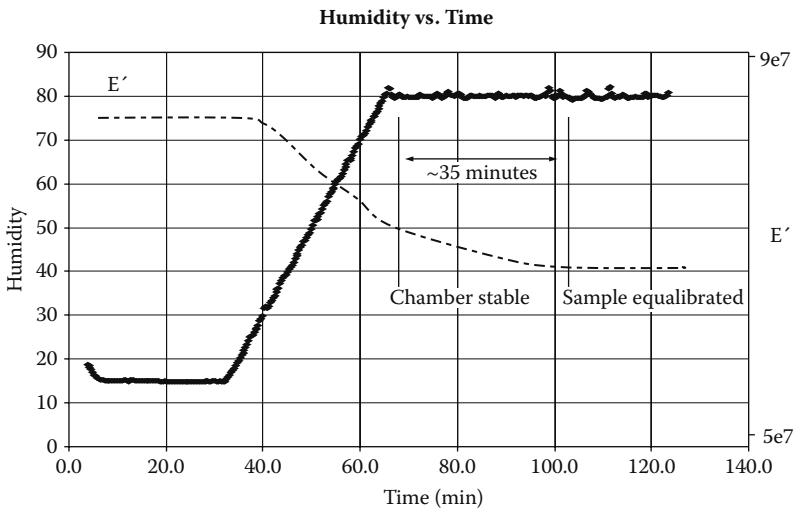


FIGURE 9.7 A strip of copier paper in the DMA was allowed to equilibrate. Note the delay from when the relative humidity stabilizes until the paper’s modulus stops dropping. Thicker and less porous samples take even longer.

The furnace chamber reaches a stable humidity after about 40 minutes but it takes another 35 minutes for the paper's modulus to stop changing. So even for a thin sample like a piece of paper, we need 75 minutes or more to have the sample in equilibrium.

9.2.2 EFFECTS OF HUMIDITY IN THE DMA

Anyone working with materials like paper, nylon fibers, or sugars is well aware that moisture levels cause changes in the T_g and the modulus values. Water is known to act as a plasticizer in polymers and most studies on the effect of water have involved soaking the material in solution or a humidity chamber and then running it under dry gas. Running the samples in humidity directly allows you to see how water changes the modulus as it is absorbed as well as the effects on the relative humidity level on final properties.

Examples of the effect of humidity are shown in Figure 9.8. In the first case, samples of dry tea leaves were loaded into a material pocket and allowed to equilibrate at 75% RH. It was then temperature scanned to measure the T_g . A second sample was tested at 40% RH. The second example shows the change in the sucrose T_g as a function of humidity. The third example shows nylon fishing line. A range of materials has been reported in the literature including cellulose films,¹¹ sunflower protein isolate,¹² Nafion™ 117 films,¹³ polyesters,¹⁴ leather,¹⁵ and polyurethanes.¹⁶

9.3 IMMERSION

Traditionally materials have been soaked in a solvent of interest and then run. This doesn't always give the desired results as can be seen in Figure 9.9. Early work with hydrogels required the samples be run in solution,¹⁷ as they dry out extremely quickly being in some cases over 90% water. As the capability to actually test in solution became known, it quickly spread to other industries. Many other materials are used while in contact with solutions and get exposed to various solvents during

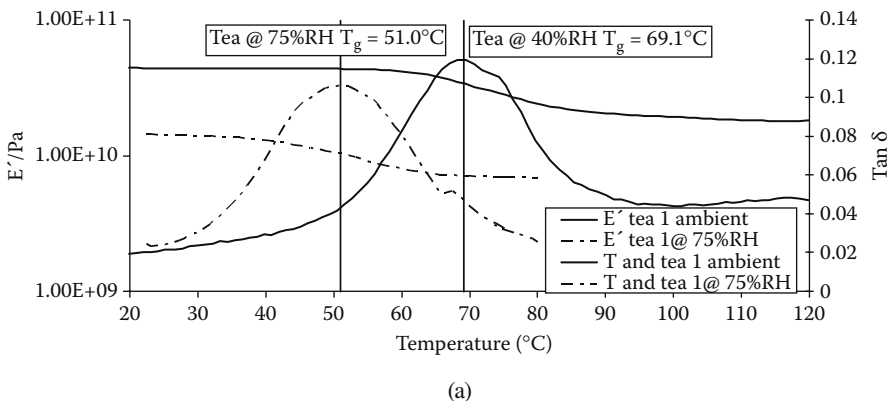
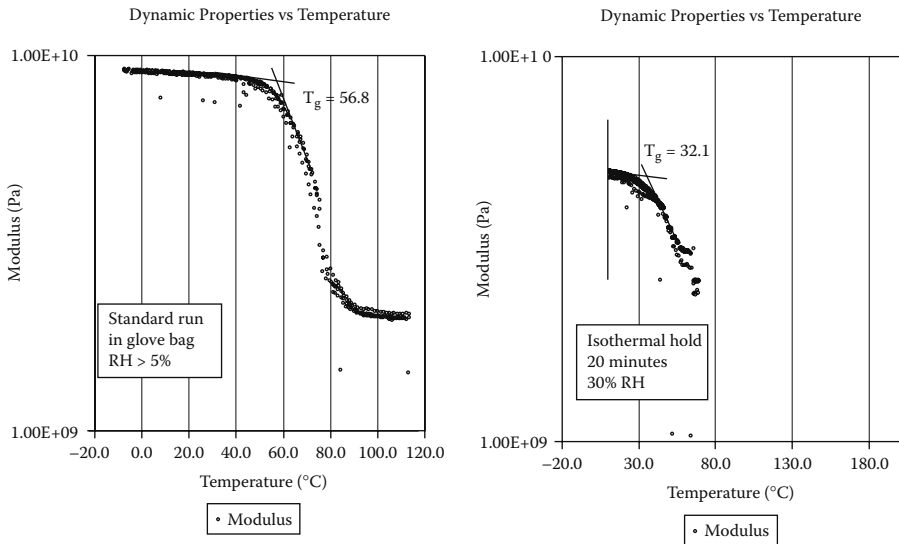
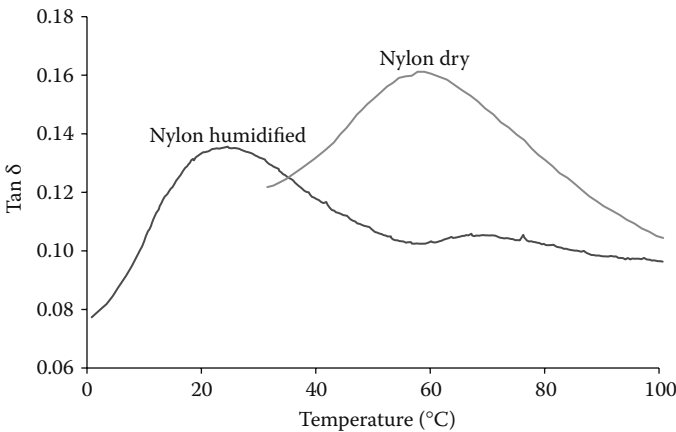


FIGURE 9.8 Examples of the effects of humidity on (a) a natural product, tea, (b) a sugar-excipient mixture, and (c) nylon fishing line. In all three cases, the increased relative humidity acts to plasticize the material.

Normal Run vs. Controlled Humidity in Material Pockets



(b)



(c)

FIGURE 9.8 (CONTINUED)

their service life.¹⁸ This interest has led to the development of instruments designed to handle solutions safely.

9.3.1 EFFECTS OF SOLVENT ON INSTRUMENTATION AND MEASUREMENT

Dealing with solutions in a DMA has several concerns that need to be addressed to not only get decent data but also to protect the instrument from damage. Certain instrument designs are more vulnerable to damage when working with solutions.

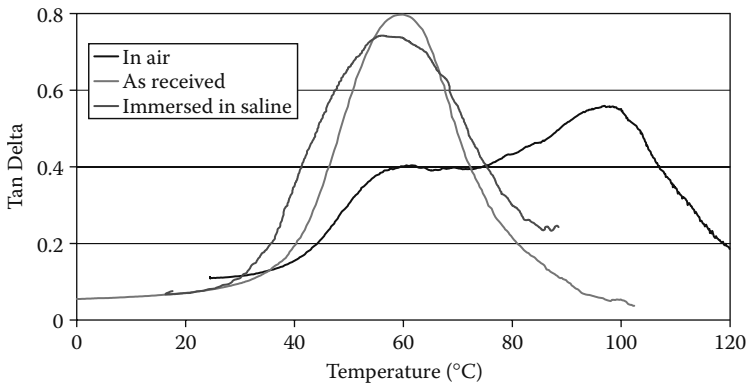


FIGURE 9.9 Epoxy paint run as a film in extension dry, immersed, and after soaking. In the soaked sample, a new peak appears that is not related to the material.

In designs where the analytical train is located under the bath, it is possible to destroy the instrument with a spill or leak. Equally important is the effect of the solution or its vapors on the fixtures and the instrument. For example, furnace liners made of aluminum have some advantages but are not suitable for work in highly caustic solutions. Similarly, the fixtures in all their parts must be resistant to the solutions used. Even low levels of corrosion can be harmful, especially if you have dissimilar materials in contact. Making a crude battery can cause depolymerization in certain systems, which can lead to interesting erroneous results.

Assuming the above concerns are addressed, there are also the effects on the inertia of the probe and the thermal lag of the solvent bath. Often referred to as floatation effects, the concern here is that the resistance of the solution to the movement of the probe or sample is much greater than that of a gas and hence the values measured for modulus are going to be high. This is a greater concern in some geometries than in others (Figure 9.10a) and the best way of confirming it is to run an inert sample in a solution and comparing that run with a similar one done in air. This is shown in Figure 9.10b.

Another concern is that of thermal mass and the heat capacity of the solvent. A solvent-filled bath has a lot of mass and requires a longer time to heat up if it is to be kept in relative equilibrium. This is a big concern on heating runs and heating rates of 1–2°C/min are as fast as you dare heat a large bath (see Figure 9.10c). Much of my own work is done at 0.5°C/min. Some researchers will use very small cups as baths to get around this slow heating but those are limited in both sample size and geometry. Cooling is even more difficult and long times must be allowed for temperature changes. All this thermal mass does help with isothermal runs that can be very stable if the furnace is properly tuned.

9.3.2 DMA IN SOLUTION

Figure 9.11 shows a DMA run on a sample of spaghetti run in a fluid bath with water as the solvent. As the water heats, the spaghetti softens. While this experiment does

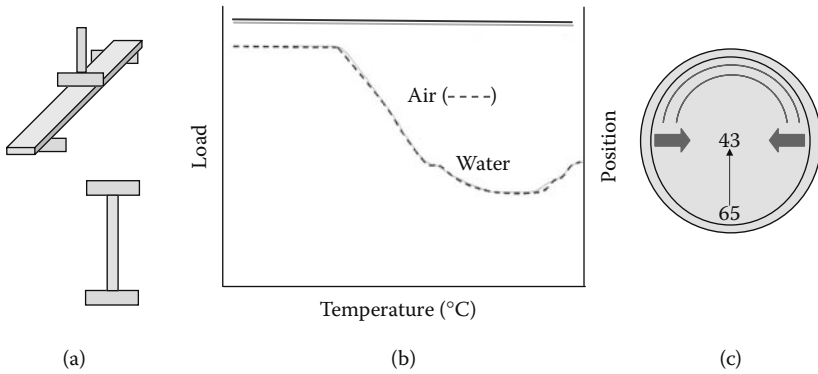


FIGURE 9.10 Sample orientation can affect your results. (a) For example, a sample in three-point bending has more surface area pushing against the fluid than the same sample in tension. (b) A good test is to run the sample in both air and a solvent that it is known to be inert to. Here a sample of monofilament shows no difference in air or water, as we would expect for the material. (c) Heat rates must be kept slow enough to maintain even heating to prevent problems like shown here.

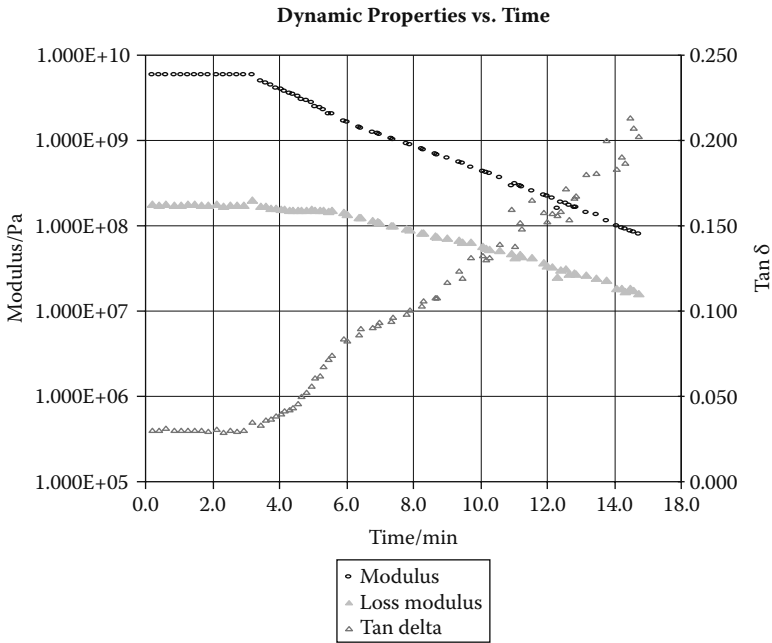


FIGURE 9.11 Pasta cooking in the DMA. A sample of commercial dry spaghetti was run in water. As the water warms, the starch absorbs water and softens.

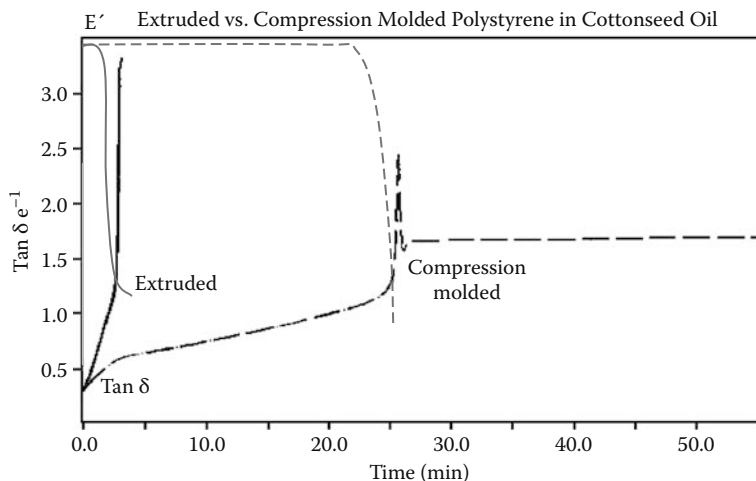


FIGURE 9.12 Immersed in cottonseed oil, the differences between extruded and compression molded polystyrene plaques is clearly seen.

not take it to al dente, it makes a nice example of the approach. In most cases, the solvent acts to plasticize the material as time and temperature increases. Studies of materials in solution are numerous¹⁹ and include polystyrene resistance to oil (Figure 9.12), dental materials, polyamide composites, epoxy films, fishing line (Figure 9.13), hydrogels tested in saline^a, fibers in solutions^b, collagen in water^c, and many others.

9.4 HYPHENATED TECHNIQUES

Several studies look at the idea of hyphenated DMA techniques. Two of the earliest approaches were DMA-DEA and DMA-DTA. A combined differential thermal analyzer (DTA) and DMA is surprisingly easy to develop. By simply having another thermocouple available that can measure the temperature of the sample as time, we can measure thermal changes in the material. We can then subtract the sample temperature from the furnace temperature, assuming no thermal lag, and get a simple delta T signal. Assuming we can do the necessary calibrations, we can now get both DTA and DMA data in one run.

The combination of dielectric analysis (DEA) and DMA is more interesting. DEA can be used to measure the dielectric constant under the right condition and it allows the application of very wide frequency ranges. DEA works by applying an oscillating electric current to a sample and measuring the effect on dipoles or

^a Q. Bao, *NATAS Proceedings*, 21, 606, 1992; J. Enns, *NATAS Proceedings*, 23, 606, 1999.

^b C. Daley and K. Menard, *SPE Technical Papers*, 39, 1412, 1994; C. Daley and K. Menard, *NATAS Notes*, 26(2), 56, 1994.

^c B. Twombly, P. Cassel, and A. Miller, *NATAS Proceedings*, 23, 208, 1994.

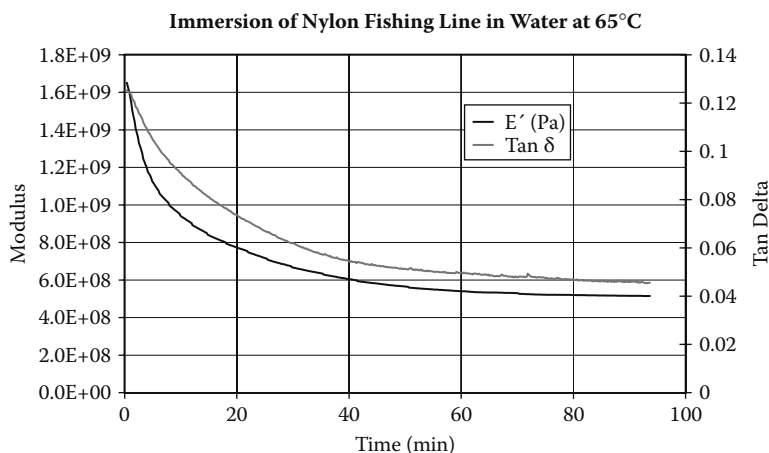


FIGURE 9.13 Many polymers are affected by water. Here nylon finishing line is soaked in a water bath and the modulus changes over time. Similar effects are seen in other polymers including medical grade polyurethanes.

induced dipoles in the material. It is a very powerful material analysis technique²⁰ and is used in aerospace quite a bit.²¹ Coupling with the DMA gains several advantages including the extended frequency range of DMA and sensitivity to material changes at the ends of the DMA's operating range.²² Most work with these systems has been done with curing and composites.²³

Coupling DMA to a spectrometer is actually a more useful exercise than the above. Using infrared, near infrared, or Raman spectroscopy to monitor chemical changes during a DMA run has the potential to greatly extend one's understanding of a material's behavior. Early work in combined rheological–optical methods was started by several companies and universities in the 1980s and optical rheology was fully presented in Fuller's book.²⁴ The use of combined DMA-FTIR has been reported for cellulose,²⁵ other wood polymers,²⁶ polyurethanes,²⁷ polyesters,²⁸ and other high polymers.²⁹ Both near infrared (NIR) and Raman have potential in this area that hasn't been exploited as of yet. To date, no commercial systems exist although the PerkinElmer DMA 8000 has a special transverse furnace with optical windows to permit these measurements to be made.

DMA has also been coupled to a Mass Spectrometer (MS) to study the degradation of nitrocellulose under both isothermal and temperature scanning conditions.³⁰ This combination of techniques has application in other cases where degradation of the material under mechanical or thermal stress can release products.

9.5 MODELING OTHER MECHANICAL TESTS

There exists possibly hundreds of specialized tests for polymer properties that developed to meet industrial needs in materials analysis. Some of these require specialized equipment or instruments and are not really adaptable to a DMA. Others are to

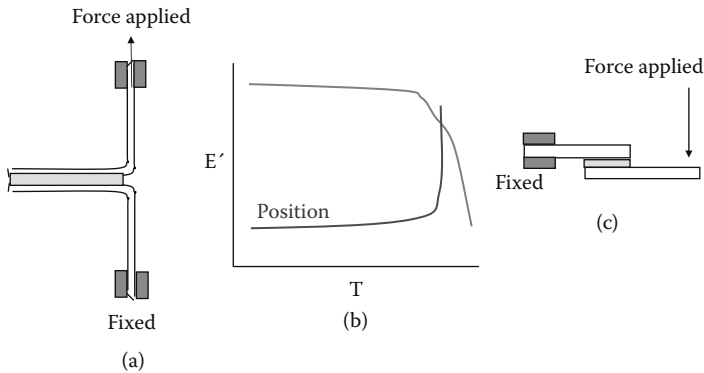


FIGURE 9.14 (a) T-peel and (c) lap shear specimens are shown with result (b). While a temperature scan under constant load is shown in (b), either experiment can also be run using a dynamic strain scan isothermally or under constant dynamic loading with a temperature ramp.

some degree. Several tests used with adhesives have been run in the DMA and I'd like to discuss three of those here as examples of exploiting modern instruments to get a better handle on material properties.

The measure of the tackiness of a prepreg is often done by some very strange tests that developed over time. An example is rolling a steel ball of known weight down a slope covered with the material. Tack has been measured in the DMA by using parallel plates. The plates are pushed firmly together and then the upward force increased, either continuously or dynamically, until they separate. Although not the most scientific test around, it gives decent values that can be correlated to actual performance.

Peel can be considered the inverse of tack. Although both tack and peel are discussed in Chapter 8, as the frequencies of the test are quite different and frequency scans can be used to compare the responses, a dynamic T-peel test has also been used. A sample of an adhesive can be used to make a small T-peel specimen and the specimen tested under either constant dynamic strain as temperature increases or by a dynamic strain ramp. Both modulus and position change at failure (Figure 9.14). The advantage of the small specimen is that evaluated temperatures are more easily obtained. Lap shear and other bond line failure tests can also be mimicked in the DMA with similar results.

NOTES

1. S. Newman, University of Colorado Dental School, private communication.
2. Graphite targets are disks of graphite used in power-compensated DSC to allow tuning the differences out of the light beam striking the two furnaces. See the PerkinElmer DPA manual for details.
3. T. Renault et al., *NATAS Notes*, 25, 44, 1994. H.L. Xuan et al., *J. Polym. Sci.: Part A*, 31, 769, 1993. W. Shi et al., *J. Appl. Polym. Sci.*, 51, 1129, 1994.

4. K. Menard, W. Chokaew, and W. Brostow, in preparation.
5. V. Litvinov and A. Dias, *Macromolecules*, 34, 4051, 2001. N. Emami et al., *Dent. Mater.*, 21, 977, 2005. R. Johnson, *SPE ANTEC Proc. V2*, 43, 186, 2003.
6. Y. Gao et al., *Polym. Degradation and Stability*, 91, 2761, 2006. D. Jia et al., *J. Polym. Res.*, 12, 473, 2005. S. Wang et al., *J. Appl. Polym. Sci.*, 89, 2757, 2003. A. Floui, *J. Phys.: Conf. Ser.*, 40, 118, 2006. K. Stovall et al., *RadTech Report*, August 2006. C. Saron and M. Felisberti, *Mater. Sci. Eng. A*, 370, 293, 2004. J. Pielichowski et al., *J. Thermal Anal.*, 43, 505, 1995. M. Amin et al., *J. Appl. Polym. Sci.*, 56, 279, 1995.
7. M. Felisberti and C. Saron, *Mater. Sci. Eng. A*, 370, 293, 2004.
8. *Humidity Controller Operator's Manual*, Manual Part Number: T100510B, Triton Technologies, Keyworth, UK, 2006, p. 21.
9. *ASTM E104-02 Standard Practice for Maintaining Constant Relative Humidity by Means of Aqueous Solutions*, ASTM International, West Conshohocken, PA, www.astm.org.
10. *ASTM WK9142 New Humidity Calibration of Humidity Generators for Use With Thermogravimetric Analyzers*, ASTM International, West Conshohocken, PA, Pennsylvania, www.astm.org.
11. I. Yakimets et al., *Mech. Mater.*, 39, 500, 2007.
12. A. Rouilly et al., *Polym. Eng. Sci.*, 46, 1635, 2006.
13. F. Bauer et al., *J. Polym. Sci. Part B: Polym. Phys.*, 43, 786, 2005.
14. G. Foster et al., *J. Thermal Anal. Calorimetry*, 73, 119, 2003.
15. S. Jeyapalina et al., *J. S. Leather Technologies Chemists*, 91, 102, 2007.
16. R. Broos et al., *J. Cell. Plast.*, 36, 207, 2000.
17. R. Smith et al., *J. Mater. Sci.: Mater. Med.*, 7, 957, 1996. J. Harmon et al., *Polymer*, 44, 207, 2003. M. Cascone et al., *Polym. Int.*, 50, 1241, 2001. A. Alvarez et al., *J. Composite Mater.*, 40, 2009, 2006.
18. A. Lopez et al., *J. Thermal Anal. Calorimetry*, 47, 1388, 1996. V. Karbhari et al., *Composites Part B: Eng.*, 35, 299, 2004. R. Brereton et al., *The Analyst*, 131, 73, 2006.
19. J. Sosa and K. Menard, *NATAS Proc.*, 25, 176, 1995. C. Daley et al., *NATAS Notes*, 26(2), 56, 1994. J. Rosenblatt et al., *J. Appl. Polym. Sci.*, 50, 953, 1993. E. McKaque et al., *J. Test. Eval.*, 1(6), 468, 1973.
20. S. Havriliak and S. J. Havriliak, *Dielectric and Mechanical Relaxations in Materials*. Hanser, Cincinnati, OH, 1997. D. Melotik et al., *Thermochimica Acta*, 217, 251, 1993. H. Block and S. Walker, in *Developments in Polymer Characterization*, J. Dawkins, Ed., Academic Press, New York, 1980, ch. 3. N. McCrum et al., *Anelastic and Dielectric Effects in Polymeric Solids*, Dover, New York, 1967, ch. 2 and 3.
21. R. Hinrichs, *Engineered Material Handbook*, ASTM, Philadelphia, 1, 649, 1987. N. Sheppard et al., *Technical Report 4/NR-039-260 Dielectric Analysis of Thermoset Cure*, Office of Naval Research, Arlington, VA, 1985. R. Hinrichs, *Engineered Material Handbook*, ASTM, Philadelphia, 1, 761, 1987. N. Roberts et al., *SAMPE Proc.*, 34, 373, 1989.
22. B. Twombly and D. Sheppard, *North American Thermal Analysis Society Proc.*, 23, 704, 1994. B. Twombly and D. Sheppard, *Thermochimica Acta*, 272, 125, 1996.
23. J. Suwardie, *ASTM ST 1402 Materials Characterization by Dynamic and Modulated Thermal Analytical Techniques*, 2001, p. 131.
24. G. Fuller, *Optical Rheology of Complex Fluids*, Oxford University Press, Oxford, UK, 1995.
25. B. Hinterstoisser and L. Salmen, *Cellulose*, 6, 251, 1999. B. Hinterstoisser and L. Salmen, *Vib. Spectrosc.*, 22, 111, 2000.

26. M. Akerholm and L. Salmen, *Polymers*, 42, 963, 2001.
27. H. Wang et al., *Macromolecules*, 35, 8794, 2002. H. Wang et al., *Macromolecules*, 34, 7084, 2001. R.A. Palmer, *AIP Conf. Proc.*, 503, 31, 2000.
28. S. Markovic et al., *J. Appl. Polym. Sci.*, 81, 1902, 2001.
29. R.A. Palmer, V.G. Gregoriou, and J.L. Chao, *Polym. Prepr.*, 33, 1222, 1992.
30. S. Vyazovkin et al., *Macromol. Rapid Commun.*, 26, 29, 2004.

10 DMA Applications to Real Problems

Guidelines

This chapter was written at the request of many of the students in my DMA course asking for a step-by-step approach to deciding which type of test, what fixtures, and what conditions to use. The following was developed to formalize the process we go through in deciding what tests to run. The process is shown in flow sheets in Figures 10.1, 10.2, and 10.3.

10.1 THE PROBLEM: MATERIAL CHARACTERIZATION OR PERFORMANCE

The first question that has to be asked and often isn't is "What are we trying to do?" There are two basic options: one could characterize the material in terms of its behavior or one can attempt to study the performance of the material under conditions as close to real as possible. Several things need to be considered. First, what do I need? Do I need to understand the material or to see what it behaves like under a special set of conditions? If I am interested in performance, is it even possible to test or model those conditions? Sometimes it isn't. Airbags open at about 10,000 Hz and no mechanical instrument generates that high a frequency. To reach that frequency, we would need to use dielectric analysis (DEA) or superposition data. So if we want to model this process, some data manipulation is needed. Otherwise, we can characterize the material at a few frequencies and use the average of a 5°C shift per decade to estimate the values at that frequency. However, unless we consider and can state a precise question, we are running tests for no real reason. This isn't to say we never do exploratory tests, but even there we need to know what we are looking for.

10.2 PERFORMANCE TESTS: TO MODEL OR TO COPY

The reason for running a performance test is to collect data under conditions that duplicate or approximate use. This is often done when one knows what material works, but is unsure of what material parameters make a good material good. In many mature industries, a material is optimized by trial-and-error over many years and no laboratory test was used to study it. Sometimes, the end use conditions are so complex or require the interaction of so many variables, you don't trust a characterization approach to give you useful information. And sometimes we just want to see how something will work.

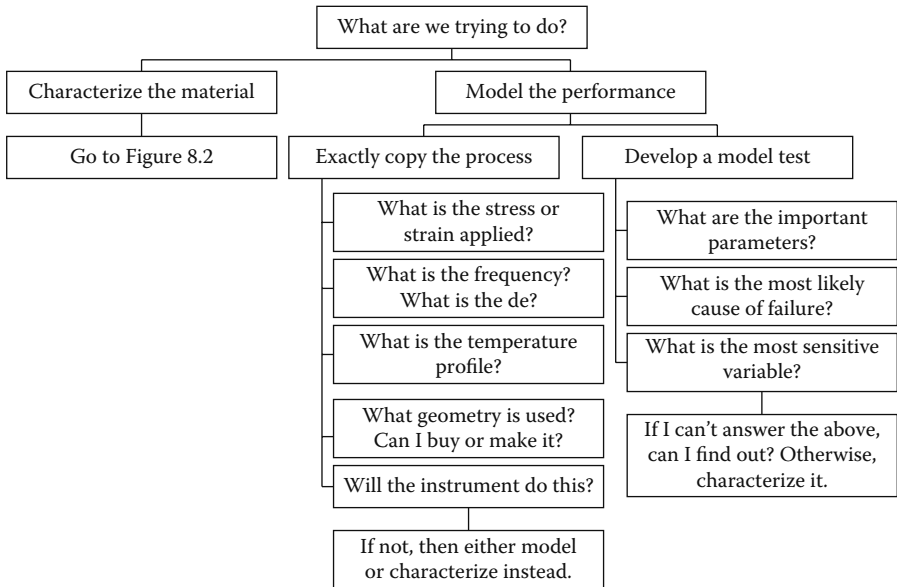


FIGURE 10.1 Choosing a DMA test method requires deciding whether you want to characterize the material, copy the process, or evaluate a model for significant properties.

One approach is to carefully measure the stresses, the frequency, the temperature range and changes, and even the wave shape of the process. One then applies as exact a copy as one can and records how the material responds. This approach has some problems as the time scale or the frequency may be outside of the instrument's limit. It also requires a high degree of understanding of the process so you copy the key step.

In order to avoid the difficulty of matching the process, many people or industries pick a performance test that either roughly models real life or should give similar results. Some of these are excellent, backed by years of experience and knowledge, while others are poor models that are used because they always have been. For this approach, standard sets of highly controlled conditions are chosen to test representative performance. Table 8.1 gives a list of the tests performed in most DMAs and how they can be used to represent certain processes.

10.3 CHOOSING A TYPE OF TEST

What type of test do we choose? The test needs to reflect the type of stress the material will see, the frequency at which this is applied, the level of stress or strain, and the sample environment. First, it is helpful to know what the stress, strain, and strain rate are for the process. This will be needed to see how the material acts. How fast are the stresses applied to the material, are the stresses steady (or constant), increasing, decreasing, or oscillatory? If the stresses are oscillatory, are they sinusoidal, stepwave, or something else? How large are they and how fast are they applied?

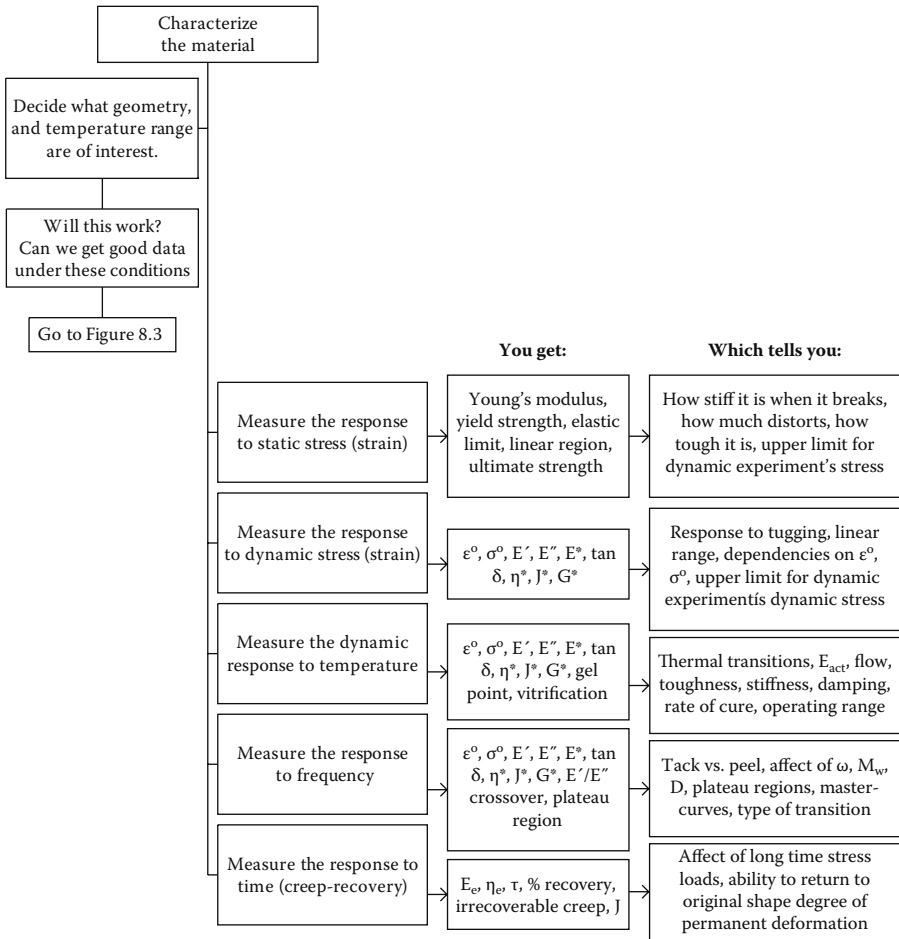


FIGURE 10.2 Characterizing a material allows you to gain a tremendous amount of information on it. Notice humidity, immersion, atmosphere, and irradiation are not mentioned. These are applied to a sample after geometry and method are chosen. A properly designed instrument for this type of work shouldn't limit either due to the use of a special environment.

Once the types of stresses or strains are defined we can choose from the tests listed in Table 10.1.

The temperature is the next question. This needs to include any heating or cooling the sample would see. Even something like baking a cake has a temperature ramp as the material comes to equilibrium in the oven. Often the material will see heating and cooling cycles that may change the forces applied to it (see compression set discussion in Chapter 3). The thermal cycle we choose should copy these changes. Sometimes we find that the time at a set temperature is less important than the getting to and from it. Other times, it is the exposure of the material to a specific gas at an elevated temperature that causes the problem and we may need to use gas switching.

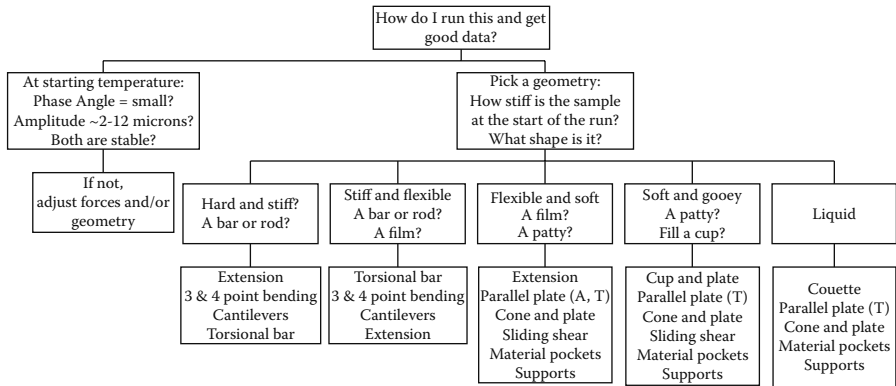


FIGURE 10.3 Some general guidelines for selecting the proper test geometry. Depending on the sample size, the strain level, and the instrument type, there may be some variation.

The shape of the stress wave is important and can vary considerably. For example, brushing hair (and modeling the degradation of hair spray) can be seen as a square wave, a heartbeat is a composite wave, and vibration can often be a sine wave. The sinusoidal wave works for a lot of processes, but for very nonlinear materials, like those used in some biomaterials, it helps to match the wave shape as closely as possible. People working with heart valves and pacemakers often desire complex waveforms that closely match those of the heart itself.

10.4 CHARACTERIZATION

The alternative to performance tests is to characterize the material as fully as possible. This has the advantage of picking up differences that are not readily seen in the test designed to measure performance. These differences might affect a material during long-term use or change how fast it degrades. In addition, since we will try to relate the tests to various molecular properties and processing conditions, this approach allows us to understand why materials are different and how to tune them.

10.5 CHOOSING THE FIXTURE

The type of fixture you pick is driven by the modulus of the material, the form it is in, and the type of stress the material experiences in use. Certain forms, like fibers and films, suggest certain fixtures, like extension in this case. This is not always true. Sometimes a very thin sample can be handled in extension, three-point bending, or dual cantilever. The choice can then be made on several grounds. I prefer to pick the fixture that is the easiest to load and gives the most reproducible data. Another argument will be to use the fixture than gives the cleanest type of deformation. Yet another is to use one that is similar to the real-life stress of the material. This sometimes requires making a specially shaped geometry, like a pair of concentric spheres to model the eye for contact lenses. Any one of these techniques will work depending on how the problem is approached.

TABLE 10.1
Test Methods Used in the DMA by Mode of Operation, Giving the Data
Calculated from the Test and What it Means

Test	Result	What it Tells You
Thermomechanical analysis	Changes in slope	Transition temperature
	Slope of curve with temperature	Thermal expansivity or CTE
	Change in volume (dilatometry)	Shrinkage on curing, volumetric expansion
Static stress-strain	Slope	Young's modulus
	Yield point	Strength before distortion
	Yield strength	Load capacity
	Proportional limit	End of linear region (max. F_T)
	Ultimate strength	Strength at breaking point
	Elongation at break	Ductility
	Area under curve	Toughness
Dynamic stress-strain	Dynamic proportional limit	End of linear region (max. F_D)
	Storage, loss modulus	Stiffness as function of load
	Tan δ	Damping
	Ultimate strength	Strength at break by tugging
Creep-recovery	Equilibrium compliance, modulus, equilibrium	Long-term behavior
	Viscosity	Extensional viscosity
	Creep compliance	Effect of load
	Creep rupture	Strength
	Relaxation spectra	Molecular modeling
Stress relaxation	Compliance and modulus	Long-term behavior, MW, crosslinks, and entanglements
	Retardation spectra	Molecular modeling
	Force as a function of temperature	Shrinkage/expansion force
Dynamic temperature/time scan	Storage and loss modulus	Change in stiffness, mapping modulus
	Complex viscosity	Change in flow
	Tan δ	Damping, energy dissipation
	Temperature of transitions as drops or peaks	$T_M T_g T_\alpha T_\beta T_\gamma T_\delta$
	Modulus of rubbery plateau	Molecular weight between crosslinks, entanglements
	Crossover of E' and E'' on curing	Gel point
	Shape of viscosity curve on curing	Minimum viscosity, E_{act} , vitrification point
Dynamic frequency scan	Complex viscosity, loss modulus	Flow as function of frequency

(Continued)

TABLE 10.1 (CONTINUED)**Test Methods Used in the DMA by Mode of Operation, Giving the Data Calculated from the Test and What it Means**

Test	Result	What it Tells You
	Storage modulus	Elasticity or stiffness as function of frequency
	E'/E'' or η^* crossover	Relative MW and D
	Plateau regions	MW estimation
	Master curve	MWD, long-term behavior, wide range behavior, molecular modeling

Table 10.2 lists the common fixtures and the type of samples for which they are most commonly used. Normally, just flexing the sample between your fingers will lead you to decide the appropriate fixture and the approximate force range. However, you can always check this by loading the sample in the DMA and applying an arbitrary load for 30 seconds. Depending on the modulus value you see, you can then select the most desirable fixture. Some of this is intuitive: stiff hard samples go into three-point bending, rubbery samples into parallel plates, and fluid ones into cups.

TABLE 10.2**Samples and Fixtures: A Quick Guide to Choosing a Geometry Based on the Way the Sample Looks at RT**

Very hard	Three-point bending (large)	Goopy	Various parallel plates
	Four-point bending (large)		
	Single cantilever		
Hard	Three-point bending (large)	Fluid	Cone and plate
	Torsion bar		
	Single cantilever		
Stiff and flexible	Three-point bending (medium)	Film	Couette
	Torsion bar		
	Single cantilever		
Pliable	Three-point bending (medium)	Fiber	Extension
	Dual cantilever		
	Torsion bar		
Soft	Three-point bending (small)	Suspension	Parallel plate
	Dual cantilever		
	Torsion bar		
Very soft	Dual cantilever	Powder	Cone and plate
	Axial parallel plates		
	Torsion bar		

Note: Large deviations in temperature from ambient will change things.

10.6 CHECKING THE RESPONSE TO LOADS

Besides being a more accurate method of determining how hard a material is for picking test conditions, the response of a material to a load measured as either stress or strain is one of the most basic studies. For solids, a stress–strain curve lets us see the region of linear behavior, the amount of force needed to make the sample yield, and the force needed to break it. This test allows one to see how a sample responds to a load. However, samples that will be held under loads often need to be tested by creep, as there will usually be time dependence in the response. Similarly, on fluids and liquids, we need to check the strain rate response to be sure we are in the linear region.

10.7 CHECKING THE RESPONSE TO FREQUENCY

As discussed at length in Chapter 8, all materials exhibit some sort of response to the frequency of testing. The frequency of testing affects the temperatures of transitions as well as the modulus and viscosity of the material. Three approaches are normally used to pick the frequency of the test: (1) use an arbitrary number for all tests (1 Hz and 10 rad/sec are common), (2) measure your process's shear rate and pick the corresponding rate for testing, and (3) run a frequency to pick a testing frequency. One can ideally pick a frequency on the zero-shear plateau, but often these are too low to be useful. The frequency normally ends up in the power law region due to instrument limits.

The third approach is also a good idea even if you have already decided to use one of the first two. How quickly the viscosity and elastic modulus change with frequency is very important for knowing how the material will respond. One needs to remember that frequency and temperature effects overlap and that frequency effects need to be studied at the temperature or in the temperature range of interest. In addition, the frequency response will help you classify transitions. Most instruments make it fairly easy to do a two or three frequency temperature scan and this allows a quick look at how the material responds at various transitions.

10.8 CHECKING THE RESPONSE TO TIME

Under this heading, we want to make sure that the material is first stable under the testing conditions. This is done by loading the sample at the chosen forces, frequency, and temperature. We should be seeing a level of deformation and percent strain under 0.5%. The sample is then held for 1–5 minutes under these conditions and $\tan \delta$, E' , and E'' are examined. If an upward or downward trend is seen, it means the material is changing as a function of the test conditions. This can be due to extremely long relaxation times or to being out of the elastic limits. One approach would be to remove the testing forces and let the material relax after mounting to see if that helps. Creep–recovery testing is also done to examine the relaxation response.

Another point of this test is that any mechanical or environmental noise in the vicinity will be seen in the test. This allows us to find and remove sources of error that have nothing to do with the test. A lot of the oddities in data are caused by environmental effects, including mechanical vibration, impure gases, poorly controlled

Best choice	Sample modulus /Pa	Preferred geometry (for indicated sample size)	Sample thickness /mm	Free length /mm	Ideal Heating /cooling rate /°C/ min
	10^{10} to 10^6	Tension	<0.02	2	5
X	10^{10} to 10^5	Tension	0.02 to 1	2 to 10	5
X	10^{10} to 10^6	Single cantilever	1 to 2	5 to 10	3
X	10^{10} to 10^6	Single cantilever	2 to 4	10 to 15	2
	10^{10} to 10^6	Single cantilever	>4	15 to 20	1
X*	10^{10} to 10^6	Dual cantilever *for highly orientated samples that are likely to retract above T_g	2 to 4	10 to 15	2
X	10^{12} to 10^8	Three-point bending	1 to 3	10 to 20	3
	10^{11} to 10^7	Three-point bending	>4	15 to 20	2
X	10^7 to 10^2	Simple shear	0.5 to 2	5 to 10 (dia)	≤ 2
	10^7 to 10^2	Compression good for irregularly shaped samples and any others that are difficult to mount	0.5 to 10 (height or thickness)	5 to 10 (dia)	≤ 2
width	Generally sample width is uncritical and 5 mm is recommended (a wider sample may not be held uniformly in the clamps). A smaller value should be used for stiff samples in tension (1 to 2 mm).				

FIGURE 10.4 Modulus and geometries for the DMA 8000. This example shows how modulus and sample dimensions lead one to select certain geometries. Note as sample size increases the suggested heating and cooling rates decrease. Used with the permission of PerkinElmer LAS, Shelton, CT.

gas rates, improper cooling, or noisy power. All of these sources of error must be eliminated before a test can be considered valid.

As mentioned earlier, creep–recovery testing is also done to see how time affects the polymer. This is done to determine the linear region for creep–recovery curves and to measure relaxation times. One first applies creep stresses to the sample in increasing amounts and plots this as compliance, J , versus time. In the linear region, J becomes independent of the stress so the curves overlay. A fast way to check this is to start at very low stresses and increase it by doubling the stress for each run. When the strain stops doubling, we are out of the linear region.

10.9 CHECKING THE TEMPERATURE RESPONSE

Using the information from the response to time, we now check the response of the material to temperature by running a temperature scan. One normally scans the widest range possible within instrumental limits. The end of the linear region from the static stress–strain curve tells us the maximum total force and the maximum from the dynamic stress–strain run tells us the maximum dynamic force. Then, we pick a dynamic force strong enough to give us a strain between $2 \mu\text{m}$ and $12 \mu\text{m}$. If we are running a solid sample, we adjust the static or clamping force to keep the specimen in good contact with the probe. For a hard glassy sample in three-point bending, this is normally 110% of the dynamic force. As the sample becomes softer and more

rubbery, this increases as necessary. For fluid samples in a torsional rheometer, we set the gap to where the sample is able to keep a smooth edge. Obviously for some geometries like the cone-and-plate, the fixture is designed to run at a fixed gap.

We adjust the positioning of the solid sample to get as low a phase angle as possible at those stresses. (Remember we are concerned about the stress, not the force.) This is especially important in cantilever and extension geometries where it is easy to misalign the specimen. The specimen needs to be set up at the lowest temperature, otherwise the forces may not be sufficient. The sample is then run at a heating rate slow enough to give even heating to the specimen. This should allow one to identify the transitions of the material. It is not uncommon to need multiple runs or special control to collect all these data, as some materials will change so much at the T_g that the specimen will fail.

10.11 PUTTING IT TOGETHER

Now that we have collected the data, we need to apply the analysis given in the previous chapters to determining what it means for our sample. We should now be able to determine the linear region, the effects of temperature, stress, and frequency, and how time dependent the material is. In addition, we should be aware of where transitions occur and to what of type of behavior they correspond.

10.12 VERIFY THE RESULTS

So how do we know that the data are good? Calibration and operation should have been checked long before reaching this point, although in the case of an unexpected result, they can be checked after the run. All of the tests should be run in triplicate (at least) to be sure that the numbers are real. Things happen. We can then use the data to check for material variations and operator errors.

The data then need to be examined for inconsistencies and abnormalities. I normally look at five charts when doing this:

1. The method used
2. A plot of storage modulus, loss modulus, and $\tan \delta$ versus temperature
3. A plot of program temperature and actual temperature versus time (If I've done a humidity run, I'll plot humidity here. Often you don't really need the program temperature, as actual temperature versus time will normally show any unexpected differences.)
4. A plot of amplitude and phase angle versus temperature or time (I often blend it with chart 3.)
5. A plot of probe position, static stress, and dynamic stress versus temperature

These are used as follows:

If I am going to be performing a time-temperature superposition (TTS), I'll look at a Wicket or Cole-Cole plot, too. I normally separate my frequencies if they are not already. Often bad data points are frequency specific because you chose too high a frequency.

So looking at the data, the method used and the plots of E' and $\tan \delta$ are examined to look at transitions and material behavior. The method is checked to make sure what was supposed to be run was actually programmed. Were the stresses or strains correct? Was the right temperature range chosen? Were the forces actually applied to the sample? The data is checked to see if the transitions and behavior of the material make sense. Are there any sharp drops or abrupt changes that suggest an electronic, mechanical, or sample-related problem? Does the sample seem to randomly change length in a step? Does the E' and E'' differ from that recorded from previous samples? If so, is the $\tan \delta$ different, too? If E' and E'' are changed but $\tan \delta$ hasn't, check the stresses and strains. Do they match up correctly? Did we mismeasure the sample?

The temperature plots are used to confirm that the analyzer did what was asked of it and that it stayed in control. Sometimes, due to sample mass or heating rate, the sample temperature will not track the programmed temperature and the data are then suspect. Are there loops in the temperature data suggesting furnace instabilities, variations in gas flow, or ice dropping on the thermocouple, which happens occasionally in subambient runs under high humidity? If it's a humidity run, did the humidity have time to stabilize?

The plots of probe position, forces, and raw signals (amplitude and phase angle) are examined for abnormalities. Does the probe position show any sharp changes that suggest sample slippage or movement? Did the stresses behave as expected? Do the raw signals appear to match the data? Does the Wicket plot show a nice curve or does it have humps and shoulders? If the latter, this means that the Williams-Landel-Ferry (WLF) conditions aren't met and we need to worry about the TTS. If the TTS is done and the data doesn't overlay, what risks are we taking? Any discrepancies need to be explained.

It is also advantageous to examine the sample after the run. Does it show marks from excessive clamping force? Is there evidence of distortion or deformation? Does it weigh the same as it did originally? Has its appearance changed? Can these changes have generated spurious transitions in the spectra?

Finally, we need to ask is this response a real event, environmental noise, or abnormality? Does the material do this consistently? Is the material variation so great that the sampling will determine the results? Unfortunately, many rheological and thermal tests seem to be done only once; at least three samples should be run to confirm that the data is correct. In addition, the normal statistics of sampling and data analysis need to be followed.

10.13 SUPPORTING DATA FROM OTHER METHODS

DMA does not always represent the best way to analyze a sample. Some changes that influence the DMA spectrum are more easily studied by other methods. For example, changes in degree of crystallinity can be measured in the differential scanning calorimeter (DSC) in one run.¹ Activation energy, degree of cure, and kinetics can also be studied in the DSC. Vitrification shows up in the C_p curve from StepScan.² Losses of water, decomposition, filler levels, and the presence of antioxidants can also be seen in the thermogravimetric analyzer (TGA)³ or in one of its hyphenated

variants.⁴ FTIR is also an excellent way to investigate questions about composition.⁵ DEA allows detection of curing past the DMA's instrument limits (both upper and lower) for thermosetting systems.⁶ Information from alternative methods is a vital part of the analysis of a material and it is foolhardy to limit one's approach to DMA (regardless of how much fun it is to use) or any other instrument.

10.14 APPENDIX: SAMPLE EXPERIMENTS FOR THE DMA

Before running any experiments on a DMA, it is important to check that it is properly set up and calibrated. For example, the purge gas type, the purge gas rate, the cooling system, the last date of calibration, and the last verification tests should be checked. After assuring the instrument is ready to run, the following series of experiments will help you gain experience on how your instrument operates.

10.14.1 TMA EXPERIMENTS

A baseline should at least also be run on the empty fixtures and ideally a known standard should be used to calibrate out the expansion of the fixtures. A sample of polystyrene⁷ 10 mm long should be run under a maximum of 50 mN load in nitrogen purge from 25°C to 125°C at 5°C to determine the T_g and the coefficient of thermal expansion (CTE). One could also do:

- A small bar run with a knife-edge probe in three-point bending to determine the T_g
- A small slab run with a 0.5 mm probe in penetration to determine the T_g

After these three runs, compare the effect of the method on the T_g and the range of the region of the transition.

10.14.2 STRESS–STRAIN SCANS

For a small bar of nylon 66 and another of PPS, set up in single cantilever, a stress ramp is applied from 0 to 2000 mN of static load at 100 mN/min ramp rate. For one specimen, repeat this experiment three times on the same sample. Also run a sample under two additional ramp rates (i.e., 200 and 400 mN/min). These should all be done at room temperature. Display the data so you can see the effect of ramp rate and multiple ramps on a sample. Calculate the initial slope of the stress–strain plot to obtain the modulus.

10.14.3 CREEP–RECOVERY EXPERIMENTS

Using a rubber Gas Chromatograph (GC) septum or disk of butyl rubber, set up a simple creep experiment at 40°C under nitrogen purge. Using a small, even recovery force such that the material shows no creep, run an experiment where 200 mN is applied for five 1-minute cycles with 3 minutes of recovery time between cycles.

Compare the first and the last cycles noting differences in percent recovery. Repeat with 1000 mN creep load and again at 80°C.

10.14.4 STRESS RELAXATION

Using the necessary controls, load a single 10 mm long polypropylene (PP) fiber (common fishing line) in extension with nitrogen purge and low temperature cooling and hold it under enough tension to keep it taut. Set up a stress relaxation experiment to distort it by 0.1 mm and track the decay of the forces.

10.14.5 DYNAMIC STRAIN SWEEPS

Using the same materials as in the stress–strain scans, run a dynamic strain sweep. Compare the results with the stress–strain scan at 200 mN/min. Then plot the storage modulus, loss modulus, and $\tan \delta$ as a function of dynamic strain.

10.14.6 DYNAMIC TEMPERATURE SCANS

Using samples of polystyrene in single cantilever, PET film (from a transparency or coke bottle) in extension, and nylon 6 in three-point bending, run temperature scans from 25°C to 250°C at 2°C/min. Choose a 50 micron-starting amplitude for both three-point bending and tension; use the appropriate controls to keep the sample loaded with 50% extra static force. Calculate the T_g from the $\tan \delta$ peak and onset as well as the onset of the E' drop. Compare the results for polystyrene with the results from the TMA experiments.

10.14.7 CURING STUDIES

Using the shear geometry and a sample of commercial two-part high-strength epoxy, set up a run to cure the material in the DMA. Assuming the material takes 2 hours to set (the back of the label gives the setting time), run isothermally at 40°C, 50°C, and 60°C. Depending on the viscosity of the initial material, you may want to float the probe and use amplitude control. Find the gelation and vitrification points. Alternately you can run a temperature ramp at 10°C/min up to 300°C. In either case, you can use Roller's method to estimate the activation energy, which you could also compare to the DSC value.

10.14.8 FREQUENCY SCANS

In either the extension or three-point bending geometry, set up a sample of PVC in single cantilever. Then set the analyzer to vary the frequency across the full range in logarithmic steps. Set up a series of isotherms 10°C apart up to about 200°C. These runs can be then used for a TTS experiment.

NOTES

1. G. Hohne et al., *Differential Scanning Calorimeter*, 2nd ed., Springer, Berlin, 2004. V. Mathot, *Calorimetry and Thermal Analysis of Polymers*, Hanser-Gardner, Cincinnati, OH, 1993. R. Wunderlich, *Thermal Analysis of Polymers*, Springer,

- Berlin, 2005. P. Gallagher, Ed., *Handbook of Thermal Analysis and Calorimetry*, Vols. 1–4, Springer, Berlin, 1998–1999.
2. B. Bilyeu, W. Brostow, and K. Menard, *J. ASTM Inter.*, 10, 2, 2005. B. Bilyeu, W. Brostow, and K. P. Menard, Evaluation of the curing process in a fiber-reinforced epoxy composite by temperature-modulated and StepScan DSC and DMA, *Materials Characterization by Dynamic and Modulated Thermal Analytical Techniques, ASTM STP 1402*, A. T. Riga and L. H. Judovits, Eds., American Society for Testing and Materials, West Conshohocken, PA, 2001.
 3. G. Ehrenstein, *Thermal Analysis of Plastics: Theory and Practice*, Hanser-Gardner, Cincinnati, OH, 2004. W. Groenewoud, *Characterization of Polymers by Thermal Analysis*, Elsevier Science, New York, 2001.
 4. T. Proveder, *Hyphenated Techniques in Polymer Characterization*, ACS, Washington D.C., 1994. S. Materazzi and R. Curini, *Appl. Spectro. Rev.*, 36, 1, 2001. B. Roduit and M. Odlyha, *J. Therm. Anal. Calorim.*, 85, 157, 2006.
 5. A. Kuptsov and G. Zhizhin, *Handbook of Fourier Transform Raman and Infrared Spectra of Polymers*, Elsevier Science, New York, 1998.
 6. S. Havriliak and S. Havriliak, *Dielectric and Mechanical Relaxations in Materials*, Hanser/Gardner, Cincinnati, OH, 1997.
 7. All samples can be obtained in convenient form from the Society of Plastic Engineers in its “ResinKit” set. This is a collection of 50 polymer samples used to teach the identification of plastics and is listed in the Society of Plastic Engineers book catalog. Instrument vendors often have small test kits, too.

Index

Note: Page numbers with “n” after them indicate a note. Page number in **bold** refer to figures or tables.

A

Accelerated aging, 167, 178
Acceleration (a), 15, 33
Acoustical damping, 102n34
Acoustic damping, 101
Acrylics, 102n40
Activation barrier, 101n28
Activation energy (E_{act}). *See also* Energy (E')
 curing studies, 202
 frequency dependencies, 156
 Newtonian fluid, 164
 relative estimates, 6
 slope of curve, 130
 studied in DSC, 200
 temperature, 139
Adhesives and sealants, 52n40, 151–152, 188
Aerospace applications of wires, 116
Aggressive environments, 10–12
Aging, 52n35, 53, 57n5, 98n10, 127, 165
Aging time, 164n38
Alpha staging (α -staged), 125
Alpha star transition (T_{α^*}), 108n58
Alpha transition (T_{α}), 4, 103
American Society for Testing and Materials (ASTM)
 ASTM D2990-91, 46
 ASTM D648, 65–67
 ASTM D-790, 24
 desorption and adsorption studies, 180n9
 methods for TMA, 59–61
 standards, **47–48**
 Tests for the DMA, **113**
Amorphous phase, 99
Amorphous polymers, 50, 108–110
Analysis of a creep-recovery curve, **42**
Analysis of stress-strain curve, 21–23
Anisotropic material, 59, 61, 65
Applied force, 2, 79
Applied stress (σ_0). *See also* Stress (σ)
 change in modulus, 75
 and four-point bending, 84–85
 to generate strain (γ), 18
 and geometric factors, 82
 and material response, 42–43
 normal force, 159
 and resultant strain difference, 72–73

 rheological concepts, 17–20
 sinusoidal oscillation of, 71–72
Area (A), 16, 32–33
Armstrong, R., 27n14, 160n26
Aspect ratio, 24n11, 25n13
ASTM. *See* American Society for Testing and Materials
Axial, 83
 dual and single cantilever, 85–86
 extension/tensile, 87
 parallel plate and variants, 86–87
 shear plates and sandwiches, 87–88
 three-point and four-point bending, 84–85
Axial analyzers
 commercial instruments, 83, 128
 measuring shear, 87
 thermomechanical analyzer (TMA), 79
Axial and torsional deformation, 79
Axial geometry, 2
Axial instruments, 79, 88, 128
Axial rheometers, 86

B

Bao, Q., 186
Behavior and creep testing, 37n1, 161
Berger model, 43, 44
Bershtein, V., 101n28, 110n63
Bessette, M., 116n79
Beta and gamma transitions, 6
Beta staging (β -staged), 125
Beta transition (T_{β}), 5n19, 99, 102
Bird, R.B., 95n2
Bitumen, 132n25
Bohlin Rheologia, 2
Boltzman and history of strain (γ), 48
Boltzman superposition principle, 8n30, 39–40, 48–49, 146n2
Bonilla-Rios, J., 173n54
Boyd, R.H., 102n49
Boyer, R., 101n27, 102n42
Boyer, R.J., 108, 110n64
Branching, 50
Brittleness, 99n22
Brostow, W., 49n17, **52**, 52n45, 165n43
 β transition, 99, 102
Bulk, 87n13

Bulk measurements, 62, 65
 Bulk properties of foam, 116
 Bulk styrene polymerization, 65n14

C

Calculation property
 deformation (elasticity), 2
 frequency scan, 76
 modulus (E), 2
 Poisson's ratio, 75
 viscosity (η), 2, 75–76
 Young's modulus, 74

Calibration issues, 91–92

Cantilever fixtures, 85

Capillary flow studies, 74

Capillary rheometers, 27

Carbon-epoxy composites, 127n9

Carreau model, 27

Cassel, P., 186

Cellulose, 187n25

Cellulose films, 182n11

Ceramics, 59

CGL. *See* Constant gauge length

Chain mobility, 58

Characterization, 20, 194

Chemical simplicity, 165

Chemists and rheology, 15

Chemorheology of thermosetting systems, 134

Cheng, S., 101n30

Chodak, I., 95n3

Choosing a type of test, 192–194

Choosing the fixture, 194–196

Coatings, 128n13

Coefficient of thermal expansion (CTE)
 dilatometry, 65
 expansion and, 61–63
 material expansion calculation, 57
 thermomechanical analyzer (TMA), 61–63
 TMA Experiments, 201
 and TMA samples, 59

Cole-Cole plot, 155n15–16, 167, 199–200

Collection of frequency data, 145

Commercial instruments
 axial analyzers, 83, 128
 Bohlin Rheologia, 2
 capillary rheometers, 27
 effects of solvent on, 183–184
 forced resonance analyzers, 76–77, 127–128
 free resonance analyzers, 79–81, 147n5, 161n31
 glass dilatometers, 65
 glass viscometer, 26
 Gnomix, 67, 68
 modeling other mechanical tests, 187–188
 rheovibron, 1
 software packages, 173n50
 strain-controlled analyzers, 77–78
 stress-controlled rheometer, 146–147n4, 161n32
 thermomechanical analyzers, 57
 torsional, 88
 torsional braid analyzers, 81
 used to measure qualities like Young's modulus, 57n1
 Weissenberg rheogoniometer, 1n6

Commercial polymers, 114

Common Products and their Use Frequencies, 153

Complex modulus (E^*), 4, 75

Complex viscosity (η^*), 4, 75–76, 148, 149, 150

Compliance (J), 38–39, 168

Compliance vs. time, 39n4, 41n10, 44, 49

Composite materials, 128

Compressive viscosity, 65n27

Computer technology revolution, 2

Concentric/coaxial cylinders, 89

Cone-and-plate, 27–28, 89, 160, 199

Constant gauge length (CGL), 10, 53, 67n30, 110

Constant-strain variable temperature test.
See Constant gauge length

Constant stress rate ($\dot{\sigma}$), 17n6

Continuous heating transformation diagram, 138

Continuous shear experiments, 160n24

Continuous shear rheometers, 27

Continuum mechanics, 15n1

Controlled humidity, 10–12

Controlled stress analyzer, 2

Conversion factors, 32–35

Conversion-temperature-property diagram, 138

Copolymer, 114–116

Corrosive gases, 117

Couette, 89

Coupling, 187

Cox, W., 149n9

Cox-Merz rule, 4n18, 76, 149, 160, 161

Crankshaft model, 58, 99

Crazing, 50n24, 52n36

Creep
 activation barrier, 101
 compliance vs. time, 39n4, 41n10, 44, 49
 data and rates, 146–147
 data and stress relaxation data, 52n29
 experiments, 40
 frequencies, 161n30
 frequency studies, 146–147
 mechanical engineering curriculums, 37n2
 postcure studies, 141

Creep experiment analysis, 44

Creep force, 79n7

- Creep recovery, 147–148
 Creep-recovery behavior models, 40–41
 Creep-recovery curve, 40n6, 41–44, 79
 Creep-recovery cycle, 37
 Creep-recovery experiment, 9n34, 9n36, 201–202
 Creep-recovery testing
 dynamic mechanical analysis (DMA), 9–10
 experiments, 50n23, 67n29, 79, 155
 material characterization, 9n33
 polymer, 37–40, 50
 rheology basic, 37–40
 structure-property relationships, 50–51
 and time, 197–198
 Creep ringing, 45, 81, 146
 Creep testing, 37, 45–48
 Critical molecular weight (M_c), 29, 103, 169
 Crosslinking
 cured thermoset, 99
 curing processes, 125
 degree of, 52n33
 polymers, 51, 63, 90
 polymers degrade by, 111
 thermal or UV aging, 103
 Crossover point
 molecular weight, 7n26, 169–170
 molecular weight distribution, 7n27, 151
 Crystalline polymers, 30
 Crystallinity, 52n34, 108
 Crystal morphology, 51
 CTE. *See* Coefficient of thermal expansion
 Cure cycle, 123, 138–139
 Cured thermosets, 30, 99, 155
 Cure profiles, 127–132, 128–130, 132–133
 Curing and time, 133–134
 Curing kinetics, 123
 Curing processes, 125
 Curing studies, 127–128, 158, 202
 Curing systems, 123, 128–130, 176–177
 Curvature, 21n9, 25, 28–29
 Cyanate esters, 127n10
- D**
- Daley, C., 186
 Damping, 4
 Dashpot
 Newton's law, 24, 25–26, 29
 and spring, 40
 viscous behavior, 74
 viscous response of strain rate, 72
 Data and stress relaxation data, 52n29
 Data from penetration run on PMMA, 64
 Data points, 145–146
 DDSC. *See* Dynamic differential scanning calorimeter
 DEA. *See* Dielectric analysis
 Dealy, J., 28n20, 146n1, 159n20, 165n46
 Deborah number, 155
 Decade, 2
 Decay curve, 79–80
 Decay of amplitude, 79–81
 Decomposition studies, 116n77, 123
 Deformation (elasticity)
 activation barrier, 101
 calculating properties, 2
 calibration issues, 91–92
 choosing the fixture, 194
 creep data and rates of, 146–147
 forced resonance analyzers, 76–77
 material slope, 54
 and phase lag calculation, 75–76
 strain (γ), 2, 16–17
 Deformation of material, 17–18
 Degradations, 99, 111, 118, 132
 Degree of crosslinking, 52n33
 Degree of cure
 frequency data, 8
 relationship to T_g , 125–126, 134
 supporting data from other methods, 200
 time-temperature superposition, 164
 UV photocures, 177
 UV studies, 175
 Dental materials, 52n38
 Dependency of transition temperature, 156–157
 Desorption and adsorption studies, 180n9
 Dielectric analysis (DEA), 2n8, 101, 131n21, 186–187, 191
 Die swell, 159n22
 Differential scanning calorimeter (DSC)
 beta and gamma transitions, 6
 and composite materials, 128
 vs. curing systems, 123
 dilatometry, 65n20, 66
 vs. DMA to measure T_g s, 95
 energy management, 175n2
 frequency and transitions, 113
 postcure studies, 140–141
 residual cure energy, 126
 supporting data from other methods, 200n1
 temperature range, 108
 vs. TMA, 57
 TTT diagram, 138n43
 Differential thermal analyzer (DTA), 95, 186
 Dilatometry
 bulk measurements, 62–63
 and bulk measurements, 65
 coefficient of thermal expansion (CTE), 65
 differential scanning calorimeter (DSC), 65n20, 66
 Dimensionless numbers, 155
 Distribution of relaxation or retardation times, 49n20

DMA. *See* Dynamic mechanical analysis

DMA and polymer melts, 145

DMA-DEA, 131n21, 186

DMA-DTA, 186

DMA-FTIR, 175, 187n25

DMA in solution, 184–186

DMA measurement, 116–117

DMA-MS, 175

DMA to measure T_{gs} , 95

DMA vs. DSC, 103–106

DMTA. *See* Dynamic mechanical thermal analysis

Doi-Edwards theory, 7, 98n14, 173n52

Double reptation mixing rule, 170

Dough, 52n37

DSC. *See* Differential scanning calorimeter

DSC or DTA sensitivity, 103

DSC or TMA, 6n20

DTA. *See* Differential thermal analyzer

Dual cantilever, 85–86, 194

Dual glass transitions in homopolymer, 95n1

Dual-layer film, 21, 22

Duncan, J., 24n12, 75n4, 95n4

Du Pont, 2

Dynamic differential scanning calorimeter (DDSC), 140

Dynamic experiments, 92–93

Dynamic force, 71

Dynamic mechanical analysis (DMA)

- aggressive environments, 10–12
- analytical laboratory tool, 1
- basic principles, 2–4
- and computer technology revolution, 2
- creep-recovery testing, 9–10
- and DEA, 2n8
- DSC or DTA sensitivity, 103
- free volume of polymers and temperature, 71
- in frequency scan, 7, 49
- history of, 1–2
- How a DMA works, 3
- material characterization, 1, 2
- measured normal forces, 2n10
- modulus, 2–4
- modulus and sine wave, 4
- oscillating force, 2
- oscillatory deformations, 1n3
- oscillatory experiments and elasticity, 1
- polymer chains, relaxation of, 2n14
- polymer properties, 1
- rheology, 1, 15
- sample applications, 4–9
- sample experiments for, 201–202
- state of the art articles, 2n13
- technique of, 1
- techniques reviewed by te Nijenhuis, 1n4

Test Methods Used, 195–196

- torsional braid analyzer, 2n9

Dynamic mechanical thermal analysis, 1

Dynamic mechanical thermal analyzer (DMTA), 2

Dynamic properties, calculating, 74–76

Dynamic strain, 202

Dynamic stress, applying, 71–74

Dynamic stress-strain curves, 92–93

Dynamic temperature scans, 202

Dynamic testing and instrumentation

- applying dynamic stress, 71–74
- axial and torsional deformation, 79
- calibration issues, 91–92
- dynamic experiments, 92–93
- dynamic properties, calculating, 74–76
- fixtures or testing geometries, 81–90
- forced resonance analyzers, 76–77
- free resonance analyzers, 79–81
- sample handling issues, 90
- stress and strain control, 77–78

Dynamic T-peel test, 188

E

E' - η^* crossover point, 151

Effect of humidity on material's properties, 12

Effect on viscosity, 6, 26, 149–150

Effects of humidity, 182

Effects of humidity in the DMA, 182

Effects of solvent on commercial instruments, 183–184

Effects of structural changes, 29n24

Egorov, V., 101n28

Eicke, H.F., 81n9

Elastic material, 21, 74

Elastic modulus (E'). *See also* Modulus (E')

- calculation of, 74, 75
- frequency increase, 151
- heat set temperature, 110
- measurement of, 4
- vs. Young's modulus, 149

Electronic materials, 116

Energy (E'), 75, 102n44

Energy, loss (E''), 4, 75

Energy, return (E'), 4

Energy management, 175n2

Epoxy-based systems, 126–127

Epoxy-graphite composite, 64

Epoxy-propylene, 115n72

Equilibration times, 181–182

Equilibrium modulus, 44

Equilibrium viscosity, 44

Ewoldt, R., 45n13, 81n10

Expansion and CTE, 61–63

Expansion studies, 63

Experiments

- and aggressive environments, 10–12
 - Analysis of a creep-recovery curve, **42**
 - characterization, 194
 - checking the response to frequency, 197
 - checking the response to loads, 197
 - checking the response to time, 197–198
 - checking the temperature response, 198–199
 - choosing a type of test, 192–194
 - choosing the fixture, 194–196
 - constant gauge length tests, 53–54
 - creep, 40
 - creep experiment analysis, 44
 - creep-recovery experiment, 9n34, 9n36, 201–202
 - creep-recovery testing, 50n23, 67n29, 79, 155
 - curing studies, 202
 - dynamic, 92–93
 - dynamic strain sweeps, 202
 - dynamic temperature scans, 202
 - extension/tensile, 87
 - frequency scans, 202
 - frequency studies, 145–147
 - heat distortion test, 64
 - material characterization or performance, 191
 - multiple cycle creep, 45–46
 - penetration tests, 64
 - performance tests, 191–192
 - photo-DMA experiment, 177
 - plate and tension, 95
 - putting it together, 199
 - recovery experiment, 9n35, 146–147n4
 - stress relaxation experiment, 18, 51–53, 67, 79, 202
 - stress-strain experiment, 17–18, 79
 - stress-strain scans, 201
 - supporting data fro other methods, 200–201
 - TMA experiment, 18
 - TMA Experiments, 201
 - verify the results, 199–200
- Extensional thickening, 28n23
- Extension/tensile, 87

F

- Ferry, J., 173n49
- Ferry, J.D., 1n7, 49n21, 75n3, 117n84, 161n33, 164n34
- Fiber-reinforced composites, 90
- Fibers, 52n39
- Film softening, 65n24
- Fingerprinting materials, 123, 138
- Fishing line, 202
- Fixtures, 59, 81–90
- Flexural and penetration mode, 64

- Flexure fixtures types, 84
- Flexure studies, 64
- Flexure tests of composites, 59
- Flow behavior, 4n17
- Flow Models, **150**
- Fluid bath, 184
- Food analysis, 123n1
- Food rheology, 40–41n9, 59, 65
- Force (F), 15–16, 33–34, 61
- Force, stress, and deformation, 15–17
- Forced resonance analyzers, 76–77, 127–128
- Four-element model, 40, 41–44, 49–50
- Fourier Transform Infrared Spectrometer (FTIR), 102n50, 175n1, 201n5
- Four-point bending, 84–85
- Free resonance analyzers, 79–81, 147n5, 161n31
- Free resonance decay, 45
- Free resonance studies, 161
- Free resonance techniques, 146n3
- Free volume (v^f)
 - bulk, 87n13
 - glass transition (T_g), 67–68, 103
 - material characterization, 57
 - polymer, 2n15
 - of polymers, 57–58, 71, 98n7
 - shifting curves approach, 165
- Frequency, 33
 - checking the response to frequency, 197
 - Common Products and their Use
 - Frequencies, **153**
 - creep, 161n30
 - curing studies, 158
 - data points, 145–146
 - dependency of transition temperature on, 156–157
 - effects during curing studies, 158
 - effects on materials, 147–154
 - effects on solid polymers, 155–157
 - rate of shear, 27
 - slope of curve, 130
 - testing methods, 112–114
- Frequency and transitions, 113
- Frequency and waveform, 146n2
- Frequency behavior, 7, **148**, 151
- Frequency changes and curves, 164
- Frequency data, 8, 8n30, 145, 167–168
- Frequency dependence, 102, 112–114
- Frequency increase, 151
- Frequency range, 153, 165
- Frequency response, 91
- Frequency scan
 - calculation property, 76
 - commercial polymers, 114
 - Deborah number, 155
 - in DMA, 7, 49
 - dynamic experiments, 92–93
 - experiments, 202

frequency effects during curing studies, 158
 frequency effects on materials, 147–154
 frequency effects on solid polymers,
 155–157
 frequency studies on polymer melts, 158–159
 low temperature-low frequency data, 165
 mater curves and time-temperature
 superposition, 161–167
 methods of performing, 145–147
 molecular weight and molecular weight
 distributions, 169–171
 normal forces and elasticity, 159–161
 polymer melt vs. polymeric solid, 28
 problems with performing, 161
 three-point bending, 202
 time-temperature superposition (TTS), 202
 transformations of data, 167–168
 on viscoelastic material, 148
 viscosity (η), 147, 152–153
 Frequency scan predictive method, 145
 Frequency shifts master curve, 170–171
 Frequency studies, 145–147, 158–159
 Frequency/temperature dependencies, 159
 Frequency transition, 156
 FTIR. *See* Fourier Transform Infrared
 Spectrometer
 Fuller, G., 187n24
 Function of temperature, 4
 Function of time, 136–137

G

Gamma transition (T_γ), 99n19
 Gas Chromatograph (GC), 201
 Gas diffusion, 101
 Gaskets and rubbers, 52n41
 Gel permeation chromatography (GPC), 7n29,
 29, 149
 Gel temperature, 137
 Gel time test, 140
 Geometric arrangements, 18–19
 Geometric factors, 81–82
 Geometry
 cone-and-plate, 89
 Couette, 89
 extension/tensile, 87
 parallel plates, 88
 sample shape, and aspect ratio, 24–25
 torsional beam and braid, 90
 Gillham, J., 79n6, 79n8, 137n41
 Gillham-Enns diagram, 123, 137–138
 Glass dilatometers, 65
 Glass transition (T_g), 4, 30, 50
 DMA vs. DSC, 103–106
 effects of humidity, 182
 free volume (v^f), 67–68, 103
 and heating, 99

 heating rate, time, frequency relationship,
 127
 of lyophilized materials, 65n18
 measurement of volume of polymer, 67–68
 metallic glasses, 116
 polymer, 58, 103
 temperature, 59
 TMA measurement, 61–62
 TMA on inorganic glass, 57
 Glass transition (T_g^c) temperature, 126
 Glass transition (T_g or T_α), 103–106
 Glass viscometer, 26
 Glassy, 102n46
 Gleissel, W., 161n28
 Gleissele's mirror relationship, 76, 149n10,
 161n28
 Gnomix, 67, 68
 Goertzen, W.K., 49n16
 Goldman, A. Ya, 164n35
 GPC. *See* Gel permeation chromatography
 Grafting in polymers, 116n75
 Graphite-epoxy composites, 128, 153
 γ transition, 99, 102

H

Halley, P.J., 134, 136
 Heat (damping), 2, 75
 Heat capacity of solvent, 184
 Heat distortion, 65
 Heat distortion test, 64
 Heating, 99
 Heating rate, time, frequency relationship, 127
 Heating rate and CTE, 61
 Heat set temperature, 110
 Heijboer, J., 99n18, 102n43
 Heterogeneous material, 61
 High frequency response, 7
 High Impact Poly Styrene (HIPS), 178n7
 High polymers, 187n29
 High pressure differential scanning calorimeter
 (HP DSC), 68
 HIPS. *See* High Impact Poly Styrene
 Homogeneous strain, 89
 Homopolymer, 114, 116
 Hookean behavior, 20n8, 31, 71
 Hooke's law, 20–23
 Hot melt adhesive, 7n25
 How a DMA works, 3
 HP DSC. *See* High pressure differential
 scanning calorimeter
 Humidity, 54, 117, 164, 181, 182
 Humidity on material's properties, effect of, 12
 Humidity systems, 179–180
 Hyphenated techniques, 186–187
 Hyphenated variants, 200–201n4

I

Imaginary (loss) modulus (E''), 4n16
 Immersion, 182–186
 Impact properties, 57n7, 98n12
 Industry and heat distortion test, 18
 Inertia, 82, **83**, 88n14, 184
 In-phase portion of curve, 72
 In-phase strains, 73
 Instrumentation and measurement effects, 183–184
 Integrated fluid bath, **63**
 Internal defects, 52n32
 International Conference on Polymer Characterization (POLYCHAR), 15
 Invar steels, 59
 IR, 131n22
 Isayev, A., 28n19
 Isothermal conditions, 92, 136
 Isothermal cures, 134–135, 140
 Isothermal curing studies, 133–134
 Isothermal irradiation, 177
 Isothermal runs for values of DSC, 6n24
 Isothermal stress-strain curve, 23

J

Johari, G., 101–102n31–32

K

Kinetic behavior, 127
 Kinetic models, 134n32
 Kinetics, 125, 128, 134–137, 175

L

Laplace transform, 38n3
 Laun's rule, 161n27
 LCTE. *See* Linear coefficient of thermal expansion
 Leather, 182n15
 Leather, shrinkage of, 53
 Length, 32, 81
 Linear coefficient of thermal expansion (LCTE), 57
 Linear region estimate, 39–40
 Linear Vertical Displacement Transducer (LVDT), **77**
 Linear viscoelastic region, 16n4, 38, 71, 82, 197–198
 Liquid crystal (rigid), 67
 Liquid-like flow or viscous limit, 25–28
 Liquid-liquid transition (T_{ll}), 108n58
 Loads, 197

Load to deformation, 19–20
 Log-log plot, 167–168
 Loss modulus (E''), 75
 Low frequency modulus, 7
 Low temperature-low frequency data, 165
 LVDT. *See* Linear Vertical Displacement Transducer
 Lyophilized materials of glass transition (T_g), 65n18

M

MacKay, M.E., 134, **136**
 MacKnight, J., 98n15
 MacKnight, W., 15n2
 Macosko, C., 15n3, 28n21, 28n22, 89n15, 116n78
 Malkin, A., 26n16, 28n19
 Mangion, M., 102n32
 Mapping thermoset behavior, 137–138
 Mark-Houwink constant, a, 149
 Mark-Houwink exponent, 169
 Mass, 33
 Mass Spectrometer (MS), 187
 Master curves, 8n31, 161–164, 165, 168
 Material, elastic response, 20
 Material behavior, 25
 Material characterization
 beta transitions, 102
 bulk properties of foam, 116
 choosing a type of test, 192–194
 creep-recovery testing, 9n33
 cure cycle, 138–139
 degradation acceleration, 118
 dilatometry and bulk measurements, 65
 and DMA, 1
 dynamic mechanical analysis (DMA), 2
 elastic and viscous, 71
 and energy, 4
 flow behavior, 4n17
 free volume, 57
 frequency behavior of, 7
 load to deformation, 19–20
 performance tests, 191–192
 postcure studies, 140–141
 and powders, 6n21
 rate of strain, 6–7
 rheologically simple and superpositioned, 165
 Samples and Fixtures, **196**
 single and dual cantilever equations, 86
 solids vs. fluids, 28, 130–131
 special area of concern, 128
 stress to deform, 21n10
 and temperature programs, 10n37
 temperature range, 99–100

- and testing, 53–54
 - testing in nonstandard environments, 9n32
 - and thermal expansion, 61–62
 - viscosity during curing, 130, 139–140
 - Viscosity of Common Materials, **132**
 - weight, 6n22
 - Material expansion calculation, 57
 - Material properties, 4–6, 75–76, 101
 - Material response, 42–43, 151–152
 - Material slope, 54
 - Material volume, 21
 - Mathematicia™, **27**
 - Maxwell model, 29, 40, 52
 - McCrum, N., 2n8, 79n8, 99n23, 102n48, 113n69
 - McKinley, G., 45n13, 81n10
 - Measured normal forces, 2n10
 - Measured stiffness, 20, 76
 - Measurement. *See also* TMA measurements
 - of material's stiffness, 20–21
 - of modulus (ϵ), 24
 - of molecular weight distribution, 170
 - and polymer systems, 113
 - of viscosity (η), 44, 52n43
 - of volume of polymer, 67–68
 - Mechanical engineering curriculums, 37n2
 - Mechanical properties, 101
 - Mechanical testing, 64, 65n26, 67n29
 - Melt indexer, 27n17
 - Melting point. *See* Melting temperature
 - Melting temperature (T_m), 4, 99, 110
 - Melt rheology, 159n20
 - Memory function, 48n15
 - Menard, K., 186
 - Merz, E., 149n9
 - Metallic glasses, 116
 - Metals, 52n42, 116
 - MgCl salt solution, 180n8
 - Miller, A., 186
 - Miller, M.L., 1n5
 - Model information, 52n28
 - Modeling cure cycles, 133
 - Modeling other mechanical tests, 187–188
 - Model linear behavior, 40n7
 - Models of behavior, 71
 - Modulus (E). *See also* Elastic modulus (E')
 - calculate a stiffness for sample, 76
 - calculation property, 2
 - change in applied stress, 75
 - to characterize material, 20
 - choosing the fixture, 194–196
 - and crystalline polymers, 30
 - cure cycle, 123
 - DMA measurement, 116–117
 - dynamic mechanical analysis (DMA), 2–4
 - frequency behavior, **148**, 151
 - and geometric factors, 82
 - how aspect ratios affects, 25n13
 - linear viscoelastic region, 38
 - measurement of, 24
 - measure of material's stiffness, 20–21
 - and mechanical tests, 65n26
 - The ratio of stress to strain, **3**
 - speed of application of stress, 31
 - stress-strain curve, 2, 4, 72
 - stress-strain scans, 201
 - and temperature, 30
 - temperature scan, 127
 - thermoset, 6
 - values during cure, 130
 - Modulus and sine wave, 4
 - Molecular motion, 5
 - Molecular weight
 - crossover point, 7n26, 169–170
 - $E'-\eta^*$ crossover point, 151
 - for Newtonian fluid, 149
 - plasticization, 50
 - related to polymer viscosity in Newtonian region, 169n51
 - shape of curve, 126
 - stress relaxation experiment, 52n31
 - stress-strain curve effects, 29
 - temperature-dependent impact tests, 102n36
 - Molecular weight and molecular weight distributions, 169–171
 - Molecular weight between entanglements (M_e), 106–108
 - Molecular weight distribution
 - crossover point, 7n27, 151
 - master curve, 165
 - measurement of, 170
 - retardation time, 43
 - rule of thumb, 169
 - stress-strain curve effects, 29
 - weight-based $[W(M)]$, 171
 - Molten state and molecular weight of polymer, 110
 - Morphological component, 116
 - MS. *See* Mass Spectrometer
 - Multiple cycle creep, 45–46
 - Multiple cycles, 45–46
 - Multistage cure cycle, 133
 - Murayani, T., 2n11
- ## N
- NaCl salt solution, 180n8
 - Nafion™ 117 films, 182n13
 - NASTA Notes (Daley), 186
 - NATAS Proceedings (Bao), 186
 - NATAS Proceedings (Twombly), 186

- National Physics Laboratory, 95n5
 Natural resonance frequency, 153
 Near infrared (NIR), 187
 Nelson, B., 146n1
 Nelson, F.C., 102n33
 Newman, S., 175n1
 Newton, Isaac, 25n15
 Newtonian behavior, 20, 149
 Newtonian fluid, 149, 164–165
 Newtonian model, 25
 Newtonian region, 151, 169
 Newton's law, 24, 25–26, 28n22, 29
 Nielsen, L., 44
 NIR. *See* Near infrared
 NIST traceable materials, 91
 Nonhomogeneous samples, 90
 Non-Newtonian behavior, 25, 31–32
 Non-Newtonian fluid mechanics, 15, 89
 Non-Newtonian materials, 26–27
 Normal distribution, 173n56
 Normal forces and elasticity, 159–161
 Normal forces under shear, 28n22
 Normal stress coefficients, 160
 Normal stresses coefficients, 159–160
- O**
- O'Neal, H., 64n13
 Optical uses of PerkinElmer DMA 8000, 187
 Orders of reaction, 137n37
 Orthodontics, 116n81
 Oscillating force, 2
 Oscillatory deformations, 1n3
 Oscillatory experiments and elasticity, 1
 Osmometry, 149n7
 Out-of-phase strains, 73
- P**
- Paints, 101, 128n12
 Parallel plate, 27–28, 86–87, 95, 160
 Parallel plate and variants, 86–87
 Parallel plates, 88
 Peanut butter, 114
 Peltier heater, 77
 Penetration by solvents, 98n11
 Penetration tests, 64
 Penetrative viscosity, 65n28
 Performance tests, 191–192
 PerkinElmer, 2
 PerkinElmer DMA-7e, 132
 PerkinElmer DMA 8000. *See also* Commercial instruments
 calibration issues, 91
 collection of frequencies, 145
 Data from penetration run on PMMA, 64
 effect of humidity on material's properties, 12
 How a DMA works, 3
 integrated fluid bath, 63
 measured stiffness, calculate values, 20
 optical uses, 187
 photocuring and UV adapter, 132
 schematic of, 77
 Stress relaxation experiments, 51
 Testing in the presence of solvents, 11
 PET film, 202
 Phase angle, 74n1, 75
 Phase lag, 72, 75, 91
 Phase lag calculation, 75–76
 Photodegradations, 175
 Photocalorimetry, 176
 Photocuring, 132–133, 176–177
 Photocuring materials, 87
 Photocuring reaction, 176
 Photocurves, 123
 Photo-DMA, 177, 178
 Photoreactions, 175
 PID. *See* Proportional, integral, and derivative control
 Plane angle, 33
 Plasticization, 50
 Plasticizers, 30–31
 Plate and tension, 95
 Plazek, D., 165n47
 Poisson's ratio
 calculation property, 75
 material volume change with deformation, 21
 Shear, compressive, and extensional flows, 27
 shear correction based on, 86
 tensile vs. shear viscosity, 40n5
 POLYCHAR. *See* International Conference on Polymer Characterization
 Polyesters, 102n38, 182n14, 187n28
 Polyethylene and polystyrene, 165n44
 PolyMath™, 27
 Polymer
 aging in, 53
 behavior and creep testing, 37n1, 161
 blend or copolymer, 114–116
 contains modifiers and fillers, 114n70
 creep-recovery testing, 37–40, 50
 crystalline, 30
 Deborah number, 155
 degrade by crosslinking, 111
 determining operating range, 5–6
 effects of structural changes, 29n24
 expansion studies, 63
 free volume, 2n15, 57n3, 71, 98n7
 frequency effects on solid, 155–158

gas diffusion, 101
 glass transition (T_g), 58, 103
 glassy, 102n46
 industry and heat distortion test, 18
 models of behavior, 71
 molten state and molecular weight of, 110
 and plasticizers, 30–31
 PVT relationship, 67n32
 relaxation process of, 95
 rule of thumb, 169
 shear/compression vs. melt, 28
 shear rate problems, 28
 sinusoidal oscillation of, 74
 solids vs. fluids, 150
 strain dependence of, 52n30
 stress controls duplicate real-life conditions, 78
 and stress-strain curve, 23
 superposition of, 48–49
 temperature and pressure dependencies, 67n31
 $T\gamma$ transitions, 102
 thermal transitions in, 98
 and TMA usage, 57
 trends in behavior, 29–30
 types of creep tests, 45–46
 and viscoelastic nature, 29, 31
 Polymer chains, relaxation of, 2n14
 Polymer extrusion, 159
 Polymeric material, 21
 Polymerization, 116n76
 Polymer labs, 2
 Polymer liquid crystals, 49n18
 Polymer melt, 26–27, 31, 111–112, 158–159
 Polymer melt vs. polymeric solid, 28
 Polymer properties, 1
 Polymer science and dynamic measurements, 1–2
 Polymer synthesis, 125n4
 Polymer viscosity, 173n51
 Polypropylene (PP) fiber, 202
 Polyurethanes, 182n16, 187n27
 Poly vinylidene Fluoride (PVDF), 49n19
 Postcure and $\tan \delta$ relationship, 103n52
 Postcure studies, 123, 140–141
 Postcuring, 125, 132
 Powders, 6n21
 Power, 34
 Power law zone, 150
 Poyntang, J.H., 1n2
 PPO, 102n39
 Pressure, 34
 Pressure-volume-temperature (PVT), 67, 87
 Probe (m), 15
 Product of force across area, 16
 Properties for DMA, 74n2

Properties of polymers, 164n37
 Proportional, integral, and derivative control (PID), 92
 PVC, 102n37, 114
 PVDF. *See* Poly vinylidene Fluoride
 PVT. *See* Pressure-volume-temperature
 PVT relationship studies, 67–68

Q

Quality control (QC), 138
 Quartz, 59, 64, 87

R

Radius, 81
 Rahalkar, R., 173n52
 Raman, 102, 131n23, 175n1, 187
 Rate of shear, 27
 Rate of strain, 6–7, 161
 Rate of stress, 71
 Ratio of stress to strain, **3**
 Read, B.E., 2n12
 Recovery experiment, 9n35, 146–147n4
 Recovery portion of creep-recovery curve, 79
 Recovery tests, 37
 Reduced variables methods, 161
 Reiner, M., 155n17
 Relationship to T_g , 125–126, 134
 Relative humidity values, 180
 Relaxation and retardation times, calculating, 50n22
 Relaxation process, 95
 Relaxation spectra, 165n45
 Relaxation time, 98n8, 155n14
 Residual cure, 126, 141
 Resonance response, 154
 Response of material to temperature, 198–199
 Response to frequency, checking, 197
 Response to loads, checking, 197
 Response to time, checking, 197–198
 Resultant strain difference and applied stress, 72–73
 Retardation and relaxation times, 49–50
 Retardation spectra, 165n45
 Retardation time (τ), 43–44
 Rheological concepts
 apply the stress, 17–20
 conversion factors, 32–35
 force, stress, and deformation, 15–17
 geometry, sample shape, and aspect ratio, 24–25
 Hooke's law, 20–23
 liquid-like flow or viscous limit, 25–28
 stress-strain curve, 28–32

- Rheologically simple and superpositioned, 165
- Rheological-optical methods, 187
- Rheologists, 1n1, 26, 145
- Rheology, 1, 15
- Rheology basic
- Boltzman superposition principle, 48–49
 - constant gauge length tests, 53–54
 - creep experiment analysis, 44
 - creep-recovery behavior models, 40–41
 - creep-recovery curve analysis, 41–44
 - creep-recovery testing, 37–40
 - creep-recovery tests, structure-property relationships, 50–51
 - creep ringing, 45
 - creep tests, other variations, 45–48
 - retardation and relaxation times, 49–50
 - stress relaxation experiments, 51–53
- “Rheology for the Mathematically Insecure” (Menard), 15
- Rheometrics Corporation, 2n10
- Rheovibron, 1
- Rigid analyzer, 88
- Roark’s Formula for Stress and Strain* (Young), 83n11
- Rohn, C.L., 28n18, 98n16
- Roller, M., 134n35, 137n39
- Roller method, 134, 139
- Roller’s method, 202
- Rosen, S., 155n14
- Rubber, 53, 63, 90
- Rubbery plateau, T_{α}^* and T_{II} , 106–110
- Rule of thumb, 169
- Rykkers’s solution, 118
- S**
- Sample applications, 4–9
- Sample experiments, 201–202
- Sample geometry, 81
- Sample handling issues, 90
- Samples and Fixtures, **196**
- Scanning temperature, 71
- Schartel, B., 102n47
- Schematic of PerkinElmer DMA 8000, **77**
- Second-order transitions, 101
- Shape of curve, 126
- Shaw, M., 15n2, 52n44, 98n15
- Shear, compressive, and extensional flows, **27**
- Shear, measuring, 87
- Shear/compression vs. melt, 28
- Shear correction based on Poisson’s ratio, 86
- Shear heating, 82
- Shearing force, 27
- Shear modulus, 81, 160–161
- Shear plates and sandwiches, 87–88
- Shear rate
- cone-and-plate, 89
 - effect on viscosity, 6, 26, 149–150
 - material’s response to various, 151–152
 - Newtonian region, 151, 169
 - polymer problems using, 28
 - scan frequency or, 4
 - tests using low, 37, 44
 - zero-shear plateau, 27
- Shear rate curve, 76
- Shear rate problems, 28
- Shear thickening behavior, 26, 150
- Shear thinning, 26, 28n22, 150
- Shifting curves approach, 165
- Shoemaker, C., 40n8
- Silly Putty™, 4, 150, 155
- Single and dual cantilever equations, 86n12
- Single cantilever, 85–86
- Single-layer film, 21, **22**
- Sintered/sandblasted plates, 86
- Sinusoidal oscillation, 71–72, 74
- Sinusoidal wave, 194
- Six-element model, 40
- Slope of curve, 43, 130
- Smith, S., 102n45
- “Soaking of resin into a shoelace”, 128
- Society of Plastic Engineers, 173n53
- Softening points, 65n25
- Software, 173n55
- Software packages, 173n50
- Solid-phase reactions, 101
- Solid polymer, 156
- Solids vs. fluids
- and analyzers, 79
 - material characterization, 28, 130–131
 - polymer, 150
- Solutions in non-Newtonian behavior, **25**
- Solvents, 57n6, 117, 182–183, 183–184, 184–186
- Spectrometer, 187
- Spectroscopy, 176
- Sperling, L.H., 44n12
- SPE Technical Papers* (Daley), 186
- Speyer, R., 65n17
- Springs and dashpots combination, 40n6
- Staging, 125
- Stain, 164
- Standard Pressure-Volume-Temperature Data for Polymers* (Zoller), **67**
- Standards. *See* American Society for Testing and Materials
- Static stress, 17n5
- Steady shear viscosity (η_s), 4, 76
- Steady-state creep, 44
- Steel, 64
- StepScan DSC, 108n58, 200n2

- Stiffness. *See* Modulus
- Strain (displacement) control, 77
- Strain (γ)
- applying stress to generate, 18
 - Boltzman and history of, 48
 - and deformation, 16–17
 - properties of polymers, 164n37
- Strain-controlled analyzers, 77–78
- Strain curve, 42, 43
- Strain dependence of polymer, 52n30
- Strain rate, 44
- Strain sine wave, 74
- Stress (force) control, 77
- Stress (σ)
- and deformation of material, 17–18
 - deformation or strain (γ), 2
 - geometric arrangements, 18–19
 - product of force across area, 16
 - relaxation time, 155n14
 - and superposition, 52–53
- Stress and strain control, 77–78
- Stress-controlled rheometer, 146–147n4, 161n32
- Stress controls duplicate real-life conditions, 78
- Stress control usefulness, 18n7
- Stress relaxation, 37
- Stress relaxation experiment
- experiments, 18, 51–53, 67, 79, 202
 - molecular weight, 52n31
 - PerkinElmer DMA 8000, **51**
- Stress relaxation modulus, 168
- Stress relaxation tests experiments, 52
- Stress sine wave, 74
- Stress-strain scans, 202
- Stress-strain curve
- analysis of, 21–23
 - checking the temperature response, 198–199
 - and curvature, 25
 - curvature in, 28–29
 - dashpot and spring, 40
 - and Hooke's law, 20–21
 - material, elastic response of, 20
 - mechanical tests, 67n29
 - modulus, 4
 - modulus (E), 2, 72
 - modulus measurement, 4
 - in non-Newtonian behavior, 31–32
 - polymer, 23
 - polymeric material, 21
 - rheological concepts, 28–32
 - temperature, 18
 - viscoelastic materials effects, 147–148
- Stress-strain experiment, 17–18, 79
- Stress-strain plot, 201
- Stress-strain scans, 201
- Stress to deform, 21n10
- Structure of Polymers* (Miller), 1n5
- Structure-property relationships, 45
- Study of curing systems, 123
- Study of material flow, 26
- Subambient beta transition, 101n29
- Sub- T_g transitions, 101–102, 156
- Sunflower protein isolate, 182n12
- Superglue™, 90
- Superposition data, 191
- Superpositioning stress, 52–53, 164n36
- Superposition of polymer, 48–49
- Sweeney, J., 98n17
- ## T
- Tack, 188
- Tan delta, 4
- Tangent of phase angle, 75
- Temperature, 35
- curing and time, 133–134
 - frequency range of analyzer, 165
 - function of time, 136–137
 - glass transition (T_g), 50, 59
 - hyphenated techniques, 186–187
 - modulus (E), 30
 - NIST traceable materials, 91
 - polymer and free volume, 71
 - response of material to, 198–199
 - stress-strain curve, 18
 - time and study of age life, 117n84
 - TMA change in dimensions, 57
 - TMA distribution of molecular weights, 59
 - UV irradiation effect, 176
- Temperature and pressure dependencies, 67n31
- Temperature calibration, 95n4
- Temperature control, 57, 59, **97**
- Temperature-dependent impact tests, 102n35, 102n36
- Temperature programs, 10n37
- Temperature range, 99–100, 103, 108
- Temperature response, checking, 198–199
- Temperature scan, 95, 113, 127, 156
- Temperature-time studies, 92–93, **96**
- Tendency to flow. *See* Viscosity (η)
- te Nijenhuis, K., 1n4
- Tensile geometry, 40
- Tensile vs. shear viscosity, 40n5
- Tension and shear geometries, 175
- Terminal region, 110–112
- Testing, 53–54
- Testing geometries, 59–60
- Testing in nonstandard environments, 9n32
- Testing in the presence of solvents, **11**
- Testing methods, 112–114
- Test Methods Used, **195–196**
- Tests for the DMA, **113**
- TGA, TG/IR, or TG/MS, 125n3
- $T\gamma$ transitions, 102
- Thermal cures, 123

- Thermal curing studies, 132n28, 177, 178
- Thermal cycles, 53, 132
- Thermal expansion, 61–62, 64, 88
- Thermal expansion curve, 59
- Thermal expansivity, 61n8
- Thermal mass of solvent, 184
- Thermal or UV aging, 103
- Thermal techniques and TMA applications, 59
- Thermal transitions, 98
- Thermocouple, 59, 91, 186
- Thermogravimetric analyzer (TGA) studies, 180n10, 200n3
- Thermomechanical analysis
- dilatometry and bulk measurements, 65
 - expansion and CTE, 61–63
 - flexure and penetration, 64
 - mechanical tests, 65–67
 - PVT relationship studies, 67–68
 - theory of, 57–58
 - TMA samples, experimental considerations, 58–61
 - and transitions, 101
- Thermomechanical analyzer (TMA) and axial analyzers, 79
- beta and gamma transitions, 6n20
 - controlled stress analyzer, 2
 - and CTE, 61–63
 - heat set temperature, 110
 - tests subset of creep testing, 57
- Thermoplastics, 123, 132, 137n40, 155
- Thermosets
- characterization, quality control approaches, 138–140
 - contraction during cure, 65nn15-16
 - cure profiles, 127–132
 - isothermal curing studies, 133–134
 - kinetics by DMA, 134–137
 - mapping thermoset behavior, 137–138
 - modeling cure cycles, 133
 - photocuring, 132–133
 - postcure studies, 140–141
 - quality control, 138–140
 - thermoset characterization, quality control approaches, 138–140
 - thermosetting materials, 123–127
 - viscosity (η), 6
- Thermosetting materials, 123–127
- Thermosetting reactions, 125
- Thermosetting systems, 201n6
- Three-dimensional forms, 28n22
- Three-point and four-point bending, 84–85
- Three-point bending, 84
- aspect ratio, 24
 - checking the temperature response, 198–199
 - choosing the fixture, 194
 - and dual cantilever fixtures, 85
 - dynamic temperature scans, 202
 - fixtures, 59
 - frequency scan on viscoelastic material, 148
 - frequency scans, 202
 - resonance response, 154
 - TMA experiment, 201
- Time, 33, 51, 197–198
- Time and study of age life, 117n84
- Time and temperature scanning in DMA, 95–98
- Time-based studies, 117–118
- Time constants, 91
- Time-temperature effects, 117
- Time-temperature equivalence, 150n11, 151
- Time-temperature scans, 95
- Time-temperature superposition (TTS)
- accelerated age testing, 178
 - Deborah number, 155
 - difficulties and failures of, 165n47
 - frequency changes and curves, 164
 - frequency scan predictive method, 145
 - frequency scans, 202
 - method of reduced variables, 161
 - verify the results, 199–200
 - Williams-Landel-Ferry (WLF) model, 164, 167
- Time-temperature-transition (TTT) diagram, 137, 138n43
- Tirrell, M., 28n22
- TMA. *See* Thermomechanical analyzer
- TMA change in dimensions, 57
- TMA distribution of molecular weights, 59
- TMA experiment, 18, 201
- TMA measurements
- free volume of polymer, 57
 - glass transition (T_g), 61–62
 - mechanical tests, 65–67
 - and testing geometries, 59–60
 - and vertical movement, 65
- TMA methods, 59–61
- TMA on inorganic glass, 57
- TMA samples, 58–61
- TMA usage, 57
- Torsional, 88, 89, 90
- Torsional analyzers, 79
- Torsional beam and braid, 90
- Torsional braid analyzers (TBAs), 2n9, 81
- Torsional rheometers, 88
- Transformations of data, 167–168
- Transitions in polymers, 4–6
- applications, 114–117
 - frequency dependencies in transition studies, 112–114
 - glass transition (T_g or T_o), 103–106
 - overview, 98–100
 - rubbery plateau, T_{α}^* and T_{β} , 106–110
 - sub- T_g transitions, 101–102
 - terminal region, 110–112

time and temperature scanning in DMA, 95–98
 time-based studies, 117–118
 Triton Technologies, 180n8
 TTS. *See* Time-temperature superposition
 TTT. *See* Time-temperature-transition (TTT) diagram
 2D-IR, 102
 Twombly, B., 186
 Two-part epoxy resin, 128–130
 Two-stage cure cycle, 133

U

Unusual conditions and specialized tests
 humanity studies, 179–182
 hyphenated techniques, 186–187
 immersion, 182–186
 modeling other mechanical tests, 187–188
 UV studies, 175–179
 UV inhibitor, 178
 UV irradiation effect, 176
 UV light source, 117, 132, 134
 UV Photocures, 177–178
 UV Photodegradations, 178–179
 UV radiation, 178
 UV studies, 175–179

V

Velocity, 33
 Verify the results, 199–200
 Vertical movement, 65
 Vicat, 65n23
 Viscoelasticity, 57n4, 98n9
 Viscoelastic materials effects, 147–148
 Viscoelastic nature, 29, 31
Viscoelastic Properties of Polymers (Ferry), 1n7
 Viscosity (dynamic), 34
 Viscosity (η)
 amorphous phase, 99
 calculation property, 2, 75–76
 during curing, 130, 139–140
 curing studies, 202
 and curing systems, 123, 128–130
 frequency effects on materials, 147–154
 frequency scan, 147
 vs. frequency scans, 152–153
 frequency/temperature dependencies, 159
 function of temperature, 4
 increase during curing, 6n23
 linear viscoelastic region, 38
 measurement of, 44, 52n43
 parallel plates, 88
 shear rate, 6, 26, 149–150
 and staging, 125

temperature scan, 127
 tendency to flow, 4
 tensile vs. shear, 40
 thermoset, 6
 torsional, 88
 Viscosity (kinematic), 34
 Viscosity, compressive, 65n27
 Viscosity, penetrative, 65n28
 Viscosity of Common Materials, 132
 Viscosity-shear rate curve, 32
 Viscosity testing, 25n14
 Viscous behavior, 74
 Viscous response of strain rate, 72
 Vitrification, 129
 Vitrification point, 131–132, 140
 Voigt-Kelvin model, 40, 42–43
 Volume, 33, 132
 Volumetric expansion, 62

W

Ward, I., 98n17
 Weight, 6n22
 Weight-based [W(M)], 171
 Weissenberg rheogoniometer, 1n6
 Wendorff, J., 102n47
 Wicket plot, 155nn15–16, 166–167, 199–200
 Williams-Landel-Ferry (WLF) model
 Boltzman superposition principle, 49
 kinetics by DMA, 134
 master curve, 8–9
 time-temperature superposition, 164, 167
 verify the results, 199–200
 Wissbrum, K., 159n20, 165n46
 Wood polymers, 187n26
 Work (energy), 34

Y

Yee, A., 102n45
 Yield stress, 32
 Young, W., 83n11
 Young's modulus
 calculation property, 74
 vs. classic stress-strain curve, 4, 21
 and curvature, 21n9
 elastic modulus (E'), 149
 and Hooke's law, 20
 instruments used to measure qualities like, 57n1

Z

Zero-shear plateau, 7n28, 27, 149n6
 Zolzer, U., 81n9

Material Science

Second Edition

DYNAMIC MECHANICAL ANALYSIS

A Practical Introduction

Once a tool reserved for specialists, dynamical mechanical analysis (DMA) or spectroscopy has left the domain of the rheologist to become a prevalent tool in the analytical laboratory. However, information on the use of this important tool is still scattered among a range of books and articles.

Updated with new material, expanded practical explanations, and new applications, ***Dynamic Mechanical Analysis, Second Edition*** —

- Provides a systematic introduction to DMA that begins with the basics of mechanical analysis, including stress–strain and creep–recovery tests
- Updates coverage with expanded practical explanations, extensive end-of-chapter references, and new applications
- Discusses major types of instrumentation, including oscillatory rotational, oscillatory axial, and torsional pendulum
- Describes analytical techniques in terms of utility, quality of data, methods of calibration, and suitability for different types of materials
- Assesses applications for thermoplastics, thermosetting systems, and thermosets
- Discusses applications of humidity, immersion, and UV in DMA testing as well as non-standard samples like pharmaceuticals and powders

 **CRC Press**
Taylor & Francis Group
an **informa** business

6000 Broken Sound Parkway, NW
Suite 300, Boca Raton, FL 33487
270 Madison Avenue
New York, NY 10016
2 Park Square, Milton Park
Abingdon, Oxon OX14 4RN, UK

53124

ISBN: 978-1-4200-5312-8



9 781420 053128

www.crcpress.com